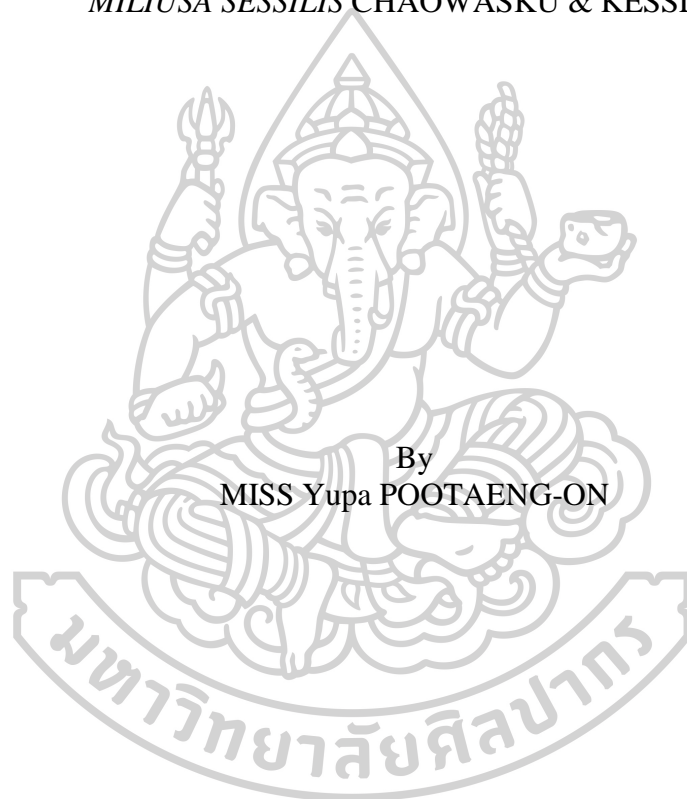




CHEMICAL CONSTITUENTS AND BIOLOGICAL ACTIVITIES FROM
MILIUSA SESSILIS CHAOWASKU & KESSLER



A Thesis Submitted in Partial Fulfillment of the Requirements
for Doctor of Philosophy ORGANIC CHEMISTRY
Department of CHEMISTRY
Graduate School, Silpakorn University
Academic Year 2019
Copyright of Graduate School, Silpakorn University

การศึกษาองค์ประกอบทางเคมีและฤทธิ์ทางชีวภาพจากใบเป็ยว้ามขวาน



วิทยานิพนธ์นี้เป็นส่วนหนึ่งของการศึกษาตามหลักสูตรปรัชญาดุษฎีบัณฑิต

สาขาวิชาเคมีอินทรีย์ แบบ 2.1 ปรัชญาดุษฎีบัณฑิต

ภาควิชาเคมี

บัณฑิตวิทยาลัย มหาวิทยาลัยศิลปากร

ปีการศึกษา 2562

ลิขสิทธิ์ของบัณฑิตวิทยาลัย มหาวิทยาลัยศิลปากร

CHEMICAL CONSTITUENTS AND BIOLOGICAL ACTIVITIES
FROM *MILIUSA SESSILIS* CHAOWASKU & KESSLER



A Thesis Submitted in Partial Fulfillment of the Requirements
for Doctor of Philosophy ORGANIC CHEMISTRY
Department of CHEMISTRY
Graduate School, Silpakorn University
Academic Year 2019
Copyright of Graduate School, Silpakorn University

Title Chemical constituents and biological activities from *Miliusa sessilis*
 Chaowasku & Kessler
By Yupa POOTAENG-ON
Field of Study ORGANIC CHEMISTRY
Advisor Assistant Professor Kanok-on Rayanil , Ph.D.

Graduate School Silpakorn University in Partial Fulfillment of the
Requirements for the Doctor of Philosophy

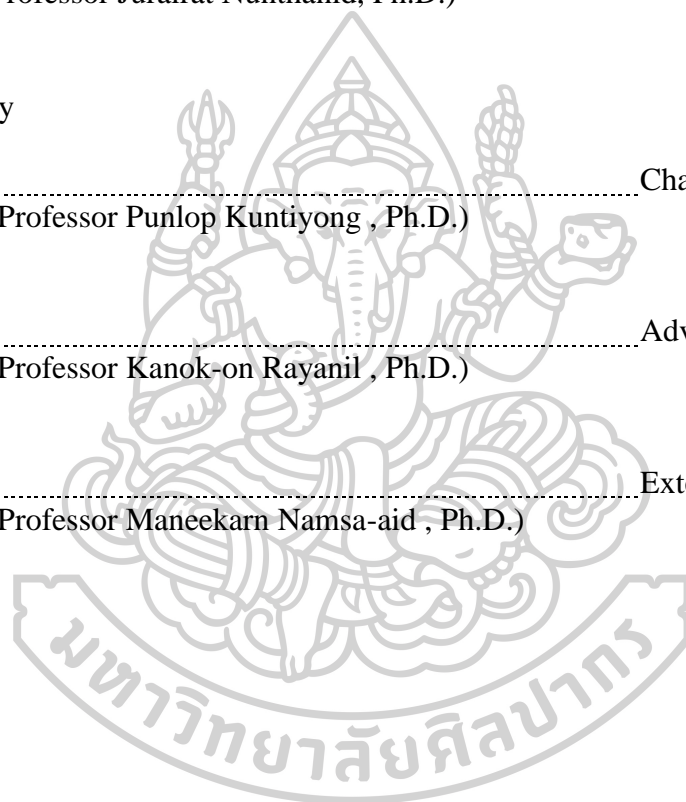
..... Dean of graduate school
(Associate Professor Jurairat Nunthanid, Ph.D.)

Approved by

..... Chair person
(Assistant Professor Punlop Kuntiyong , Ph.D.)

..... Advisor
(Assistant Professor Kanok-on Rayanil , Ph.D.)

..... External Examiner
(Assistant Professor Maneekarn Namsa-aid , Ph.D.)



58302803 : Major ORGANIC CHEMISTRY

Keyword : *Miliusa sessilis*, Annonaceae, Dihydro[*b*]benzofurans, 8-O-4'-Neolignans, Lanostane triterpenoids, Cytotoxicity

MISS YUPA POOTAENG-ON : CHEMICAL CONSTITUENTS AND BIOLOGICAL ACTIVITIES FROM *MILIUSA SESSILIS* CHAOWASKU & KESSLER THESIS ADVISOR : ASSISTANT PROFESSOR KANOK-ON RAYANIL, Ph.D.

Bioassay-guided fractionation of the hexane and ethyl acetate extracts of the leaves of *Miliusa sessilis* Chaowasku & Kessler sp. nov. (Annoaceae) led to the isolation of nine new neolignans including four dihydro[*b*]benzofuran neolignans: (7*S*,8*R*)-5'-hydroxy-3,4-dimethoxy-4',7-epoxy-8,3'-neolign-8'-en-9-acetate (MS12), (7*S*,8*R*)-3,4,5'-trimethoxy-4',7-epoxy-8,3'-neolign-8'-en-9-ol (MS15), (7*S*,8*R*)-5'-hydroxy-3,4-dimethoxy-4',7-epoxy-8,3'-neolign-8'-en-9-ol (MS17) and (7*R*,8*S*)-3,4,5'-trimethoxy-4',7-epoxy-8,3'-neolign-8'-en-9-acetate (MS11), three 8-*O*-4' neolignans: *threo*-(7*R*,8*R*)-3,3',4-trimethoxy-8,4'-oxyneolign-8'-en-7-ol-9-acetate (MS16), *threo*-(7*R*,8*R*)-3,3',4-trimethoxy-8,4'-oxyneolign-8'-en-7,9-diol (MS19) and *threo*-3,4-dihydroxy-3',5'-dimethoxy-8,4'-oxyneolign-8'-en-7,9-diol (MS20), one dineolignan: (7*R*,8*R*)-4'-hydroxy-3,4,5'-trimethoxy-8,3'-neolign-8'-en-7,9-diol (MS14) and one phenylpropanoid dimer: 4-hydroxy-3',5'-dimethoxy-3,4'-oxyneolign-7',8'-dien-9'-ol (MS18), and four new triterpenes: (3*β*,23*S*)-23-methoxy-24-methylenelanost-9-en-3-ol (MS3), (3*β*,23*S*)-23-methoxy-24-methylenenorlanost-9-en-3-ol (MS5), (3*β*)-24,24¹-epoxy-lanost-9-en-3-ol (MS6) and (3*β*,16*β*)-24-methylenelanost-9-en-3,16-diol (MS7), together with seven other known compounds, including, two neolignans: dehydrodieugenol A (MS10) and dehydrodieugenol B (MS13), two sesquiterpenes: (+)-spathulenol (MS1) and T-muurolol (MS4), phytol (MS2) and a mixture of stigmasterol (MS8) and *β*-sitosterol (MS9). Their structures were elucidated by extensive spectroscopic analysis. The structures of MS12, MS3, MS5 and MS7 were further confirmed by X-ray crystallographic analysis. The absolute configurations were determined using circular dichroism (CD) data analysis and the modified Mosher's method. All isolated compounds were also evaluated for their cytotoxic activities against four human cancer cell lines (HeLa, HN22, HepG2 and HCT116), including one normal-type cell line (HaCaT) using MTT assay. MS17 was found to exhibit the most promising cytotoxic effect against Hela cells with the lowest IC₅₀ value of 0.04 mM and the highest selective index of 187.8.

ACKNOWLEDGEMENTS

I would like to thank all professors from the Faculty of Science, Silpakorn University who taught me and gave me invaluable advice throughout my graduate study at Silpakorn University. Also, I would like to thank the Faculty of Animal Sciences and Agricultural Technology, Silpakorn University who gave me initial financial support and permit me to pursue my Ph.D. degree.

I would like to express my sincere thanks to Asst. Prof. Dr. Kanok-on Rayanil, my thesis advisor, for her invaluable help and constant encouragement throughout my research. I am most grateful for her teaching and advice, not only the research methodologies but also many other methodologies in life. I would not have achieved this far and my thesis would not have been completed without all the support that I have always received from her.

I am indebted to the thesis defense committee for the comments and suggestions, especially, Asst. Prof. Dr. Maneekarn Namsaaid, Department of Chemistry, Faculty of Science, Srinakharinwirot University, who spent valuable time as an external thesis committee and kindly understand my limitation.

I would like to thank Asst. Prof. Dr. Punlop Kuntiyong for material support, valuable discussion and answers concerning NMR interpreting the absolute stereochemistry by the modified Mosher's method.

I am grateful to Dr. Piya Chalermglin, Thailand Institute of Scientific and Technological Research and Assoc. Prof. Dr. Uma Prawat, Phuket Rajabhat University, for their support in collecting and identifying the plant material.

I am grateful to Dr. Purin Charoensuksai, Dr. Pawaris Wongprayoon and Ms. Suwadee Jiajaroen, Department of Biopharmacy, Faculty of Pharmacy, Silpakorn University for enabling me to carry out the bioactivity assay in their laboratory and for their helpful suggestions.

Besides, I would like to thank Asst. Prof. Dr. Kittipong Chainok, Materials and Textile Technology, Faculty of Science and Technology, Thammasat University for collecting X-ray crystallographic data.

I gratefully acknowledge Chulabhorn Research Institute (CRI) for collecting HRESIMS data.

I am also grateful to the Graduate School, Silpakorn University for financial support.

A special acknowledgment is extended to the Department of Chemistry, Faculty of Science, Silpakorn University for providing research facilities.

I thank scientists at the Department of Chemistry, Faculty of Science, Silpakorn University for their helpful assistance in research facilities such as UV, IR and NMR experiments.

I also would like to acknowledge several partner laboratories, Ms. Wirunya Sutassanawichanna, Ms. Jintana Jantham, Asst. Prof. Sarinrat Chattiranan and others who I remember fondly because of their helpfulness, some very enjoyable experiences that we shared.

Finally, I am grateful to my family for their love, understanding, encouragement and support in everything throughout this research. This accomplishment would not have been possible without them. Thank you.

Yupa POOTAENG-ON

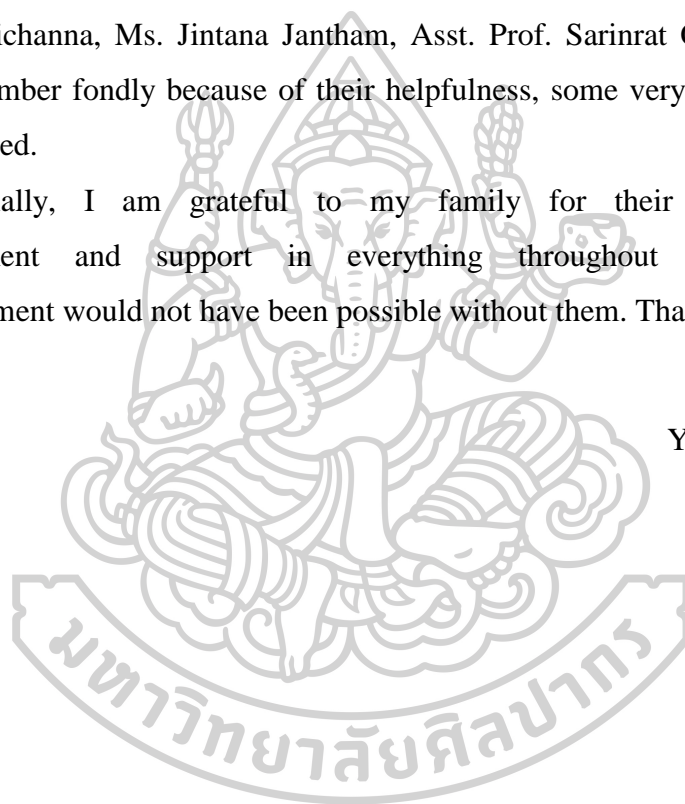


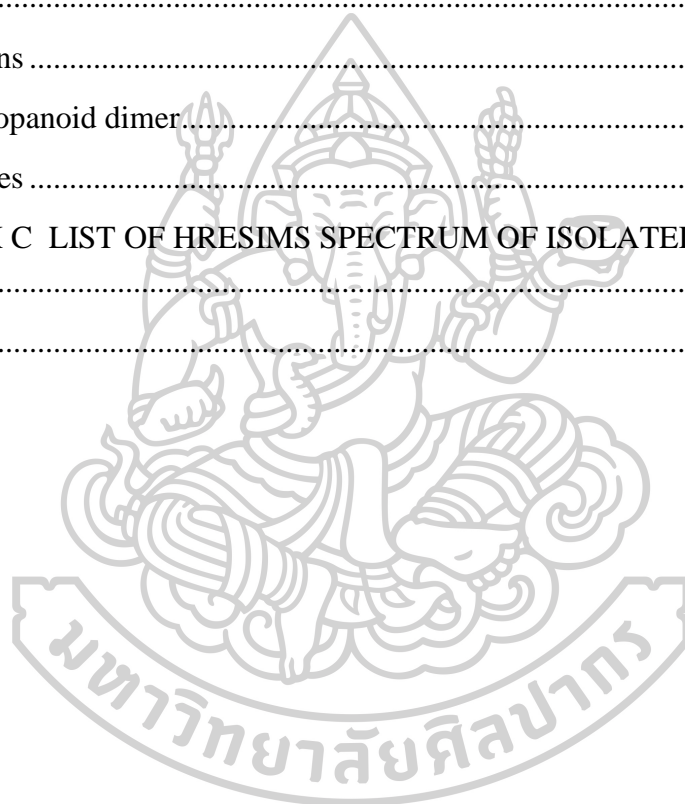
TABLE OF CONTENTS

	Page
ABSTRACT.....	D
ACKNOWLEDGEMENTS.....	E
TABLE OF CONTENTS.....	G
LIST OF TABLES.....	K
LIST OF FIGURES.....	N
CHAPTER 1 INTRODUCTION.....	2
1.1 The genus <i>Miliusa</i>	2
1.2 Morphological characters of <i>Miliusa sessilis</i> Chaowasku & Kessler sp. nov.....	4
1.3 Chemical constituent investigation of the genus <i>Miliusa</i>	8
1.3.1 <i>Miliusa cf. banacea</i>	8
1.3.2 <i>Miliusa velutina</i> (DC.) Hook. f. & Thomson.....	8
1.3.4 <i>Miliusa sinensis</i> Finet & Gagnep.....	25
1.3.5 <i>Miliusa mollis</i> Pierre.....	29
1.3.6 <i>Miliusa fragrans</i> Chaowasku & Kessler sp. nov.....	32
1.3.7 <i>Miliusa umpangensis</i> Chaowasku & Kessler sp. nov.....	34
1.3.8 <i>Miliusa cuneata</i> Craib.....	35
1.3.9 <i>Miliusa thorelii</i> Finet & Gagnep.....	37
1.3.10 <i>Miliusa sessilis</i> Chaowasku & Kessler sp. nov.....	39
CHAPTER 2 EXPERIMENTAL.....	1
2.1 Instrumentals and Chemicals.....	1
2.2 Plant materials.....	2
2.3 Chemical investigation of the leaves.....	3
2.3.1 Extraction and isolation.....	3
2.3.2 Chemical investigation of hexane extract fraction.....	5
2.3.3 Chemical investigation of EtOAc extract fraction.....	15

2.4 Hydrolysis of MS12.....	20
2.5 Methylation of MS12.....	21
2.6 Dehydration of MS14	21
2.7 Preparation of <i>S</i> -(-)-MTPA ester MS16 and <i>R</i> -(+)-MTPA ester MS16	22
2.8 Hydrolysis of MS16.....	23
2.9 Acetylation of MS20.....	23
2.10 X-ray crystallographic analysis of MS12, MS3, MS5 and MS7	24
2.10.1 Crystallographic data of (7 <i>S</i> ,8 <i>R</i>)-5'-hydroxy-3,4-dimethoxy-4',7-epoxy-8,3'-neolign-8'-en-9-acetate (MS12)	25
2.11 Biological assays	25
2.11.1 Cell culture	25
2.11.2 Cytotoxicity evaluation	26
2.12 Physical and spectral properties of isolated compounds	27
2.12.1 MS1	28
2.12.2 MS2	29
2.12.3 MS3	30
2.12.4 MS4	31
2.12.5 MS5	32
2.12.6 MS6	33
2.12.7 MS7	69
2.12.8 a mixture of MS8 and MS9	70
2.12.9 MS10	71
2.12.10 MS11	72
2.12.11 MS12	73
2.12.12 MS13	74
2.12.13 MS14	75
2.12.14 MS15	76
2.12.15 MS16	77
2.12.16 MS17	78

2.12.17 MS18	79
2.12.18 MS19	80
2.12.20 MS20a	82
CHAPTER 3 RESULTS AND DISCUSSION.....	104
3.1 Structure elucidation and identification.....	104
3.1.1 Neolignans.....	105
3.1.1.1 (7S,8R)-5'-Hydroxy-3,4-dimethoxy-4',7-epoxy-8,3'-neolign-8'- en-9-acetate (MS12)	105
3.1.1.2 (7S,8R)-5'-Hydroxy-3,4-dimethoxy-4',7-epoxy-8,3'-neolign-8'- en-9-ol (MS17)	109
3.1.1.3 (7S,8R)-3,4,5'-Trimethoxy-4',7-epoxy-8,3'-neolign-8'-en-9-ol (MS15).....	111
3.1.1.4 (7R,8S)-3,4,5'-Trimethoxy-4',7-epoxy-8,3'-neolign-8'-en-9-acetate (MS11).....	113
3.1.1.5 (7R,8R)-4'-Hydroxy-3,4,5'-trimethoxy-8,3'-neolign-8'-en-7,9-diol (MS14).....	115
3.1.1.6 <i>threo</i> -(7R,8R)-3,3',4'-Trimethoxy-8,4'-oxyneolign-8'-en-7-ol-9- acetate (MS16).....	117
3.1.1.7 <i>threo</i> -(7R,8R)-3,3',4'-Trimethoxy-8,4'-oxyneolign-8'-en-7,9-diol (MS19).....	120
3.1.1.8 <i>threo</i> -3,4-Dihydroxy-3',5-dimethoxy-8,4'-oxyneolign-8'-en-7,9- diol (MS20).....	123
3.1.2 Phenylpropanoid dimers.....	126
3.1.2.1 4-Hydroxy-3',5-dimethoxy-3,4'-oxyneolign-8,8'-dien (dehydrodieugenol B) (MS10).....	126
3.1.2.2 4,4'-Dihydroxy-3,3'-dimethoxy-5,5'neolign-8,8'-dien, (dehydrodieugenol A) (MS13)	127
3.1.2.3 4-Hydroxy-3',5-dimethoxy-3,4'-oxyneolign-7',8-dien-9'-ol (MS18).....	129
3.1.3 Triterpenes.....	131
3.1.3.1 (3 β ,23S)-23-Methoxy-24-methylenenorlanost-9-en-3-ol (MS5).....	131
3.1.3.2 (3 β ,23S)-23-Methoxy-24-methylenelanost-9-en-3-ol (MS3).....	134

3.1.3.3 (3 β ,16 β)-24-Methylenelanost-9-en-3,16-diol (MS7)	136
3.1.3.4 (3 β)-24,24 ¹ -Epoxy- lanost-9-en-3-ol (MS6)	138
3.2 Biological evaluation	139
CHAPTER 4 CONCLUSIONS	141
REFERENCES	142
APPENDIX A LIST OF ABBREVIATIONS	147
APPENDIX B LIST OF NMR SPECTRAL DATA OF ISOLATED COMPOUNDS	151
Neolignans	156
Phenylpropanoid dimer.....	213
Triterpenes	220
APPENDIX C LIST OF HRESIMS SPECTRUM OF ISOLATED COMPOUNDS	255
VITA.....	270



LIST OF TABLES

	Page
Table 1.1 Antiherpetic activity and cytotoxicity of compounds isolated from the leaves and the stems of <i>M. fragrans</i> Chaowasku & Kessler sp. nov.	33
Table 2.1 Fractions obtained from hexane extract fraction.	5
Table 2.2 Fractions obtained from H22.	6
Table 2.3 Fractions obtained from hexane extract fraction.	7
Table 2.4 Fractions obtained from H27.9.	10
Table 2.5 Fractions obtained from H27.12.	11
Table 2.6 Fractions obtained from H27.13.	11
Table 2.7 Fractions obtained from H27.14.	12
Table 2.8 Fractions obtained from H27.21.	13
Table 2.9 Fractions obtained from H27.41.	13
Table 2.10 Fractions obtained from H27.59.	14
Table 2.11 Fractions obtained from ethyl acetate extract fraction.	15
Table 2.12 Fractions obtained from E27.	17
Table 2.13 Fractions obtained from E27.4.	17
Table 2.14 Fractions obtained from E30.	19
Table 2.15 Fractions obtained from E35.	20
Table 2.16 ¹ H NMR (300 Hz), ¹³ C NMR (75 MHz) and HMBC NMR data for MS1 in CDCl ₃ (<i>J</i> in Hz in parentheses).	83
Table 2.17 ¹ H NMR (300 Hz) and ¹³ C NMR (75 MHz) data for MS2 in CDCl ₃ (<i>J</i> in Hz in parentheses).	84
Table 2.18 ¹ H NMR (300 Hz), ¹³ C NMR (75 MHz) and HMBC NMR data for MS3 in CDCl ₃ (<i>J</i> in Hz in parentheses).	85
Table 2.19 ¹ H NMR (300 Hz), ¹³ C NMR (75 MHz) and HMBC NMR data for MS4	86
Table 2.20 ¹ H NMR (300 Hz), ¹³ C NMR (75 MHz) and HMBC NMR data for MS5 in CDCl ₃ (<i>J</i> in Hz in parentheses).	87

Table 2.21 ^1H NMR (300 Hz), ^{13}C NMR (75 MHz) and HMBC NMR data for MS6 in CDCl_3 (J in Hz in parentheses).....	88
Table 2.22 ^1H NMR (300 Hz), ^{13}C NMR (75 MHz) and HMBC NMR data for MS7 in CDCl_3 (J in Hz in parentheses).....	88
Table 2.23 ^1H NMR (300 Hz) data for a mixture of MS8 and MS9 in CDCl_3 (J in Hz in parentheses).	91
Table 2.24 ^1H NMR (300 Hz), ^{13}C NMR (75 MHz) and HMBC NMR data for MS10 in CDCl_3 (J in Hz in parentheses).....	91
Table 2.25 ^1H NMR (300 Hz), ^{13}C NMR (75 MHz) and HMBC NMR data for MS11 in CDCl_3 (J in Hz in parentheses).....	92
Table 2.26 ^1H NMR (300 Hz), ^{13}C NMR (75 MHz) and HMBC NMR data for MS12 in CDCl_3 (J in Hz in parentheses).....	93
Table 2.27 ^1H NMR (300 Hz), ^{13}C NMR (75 MHz) and HMBC NMR data for MS13 in CDCl_3 (J in Hz in parentheses).....	94
Table 2.28 ^1H NMR (300 Hz), ^{13}C NMR (75 MHz) and HMBC NMR data for MS14 in CDCl_3 (J in Hz in parentheses).....	95
Table 2.29 ^1H NMR (300 Hz), ^{13}C NMR (75 MHz) and HMBC NMR data for MS15 in CDCl_3 (J in Hz in parentheses).....	96
Table 2.30 ^1H NMR (300 Hz), ^{13}C NMR (75 MHz) and HMBC NMR data for MS16 in CDCl_3 (J in Hz in parentheses).....	97
Table 2.31 ^1H NMR (300 Hz), ^{13}C NMR (75 MHz) and HMBC NMR data for MS17 in CDCl_3 (J in Hz in parentheses).....	98
Table 2.32 ^1H NMR (300 Hz), ^{13}C NMR (75 MHz) and HMBC NMR data for MS18 in CDCl_3 (J in Hz in parentheses).....	99
Table 2.33 ^1H NMR (300 Hz), ^{13}C NMR (75 MHz) and HMBC NMR data for MS19 in CDCl_3 (J in Hz in parentheses).....	100
Table 2.34 ^1H NMR (300 Hz), ^{13}C NMR (75 MHz) and HMBC NMR data for MS20 in CDCl_3 (J in Hz in parentheses).....	101
Table 2.35 ^1H NMR (300 Hz), ^{13}C NMR (75 MHz) and HMBC NMR data for MS20a in CDCl_3 (J in Hz in parentheses).	102
Table 2.36 ^1H NMR (300 Hz) and $\Delta\delta$ values [$\Delta\delta$ (in ppm) = $\Delta\delta_S - \Delta\delta_R$] for <i>S</i> -(-)-MTPA ester MS16 and <i>R</i> -(+)-MTPA ester MS16 in CDCl_3 (J in Hz in parentheses).	103

Table 3.1 Cytotoxic activity and selectivity index (SI) of compounds isolated from <i>M. sessilis</i> leaves.....	140
---	-----



LIST OF FIGURES

	Page
Figure 1.1 Distribution of <i>Miliusa</i> A.DC.....	3
Figure 1.2 <i>Miliusa sessilis</i> sp. nov. (A) habit, (B) flower bud, (C) flower with two inner petals removed, (D) inside (adaxial surface) of an inner petal, (E) fruit. (A) – (E) van Beusekom and Santisuk 2807.	5
Figure 1.3 <i>Miliusa sessilis</i> Chaowasku & Kessler sp. Nov (A) leaves and fruits (B) fruits.	6
Figure 1.4 <i>Miliusa sessilis</i> Chaowasku & Kessler sp. Nov. (A, B and C) leaves, (D) stem.	7
Figure 1.5 Oxoaporphine alkaloids isolated from <i>M. cf. banacea</i>	8
Figure 1.6 Chemical constituents isolated from <i>M. velutina</i>	9
Figure 1.7 Goniotalamusin and partial structures of the principal constituents of mixtures of acetogenins-A and acetogenins-B isolated from the hexane extract of the stem bark of <i>M. velutina</i>	10
Figure 1.8 Acetogenins isolated from the stem bark of <i>M. velutina</i>	11
Figure 1.9 Chemical constituents isolated from the leaves of <i>M. velutina</i>	13
Figure 1.10 Some chemical constituents isolated from the hexane and ethyl acetate extracts of the fruits and flowers of <i>M. velutina</i>	15
Figure 1.11 Chemical constituents isolated from the ethyl acetate extract of the leaves and branches of <i>M. balansae</i> Fin. & Gagn.....	17
Figure 1.12 Chemical constituents isolated from the methanol-H ₂ O extract of the leaves and branches of <i>M. balansae</i> Fin. & Gagn.....	18
Figure 1.13 Chemical constituents isolated from the methanol-H ₂ O extract of the leaves and branches of <i>M. balansae</i> Fin. & Gagn.	19
Figure 1.14 Glycosides isolated from the BuOH extract of the stems of <i>M. balansae</i> Fin. & Gagn.	21
Figure 1.15 Chemical constituents isolated from the stems of <i>M. balansae</i> Fin. & Gagn.....	22
Figure 1.16 Chemical constituents isolated from the methanol extract of the leaves of <i>M. balansae</i> Fin. & Gagn.	24

Figure 1.17 Geranylated homogentisic acid derivatives contained γ -lactone spiro-ring system isolated from the CH_2Cl_2 extract of the leaves, twigs and flowers of <i>M. sinensis</i> Fin. & Gagn.	26
Figure 1.18 Geranylated homogentisic acid derivatives contained the opening of γ -lactone spiro-ring system isolated from the CH_2Cl_2 extract of the leaves, twigs and flowers of <i>M. sinensis</i> Fin. & Gagn.	26
Figure 1.19 Geranylated homogentisic acid derivatives contained tetrahydrofuran ring system.	27
Figure 1.20 Biogenetic pathways for miliusanes.	27
Figure 1.21 Chemical constituents isolated from the methanol extract of the leaves of <i>M. sinensis</i>	29
Figure 1.22 Chemical constituents isolated from the MeOH extract of the twigs of <i>M. mollis</i> Pierre in 2010.	30
Figure 1.23 Chemical constituents isolated from the MeOH extract of the leaves of <i>M. mollis</i> Pierre in 2013.	32
Figure 1.24 Lignans and neolignans isolated from the MeOH extract of the leaves and stems <i>M. fragrans</i> Chaowasku & Kessler sp. nov.	34
Figure 1.25 Geranylated homogentisic acid and flavonols isolated from the MeOH extract of the leaves of <i>M. umpangensis</i> Chaowasku and Kessler sp. nov.	35
Figure 1.26 Chemical constituents isolated from the acetone extracts of leaves and the twigs of <i>M. cuneata</i>	36
Figure 1.27 constituents isolated from the acetone extract of the stems, roots and leaves of <i>M. thorelii</i>	38
Figure 2.1 Extraction and fractionation of <i>Miliusa sessilis</i> leaves.	4
Figure 2.2 Fractionation of the hexane extract of <i>Miliusa sessilis</i>	9
Figure 2.3 Fractionation of the EtOAc extract of <i>Miliusa sessilis</i>	18
Figure 2.4 Structures of MS1-MS20.	27
Figure 3.1 Structure, ^1H - ^1H COSY (bold line) and of HMBC (H \rightarrow C) correlation of MS12.	107
Figure 3.2 X-ray ORTEP diagram of MS12.	108
Figure 3.3 Circular dichroism (CD) spectra of MS12.	108
Figure 3.4 Structure, ^1H - ^1H COSY (bold line) and of HMBC (H \rightarrow C) correlation of MS17.	110

Figure 3.5 CD spectra of MS17.	110
Figure 3.6 Structure, ^1H - ^1H COSY (bold line) and of HMBC (H→C) correlation of MS15.	112
Figure 3.7 CD spectra of MS15.	112
Figure 3.8 Structure, ^1H - ^1H COSY (bold line) and of HMBC (H→C) correlation of MS11.	114
Figure 3.9 CD spectra of MS11.	114
Figure 3.10 Structure, ^1H - ^1H COSY (bold line) and of HMBC (H→C) correlation of MS14.	116
Figure 3.11 CD spectra of MS14 compared with MS11, MS12, MS15 and MS17.	116
Figure 3.12 Structure, ^1H - ^1H COSY (bold line) and of HMBC (H→C) correlation of MS16.	119
Figure 3.13 Difference in the $\Delta\delta$ values [$\Delta\delta$ (in ppm) = $\Delta\delta_S - \Delta\delta_R$] obtained from (<i>S</i> - and (<i>R</i>)-MTPA esters of MS16.	119
Figure 3.14 CD spectra of MS16.	120
Figure 3.15 Structure, ^1H - ^1H COSY (bold line) and of HMBC (H→C) correlation of MS19.	121
Figure 3.16 CD spectra of MS16.	122
Figure 3.17 Structure, ^1H - ^1H COSY (bold line) and of HMBC (H→C) correlation of MS20.	125
Figure 3.18 CD spectra of MS20 compared with MS16 and MS19.	125
Figure 3.19 Structure, ^1H - ^1H COSY (bold line) and of HMBC (H→C) correlation of MS10.	127
Figure 3.20 Structure, ^1H - ^1H COSY (bold line) and of HMBC (H→C) correlation of MS13.	128
Figure 3.21 Structure, ^1H - ^1H COSY (bold line) and of HMBC (H→C) correlation of MS18.	130
Figure 3.22 Structure, ^1H - ^1H COSY (bold line) and of HMBC (H→C) correlation of MS5.	133
Figure 3.23 X-ray ORTEP diagram of MS5.	133
Figure 3.24 Structure, ^1H - ^1H COSY (bold line) and of HMBC (H→C) correlation of MS3.	135

Figure 3.25 X-ray ORTEP diagram of MS3.....	135
Figure 3.26 Structure, ^1H - ^1H COSY (bold line) and of HMBC (H \rightarrow C) correlation of MS7.....	137
Figure 3.27 X-ray ORTEP diagram of MS7.....	137
Figure 3.28 Structure, ^1H - ^1H COSY (bold line) and of HMBC (H \rightarrow C) correlation of MS6.....	138



CHAPTER 1

INTRODUCTION

Natural products and traditional medicines are highly important as they have been recognized in term of a source of therapeutic agents and diversity of their structures. Natural products are various in multidimensional chemical structures; in the meantime, their biological function modifiers have also been in attention.

Natural products played an important role in this world because of the achievement of drug discovery. The existence of the medicinal plants on this earth has been globally important. The earth is full of medicinal herbs being rich of endurance. Each plant has its own different therapeutic properties following their active bioactive molecule. Natural drug substances play essential roles in the modern medical system. Natural products therapeutic roles are extremely useful for disease-inhabiting capabilities. They provide basic bioactive compounds which are less toxic but more effective. They also bring biological and chemical means of modification and extraction of natural products into potent drug.

1.1 The genus *Milium*

Milium was placed in the tribe Milieae of the subfamily Malmoideae, which belongs to the Annonaceae family. The plant *Milium* is an Asian palaeotropical genus comprises about 60 species of shrubs and trees distributed from the Indian subcontinent through Indochina, Peninsular Malaysia, the Southeast Asian islands to New Guinea and northern Australia (Figure 1.1) [1, 2]. *Milium* is circumscribed by having four characters: 1) similarly-sized sepals and outer petals both of which are

much smaller than the inner petals, 2) a densely hairy torus, 3) miliusoid stamens, that are stamens with tiny connective prolongation not covering the thecae or without connective prolongation, and 4) fourpart lamelliform ruminations of the endosperm [3].

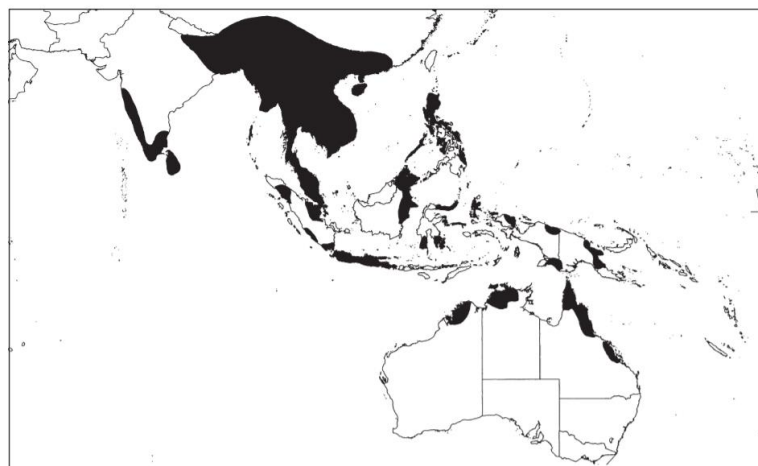


Figure 1.1 Distribution of *Miliusa* A.DC.
From Mols and Kessler (2003)

At least 20 species of *Miliusa* have been found in Thailand, including *M. amplexicaulis* Ridl., *M. chantaburiana* Damthongdee & Chaowasku, *M. campanulata* Pierre, *M. cuneata* Craib, *M. filipes* Ridl., *M. fragrans* Chaowasku & Kessler sp. nov., *M. fusca* Pierre, *M. hirsuta* Chaowasku & Kessler sp. nov., *M. horsfi eldii* (Benn.) Baill. ex Pierre, *M. intermedia* Chaowasku & Kessler sp. nov., *M. longipes* King, *M. mollis* Pierre, *M. nakhonsiana* Chaowasku & Kessler sp. nov., *M. parviflora* Ridl., *M. pumila* Chaowasku, *M. sclerocarpa* (A. DC.) Kurz., *M. sessilis* Chaowasku & Kessler sp. nov., *M. thailandica* Chaowasku & Kessler sp. nov., *M. thorelii* Finet & Gagnep., *M. umpangensis* Chaowasku & Kessler sp. nov. and *M. velutina* (DC.) Hook. f. & Thomson [2, 4]. Nine of the *Miliusa* genera growing worldwide have been investigated for their photochemistry and biological activity. Previous chemical

investigations of plants in this genus have disclosed different classes of natural products, including aporphine alkaloids and alkaloids [5-8], geranylated homogentisic acid derivatives [9-11], flavonoids [5, 6, 12], styryl compounds [12-14], lignans and neolignans [15-17], acetogenins [12, 18] and other aliphatic and aromatic compounds [19-23]. In particular, alkaloids [6, 8], geranylated homogentisic acid derivatives [6, 9, 11] and neolignan [15, 16] were showed antiherpetic activities and cytotoxic activities.

1.2 Morphological characters of *Miliusa sessilis* Chaowasku & Kessler sp. nov.

Miliusa sessilis was reported first time in 2013 by Chaowasku and Kessler [2]. The plant was collect first time at Bang Saphan, Prachuab Khiri Khan, Thailand in Feb 1970, The name of *M. sessilis* refers to the nearly sessile monocarps (and also sessile leaves) and the name in Thai is “Bai-Biaw-Dam-Kwan”. The morphological character (Figure 1.2-1.4) is shrubs, evergreen, 1-2 m high. The wood appeared yellow when fresh but became darker on exposure. The parenchyma is in fine tangential lines, forming a network with the narrow to moderately broad to broad rays, which is typical for Annonaceae [1].

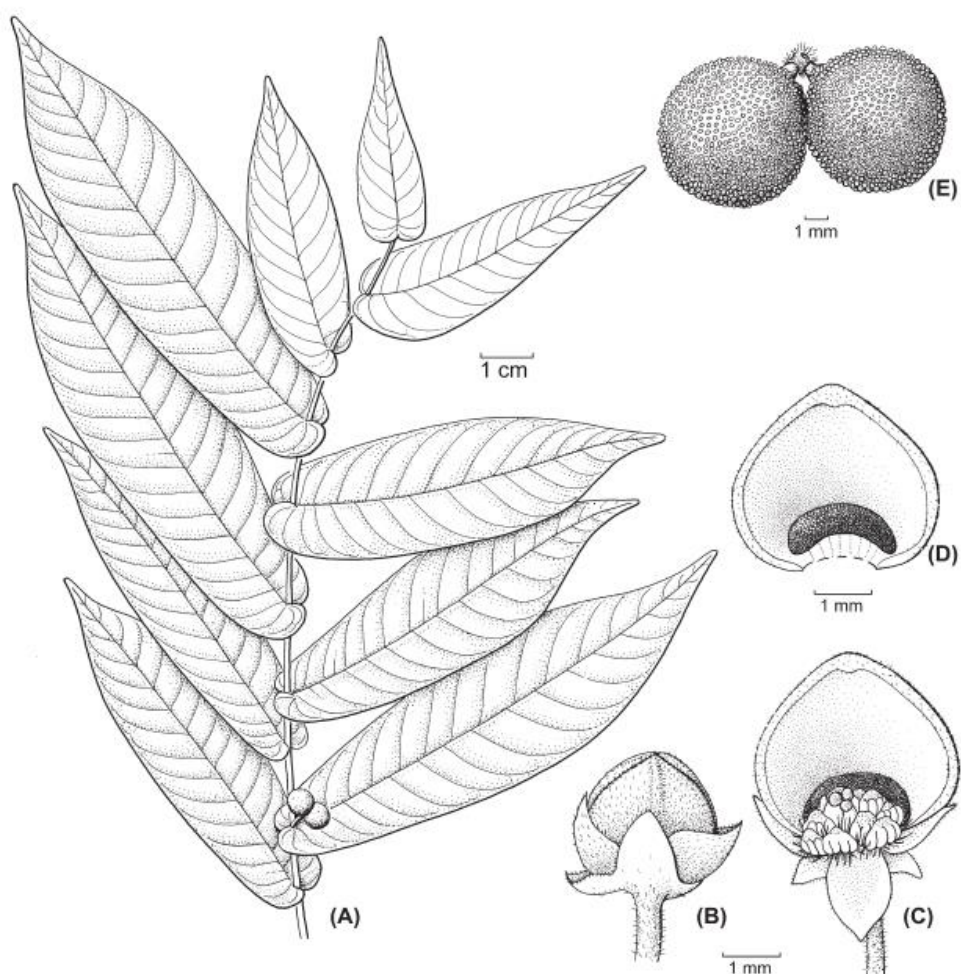
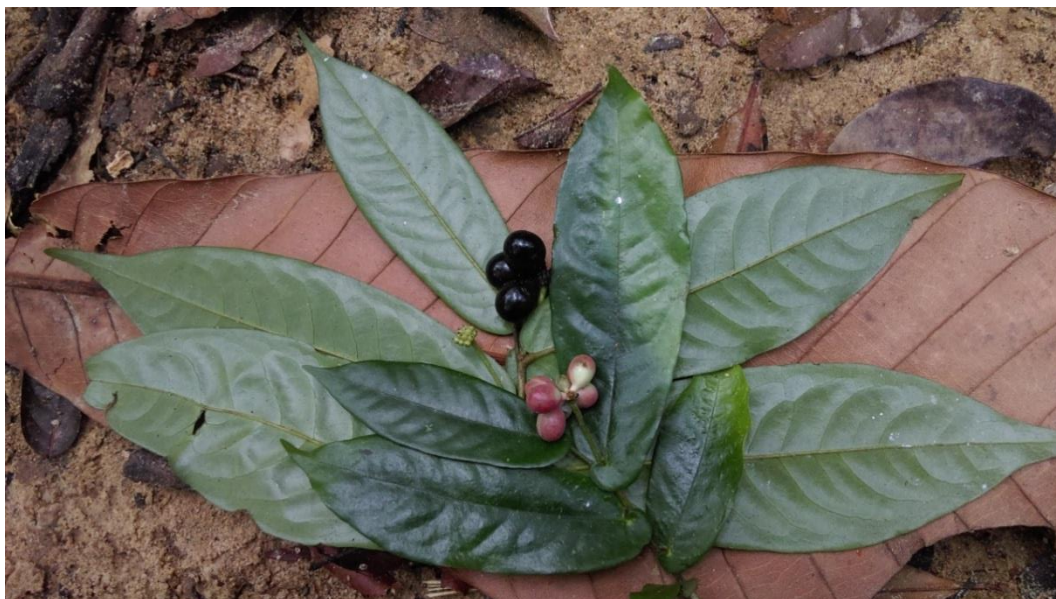


Figure 1.2 *Miliusa sessilis* sp. nov. (A) habit, (B) flower bud, (C) flower with two inner petals removed, (D) inside (adaxial surface) of an inner petal, (E) fruit. (A) – (E) van Beusekom and Santisuk 2807.

From Chaowasku and Kessler (2013)

A.



B.



Figure 1.3 *Miliusa sessilis* Chaowasku & Kessler sp. Nov (A) leaves and fruits (B) fruits.

Pootaeng-on, Y. [February, 2016]



Figure 1.4 *Miliusa sessilis* Chaowasku & Kessler sp. Nov. (A, B and C) leaves, (D) stem.

Pootaeng-on, Y. [February, 2016]

1.3 Chemical constituent investigation of the genus *Milium*

1.3.1 *Milium cf. banacea*

In 1994, phytochemical investigation of the methyl ethyl ketone extract from the root of *Milium cf. banacea* led to the isolation of two oxoaporphine alkaloids, lauterine (**1**) and 10-hydroxyliriodenine (**2**) (Figure 1.5). The structure of 10-hydroxyliriodenine (**2**), a novel oxoaporphine alkaloid, was determined by spectroscopic methods and chemical conversion to lauterine (**1**). Both lauterine (**1**) and 10-hydroxyliriodenine (**2**) are significantly toxic to the *rad 52. top1* mutant and inhibit DNA topoisomerase II activity. [8]

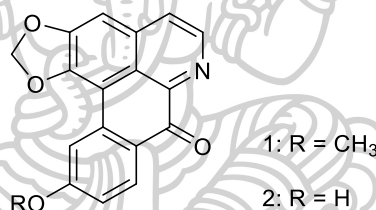


Figure 1.5 Oxoaporphine alkaloids isolated from *M. cf. banacea*.

1.3.2 *Milium velutina* (DC.) Hook. f. & Thomson

In 2000, five alkaloids were isolated from ethanolic extract of the stem bark of *M. velutina* by acid-base treatment followed by preparative silica gel TLC using chloroform-methanol-ammonia as the developing solvent. The structures were elucidated as benzulisoquinoline; reticuline (**3**), and aporphines; liriodenine (**4**), isocordine (**5**), nor-corydine (**6**), (+)-isocordine α -oxide (**7**), stigmasterol (**8**), spathulenol (**9**) and an ester, benzyl benzoate (**10**) (Figure 1.6) [7, 23].

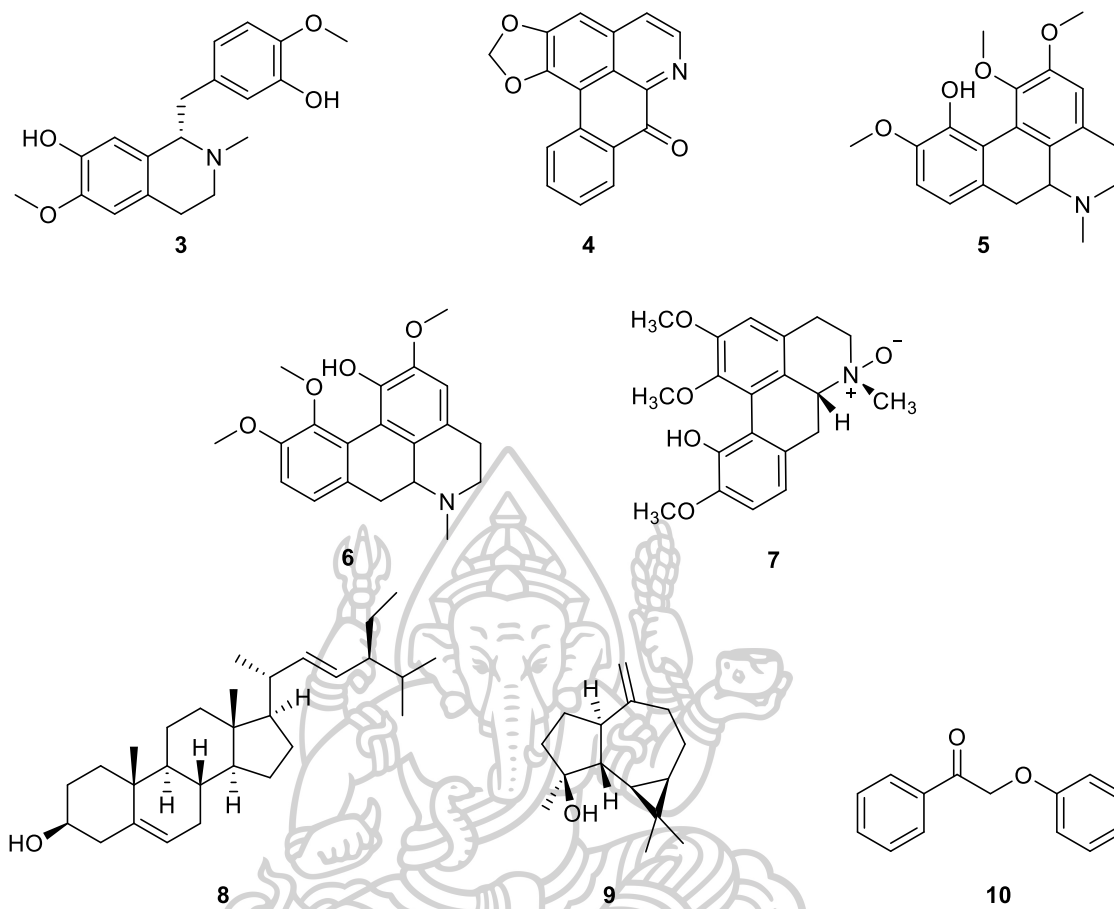


Figure 1.6 Chemical constituents isolated from *M. velutina*.

In 2000, the purified acetogenin, goniotalamusin (**11**) and two acetogenine mixtures, the mixtures of acetogenins-A (**12**) and the mixtures of acetogenins-B (**13**) (Figure 1.7) were isolated from petroleum ether extract of the stem bark of *M. velutina* Hook. f. & Thomson. Both goniotalamusin (**11**) and acetogenine mixtures-A (**12**) showed moderate antibacterial activity, whereas the acetogenins mixtures-B (**13**) was slightly active against only *Bacillus cereus* [24].

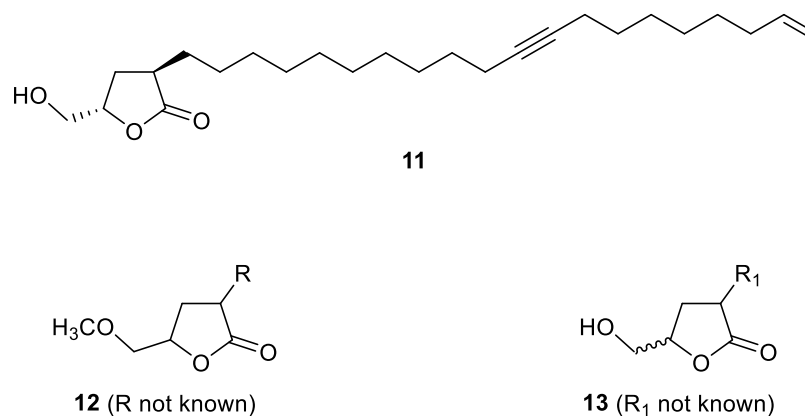


Figure 1.7 Goniiothalamusin and partial structures of the principal constituents of mixtures of acetogenins-A and acetogenins-B isolated from the hexane extract of the stem bark of *M. velutina*.

In 2011 and 2015, nine new C23 and C21 linear acetogenins, cananginones A-I (**14-22**) (Figure 1.8) were isolated from the hexane extract of the stem bark of *M. velutina*. Their structures were identified by 1D, 2D NMR as well as by intensive examination of EIMS fragmentation. The stereochemistry of the γ -lactone ring of the isolated compounds was assigned to be *2R*, *22S* (*20S**) as reported for goniiothalamusin (**11**). These compounds exhibited weak cytotoxicity (IC_{50}) against three cancer cell lines, including the epidermoid carcinoma (KB) cell lines with IC_{50} values in the range of 33.9-112.6 μ M, human breast cancer (MCF7) cell lines with IC_{50} values in the range of 16.6-129.7 μ M and human small cell lung cancer (NCI-H187) cell lines with IC_{50} values in the range of 27.0-66.7 μ M. Compounds **21** and **22** also showed weak antifungal activity against *Candida albicans* with IC_{50} values of 37.4 and 75.2 μ M, respectively. Only compound **18** showed antimalarial activity against *P. falciparum* with an IC_{50} value of 24.4 μ M. [18, 24, 25].

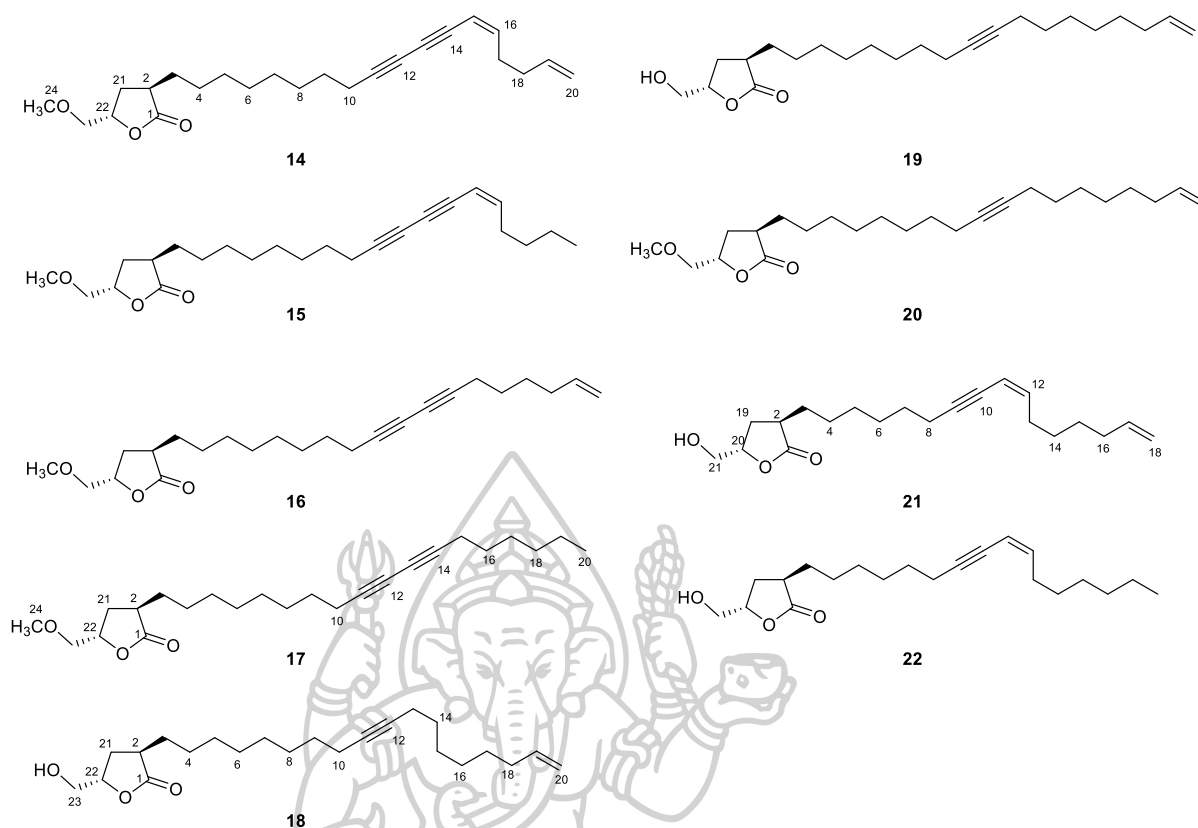


Figure 1.8 Acetogenins isolated from the stem bark of *M. velutina*.

In 2011, a unique class of eight bicyclic lactones with a C18 carbons architecture, velutinoes A-H (**23-30**), three new dimeric styrylpyrones, velutinindimer A-C (**31-33**) and five known compounds including the kawapyrone, yangonin (**34**), three flavonoids (**35-37**) and an acetogenin, cananginone H (**38**) (Figure 1.9) were isolated from the hexane and ethyl acetate extracts of the leaves of *M. velutina* [12]. Velutinindimers A-C (**31-33**) are dimers occurring from symmetrical and asymmetrical 2+2 cycloaddition of the isolated styrylpyrone, yangonin (**34**). The structures of velutinindimer B and C (**32** and **33**) were isolated as a mixture which were confirmed by X-ray crystallographic, ECD, and specific rotation analyses. Velutinoes B-D (**24-26**), velutinoes G-H (**29-30**), and velutinindimer A-C (**31-33**)

exhibited antimalarial activity with IC_{50} values in the range of 5.4 -10.0 μM . Moreover, velutinoes A-D (23-26) and velutinoes F-H (28-30) showed cytotoxicity against the KB, MCF7, and NCI-H187 cancer cell lines and Vero cell lines with IC_{50} values in the range of 4.0-24.1 μM [12].



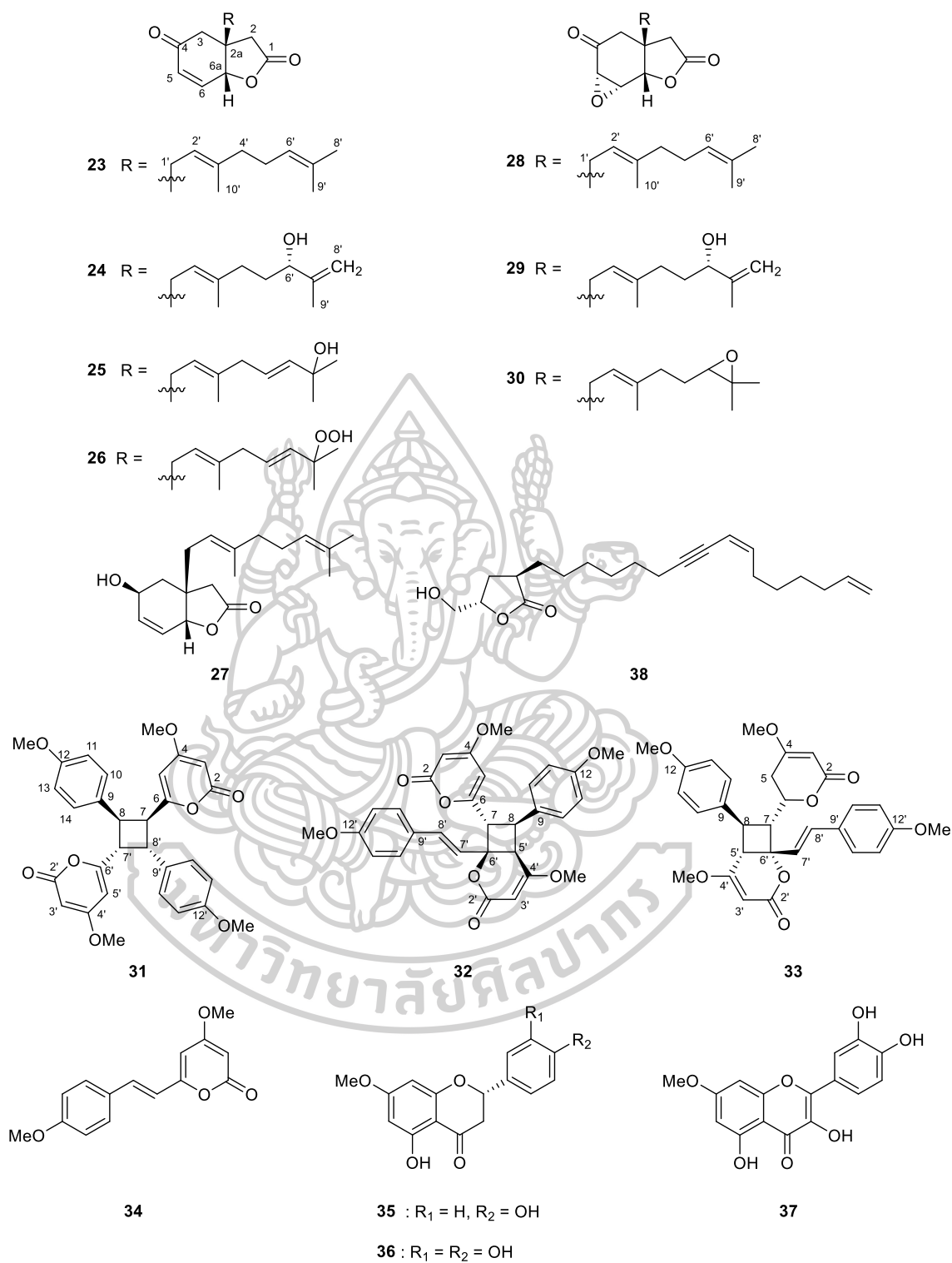


Figure 1.9 Chemical constituents isolated from the leaves of *M. velutina*.

Recently in 2019, five new rare homogentisic acid derivatives, miliusanal (**39**) and miliusanoned A-D (**40-43**) (Figure 1.10) were isolated from the hexane and ethyl acetate extracts of the fruits and flowers of *M. velutina*. In addition, the known compounds were identified by physical properties and spectroscopic data analysis, as well as two homogentisic acid derivatives, methyl-2-(1' β -geranyl-5' β -hydroxy-2'-oxocyclohex-3'-enyl)acetate (**44**) and 2-(1' β -geranyl-5' β -hydroxy-2'oxocyclohex-3'-eny) acetic acid (**45**), an isolated styrylpyrone, yanonin (**34**), two dimeric styrylpyrones, velutinindimer A (**31**) and velutinindimer B (**32**), two acetognins, cananginones A (**14**) and cananginones H (**38**), three small phenolics, 4-hydroxybenzoxazole (**46**), 4-hydroxybenzaldehyde (**47**), and isovanillin (**48**), three furfurals, 5-acetyloxymethylfurfural (**49**), 5-methoxyfurfural (**50**), and 5-hydroxymethylfurfural (**51**), and two common phytosterols, β -sitosterol (**52**) and stigmasterol (**53**) (Figure 1.10). Compounds **39** and **44** showed moderate antibacterial activities against three Gram-positive bacteria tests, including *Bacillus cereus* DMST 5040, *Staphylococcus aureus* DMST 8013, and Methicillin resistant *S. aureus*, with MICs in the range of 32-64 $\mu\text{g/mL}$. Compounds **32**, **34**, **40**, and **45** showed antibacterial against *B. cereus* with MICs in the range of 64-128 $\mu\text{g/mL}$ and **40** also showed antibacterial against *S. aureus* with an MICs of 128 $\mu\text{g/mL}$. Moreover, compounds **31**, **32**, **34**, **39**, **40**, **44**, and **45** showed antibacterial activities against Gram-negative bacteria *Pseudomonas aeruginosa* DMST 4739, with MICs in the range of 64-128 $\mu\text{g/mL}$. Compound **39** also exhibited antibacterial activity against *Salmonella enterica* serovar *Typhimurium* DMST 562 with an MICs of 128 $\mu\text{g/mL}$. It should be noted that the transformations at the terminal side chain of the geranyl group in **42** and **43** result in the lack of activities for all tests [26].

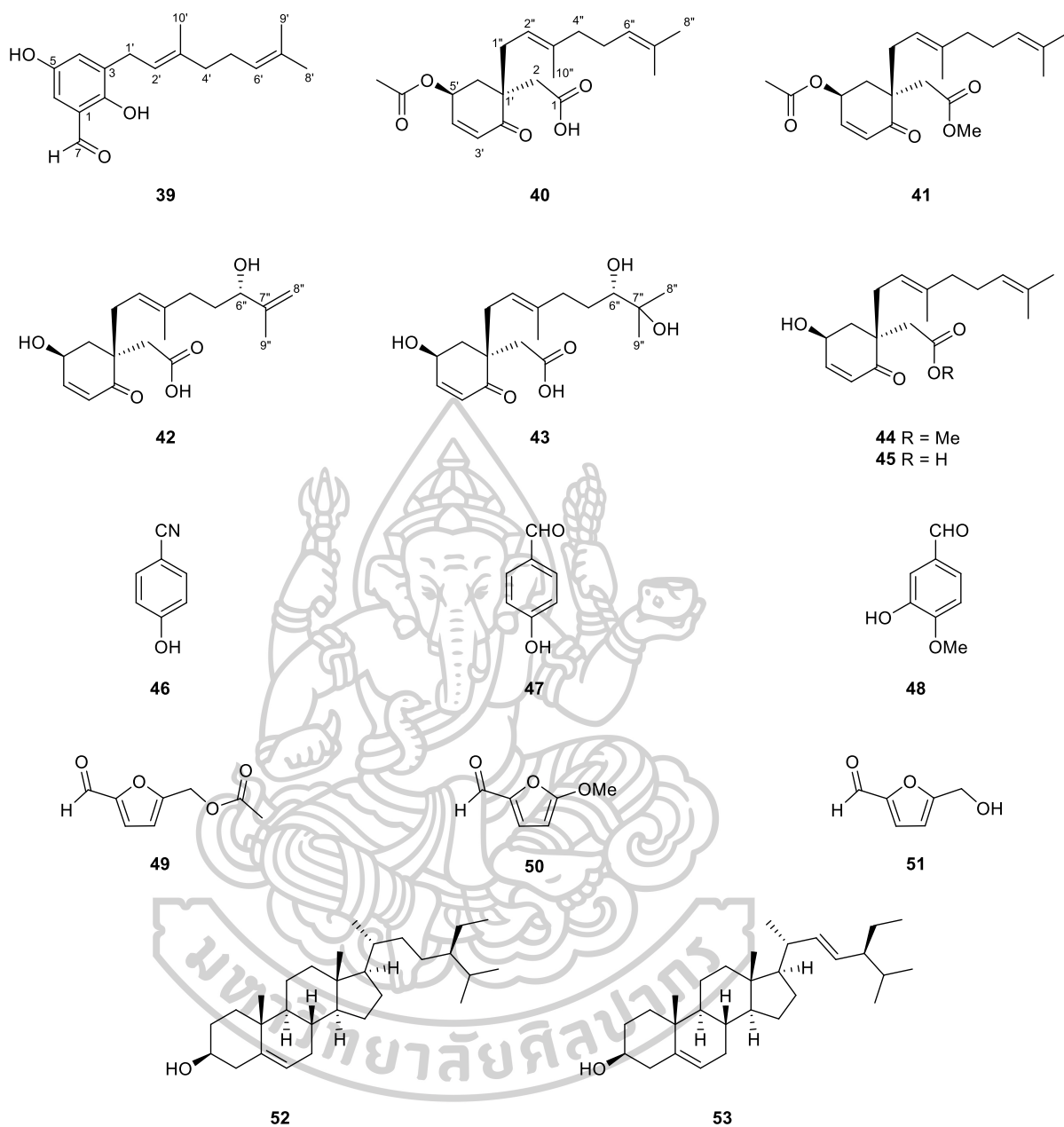


Figure 1.10 Some chemical constituents isolated from the hexane and ethyl acetate extracts of the fruits and flowers of *M. velutina*.

1.3.3 *Milium balansae* Finet & Gagnep

Phytochemical analysis of Vietnamese and Chinese *M. balansae* Finet & Gagnep from 2000 to 2015 had been found various of secondary metabolites, especially flavonoids, terpenoids, or geranylated homogentisic acid derivatives. In 2002, two styryl derivatives, 3,4-dimethoxy-6-styryl-pyran-2-one (**54**) and (2*E*,5*E*)-2-methoxy-4-oxo-6-phenyl-hexa-2,5-dienoic acid methyl ester (**55**) were isolated from the ethyl acetate extract of the leaves and branches of *M. balansae*. In addition, the known geranylated homogentisic acid derivative, miliusate (9-acetoxy-1-[(1*E*)-2,6-dimethyl-hepta-1,5-dienyl]-3,6-dioxo-2-oxa-spiro[4.5]dec-7-ene) (**56**) was also isolated. This compound has been previously reported as a chemical constituent in this species by Wu group [19] (Figure 1.11). Moreover, four known flavonoids, 4,5-hydroxy-7-methoxyflavanone (pinostrobin) (**57**), 4,5-hydroxy-7,4'-dimethoxyflavanone (**58**), 5-hydroxy-7,8-dimethoxyflavanone (**59**) and 5-hydroxy-6,7-dimethoxyflavanone (onysilin) (**60**), and two known dihydrochalcones, 2',6'-dihydroxy-3',4'-dimethoxydihydrochalcone (dihydropashanone) (**61**) and 2',6'-dihydroxy-4'-methoxydihydrochalcone (**62**) [14] were isolated.

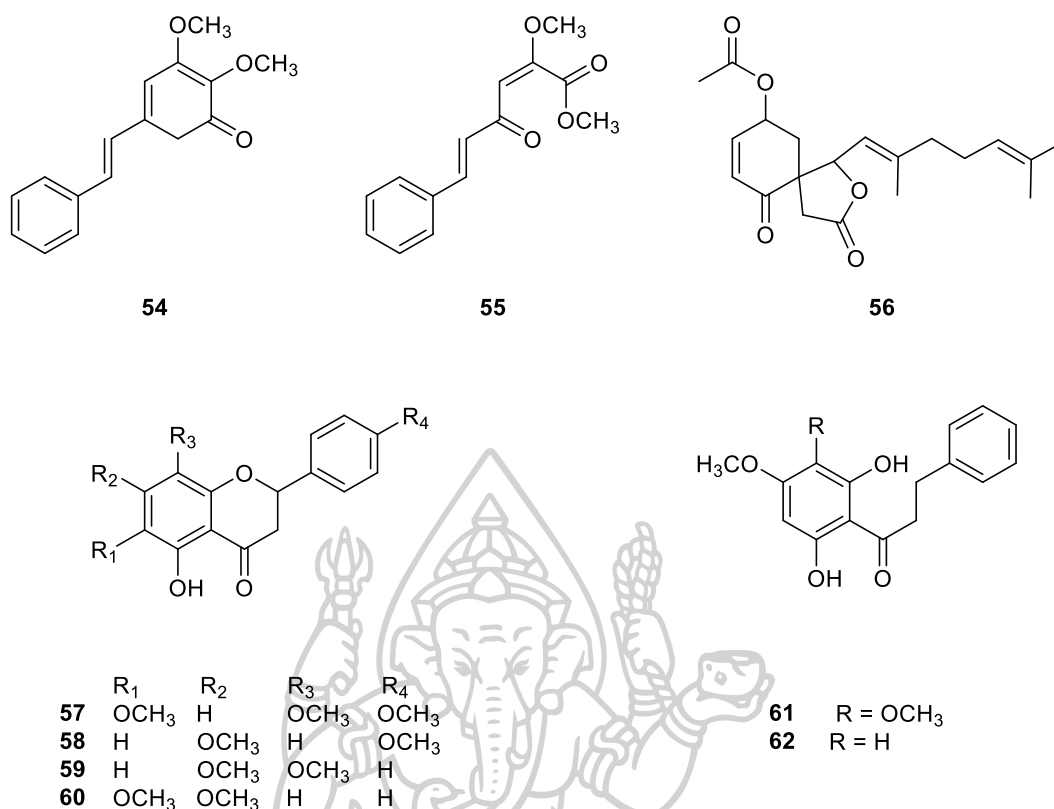


Figure 1.11 Chemical constituents isolated from the ethyl acetate extract of the leaves and branches of *M. balansae* Fin. & Gagn.

In 2004, two new homogentisic acid derivatives, (1'*E*)-(1*R**,5*R**,9*S**)-9-hydroxy-1-(2,6-dimethylhepta-1,5-dienyl)-3,6-dioxo-2-oxa-spiro[4.5]dec-7-ene (miliusol) (**63**) and 3*aS**,5*S**,7*aR**)-5-benzoyloxy-3*a*,4,5,7*a*-tetrahydro-3*H*-benzofuran-2-one (miliusolide) (**64**) were isolated from the methanol-H₂O extract of the leaves and branches of *M. balansae* Fin. & Gagn. together with two known flavanones, 4',5-dihydroxy-3,3',7-trimethoxyflavone (pachypodol) (**65**) and 4',5,6-trihydroxy-3,3',7-trimethoxyflavone (chrysosplenol C) (**66**), the symmetric ether, *bis*(2-hydroxyphenyl)-methyl ether (**67**) (Figure 1.12) and sodium benzoate. The relative configuration of miliusol (**63**) was deduced from the NOESY spectrum [11].

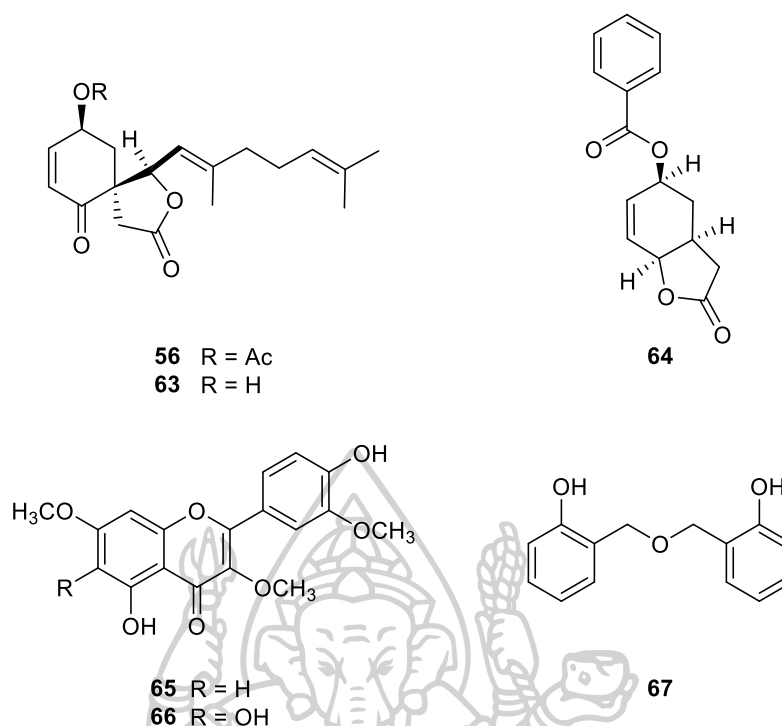


Figure 1.12 Chemical constituents isolated from the methanol-H₂O extract of the leaves and branches of *M. balansae* Fin. & Gagn.

In 2005, Huong and co-workers reported the isolation of a new flavone, 8-(2-hydroxybenzyl)-5-hydroxy-2-(4-hydroxy-3-methoxyphenyl)-3,7-dimethoxy-4*H*-chromen-4-one or 8-*C*-(*o*)-hydroxybenzylpachypodol (miliufavol) (**68**) from the methanol-H₂O extract of the leaves and branches of *M. balansae* Fin. & Gagn. together with four known flavones, 3,3',5-trihydroxy-4',7-dimethoxyflavone (ombuine) (**69**), 4',5-dihydroxy-3,3',6,7-tetramethoxyflavone (chryso splenol B) (**70**), pachypodol (**65**), and chryso splenol C (**66**) (Figure 1.13). Among them, pachypodol (**65**) has strong activities against two cancer cell lines (KB: IC₅₀ = 0.7 μg/ml and Hep-G2: IC₅₀ = 0.55 μg/ml) [27].

In 2008, Huong et al. also reported the isolation of two new bis-styryls, miliubisstyryl A (**71**) and miliubisstyryl B (**72**), and octacosanoic acid (**73**) (Figure

1.13) from the methanol-H₂O extract of the leaves and branches of *M. balansae* Fin. & Gagn. [13]. Their structures are closely related to the structure of the styryl derivative (2*E*,5*E*)-2-methoxy-4-oxo-6-phenyl-hexa-2,5-dienoic acid methyl ester (**55**), which had been isolated from this plant and reported in the previous paper [14].

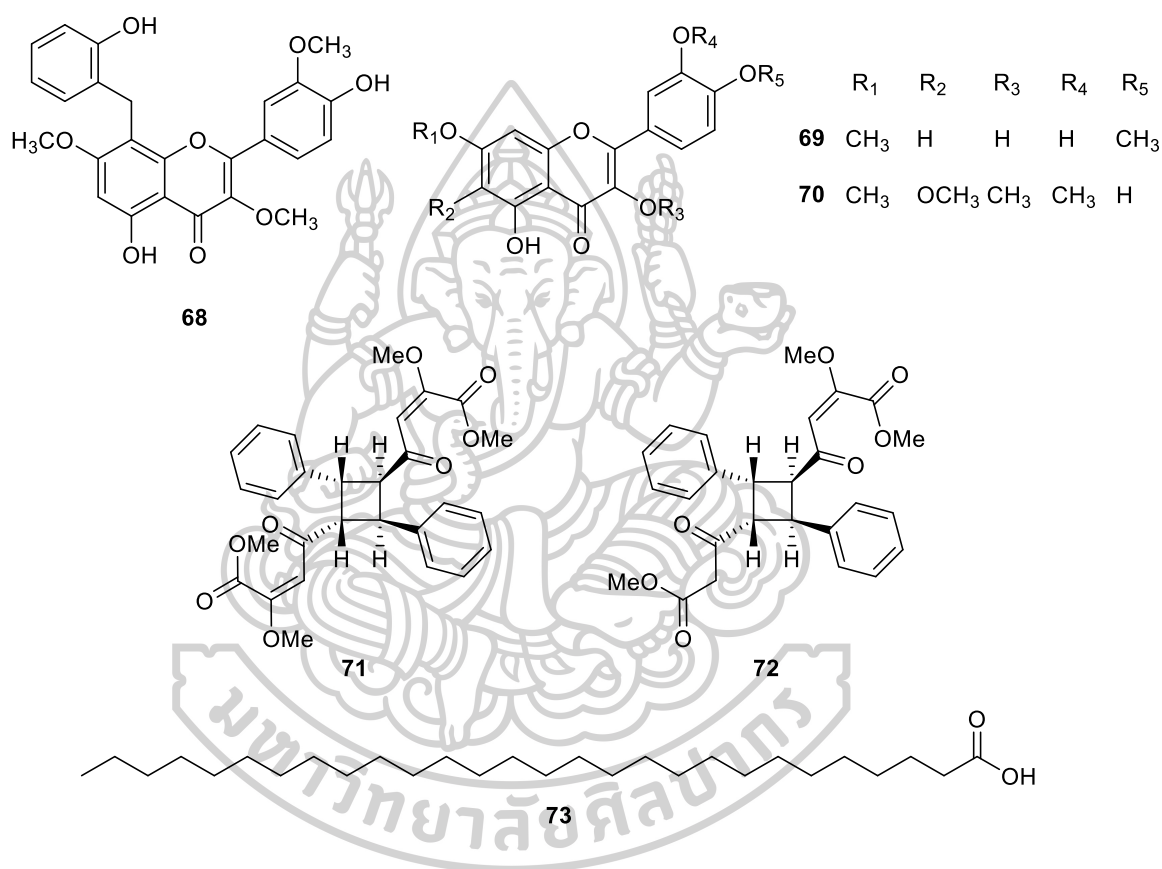
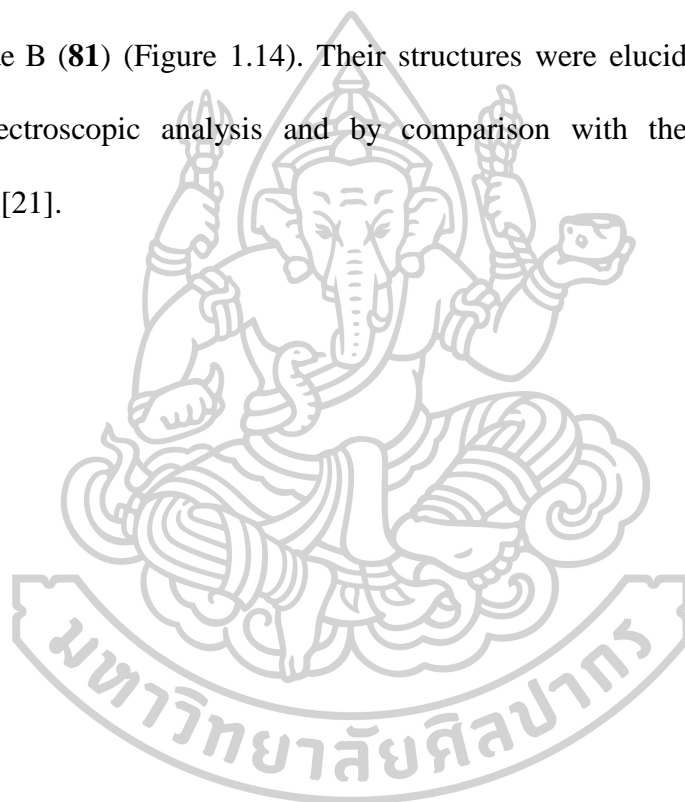


Figure 1.13 Chemical constituents isolated from the methanol-H₂O extract of the leaves and branches of *M. balansae* Fin. & Gagn.

In 2008, Lei and co-workers, the researcher group from China reported the isolation of three new glycosides together with five known glycosides from the BuOH extract of the stems of *M. balansae* Fin. & Gagn. The three new glycosides were identified as 2-hydroxy-5-(2-hydroxymethyl)phenyl *O*- α -D-apiofuranosyl-(1 \rightarrow 6)-*O*- β -

D-glucopyranoside (milioside A, **74**), 2-(4-hydroxymethyl)ethyl *O*- α -D-apiofuranosyl-(1 \rightarrow 6)-*O*- β -D-glucopyranoside (milioside B, **75**) and megastigm-7-ene-3,6,9-triol-9-*O*- α -D-apiofuranosyl-(1 \rightarrow 6)-*O*- β -D-glucopyranoside (milioside C, **76**) and the five known glycosides were 2-(4-hydroxyphenyl)ethyl- β -D-apiosyl-(1 \rightarrow 6)-*O*- β -D-glucopyranoside (osmanthuside H, **77**), cuchiloside (**78**), 1-(α -L-rhamnosyl-(1 \rightarrow 6)- β -D-glucopyranosyloxy)-3,4,5-trimethoxybenzene (**79**), D-glucopyranoside (**80**) and alangionoside B (**81**) (Figure 1.14). Their structures were elucidated on the basis of detailed spectroscopic analysis and by comparison with the spectra of related compounds [21].



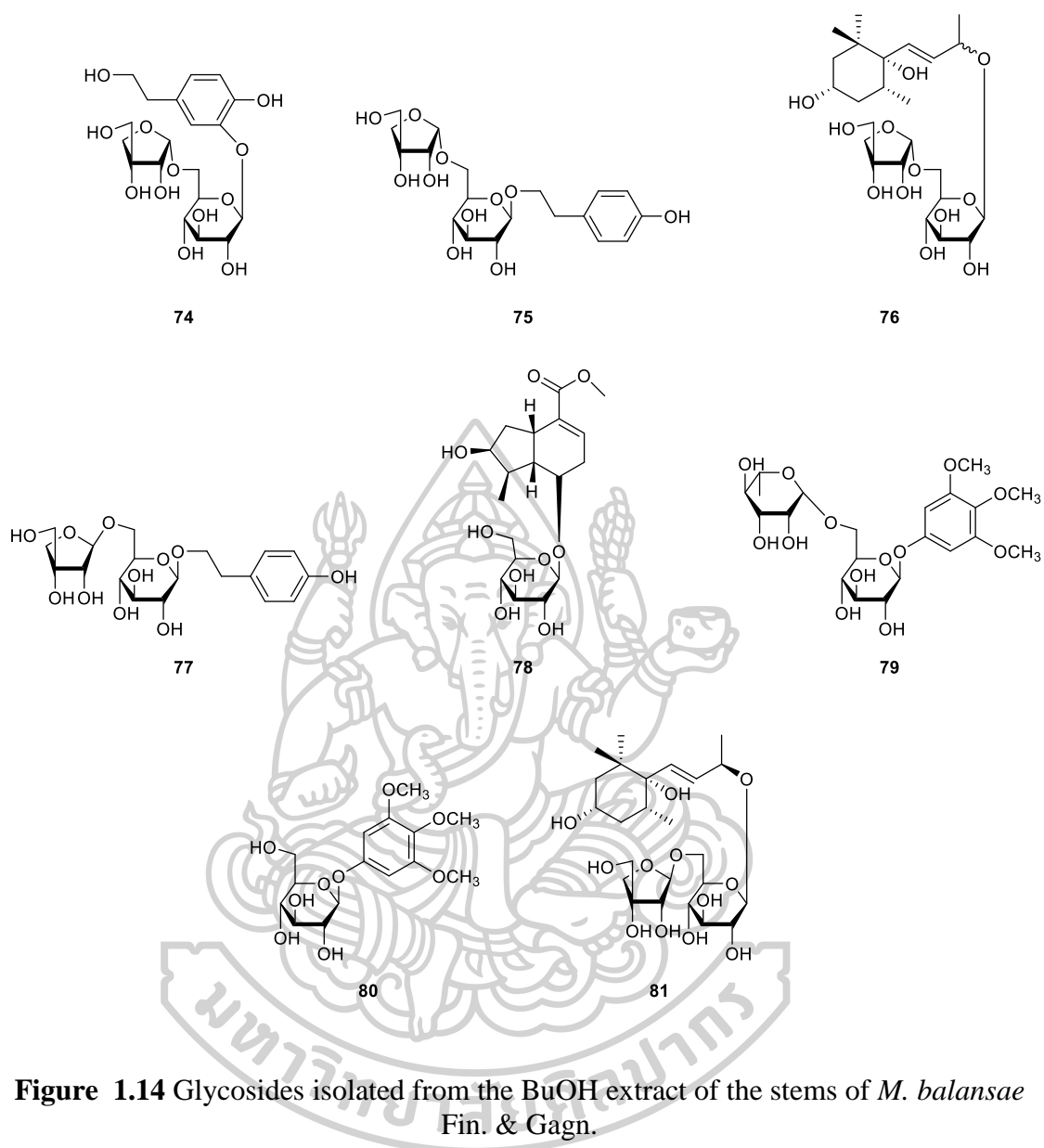


Figure 1.14 Glycosides isolated from the BuOH extract of the stems of *M. balansae* Fin. & Gagn.

In 2009, Lei and co-workers also reported the isolation of alkaloids and alkaloid pyranosides, including allantoin (**82**), coclaurine (**83**), 1-*N*-methylcoclaurine (**84**), liriodenine (**85**), adenine riboside (**86**) and uridine (**87**) (Figure 1.15). In addition, β -sitosterol (**52**), daucosterol (**88**) and two glucosides (sucrose (**89**) and glucose (**90**)) (Figure 1.15) were isolated from the stems of *M. balansae* Fin. & Gagn. [22].

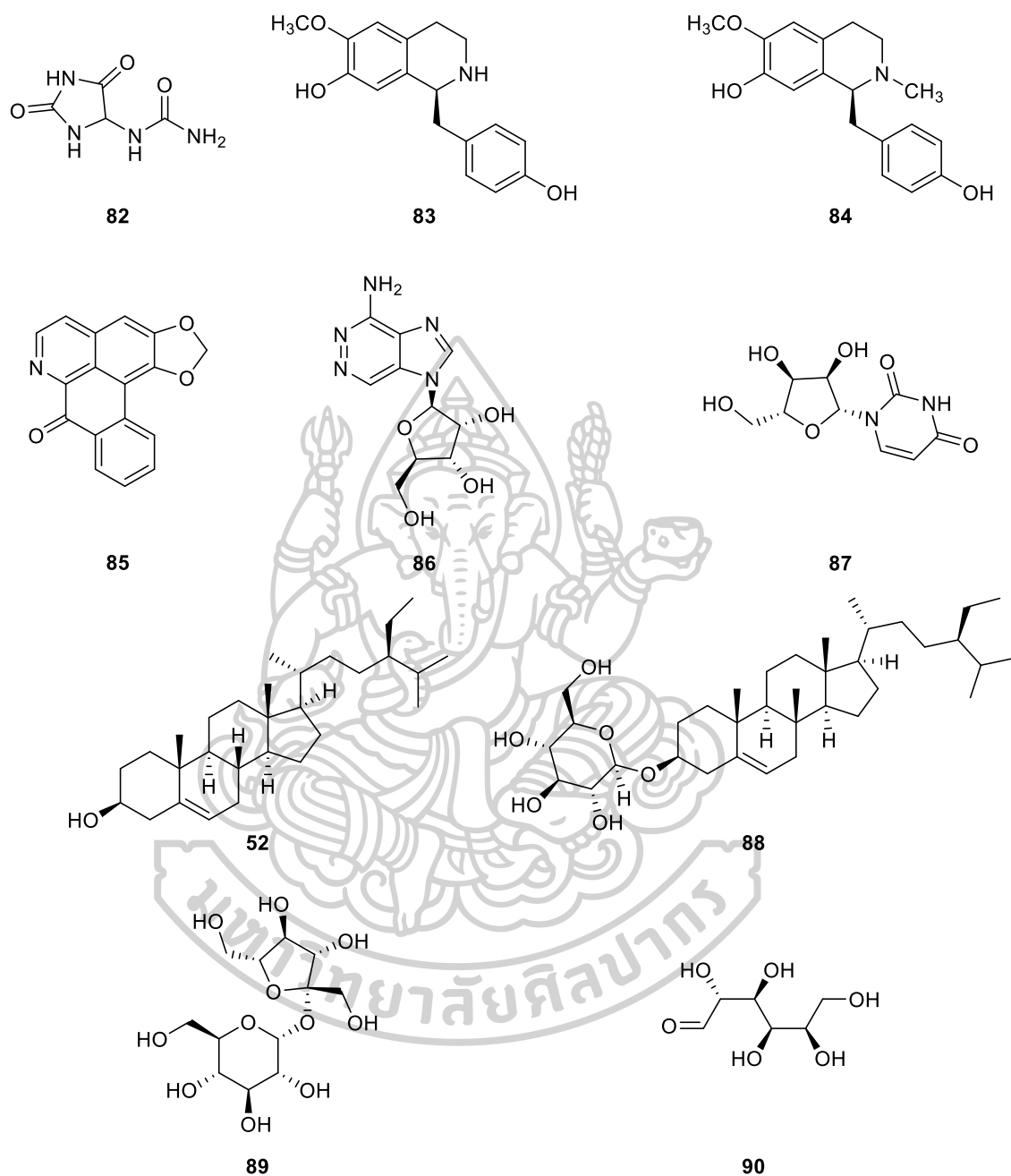


Figure 1.15 Chemical constituents isolated from the stems of *M. balansae* Fin. & Gagn.

In 2015, Tao and co-workers, the researchers from Viet Nam, isolated three new megastigmane glycosides together with fifteen known compounds from the methanol extract of the leaves of *M. balansae* Fin. & Gagn. The three new

megastigmane glycosides were elucidated as (2*R*,3*S*,5*S*,6*S*,7*E*)-3,6-epoxy-7-megastigmen-9-one-2,5-diol 5-*O*- β -D-glucopyranoside (milbaside A, **91**), (2*R*,3*S*,5*S*,6*S*,7*E*)-3,6-epoxy-7-megastigmen-9-one-2,5-diol 5-*O*- β -D-(6'-*O*- β -D-apiofuranosyl)glucopyranoside (milbaside B, **92**) and (3*S*,5*R*,6*R*,7*E*)-3,6-epoxy-7-megastigmen-9-one-5-ol 5-*O*- β -D-glucopyranoside (milbaside C, **93**). The fifteen known compounds were myrsinioside D (**94**), ampelopsioside (**95**), myrsinioside A (**96**), *threo*-1-*C*-syringylglycerol (**97**), *erythro*-1-*C*-syringylglycerol (**98**), *threo*-guaiacylglycerol (**99**), *erythro*-guaiacylglycerol (**100**), (*L*)-guaiacyl glycerol 2'-*O*- β -D-glucopyranoside (**101**), curcolide (**102**), serralactone (**103**), β -D-glucopyranosyl (*Z*)-3-hexenol (**104**), 1-(3-methylbutyryl)phloroglucinol-glucopyranoside (**105**), epicatechin (**106**), chrysosplenol C (**66**) and rutin (**107**) (Figure 1.16) (Thao et al., 2015). Their chemical structures were elucidated using extensive spectroscopic analysis, including 1D and 2D NMR, HRESIMS, and CD analysis, as well as comparison with previously reported data. Compounds **91**, **92**, **93**, **101**, and **104** exhibited potently inhibitory activities on LPS-induced production of inflammatory mediator NO in RAW 264.7 cells with inhibition values of 98.5 \pm 1.6%, 90.9 \pm 7.8%, 84.8 \pm 3.5%, 91.5 \pm 8.7% and 91.8 \pm 2.7% respectively, relatively compared to the positive control, sulfuretin (81.3 \pm 4.9% at 20.0 μ M). In addition, myrsinioside D (**94**) and epicatechin (**106**) showed moderate or weak activity at 10.0 and 20.0 μ M, but strong inhibitory effects at 40.0 μ M (with inhibition values of 82.0 \pm 5.9% and 91.8 \pm 5.6%, respectively) [20].

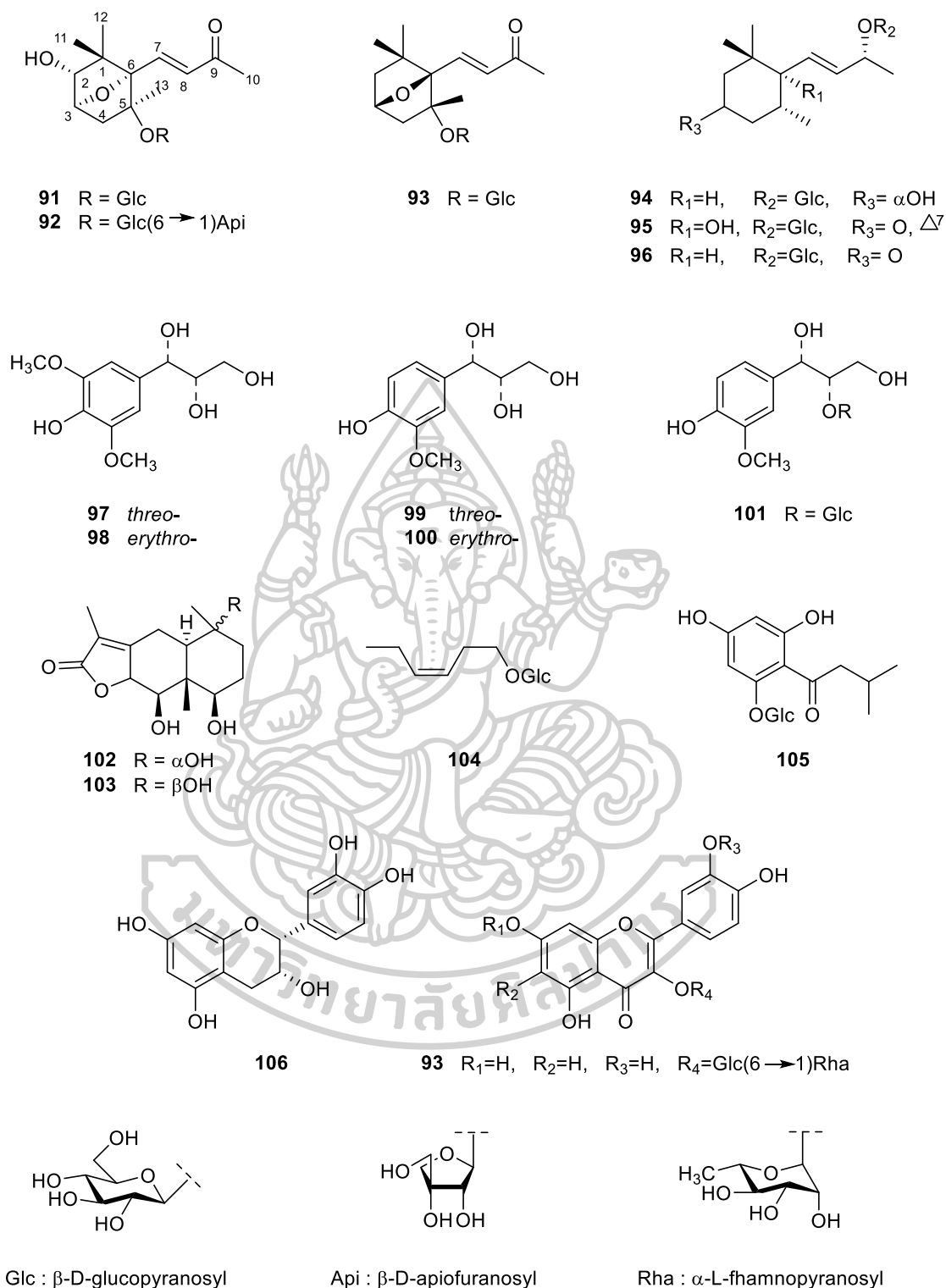


Figure 1.16 Chemical constituents isolated from the methanol extract of the leaves of *M. balansae* Fin. & Gagn.

1.3.4 *Milusa sinensis* Finet & Gagnep

In 2006, phytochemical investigation of the CH₂Cl₂ extract from the leaves, twig and flowers of *M. sinensis* Fin. & Gagn by Zhang and co-workers, the researcher group from Viet Nam, led to the isolation of miliusate (**56**) and miliusol (**63**) and 20 new miliusanes, miliusanes I-XX (**108-127**) (Figure 1.17-1.19). All of these compounds belong to a C18 carbon skeleton, which a new class of potential anticancer lead molecule, had designated as miliusane [9]. The two known compounds, miliusate (**56**) and miliusol (**63**), were reported previously from *M. balansae* Fin. & Gagn. [11, 14].

The absolute stereochemistry of miliusanes was determined using Mosher's method, various diagnostic chemical reactions and the X-ray crystallographic analysis. Distribution of the positive and negative δ values of the MTPA ester established the chiral centers of both C-1 and C-1' in the *R*-configuration. Successful chemical conversions of miliusol (**63**) to miliusate (**56**) and (+)-milusane VIII (**115**), (+)-milusane IX (**116**) to miliusol (**63**), (+)-milusane I (**108**) to (+)-milusane VI (**113**) and (+)-milusane II (**109**) to (+)-milusane VII (**114**) confirmed that compounds **56**, **109** and **113-116** occupy the same chiral centers at C-1 and C-1'. Besides, the double bonds at $\Delta^{2,3'}$ of the miliusanes were established as *E*-configured due to the observed ROE correlations between H-1' and H-9', between H-7 β and H-2' and between H-2' and H-4' in the ROESY spectra.

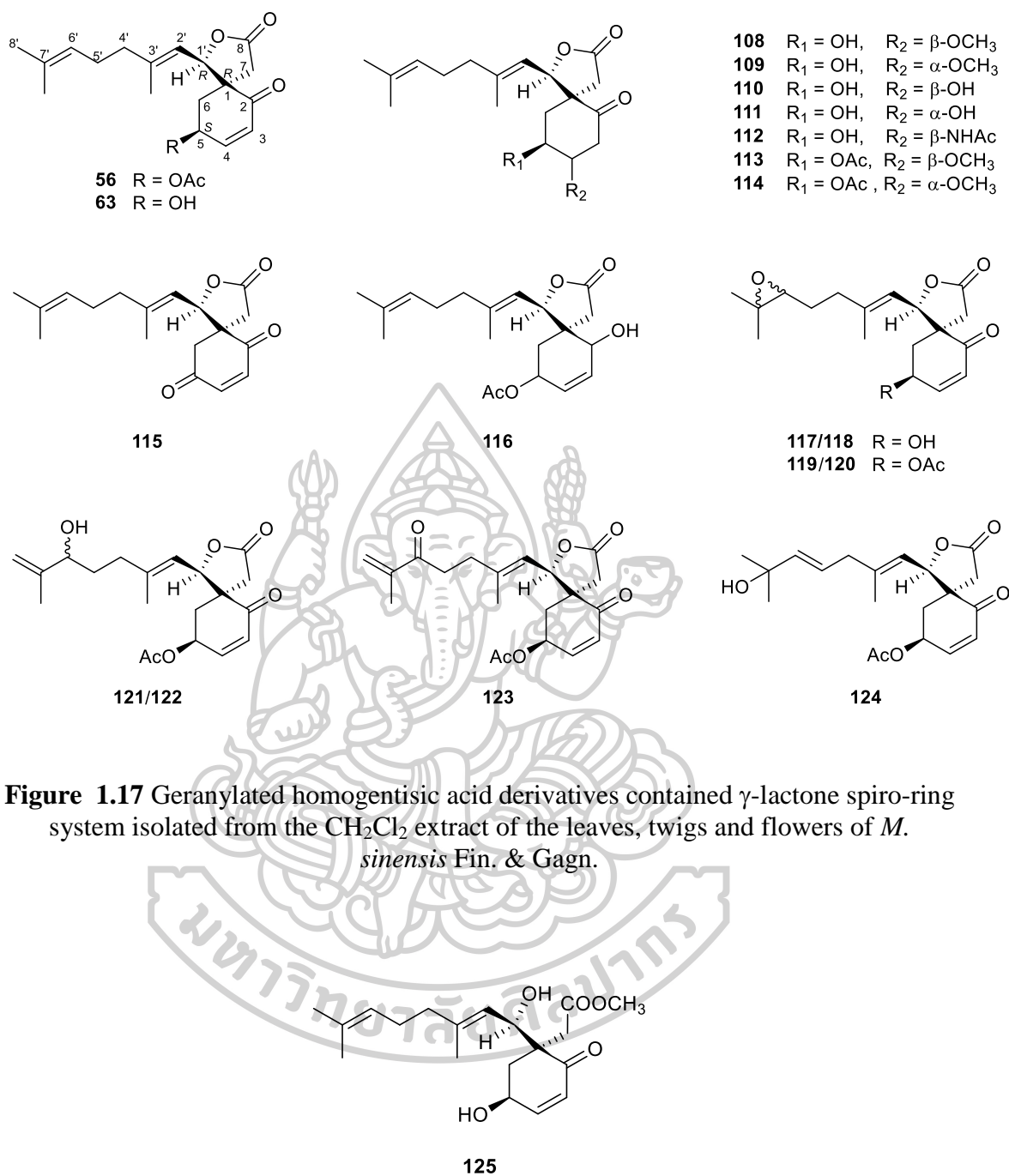


Figure 1.17 Geranylated homogentisic acid derivatives contained γ -lactone spiro-ring system isolated from the CH₂Cl₂ extract of the leaves, twigs and flowers of *M. sinensis* Fin. & Gagn.

Figure 1.18 Geranylated homogentisic acid derivatives contained the opening of γ -lactone spiro-ring system isolated from the CH₂Cl₂ extract of the leaves, twigs and flowers of *M. sinensis* Fin. & Gagn.

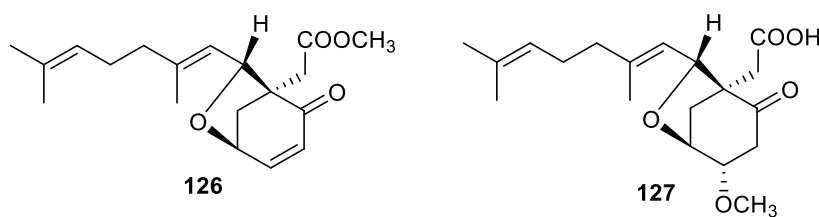


Figure 1.19 Geranylated homogentisic acid derivatives contained tetrahydrofuran ring system.

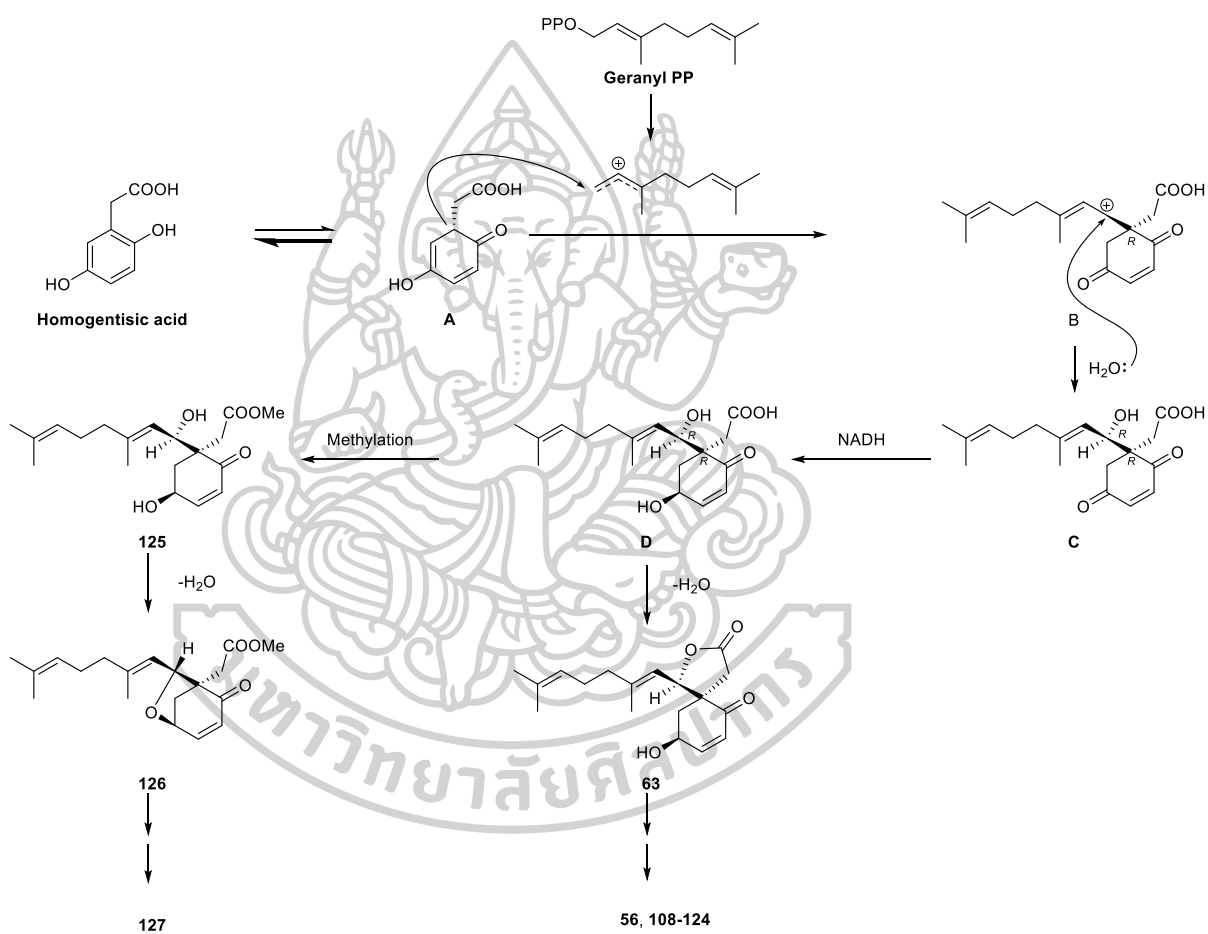


Figure 1.20 Biogenetic pathways for miliusanes.

The miliusanes belong to a novel class of natural product comprising of 18 carbons in their skeletons, which were classified as geranylated homogentisic acid. A plausible biogenetic pathway for miliusanes was shown in figure 1.20. In the first

step, the precursor, homogentisic acid combined with geranyl diphosphate (geranyl PP) by electrophilic alkylation reaction to generate an intermediate cation (**B**), which would be combined with water to form compound **C**. The C-5 carbonyl group in compound **C** would be reduced to a hydroxyl group to afford compound **D**. Compound **D** could then be transformed to the γ -lactone spiro-ring system, miliusol (**63**) by the formation of a γ -lactone group between the 1'-OH group and the 7-COOH group. Compounds **108-114** could then be produced from either **63** or its acetylated analog (**56**) through the Micheal type nucleophilic addition of a hydroxyl group, or an acetylamine group to an α,β -unsaturated ketone. The 5-OH of milusol (**63**) could then be oxidized to afford **115**, while the C-2 carbonyl carbon of miliusane (**56**) could then be reduced to provide **116**. Besides, the $\Delta^{6',7'}$ double bond in the side chain of **63** or **56** would then be oxidized to afford their corresponding analogs (**117-124**). Cyclization between the 5-OH and the 1'-OH in **125** through the loss of a H₂O molecule will then result in the tetrahydrofuran ring system, such as **126**, whose dimethyl isomer would produce **127** by the Michael nucleophilic addition of a methoxy group to an α,β -unsaturated ketone [9].

In 2011, Thuy and coworkers reported the isolation of the hexane and the ethyl acetate extracts of the leaves and branches of *M. sinensis*. A new dihydrochalcone, 4',6'-dihydroxy-2',3',4'-trimethoxydihydrochalcone (**128**), a dihydrochalcone, dihydropashanone (**61**), a chalcone, pashanone (**129**), five flavonoids, pinostrobin (**57**), 5-hydroxy-7,4'-dimethoxyflavanone (**130**), 5-hydroxy-6,7,-dimethoxyflavanone (**60**), 5-hydroxy-7,8-dimethoxyflavanone (**59**) and 3,5-dihydroxy-7,3',4'-trimethoxyflavone (**131**), an alkaloid, liriodenine (**4**), a triterpene,

24-methylcycloartane-3 β ,21-diol (**132**) (Figure 1.21) were isolated. Among these isolated compounds, liriodenine (**4**) had a good activity against four human cancer cell lines, including MCF-7, KB, Hep-G2 and LU cancer cell lines with IC₅₀ values in the range of 4.0-24.1 μ M [28].

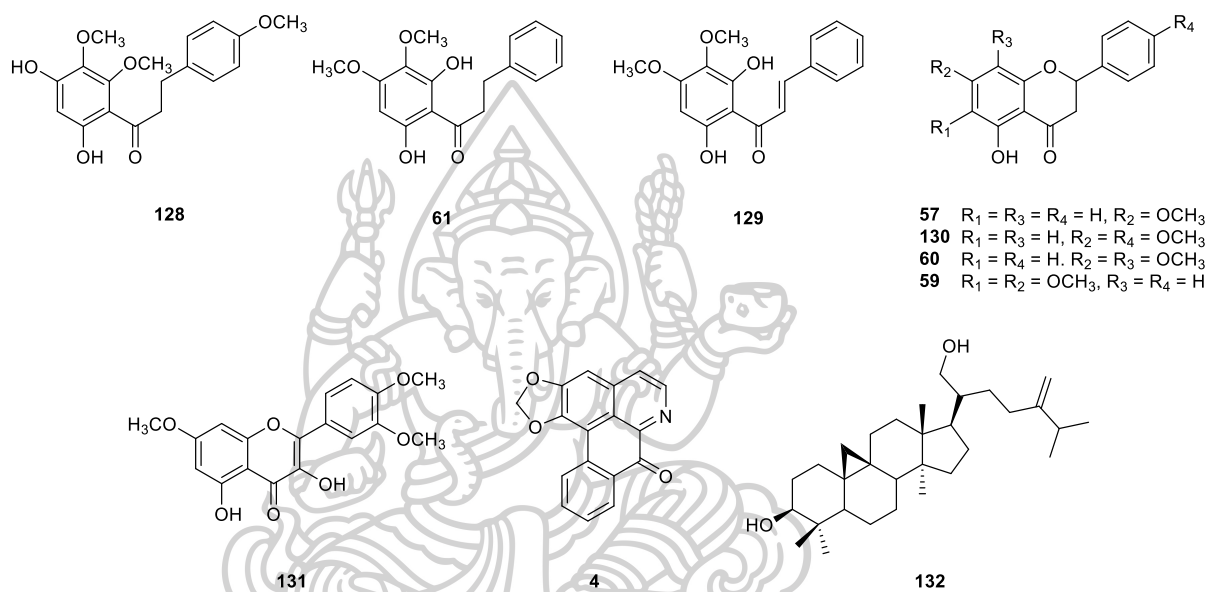


Figure 1.21 Chemical constituents isolated from the methanol extract of the leaves of *M. sinensis*.

1.3.5 *Milusa mollis* Pierre.

In 2010, Sawasdee and co-workers, a researcher group from Thailand, investigated the MeOH extract of the twigs of *M. mollis* Pierre. They reported the isolation of two new neolignans, including (2*S*,3*S*)-2,3-dihydro-2-(4-methoxyphenyl)-3-methyl-5-[1(*E*)-propenyl] benzofuran (**133**) and (7*S*,8*S*)-*threo*- Δ^8 -4-methoxyneolignan (**134**), and a new glycosidic phenylpropanoid, tyrosol-1-*O*- β -xylopyranosyl-(1 \rightarrow 6)-*O*- β -glucopyranoside (**135**). In addition, seven known compounds, including two neolignans, (2*R*,3*R*)-2,3-dihydro-2-(4-hydroxy-3-

methoxyphenyl)-3-methyl-5-(*E*)-propenylbenzofuran (**136**) and conocarpan (**137**), a favonol, epicatechin (**106**), an oxoaporphine, liriodenine (**4**), two aporphine alkaloids, asimilobine (**138**) and (-)-norushinsunine (**139**) and a glycosidic phenylpropanoid, icarisside D₂ (**140**) (Figure 1.22) were also isolated [17].

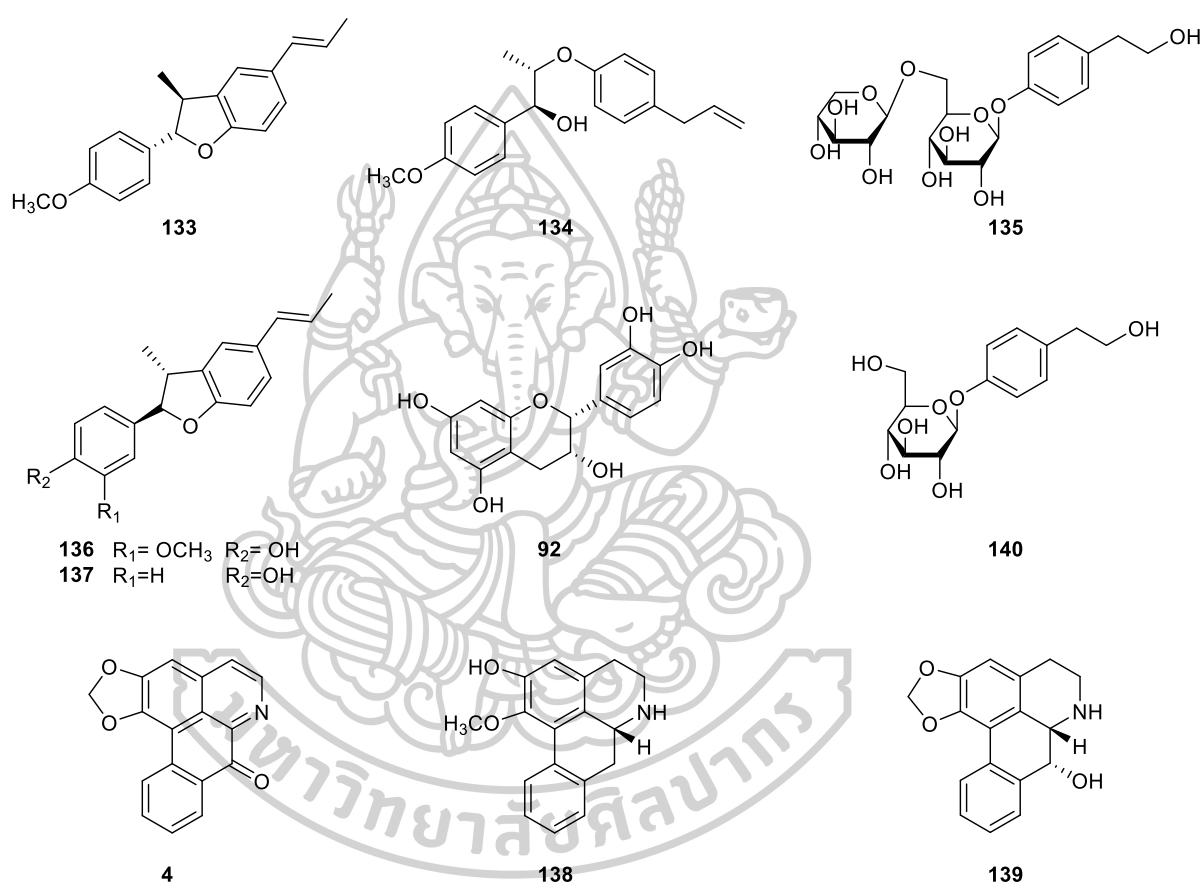


Figure 1.22 Chemical constituents isolated from the MeOH extract of the twigs of *M. mollis* Pierre in 2010.

Sawasdee and co-workers (2013) also reported the isolation of six new neolignans (**141-146**) together with a known neolignan, decurrenal (**147**) (Figure 1.23) from the methanol extract of the leaves of *M. mollis* Pierre. The five new neolignans contained a dihydrobenzofuran skeleton, including (2*S*,3*S*)-5-allyl-2,3-

dihydro-2-(4-methoxyphenyl)-3-methylbenzofuran (4'-*O*-methylmiliumollin, **141**), (2*R*,3*R*)-5-allyl-2,3-dihydro-2-(4-hydroxy-3-methoxyphenyl)-3-methylbenzofuran (3'-methoxymiliumolin, **142**), (2*R*,3*R*)-5-allyl-2,3-dihydro-2-(4-hydroxyphenyl)-3-methylbenzofuran (miliumollin, **143**), 7-methoxymiliumollin (**144**) and (2*R*,3*R*)-2,3-dihydro-2-(4-hydroxyphenyl)-3-methyl-5-(2-oxopropyl)-benzofuran (miliumollinone, **145**), while another a new 8-*O*-4'-neolignan was (7*R*,8*R*)-*threo*- Δ^8 -7-acetoxy-4-methoxy-8-*O*-4'-neolignan (miliusamolliin, **146**). Due to the limited amounts of the isolates, only neolignans **142**, **143**, **145** and **147** were subjected to further biological activity evaluation. All of these compounds exhibited weak cytotoxicity against KB, MCF and NCI-H187 human cancer cells with IC₅₀ values in the range of 27.2-137.4 μ M, 71.9-169.1 μ M and 61.3-115.9 μ M, respectively. Compound **145** showed weak activity against herpes simplex virus types 1 and 2 with IC₅₀ values of 155.3 and 222.0 μ M, respectively (positive control acyclovir: IC₅₀ 1.9 and 2.1 μ M, respectively), whereas the remaining compounds were inactive at 100 μ g/mL.

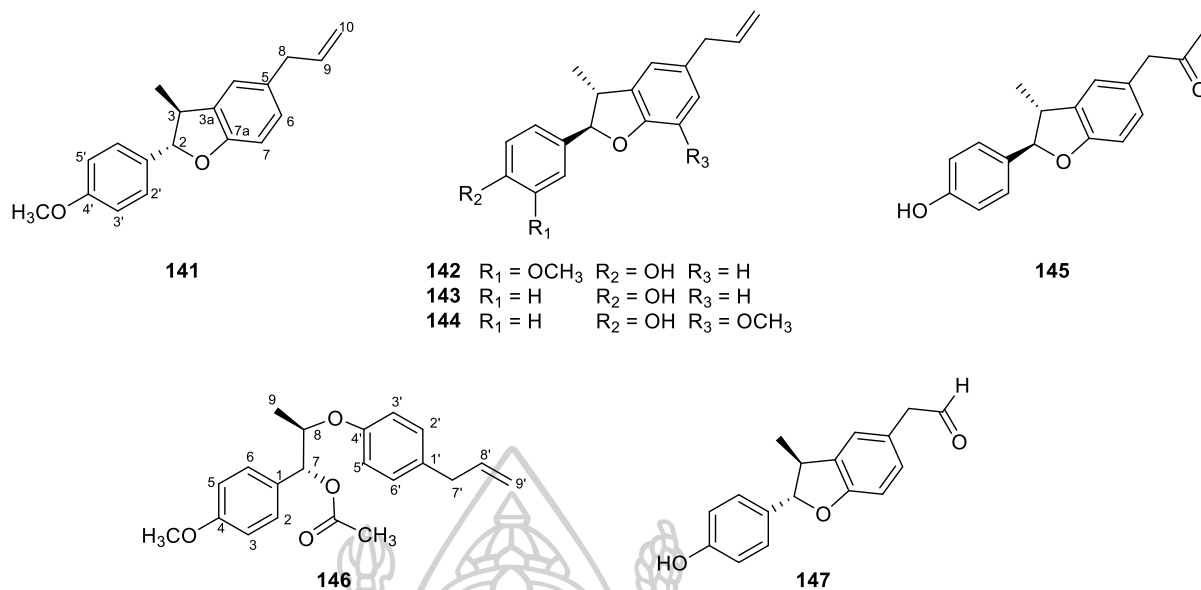


Figure 1.23 Chemical constituents isolated from the MeOH extract of the leaves of *M. mollis* Pierre in 2013.

1.3.6 *Milusa fragrans* Chaowasku & Kessler sp. nov.

In 2013, Sawasdee and co-workers reported of the isolation of thirteen neolignans (**148-154**, **156-161**), three lignans (**155**, **162-163**), and a flavonoid (**106**) (Figure 1.24) from the MeOH extract from the leaves and stems *M. fragrans* Chaowasku and Kessler. Among these isolates, eight were new compounds, which included five 7.O.3',8.O.4'-neolignans, ((7*S*,8*R*)- Δ^8 -3-hydroxy-4,5,5'-trimethoxy-7.O.3',8.O.4'-neolignan (**148**), (7*S*,8*R*)- Δ^8 -4-hydroxy-3,5,5'-trimethoxy-7.O.3',8.O.4'-neolignan (**149**), (7*R*,8*R*)- Δ^8 -4-hydroxy-3,5'-dimethoxy-7.O.3',8.O.4'-neolignan (**150**), (7*R*,8*R*)- Δ^8 -3,4,5'-trimethoxy-7.O.3',8.O.4'-neolignan (**151**) and (7*S*,8*S*)-benzodioxane-type (**152**), two 8.O.4'-neolignans, Δ^7 -9'-hydroxy-3,4,3'5'-tetramethoxy-8.O.4'-neolignan (**153**) and Δ^8 -4-hydroxy-3,5'-dimethoxy-8.O.4'-neolignan (**154**) and one tetrahydrofuran lignin, (+)-3-hydroxyveraguensin (**155**). The

remaining nine known compounds were two 7.O.3',8.O.4'-neolignans, eusiderin C (**156**) and eusiderin D (**157**), three 8.O.4'-neolignans, 2-(4-allyl-2,6-dimethoxyphenoxy)-1-(3,4-dimethylphenoxy)propane (**158**), virolongin B (**159**) and (7*S*,8*R*)-7-hydroxy-3,4,3'-trimethoxy- $\Delta^{1,3,5,1',3',5',8'}$ -8.O.4'-neolignan (**160**), a dihydrobenzofuran neolignan, licarin A (**161**), two tetrahydrofuran lignans, veraguensin (**162**) and (7*S*,8*S*,7'*R*,8'*S*)-3,4,5,3',4'-pentamethoxy-7,7'-epoxylignan (**163**) and a flavonoid, (-)-epicatechin (**92**). Compounds **149** and **161** showed recognizable anti-herpetic activity whereas compounds **148**, **149**, **150**, **157**, **160** and **161** possessed appreciable cytotoxicity against KB, MCF-7, and NCI-H187 cancer cells (Table 1.1) [15].

Table 1.1 Antiherpetic activity and cytotoxicity of compounds isolated from the leaves and the stems of *M. fragrans* Chaowasku & Kessler sp. nov.

compounds	Antiherpetic activity (IC ₅₀ , µg/ml)		Cytotoxicity (IC ₅₀ , µg/ml)		
	HSV-1	HSV-2	KB	MCF-7	NCI-H187
148	NA	NA	20.3	22.1	17.1
149	62.5	87.5	17.9	28.4	15.9
150	NA	NA	18.4	22.6	20.6
151	NA	NA	23.8	24.4	16.7
160	NA	NA	14.4	13.0	12.7
161	66.7	87.5	12.9	45.6	16.7
acyclovir	0.6	0.6	-	-	-
tamoxifen	-	-	-	9.9	-
doxorubicin	-	-	0.5	8.6	0.2
ellipticine	-	-	0.8	-	0.4

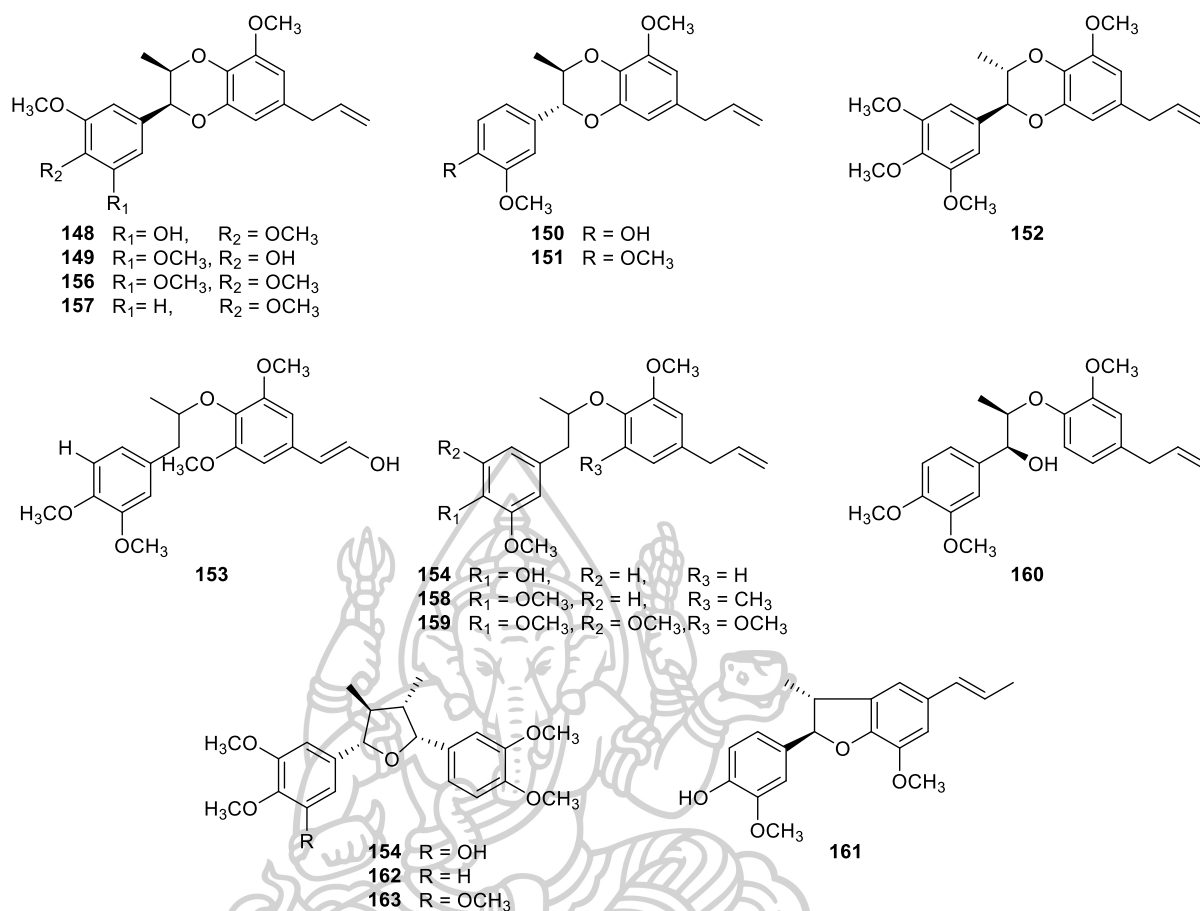


Figure 1.24 Lignans and neolignans isolated from the MeOH extract of the leaves and stems *M. fragrans* Chaowasku & Kessler sp. nov.

1.3.7 *Miliuma umpangensis* Chaowasku & Kessler sp. nov.

In 2014, Sawasdee and co-workers reported the isolation of geranylated homogentisic acids and flavonols from the MeOH extract of the leaves of *M. umpangensis* Chaowasku and Kessler sp. nov. These geranylated homogentisic acids were identified as (+)-miliusate (**56**), (+)-miliusol (**63**), (+)-miliusane I (**108**) and methyl 2-(1 β -geranyl-5 β -hydroxy-2'-oxocyclohex-3'-enyl) acetate (**164**) while, flavonols were identified as 7,3',4'-trimethylquercetin (**165**), ayanin (**166**), ombuin (**167**), quercetin 3,7-dimethyl ether (**168**), chrysosplenol-D (**169**) and rutin (**107**) (Figure 1.25). Compounds **168** and **169** showed weak anti-viral activity against HSV-

1 (IC₅₀ 94.7 and 86.8 μM, respectively) and HSV-2 (IC₅₀ 189.5 and 86.7 μM, respectively) comparing with the positive control acyclovir (IC₅₀ 1.9 and 2.1 μM, respectively) [10].

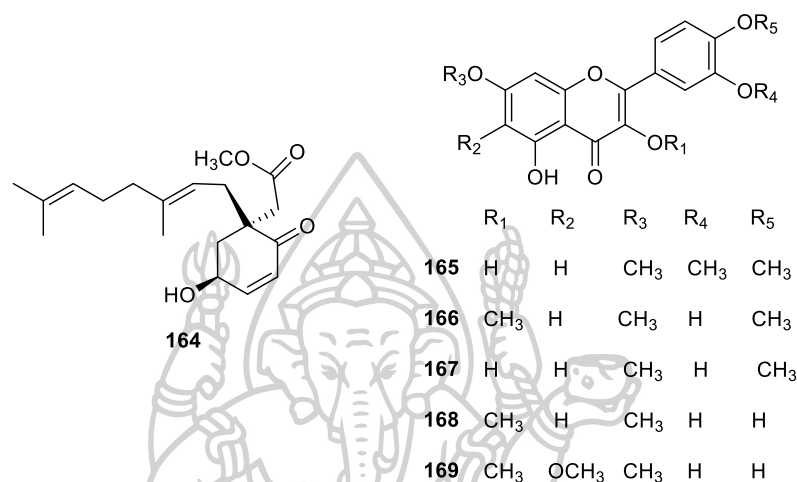


Figure 1.25 Geranylated homogentisic acid and flavonols isolated from the MeOH extract of the leaves of *M. umpangensis* Chaowasku and Kessler sp. nov.

1.3.8 *Milusa cuneata* Craib

In 2016, Promchai and co-workers reported the isolation of the acetone extract of the leaves and twigs of *M. cuneata* Craib. Separation of the acetone extract of the leaves provided five new alkaloids, miliusacunines A-E (**170-174**) along with five known compounds including, three flavones, 5-hydroxy-3,7-dimethoxy-3',4'-methylenedioxyflavone (**175**), pachypodol (**65**) and 4'-hydroxy-3,5,7,3'-tetramethoxyflavone (**176**), a geranylated homogentisic acid, miliusol (**63**, Figure 1.12) and a lignan, (+)-syringaresinol (**177**). The acetone extract of the twigs afforded six known substances, including three flavones, 5-hydroxy-3,7-dimethoxy-3',4'-methylenedioxyflavone (**175**), pachypodol (**65**), and chrysopenetin (**178**) and three

amides, *N-trans*-feruloyltyramine (**179**), *N-trans*-caffeoyltyramine (**180**), and *N-trans*-coumaroyltyramine (**181**) (Figure 1.26). Compound **63** exhibited cytotoxic activity against the KB cell line with an IC_{50} value of $10.2 \pm 0.1 \mu\text{M}$ and showed antimalarial activity against *P. falciparum* both TM4 and K1 (multi-drug-resistant strains) strains with IC_{50} values of 11.1 ± 2.0 and $9.1 \pm 1.0 \mu\text{M}$, respectively. However, this compound was relatively cytotoxic, with an IC_{50} value of $13.5 \pm 0.5 \mu\text{M}$ against the normal Vero cells. Compounds **170-174**, **176** and **178-180** displayed weaker antimalarial activity than compound **63**, with IC_{50} values ranging from 19.3-41.4 and 10.8-54.9 μM against the TM4 and K1 strains, respectively [6].

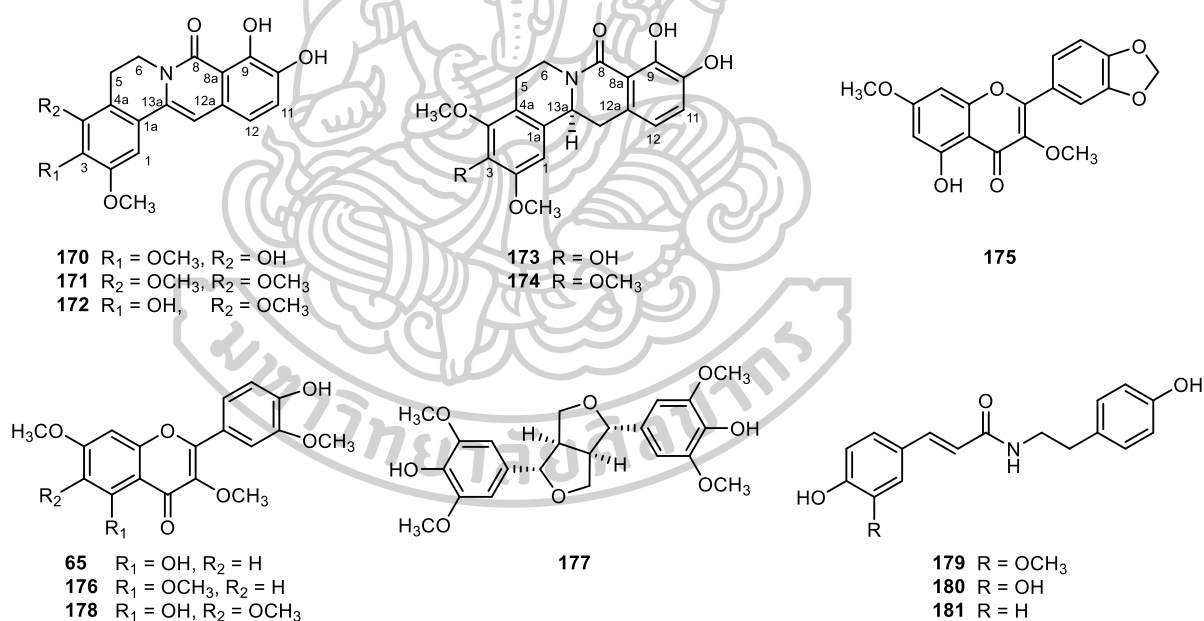
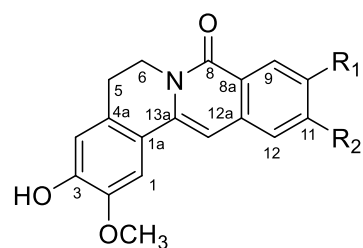


Figure 1.26 Chemical constituents isolated from the acetone extracts of leaves and the twigs of *M. cuneata*.

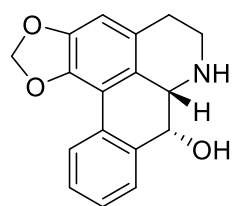
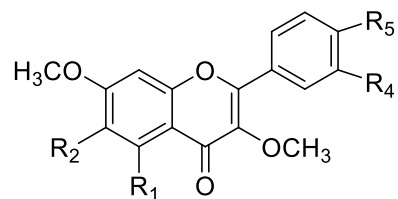
1.3.9 *Milusa thorelii* Finet & Gagnep.

In 2018, Promchai and co-workers reported phytochemical investigation of the acetone extract of the combined stems, roots and leaves of *M. thorelii* Finet & Gagnep., an analgesic and an aphrodisiac traditional medicine. Twenty five chemical constituents were isolated, including 2 new dihydrooxoprotoberberine alkaloids, miliusathorines A (**182**) and miliusathorines B (**183**), a new flavone, miliusathorone (**184**) (Figure 1.27) along with a known aporphine alkaloid, (-)-norushisunine (**185**), two known amines, *N-trans*-feruloyltyramine (**186**), *N-trans*-caffeoyltyramine (**187**) and nineteen known flavones, quercetagenin-3,5,7-trimethyl ether (**188**), 5,3',4'-trihydroxy-3,7-dimethoxyflavone (**189**), quercetagenin-3,5,7,3'-tetramethyl ether (**190**), 6,4'-dihydroxy-3,5,7-trimethoxyflavone (**191**), retusin (**192**), 5-hydroxy-3,6,7,4'-tetramethoxyflavone (**193**), dimethylmikanin (**194**), 3,5,7,3',4'-pentamethoxyflavone (**195**), 3-*O*-methylkaemferol (**196**), quercetin-3-*O*-methyl ether (**197**), quercetin-3,5,3'-trimethyl ether (**198**), 4'-hydroxy-3,5,6,7-tetramethoxyflavone (**199**), 5-hydroxy-3,7-dimethoxy-3',4'-methylene-dioxyflavone (**200**), melisimplexin (**201**), melisimplin (**202**), isokanugin (**203**), pachypodol (**65**), 3,5,6,7,3',4'-hexamethoxyflavone (**204**) and artemetin (**205**) (Figure 1.27) [5]. The isolated compounds were evaluated for their acetylcholinesterase (AChE) inhibitory activities at 100 μ M. The aporphine alkaloid **185** had the best exhibiting result with $50.17 \pm 0.07\%$ inhibition, while the oxoprotoberberines **182** and **183** were less active ($40.70 \pm 0.70\%$ and 27.93% enzyme inhibition, respectively). The flavones **184** and **188-204** showed AChE inhibition percentages ranging from <10 to $38.68 \pm 1.54\%$.

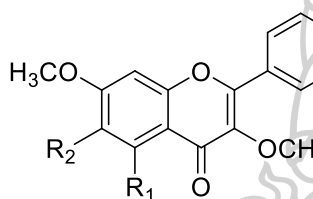


182 R₁ = OCH₃, R₂ = OH

183 R₂ = OH, R₂ = OCH₃



185



184 R₁ = OCH₃, R₂ = OH

200 R₁ = OH, R₂ = H

201 R₁ = OCH₃, R₂ = OCH₃

202 R₁ = OH, R₂ = OCH₃

203 R₁ = OCH₃, R₂ = H

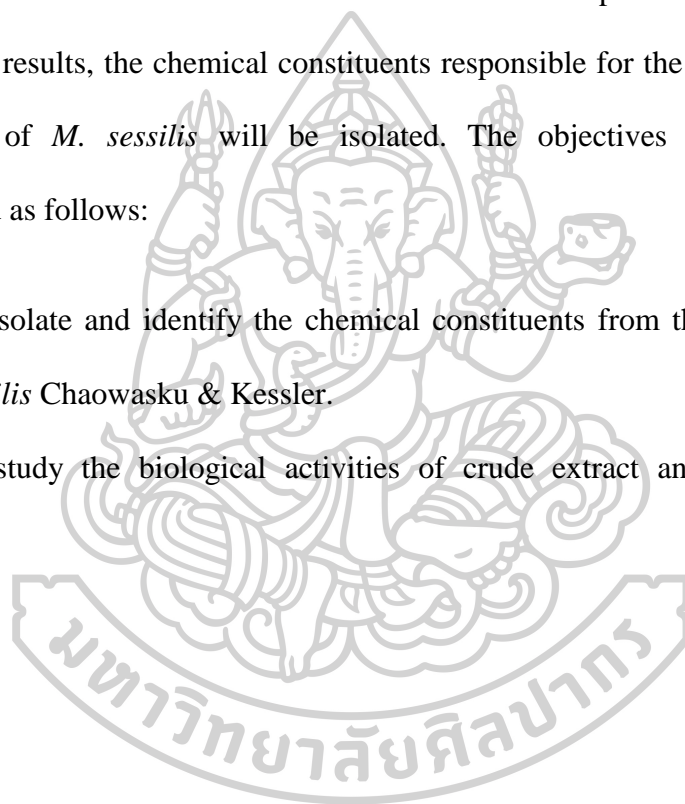
	R ₁	R ₂	R ₃	R ₄	R ₅
188	OCH ₃	OH	OCH ₃	OH	OH
189	OH	H	OCH ₃	OH	OH
190	OCH ₃	OH	OCH ₃	OCH ₃	OH
191	OCH ₃	OH	OCH ₃	H	OH
192	OH	H	OCH ₃	OCH ₃	OCH ₃
193	OH	OCH ₃	OCH ₃	H	OCH ₃
194	OCH ₃	OCH ₃	OCH ₃	H	OCH ₃
195	OCH ₃	H	OCH ₃	OCH ₃	OCH ₃
196	OH	H	OH	H	OH
197	OH	H	OH	OH	OH
198	OCH ₃	H	OH	OCH ₃	OH
199	OCH ₃	OCH ₃	OCH ₃	H	OH
65	OH	H	OCH ₃	OCH ₃	OH
204	OCH ₃	OCH ₃	OCH ₃	OCH ₃	OCH ₃
205	OH	OCH ₃	OCH ₃	OCH ₃	OCH ₃

Figure 1.27 constituents isolated from the acetone extract of the stems, roots and leaves of *M. thorelii*.

1.3.10 *Milium sessilis* Chaowasku & Kessler sp. nov.

In the present study, the hexane extract and the ethyl acetate extract prepared from the leaves of *M. sessilis* were test at the concentration of 50 µg/ml, showed cytotoxicity against MCF7 (93.52 and 82.15% inhibition, respectively) and NCI-H187 (98.82 and 98.37% inhibition, respectively) cancer cell. Moreover, no previous phytochemical studies have been carried out on this plant. According to these preliminary results, the chemical constituents responsible for the cytotoxic activity of the leaves of *M. sessilis* will be isolated. The objectives of this study were summarized as follows:

1. To isolate and identify the chemical constituents from the leaves of *Milium sessilis* Chaowasku & Kessler.
2. To study the biological activities of crude extract and pure compounds.



CHAPTER 2

EXPERIMENTAL

2.1 Instrumentals and Chemicals

The following instruments were used to obtain physical data. Melting points were determined by a Kofler hot stage apparatus (uncorrected). Specific optical rotations were measured in chloroform solutions on KRÜSS OPTRONIC digital polarimeters P300 series. Ultraviolet spectra (UV) were obtained on a Hewlett Packard 8453 UV-vis spectrophotometer. Electronic circular dichroism spectra (ECD spectra) were recorded using MeOH on a JASCO J-815 spectropolarimeter. Principal bands (λ_{max}) were recorded as wavelengths (nm) in methanol solutions. Infrared spectra (IR) were recorded on a Perkin Elmer GX FT-IR spectrophotometer. ^1H NMR and ^{13}C NMR spectroscopic data were recorded in CDCl_3 solutions on a Bruker AVANCE 300 MHz (300 MHz for ^1H NMR and 75 MHz for ^{13}C NMR) spectrometer. Chemical shifts are in δ (ppm) with tetramethylsilane (TMS) as an internal standard. Inverse-detected heteronuclear correlations were measured using HMQC and HMBC pulse field gradient. Mass spectrometric data (HRESIMS) were obtained using a Micro TOF, Bruker Daltonic mass spectrometer. X-ray data were recorded on a X8 APEX Single Crystal X-Ray Diffractometer.

The following experimental conditions were used for chromatography. Normal phase silica gel column chromatography (CC) and flash CC were carried out using silica gel 60 (Merk, 0.063-0.200 and 0.015-0.040 mm). Reversed-phase CC was

carried out using silica gel RP-18 (Merk, 40-63 μm). Preparative thin layer chromatography (PLC) was carried out on glass plates using silica gel 60 F₂₅₄ (Merk, 20×20 cm, layer thickness, 0.25, 0.5, and 1.0 mm). Pre-coated thin layer chromatography (TLC) aluminum sheets of silica gel 60 F₂₅₄ (Merk, layer thickness 0.2 mm, normal phase) and silica gel RP-18 WF_{254s} (Merk, layer thickness 0.2 mm, reversed-phase) were used for analytical purposes and the compounds were visualized under ultraviolet light (254 and 365 nm) or sprayed with 1% CeSO₄ in 10% aqueous H₂SO₄ following by heating. Organic solvents for extraction and chromatography were distilled at their boiling point ranges prior to use. Methanol and chloroform (analytical grade, Merck, Germany) were used for the ultraviolet, CD spectral data and optical rotation analysis.

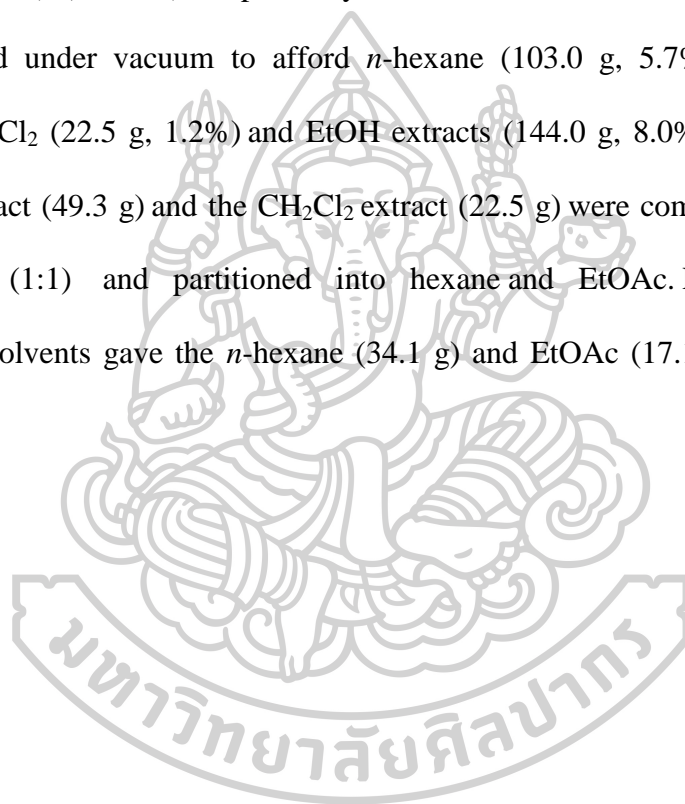
2.2 Plant materials

The leaves of *Miliusa sessilis* Chaowasku & Kessler sp. Nov. (Annonaceae) were collected in Tamot district, Phattalung province, Thailand (Coordinates: 7° 18' 15" N 100° 1' 26" E) in February 2016. The identification of the plant was performed by Dr. Piya Chalermglin. A voucher specimen (van Beusekom & Santisuk 2807) was deposited at The Forest Herbarium, Department of National Parks, Wildlife and Plant Conservation, Chatuchak, Bangkok, Thailand.

2.3 Chemical investigation of the leaves

2.3.1 Extraction and isolation

The dried, ground leaves of *M. sessilis* (1.8 kg) were extracted with *n*-hexane (20 L×2) at room temperature. The residue was continuously extracted with ethyl acetate (EtOAc) (18 L×2), followed by dichlorometane (CH₂Cl₂) (18 L×2), and ethanol (EtOH) (18 L×3), respectively. The combined extract of each solvent was concentrated under vacuum to afford *n*-hexane (103.0 g, 5.7%), EtOAc (49.3 g, 2.7%), CH₂Cl₂ (22.5 g, 1.2%) and EtOH extracts (144.0 g, 8.0%), respectively. The EtOAc extract (49.3 g) and the CH₂Cl₂ extract (22.5 g) were combined to dissolve in H₂O:EtOH (1:1) and partitioned into hexane and EtOAc. Evaporation of the respective solvents gave the *n*-hexane (34.1 g) and EtOAc (17.1 g) extracts (Figure 2.1).



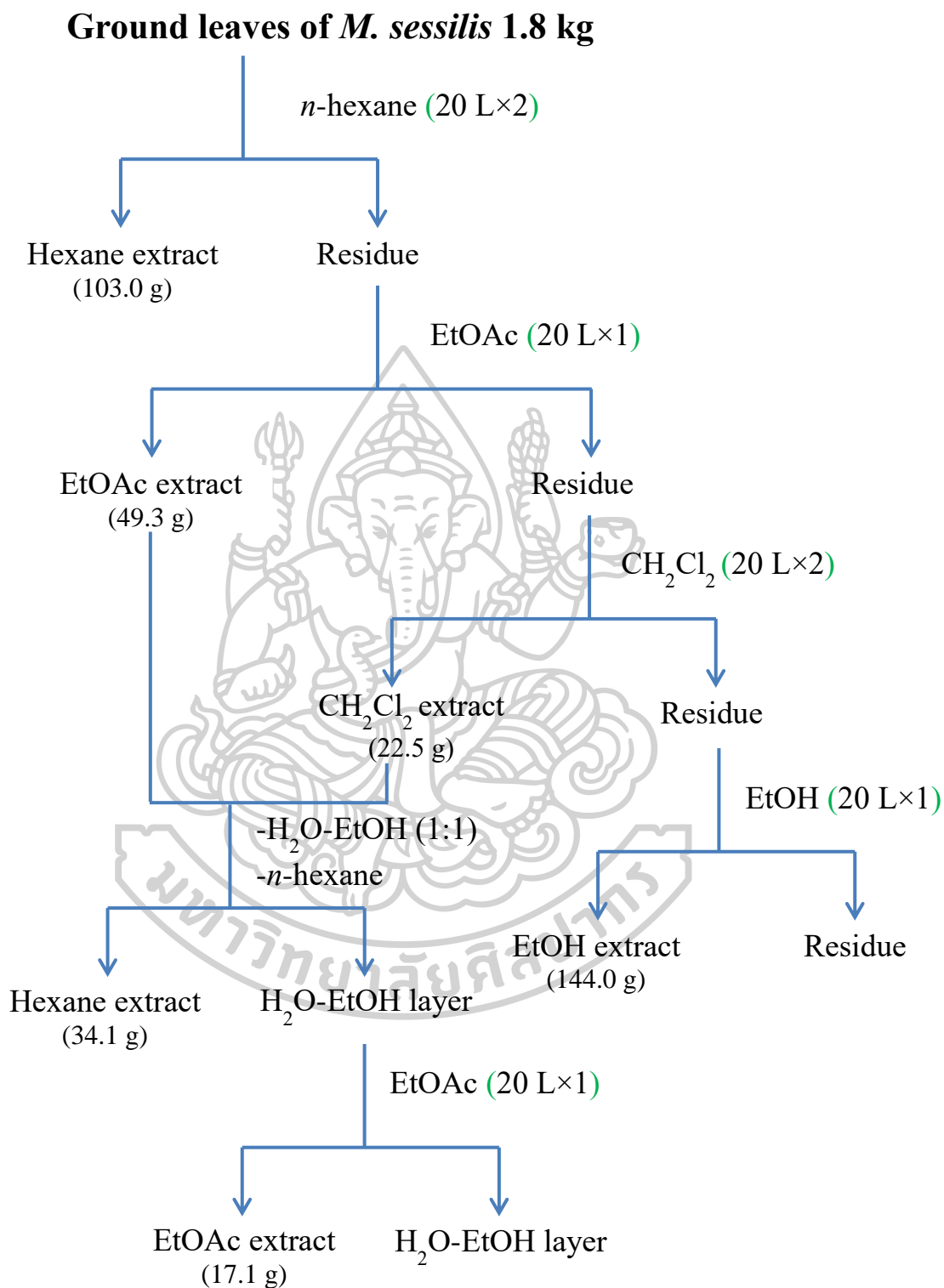


Figure 2.1 Extraction and fractionation of *Miliusa sessilis* leaves.

2.3.2 Chemical investigation of hexane extract fraction.

The *n*-hexane extract (100 g) was subjected to silica gel flash column chromatographic separation using a gradient system of *n*-hexane:EtOAc as the eluent. On the basis of their TLC characteristics, similar fractions were combined to afford 37 fractions (H1-H37, Table 2.1).

Table 2.1 Fractions obtained from hexane extract fraction.

Fraction	Eluent	Weight (g)	Physical characteristic
H1	100% hexane	6.000	light yellow oil
H2	100% hexane	7.1757	light yellow oil
H3	100% hexane	0.9000	red oil
H4	1% EtOAc in hexane	1.0230	Orang oil
H5	1% EtOAc in hexane	1.8349	yellowish orange wax
H6	1% EtOAc in hexane	1.5397	yellowish orange wax
H7	1% EtOAc in hexane	0.8528	yellowish orange wax
H8	1% EtOAc in hexane	0.4561	reddish orange wax
H9*	1% EtOAc in hexane	0.2820	reddish orange wax
H10	1% EtOAc in hexane	0.0743	reddish orange wax
H11	1% EtOAc in hexane	0.0548	reddish orange wax
H12	1% EtOAc in hexane	0.0833	reddish orange wax
H13	2% EtOAc in hexane	0.9698	reddish orange wax
H14	2% EtOAc in hexane	0.2059	red wax
H15	3% EtOAc in hexane	0.0930	red wax
H16	3% EtOAc in hexane	0.1394	red wax
H17	3% EtOAc in hexane	0.3546	red wax
H18	3% EtOAc in hexane	0.3675	red wax
H19	4% EtOAc in hexane	0.3081	red wax
H20	4% EtOAc in hexane	0.2762	red wax
H21	4% EtOAc in hexane	0.7057	red wax
H22*	4% EtOAc in hexane	2.9065	red wax
H23	5% EtOAc in hexane	0.8512	red wax
H24	5% EtOAc in hexane	1.1500	red wax
H25	5% EtOAc in hexane	0.4849	red wax
H26	100% EtOAc	0.4312	red wax
H27*	1% MeOH in EtOAc	40.6401	dark green viscose solid
H28	2% MeOH in EtOAc	0.0911	dark green viscose solid

*TLC characteristics of these fractions showed major spots under UV and obviously color and their ¹H NMR spectra showed noticeable signal.

Table 2.1 Fractions obtained from hexane extract fraction (continued).

Fraction	Eluent	Weight (g)	Physical characteristic
H29	3% MeOH in EtOAc	0.1421	dark green viscose solid
H30	4% MeOH in EtOAc	0.0532	dark green viscose solid
H31	5% MeOH in EtOAc	0.0485	dark green viscose solid
H32	10% MeOH in EtOAc	0.0576	dark green viscose solid
H33	15% MeOH in EtOAc	0.0856	dark green viscose solid
H34	20% MeOH in EtOAc	0.0592	dark green viscose solid
H35	20% MeOH in EtOAc	0.0823	dark green viscose solid
H36	20% MeOH in EtOAc	0.0687	dark green viscose solid
H37	20% MeOH in EtOAc	0.0429	dark green viscose solid

*TLC characteristics of these fractions showed major spots under UV and obviously color and their ¹H-NMR spectra showed noticeable signal.

Subfraction H22 (2.91 g) was subjected to silica gel CC using 5% EtOAc in *n*-hexane:benzene (1:1) as the eluent to provide 10 fractions (H22.1-10, Table 2.2).

Table 2.2 Fractions obtained from H22.

Fraction	Weight (mg)	Physical characteristic
H22.1	14.1	yellow wax
H22.2	10.4	yellow wax
H22.3	59.6	yellow wax
H22.4	613.7	yellowish orange wax
H22.5	495.4	yellowish orange wax
H22.6	740.6	yellowish orange wax
H22.7	173.9	yellowish orange wax
H22.8	285.6	yellowish orange oil
H22.9 *	244.4	yellow oil
H22.10	34.8	yellow oil

*Fractions were further investigated.

Fraction H22.9 (122.0 mg) was purified by RP-18 CC using MeOH:H₂O (10:1) as the eluent to obtain **MS1** as colorless oil.

Subfraction H27 (40.64 g) was separated by silica gel flash CC using EtOAc in *n*-hexane as gradient mixtures (1-45% EtOAc in hexane) to afford 67 fractions (H27.1-H27.67), Table 2.3).

Table 2.3 Fractions obtained from hexane extract fraction.

Fraction	Eluent	Weight (g)	Physical characteristic
H27.1	100% hexane	0.0151	light yellow solid
H27.2	1% EtOAc in hexane	0.4271	dark green viscous oil
H27.3	2% EtOAc in hexane	0.0910	dark green viscous oil
H27.4	3% EtOAc in hexane	0.0411	dark green viscous oil
H27.5	4% EtOAc in hexane	0.0525	dark green viscous oil
H27.6	5% EtOAc in hexane	0.0544	green wax
H27.7	6% EtOAc in hexane	0.6908	green wax
H27.8	6% EtOAc in hexane	0.5259	dark green viscous oil
H27.9*	6% EtOAc in hexane	0.4941	dark green semisolid
H27.10	7% EtOAc in hexane	0.3776	dark green semisolid
H27.11	7% EtOAc in hexane	0.3775	dark green semisolid
H27.12*	7% EtOAc in hexane	0.3309	dark green semisolid
H27.13*	7% EtOAc in hexane	0.5245	dark green solid
H27.14*	7% EtOAc in hexane	0.4896	dark green solid
H27.15	8% EtOAc in hexane	0.7690	dark green semisolid
H27.16	8% EtOAc in hexane	1.0933	dark green semisolid
H27.17	8% EtOAc in hexane	1.0078	dark green semisolid
H27.18	8% EtOAc in hexane	1.6440	dark green viscous oil
H27.19	8% EtOAc in hexane	1.4243	dark green viscous oil
H27.20	8% EtOAc in hexane	1.2573	dark green viscous oil
H27.21*	8% EtOAc in hexane	0.6504	dark green viscous oil
H27.22	9% EtOAc in hexane	0.8878	dark green oil
H27.23	9% EtOAc in hexane	1.2759	dark green oil
H27.24	9% EtOAc in hexane	1.0997	dark green oil
H27.25	9% EtOAc in hexane	0.9042	dark green oil
H27.26	9% EtOAc in hexane	0.4702	dark green oil
H27.27	10% EtOAc in hexane	0.4055	dark green semisolid
H27.28	10% EtOAc in hexane	0.5864	dark green semisolid
H27.29	10% EtOAc in hexane	0.4595	dark green semisolid
H27.30	10% EtOAc in hexane	0.3031	dark green semisolid
H27.31	10% EtOAc in hexane	0.2922	dark green semisolid
H27.32	11% EtOAc in hexane	0.1634	dark green semisolid
H27.33*	11% EtOAc in hexane	0.3501	dark green semisolid
H27.34	11% EtOAc in hexane	0.1781	dark green semisolid

*Fractions were further investigated.

Table 2.3 Fractions obtained from hexane extract fraction (continued).

Fraction	Eluent	Weight (g)	Physical characteristic
H27.35	11% EtOAc in hexane	0.0977	dark green semisolid
H27.36	11% EtOAc in hexane	0.1180	dark green semisolid
H27.37	13% EtOAc in hexane	0.0681	dark green semisolid
H27.38	13% EtOAc in hexane	0.01671	dark green semisolid
H27.39	13% EtOAc in hexane	0.2464	dark green semisolid
H27.40	13% EtOAc in hexane	0.2373	dark green semisolid
H27.41*	13% EtOAc in hexane	0.2514	dark green semisolid
H27.42*	15% EtOAc in hexane	0.3537	dark green semisolid
H27.43*	15% EtOAc in hexane	0.2654	dark green semisolid
H27.44	15% EtOAc in hexane	0.2936	dark green semisolid
H27.45	15% EtOAc in hexane	0.3801	dark green semisolid
H27.46	15% EtOAc in hexane	0.4738	dark green semisolid
H27.47	17% EtOAc in hexane	0.3740	dark green solid
H27.48	17% EtOAc in hexane	0.4884	dark green solid
H27.49	17% EtOAc in hexane	0.8275	dark green solid
H27.50	17% EtOAc in hexane	0.6234	dark green solid
H27.51	17% EtOAc in hexane	0.3937	dark green solid
H27.52	20% EtOAc in hexane	0.5381	dark green solid
H27.53	20% EtOAc in hexane	0.9482	dark green solid
H27.54	20% EtOAc in hexane	0.6806	dark green solid
H27.55	25% EtOAc in hexane	0.6935	dark green solid
H27.56	25% EtOAc in hexane	0.8220	dark green solid
H27.57	25% EtOAc in hexane	0.7726	dark green viscous solid
H27.58	30% EtOAc in hexane	1.2908	dark green viscous solid
H27.59*	30% EtOAc in hexane	2.4150	dark green viscous solid
H27.60	30% EtOAc in hexane	1.1048	dark green viscous solid
H27.61	35% EtOAc in hexane	0.3654	dark green viscous solid
H27.62	35% EtOAc in hexane	0.3992	dark green viscous solid
H27.63	35% EtOAc in hexane	0.5035	dark green viscous solid
H27.64	40% EtOAc in hexane	0.3997	dark green viscous solid
H27.65	40% EtOAc in hexane	0.3626	dark green viscous solid
H27.66	40% EtOAc in hexane	0.6192	dark green viscous solid
H27.67	45% EtOAc in hexane	0.5051	dark green viscous solid

*Fractions were further investigated.

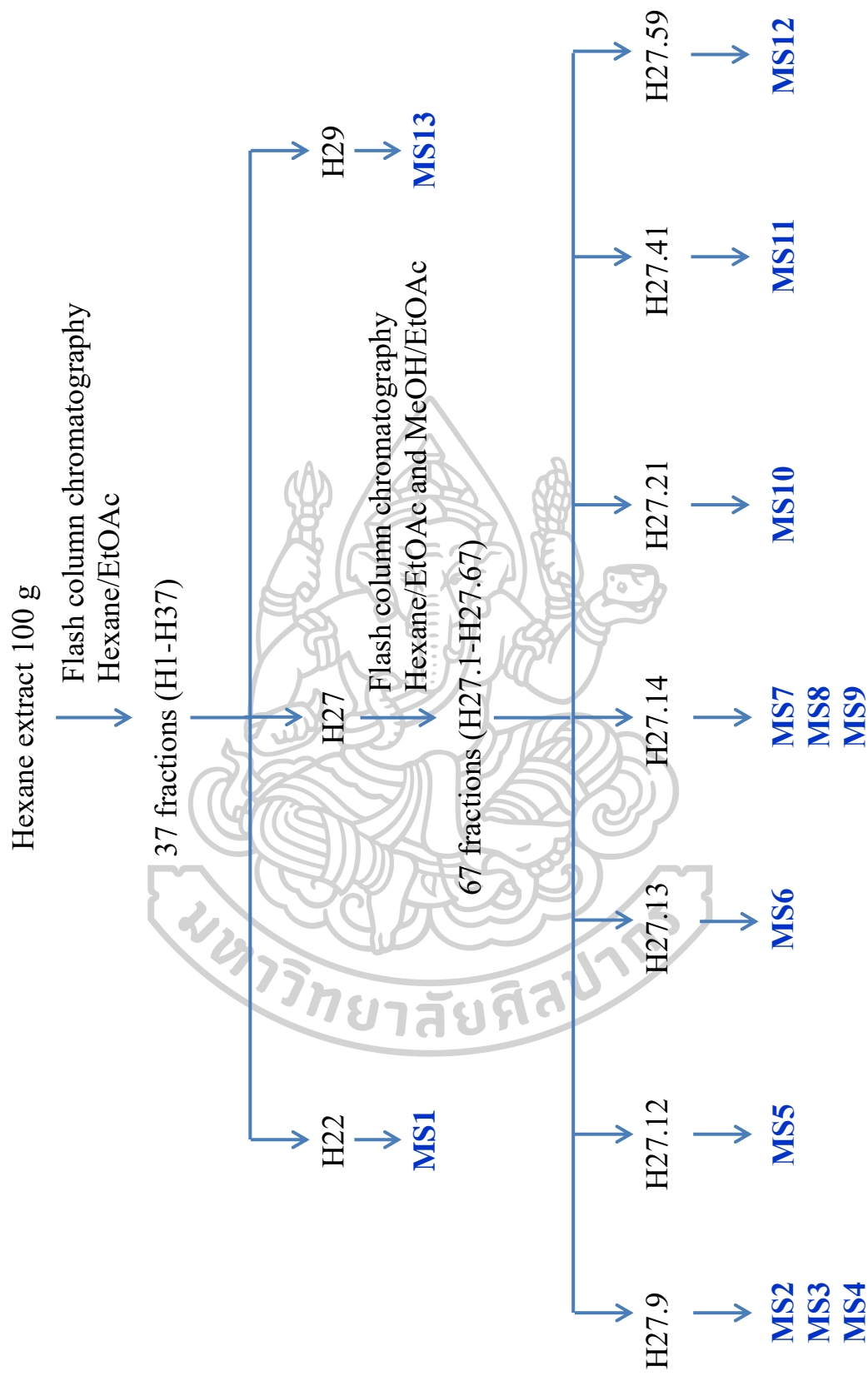


Figure 2.2 Fractionation of the hexane extract of *Miliusa sessilis*.

Subfraction H27.9 (494.1 mg) was subjected to silica gel CC using 5% EtOAc in *n*-hexane:benzene (1:1) as the eluent to provide 14 fractions (H27.9.1-14, Table 2.4).

Table 2.4 Fractions obtained from H27.9.

Fraction	Weight (mg)	Physical characteristic
H27.9.1	-	-
H27.9.2	8.3	dark green semisolid
H27.9.3	5.4	dark green semisolid
H27.9.4	22.4	dark green semisolid
H27.9.5	9.7	dark green semisolid
H27.9.6	6.1	white-green semisolid
H27.9.7	83.5	white-green semisolid
H27.9.8	33.6	white-green solid
H27.9.9	23.0	white needle crystalline
H27.9.10 *	67.0	white needle crystalline
H27.9.11	26.6	white needle crystalline
H27.9.12	15.6	white wax
H27.9.13	11.8	white wax
H27.9.14 *	12.5	white powder

*Fractions were further investigated.

Fraction H27.9.10 was separated by RP-18 CC using MeOH as the eluent to obtain **MS2** as white powder (10.1 mg) and a white solid (43.3 mg) which was recrystallized from EtOH:EtOAc (8:1) to afford **MS3** as colorless needles.

Fraction H27.9.14 was obtained as white powder which was recrystallized from EtOH:EtOAc (8:1) to afford **MS4** as colorless needles.

Subfraction H27.12 (330.9 mg) was subjected to silica gel CC using 1- 3% EtOAc in *n*-hexane:benzene (1:1) as the eluent to afford 11 fractions (H27.12.1-11, Table 2.5).

Table 2.5 Fractions obtained from H27.12.

Fraction	Weight (mg)	Physical characteristic
H27.12.1	8.6	dark yellow wax
H27.12.2	24.8	dark yellow wax
H27.12.3	21.1	dark yellow solid
H27.12.4	17.4	dark yellow solid
H27.12.5*	43.2	dark yellow solid
H27.12.6	38.2	dark yellow solid
H27.12.7	27.9	dark yellow solid
H27.12.8	7.9	dark yellow wax
H27.12.9	9.0	dark yellow wax
H27.12.10	5.3	dark yellow wax
H27.12.11	9.6	dark yellow wax

*Fractions were further investigated.

Fraction H27.12.5 was purified by RP-18 CC using acetonitrile:H₂O (100:1) as the eluent to give a white powder (12.3 mg) which was recrystallized from EtOH:EtOAc (8:1) to afford **MS5** as colorless needles.

Subfraction H27.13 (524.9 mg) was subjected to silica gel CC using (1- 4%) EtOAc in *n*-hexane:benzene (1:1) as the eluent to provide 7 fractions (H27.13.1-7, Table 2.6).

Fraction H27.13.5 and H27.13.6 were combined to purify by RP-18 CC using MeOH-H₂O (10:1) as the eluent to give **MS6** (7.1 mg).

Table 2.6 Fractions obtained from H27.13.

Fraction	Weight (mg)	Physical characteristic
H27.13.1	24.4	Greenish-white solid
H27.13.2	10.9	Greenish-white solid
H27.13.3	67.3	Greenish-white solid
H27.13.4	116.5	White solid
H27.13.5*	11.5	White solid
H27.13.6*	19.1	White solid
H27.13.7	20.7	White solid

*Fractions were further investigated.

Subfraction H27.14 (489.6 mg) was subjected to silica gel CC using 1- 5% EtOAc in *n*-hexane:benzene (1:1) as the eluent to provide 9 fractions (H27.14.1-9, Table 2.7).

Table 2.7 Fractions obtained from H27.14.

Fraction	Weight (mg)	Physical characteristic
H27.14.1	13.1	dark yellow semisolid
H27.14.2*	8.7	dark yellow semisolid
H27.14.3*	26.6	dark yellow solid
H27.14.4*	15.2	dark yellow solid
H27.14.5	36.1	dark yellow solid
H27.14.6	32.7	dark yellow solid
H27.14.7	61.8	dark yellow solid
H27.14.8	67.2	dark yellow semisolid
H27.14.9*	78.0	dark yellow semisolid

*Fractions were further investigated.

The combined fraction H27.14.2, H27.14.3 and H27.14.4 (50.5 mg) were purified by PLC using 10% EtOAc in hexane:benzene (1:1) (2 runs) as the mobile phase to provide **MS5** (12.5 mg)

Fraction H27.14.9 (78.0) was separated by PLC with 10% EtOAc in (1:1) *n*-hexane-benzene (3 times) as mobile phase to obtain two fractions (H27.14.9.1-2). Subfraction H27.14.9.1 (22.8 mg) was purified by RP-18 CC using MeOH:H₂O (10:1) as the eluent to give **MS7** (9.8 mg). Subfraction H27.14.9.2 (21.3 mg) was recrystallized with EtOH to yield **MS8** and **MS9** (14.2 mg)

Subfraction H27.21 (650.4 mg) was purified by silica gel CC using (5-10%) EtOAc in *n*-hexane as the eluent to obtain 5 fractions (H27.21.1-5, Table 2.8). The pure fraction H27.21.5 gave a pale green oil as **MS10** (310.4 mg)

Table 2.8 Fractions obtained from H27.21.

Fraction	Weight (mg)	Physical characteristic
H27.21.1	21.4	dark green semisolid
H27.21.2	68.8	dark green oil
H27.21.3	58.3	dark green oil
H27.21.4	148.3	green oil
H27.21.5*	310.4	pale green oil

*Fraction was further investigated.

Subfraction H27.41 (870.5 mg) was separated by silica gel CC using 5- 20% EtOAc in *n*-hexane as the eluent to provide 8 fractions (H27.41.1-8, Table 2.9).

Table 2.9 Fractions obtained from H27.41.

Fraction	Weight (mg)	Physical characteristic
H27.41.1	12.0	dark red thick oil
H27.41.2	29.2	dark green thick oil
H27.41.3	48.0	dark green thick oil
H27.41.4	84.5	dark green thick oil
H27.41.5	275.3	dark green solid
H27.41.6*	160.2	dark green solid
H27.41.7	36.9	dark green solid
H27.41.8	16.9	dark green solid

*Fraction was further investigated.

Fraction H27.41.6 (160.2 mg) was purified by RP-18 CC using MeOH:H₂O (10:1) as the eluent to give **MS11** (69.0 mg) as pale green-brown viscous liquid.

Subfraction H27.59 (300.8 mg) was subjected to silica gel CC using 5-25% EtOAc in *n*-hexane as the eluent to provide 4 fractions (H27.59.1-4, Table 2.10).

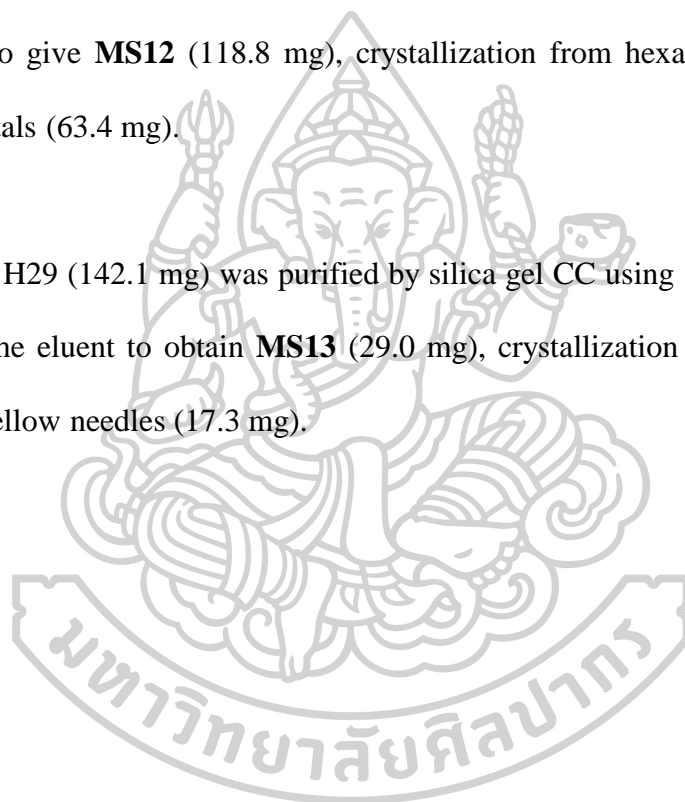
Table 2.10 Fractions obtained from H27.59.

Fraction	Weight (mg)	Physical characteristic
H27.59.1	6.0	dark green thick oil
H27.59.2	68.1	dark green thick oil
H27.59.3*	153.2	dark green solid
H27.59.4	10.2	dark green solid

*Fraction was further investigated.

Fraction H27.59.3 (153.2 mg) was purified by RP-18 CC using MeOH:H₂O (5:1) as the eluent to give **MS12** (118.8 mg), crystallization from hexane:EtOAc gave pale yellow crystals (63.4 mg).

Subfraction H29 (142.1 mg) was purified by silica gel CC using 10-30% EtOAc in *n*-hexane as the eluent to obtain **MS13** (29.0 mg), crystallization from hexane:EtOAc gave pale yellow needles (17.3 mg).



2.3.3 Chemical investigation of EtOAc extract fraction

The EtOAc extract (17.0 g) was chromatographed on a silica gel flash column eluted with EtOAc in hexane (5-100%) followed by MeOH in EtOAc (1-50%) gradient mixture to afford 66 fractions (E1-66, table 2.11).

Table 2.11 Fractions obtained from ethyl acetate extract fraction.

Fraction	Eluent	Weight (g)	Physical characteristic
E1	5% EtOAc in hexane	0.0	pale greenish yellow solid
E2	5% EtOAc in hexane	0.0067	pale greenish yellow solid
E3	5% EtOAc in hexane	0.0176	pale greenish yellow solid
E4	10% EtOAc in hexane	0.0109	pale greenish yellow solid
E5	10% EtOAc in hexane	0.0152	pale greenish yellow solid
E6	10% EtOAc in hexane	0.0198	pale greenish yellow solid
E7	10% EtOAc in hexane	0.0878	dark green oil
E8	10% EtOAc in hexane	0.1103	dark green oil
E9*	15% EtOAc in hexane	0.3289	dark green oil
E10	15% EtOAc in hexane	0.2179	dark green oil
E11	15% EtOAc in hexane	0.0852	dark green oil
E12	15% EtOAc in hexane	0.0613	dark green oil
E13	15% EtOAc in hexane	0.0731	dark green oil
E14	15% EtOAc in hexane	0.0701	dark green oil
E15	15% EtOAc in hexane	0.0942	dark green oil
E16	20% EtOAc in hexane	0.3353	dark green crystalline
E17	20% EtOAc in hexane	0.614.2	dark green crystalline
E18	20% EtOAc in hexane	0.3510	dark green crystalline
E19	20% EtOAc in hexane	0.3170	dark green crystalline
E20	20% EtOAc in hexane	0.6347	dark red thick oil
E21	20% EtOAc in hexane	1.3774	greenish brown crystalline
E22	20% EtOAc in hexane	1.7195	greenish brown crystalline
E23	20% EtOAc in hexane	1.2566	greenish brown crystalline
E24	20% EtOAc in hexane	0.8206	dark red thick oil
E25	25% EtOAc in hexane	0.5756	dark red thick oil
E26	25% EtOAc in hexane	0.2841	dark red thick oil
E27*	25% EtOAc in hexane	0.6497	dark red thick oil
E28	30% EtOAc in hexane	0.0866	dark red thick oil
E29	30% EtOAc in hexane	0.1764	dark red thick oil
E30*	30% EtOAc in hexane	0.5737	dark red thick oil
E31	30% EtOAc in hexane	0.2932	dark red thick oil
E32	30% EtOAc in hexane	0.2540	dark red thick oil

*Fraction was further investigated.

Table 2.11 Fractions obtained from ethyl acetate extract fraction (continued).

Fraction	Eluent	Weight (g)	Physical characteristic
E33	35% EtOAc in hexane	0.2519	dark red thick oil
E34	35% EtOAc in hexane	0.0927	dark red thick oil
E35*	35% EtOAc in hexane	0.5615	dark greenish red thick oil
E36	40% EtOAc in hexane	0.1546	dark greenish red thick oil
E37	40% EtOAc in hexane	0.1338	dark greenish red thick oil
E38	40% EtOAc in hexane	0.0878	dark greenish red thick oil
E39	40% EtOAc in hexane	0.1051	dark greenish red thick oil
E40	40% EtOAc in hexane	0.1183	dark greenish red thick oil
E41	50% EtOAc in hexane	0.1510	dark greenish red thick oil
E42	50% EtOAc in hexane	0.1985	dark greenish red thick oil
E43	50% EtOAc in hexane	0.1309	dark greenish red thick oil
E44	50% EtOAc in hexane	0.1020	dark greenish red thick oil
E45	75% EtOAc in hexane	0.1231	dark green thick oil
E46	75% EtOAc in hexane	0.3661	dark green semi-solid
E47	75% EtOAc in hexane	0.3632	dark green semi-solid
E48*	100% EtOAc in hexane	0.5265	dark green semi-solid
E49	100% EtOAc in hexane	0.0867	dark green semi-solid
E50	1% MeOH in EtOAc	0.0816	dark green semi-solid
E51	1% MeOH in EtOAc	0.0798	dark green semi-solid
E52	1% MeOH in EtOAc	0.1513	dark green semi-solid
E53	3% MeOH in EtOAc	0.1203	dark green semi-solid
E54	3% MeOH in EtOAc	0.1032	dark green semi-solid
E55	3% MeOH in EtOAc	0.0791	dark green semi-solid
E56	5% MeOH in EtOAc	0.1001	dark green semi-solid
E57	5% MeOH in EtOAc	0.1012	dark green semi-solid
E58	5% MeOH in EtOAc	0.1190	dark green semi-solid
E59	10% MeOH in EtOAc	0.1838	dark green semi-solid
E60	10% MeOH in EtOAc	0.2018	dark green semi-solid
E61	10% MeOH in EtOAc	0.1985	dark green semi-solid
E62	30% MeOH in EtOAc	0.2799	dark green semi-solid
E63	30% MeOH in EtOAc	0.1439	dark green semi-solid
E64	50% MeOH in EtOAc	0.1083	dark green semi-solid
E65	50% MeOH in EtOAc	0.0655	dark green semi-solid
E66	50% MeOH in EtOAc	0.0393	dark green semi-solid

*Fraction was further investigated.

Subfraction E27 (649.7 mg) was separated by silica gel CC using *n*-hexane:EtOAc (3:2) as the eluent to afford 7 fractions (E27.1-7, Table 2.12).

Table 2.12 Fractions obtained from E27.

Fraction	Weight (mg)	Physical characteristic
E27.1	37.0	brown viscous oil
E27.2	39.7	brown viscous oil
E27.3*	37.3	brown viscous oil
E27.4*	149.1	brown viscous oil
E27.5	20.2	light brown viscous oil
E27.6	110.1	light brown viscous oil
E27.7	66.3	light brown viscous oil

*Fraction was further investigated.

Fraction E.27.3 (37.3 mg) was purified by preparative TLC with CH₂Cl₂:MeOH:H₂O (300:3:1) as the mobile phase to provide **MS14** (8.9 mg) as a pale green-brown viscous liquid.

Fraction E27.4 (149.1 mg) was subjected to silica gel CC using CH₂Cl₂:MeOH:H₂O (500:3:1) as the eluent to afford 9 fractions (E27.4.1-9, table 2.13).

Table 2.13 Fractions obtained from E27.4.

Fraction	Weight (mg)	Physical characteristic
E27.4.1	5.6	light brown viscous oil
E27.4.2	15.6	light brown viscous oil
E27.4.3*	32.4	light brown viscous oil
E27.4.4	21.8	light brown viscous oil
E27.4.5	28.1	light brown viscous oil
E27.4.6	10.1	light brown viscous oil
E27.4.7	2.4	light brown viscous oil
E27.4.8	5.4	light brown viscous oil
E27.4.9	4.4	light brown viscous oil

*Fraction was further investigated.

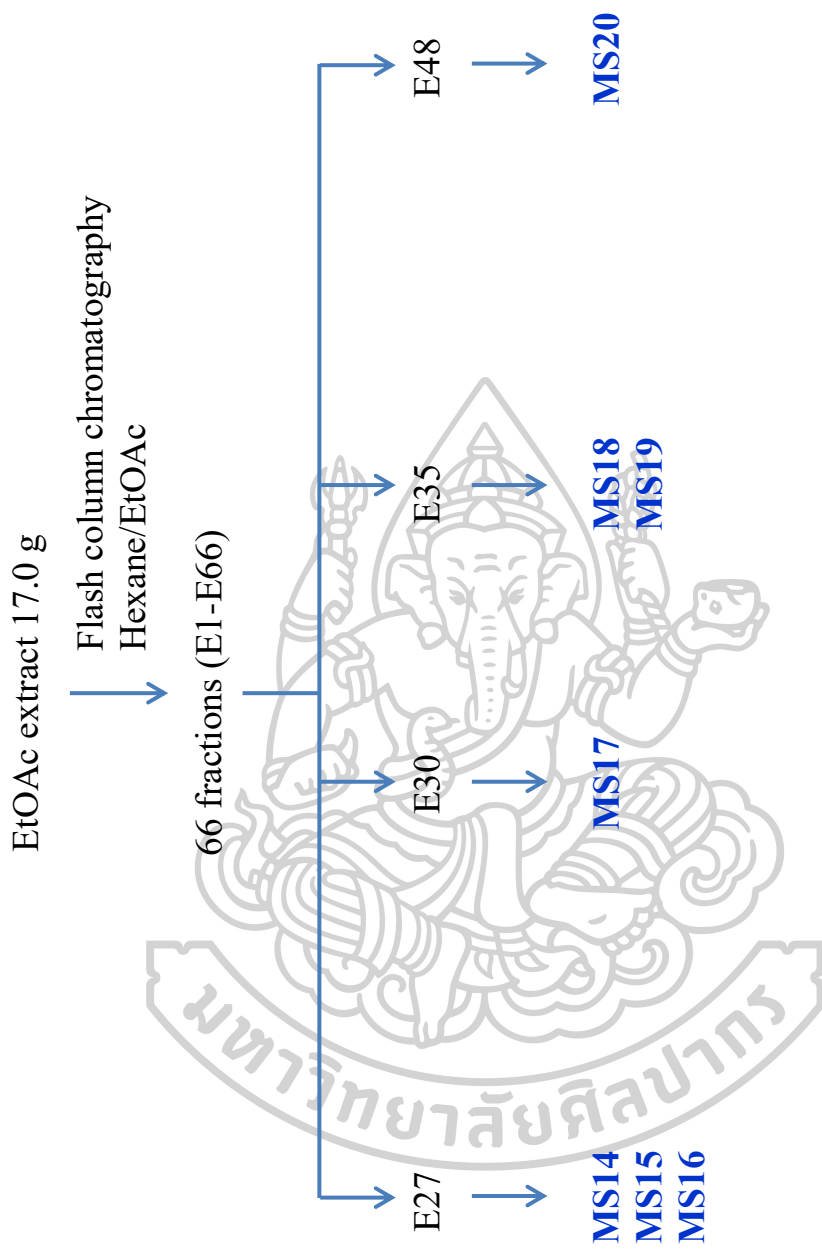


Figure 2.3 Fractionation of the EtOAc extract of *Miliusa sessilis*.

Fraction E.27.4.3 (32.4 mg) was separated by preparative TLC with $\text{CH}_2\text{Cl}_2:\text{MeOH}:\text{H}_2\text{O}$ (500:3:1) as the mobile phase to obtain **MS15** (8.9 mg) and **MS16** (11.8 mg).

Subfraction E30 (544.4 mg) was purified by silica gel CC using EtOAc in *n*-hexane (20-40%) as the eluent to obtain 8 fractions (E30.1-8, Table 2.14). Fraction E30.3 was identified as **MS 17** (201.0 mg).

Table 2.14 Fractions obtained from E30.

Fraction	Weight (mg)	Physical characteristic
E30.1	39.9	light brown viscous oil
E30.2	122.2	light brown viscous oil
E30.3*	201.0	light brown viscous oil
E30.4	75.8	light brown viscous oil
E30.5	24.0	light brown viscous oil
E30.6	10.6	light brown viscous oil
E30.7	23.4	light brown viscous oil
E30.8	6.8	light brown viscous oil

Subfraction E35 (561.5 mg) was separated by silica gel CC using 20-40% EtOAc in *n*-hexane as the eluent to afford 11 fractions (E35.1-11, Table 2.15).

Fraction E35.4 (36.3 mg) was purified by RP-18 CC using $\text{MeOH}:\text{H}_2\text{O}$ (3:2) as the eluent to give **MS18** (5.0 mg). Fraction E35.7 (57.0 mg) was separated by preparative TLC with $\text{CH}_2\text{Cl}_2:\text{MeOH}:\text{H}_2\text{O}$ (150:3:1) as the mobile phase to obtain **MS19** (20.6 mg).

Table 2.15 Fractions obtained from E35.

Fraction	Weight (mg)	Physical characteristic
E35.1	6.2	light brown viscous oil
E35.2	11.5	light brown viscous oil
E35.3	9.7	light brown viscous oil
E35.4*	36.3	light brown viscous oil
E35.5	89.9	light brown viscous oil
E35.6	36.9	light brown viscous oil
E35.7*	57.0	light brown viscous oil
E35.8	49.6	light brown viscous oil
E35.9	45.6	light brown viscous oil
E35.10	38.5	light brown viscous oil
E35.11	29.7	light brown viscous oil

*Fractions were further investigated.

Subfraction E48 (422.4 mg) was subjected to silica gel CC using CH₂Cl₂:MeOH:H₂O (120:3:1) as the eluent to provide 5 fractions (E48.1-5). Subfraction E48.4 (51.7 mg) was purified by RP-18 CC using MeOH:H₂O (5:6) as the eluent to give **MS20** (24.1 mg).

2.4 Hydrolysis of MS12

0.5 N NaOH (0.5 mL) was added into a stirred solution of **MS12** (21.4 mg) in MeOH (1.5 mL). The mixture was stirred at room temperature for 5 h. After the reaction was completed, the mixture was neutralized with 1 N HCl (1.0 mL), then 10.0 mL of water was added. The mixture was extracted with CH₂Cl₂ (5.0 mL×3). The organic layers were separated and washed with water (10.0 mL). The organic phase was dried over anhydrous sodium sulfate and evaporated. The hydrolysis product was identified as **MS17** by mean of TLC, ¹H NMR and ¹³C NMR spectral data and specific optical rotation ($[\alpha]_D^{28}$) +13.58, c 0.12, CHCl₃).

2.5 Methylation of MS12

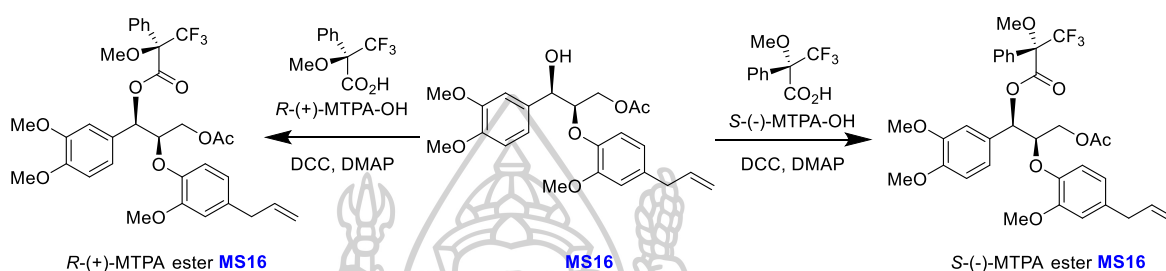
To a stirred suspension of NaH (1.5 mg, 62.5 μmol , 1.2 eq.) in DMF (1.0 mL), was added a solution of **MS12** (20.0 mg, 52.1 μmol) in dry DMF (1.0 mL, [**MS12**] = 0.026 M). The mixture was stirred at 0-5 $^{\circ}\text{C}$ for 15 min. and then 2 M CH_3I (30 μL , 0.06 mmol, 1.15 eq.) was added. The reaction mixture was continuously stirred at 0 -5 $^{\circ}\text{C}$ for 1 h. After reaction was completed, the mixture was added water (30 mL) and was extracted with EtOAc (10.0 mL \times 3). The combined organic layers were washed with water (30 mL) and followed by brine (30 mL). The organic layers were dried over anhydrous sodium sulfate and evaporated. The crude methylated product was purified by silica gel CC using hexane:ethyl acetate (1:100 to 30:70) as the eluent to provide two compounds, which were identified as a methylated product of **MS12** (11.3 mg, ($[\alpha]_{\text{D}}^{28}$ +20.59 $^{\circ}$, c 0.03, CHCl_3)) as colorless oil and a methylated and hydrolyzed product of **MS12** (11.3 mg) as colorless oil. The methylated product of **MS12** was identified as an enantiomer of **MS11** by mean of TLC, ^1H NMR and ^{13}C NMR spectral data and specific optical rotation ($[\alpha]_{\text{D}}^{28}$ +46.18, c 0.06, CHCl_3).

2.6 Dehydration of MS14

MS14 (10.5 mg) in 4.0 ml 20% H_3PO_4 was refluxed for overnight. After the reaction was completed, the reaction mixture was extracted with CHCl_3 . The organic fraction was dried over anhydrous sodium sulfate and evaporated (Kawanishi, 1982). The crude dehydrated product (9.5 mg) was purified by PLC using hexane:ethyl acetate (7:3) as mobile phase to afford a pure compound (6.2 mg) which was

identified as **MS15** by mean of TLC, ^1H NMR, ^{13}C NMR spectral data and specific optical rotation ($[\alpha]_{\text{D}}^{28}$ +21.82, c 0.05, CHCl_3).

2.7 Preparation of *S*-(-)-MTPA ester **MS16** and *R*-(+)-MTPA ester **MS16**



A stirred solution of **MS16** (5.1 mg, 12.0 μmol), *N,N'*-Dicyclohexylcarbodiimide (DCC, 19.9 mg, 69.7 μmol , 8 eq.), and 4-Dimethylaminopyridine (DMAP, 3.1 mg, 25.4 μmol , 2.1 eq.) in dry CH_2Cl_2 (0.5 ml, [**MS16**] = 0.012 M) at room temperature and *S*-(-)- α -methoxy- α -(trifluoromethyl)phenylacetic acid (*S*-(-)-MTPA-OH, 15.0 mg, 64.1 μmol , 5.0 eq.) in dry CH_2Cl_2 (0.5 ml) was added. The reaction progress was monitored by thin-layer chromatography (TLC on silica gel, hexane: ethyl acetate (3:2)). After complete consumption of the **MS16** (3 days), the reaction mixture was concentrated under vacuum. The crude mixture was purified by silica gel column, eluting with hexane:ethyl acetate (5:1) to afford the *S*-(-)-MTPA ester **MS16** (3.5 mg, 46%) as colorless oil. For ^1H NMR spectroscopic data of *S*-(-)-MTPA ester **MS16**, see Table 2.36.

The *R*-(+)-MTPA ester **MS16** was prepared using *R*-(+)-MTPA-OH. A stirred solution of **MS16** (4.7 mg, 12.0 μmol), DCC (14.7 mg, 71.2 μmol , 5.9 eq.) and DMAP (3.1 mg, 25.4 μmol , 2.1 eq.) in dry CH_2Cl_2 (0.5 ml, [**MS16**] = 0.012 M) at room temperature and (*R*-(+)-MTPA-OH, 13.1 mg, 55.9 μmol , 4.7 eq.) in dry CH_2Cl_2 (0.5 ml) was added. The reaction progress was monitored by thin-layer

chromatography (TLC on silica gel, hexane: ethyl acetate (2:3)). After complete consumption of the **MS16** (3 days), the reaction mixture was concentrated under vacuum. The crude ester was purified by silica gel CC using hexane:ethyl acetate (5:1) as the eluent to provide the *R*-(+)-MTPA ester **MS16** (2.1 mg, 28%) as colorless oil. For ^1H NMR spectroscopic data of *R*-(+)-MTPA ester **MS16**, see Table 2.36.

2.8 Hydrolysis of MS16

To a stirred solution of **MS16** (9.0 mg) in MeOH (1.5 mL) was added 0.5 N NaOH (0.5 mL). The mixture was allowed to stir at room temperature for 5 h. Upon completion, the mixture was quenched with 1.0 mL of 1 N HCl. The resulting mixture was added 10.0 mL of water and extracted with CH_2Cl_2 (5.0 mL \times 4). The combined organic layers were separated, washed with water (10.0 mL), dried over anhydrous sodium sulfate and evaporated. The crude hydrolysis product was purified by CC using hexane: ethyl acetate (5:1 to 3:1) as eluent to afford pure colorless oil (7.1 mg). The hydrolysis product was identified as **MS19** by mean of TLC, ^1H NMR and ^{13}C NMR spectral data and specific optical rotation ($[\alpha]_{\text{D}}^{28}$ +52.50, c 0.04, CHCl_3).

2.9 Acetylation of MS20

A mixture of **MS20** (19.3 mg) and acetic anhydride (1.0 mL) in pyridine (1.0 ml) was refluxed at 110 °C for 1 h. The reaction progress was monitored by thin-layer chromatography (TLC on silica gel, hexane: ethyl acetate (1:1)). After the reaction was completed, the mixture was added saturated NH_4Cl (1.0 mL) and then extracted

with CH_2Cl_2 (2.0 mL \times 3). The combined organic layers were washed with water, dried over anhydrous sodium sulfate and evaporated under vacuum. The crude acetylated product (23.1 mg) was further purified by column chromatography using hexane:ethyl acetate (1:1) as mobile phase to provide pure acetylated product **MS20a** as colorless solid (10.7 mg).

2.10 X-ray crystallographic analysis of MS12, MS3, MS5 and MS7

The crystal data of **MS12**, **MS3**, **MS5** and **MS7** were collect on Bruker D8 QUEST CMOS PHOTON II with graphite monochromated Mo-K α ($\lambda = 0.71073 \text{ \AA}$) radiation at 296(2) K. Data collection, cell refinement and data reduction were perform using *SAINT* program and *SADABS* were used for absorption correction (Bruker, 2016). The integrity of the symmetry was checked by using *PLATON* (Spek, 2015). The structure was solved with the *ShelXT* structure solution program using combined Patterson and dual-space recycling methods (Sheldrick, 2015a). The structure was refined by least squares using *ShelXL* program packages (Sheldrick, 2015b). All non-H atoms were found from electron density maps and refined with anisotropic parameters. The O–H hydrogen atoms were located in difference Fourier maps but refined with O–H = $0.82 \pm 0.01 \text{ \AA}$. CCDC-1976013, containing the supplementary crystallographic data, can be obtained free of charge from the Cambridge Crystallographic Data Centre via www.ccdc.cam.ac.uk/data_request/cif.

2.10.1 Crystallographic data of (7*S*,8*R*)-5'-hydroxy-3,4-dimethoxy-4',7'-epoxy-8,3'-neolign-8'-en-9-acetate (MS12)

pale yellow block shaped crystals obtained from a solution of EtOH, C₂₂H₂₄O₆, M = 384.41, Monoclinic, Space group *P*2₁, *a* = 11.3256(16) Å, *b* = 8.4544(13) Å, *c* = 11.8877(18) Å, $\alpha = \beta = 90^\circ$, $\gamma = 118.261(5)^\circ$, *V* = 1002.6(3) Å³, *Z* = 2, *D*_{calcd} = 1.273 Mg/m³, Crystal size 0.30 × 0.28 × 0.28 mm³, *F*(000) = 408, 36993 Reflections collected, 5206 Independent reflections (*R*_{int} = 0.0408), *R*₁ = 0.0562 [*I* > 2σ(*I*)], *wR*₂ = 0.1320 [*I* > 2σ(*I*)], *R*₁ = 0.0682 (all data), *wR*₂ = 0.1439 (all data), Goodness of fit = 1.050, Flack parameter = -0.3(13).

2.11 Biological assays

2.11.1 Cell culture

HaCaT cancer cell line (Human immortalized keratinocyte) was obtained from Dr. Veerawat Teeranachaideekul, Faculty of Pharmacy, Mahidol University. HepG2 cell line (Hepatocellular carcinoma), HCT116 cancer cell line (colorectal), HN22 cancer cell line (head-and-neck cancer) and HeLa cancer cell line (cervical cancer cell line) were obtained from Professor Praneet Opanasopit, Faculty of Pharmacy, Silpakorn University. HeLa was maintained and cultured in Minimum Essential Medium Eagle (MEM, Gibco) while HN22, HCT116 and HepG2 were maintained and cultured in Dulbecco's modified Eagle's medium (DMEM, Gibco, Waltham, MA, USA). Media for all cancer cell lines were supplemented with fetal bovine serum (FBS, Gibco, 10%), Pen-Strep (Gibco, 1%), L-glutamine (Gibco, 1%), and non-essential amino acid (Gibco, 1%) at 37 °C. HaCaT was maintained and cultured in

DMEM supplemented with FBS (10%) and Pen-Strep (1%). All cells were incubated at 37 °C in a humidified atmosphere with 5% CO₂.

2.11.2 Cytotoxicity evaluation

Assay of the isolated compounds for cytotoxicity against the cancer cell lines were conducted by MTT assay and IC₅₀ determination. In brief, cells were maintained and diluted to 8×10^4 cells/well onto 96-well plate and incubated for 12 h. Onward, 100 µl of serial 5-fold diluted compounds are added to each well to the final concentration of 250 µg/mL to 0.08 µg/mL. DMSO was used as vehicle control. Irinotecan (Fresenius Kabi, India), a cytotoxic drug, was used as positive control at 100 µM for HeLa and 40 µM for all other cell lines. After the incubation period for 72 h, cell viability was determined by MTT assay. Briefly, cells were washed with phosphate buffer saline (PBS) solution then incubated with 1 mg/mL thiazolyl blue tetrazolium bromide (Sigma-Aldrich, St. Louis, MO, USA) for 4 h. After removal of the supernatant, DMSO (100 µL) was added to each well to dissolve the formazan crystals. The absorbance was read by a microplate reader (Packard bioscience) at 550 nm. All the tests were repeated in three independent experiments. Data were expressed as the IC₅₀ and 95% confidence interval. The IC₅₀ was calculated by a non-linear regression analysis using the scientific statistic software GraphPad Prism version 7 (GraphPad Software Inc., La Jolla, CA).

2.12 Physical and spectral properties of isolated compounds

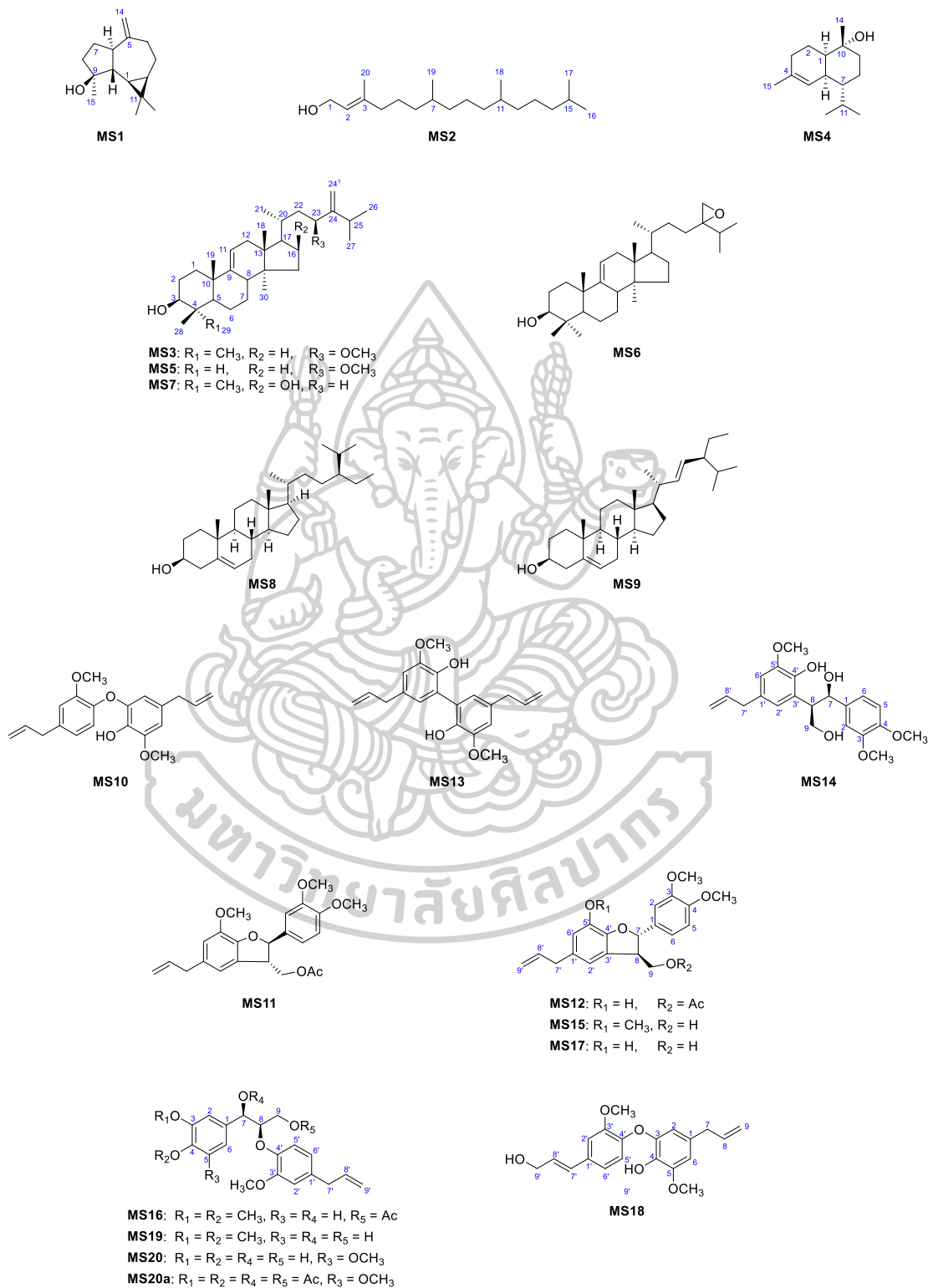
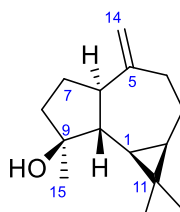


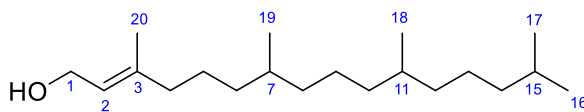
Figure 2.4 Structures of MS1-MS20.

2.12.1 MS1



IUPAC name:	-
Common name:	(+)-spathulenol
Appearance:	colorless viscous liquid
Melting Point:	-
Optical rotation:	$[\alpha]_D^{23} +21.5$ (c=0.08, CHCl ₃)
CD:	-
UV:	-
IR:	(thin film): $\nu_{\max}, \text{cm}^{-1}$; 3402, 3108, 2945, 1637, 919 and 888
HRESIMS:	-
Chemical Formula:	C ₁₅ H ₂₄ O
Exact Mass:	220.1827 g/mol
¹ H NMR spectroscopic data	δ ppm, 300 Hz in CDCl ₃ see Table 2.16
¹³ C NMR spectroscopic data	δ ppm, 75 Hz in CDCl ₃ see Table 2.16

2.12.2 MS2



IUPAC name: (E)-3,7,11,15-tetramethylhexadec-2-en-1-ol

Common name: phytol

Appearance: colorless viscous liquid

Melting Point: -

Optical rotation: -

CD: -

UV: -

IR: (thin film): ν_{\max} , cm^{-1} ;
3250, 2900, 1450 and 1005

HRESIMS: -

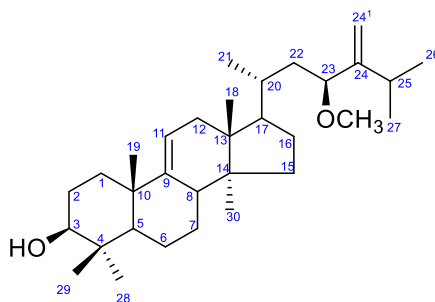
Chemical Formula: $\text{C}_{20}\text{H}_{40}\text{O}$

Exact Mass: 296.3079 g/mol

^1H NMR spectroscopic data δ ppm, 300 Hz in CDCl_3
see Table 2.17

^{13}C NMR spectroscopic data δ ppm, 75 Hz in CDCl_3
see Table 2.17

2.12.3 MS3



IUPAC name: (3 β ,23*S*)-23-methoxy-24-methylenelanost-9-en-3-ol

Common name: -

Appearance: colorless needle (ethanol:ethyl acetate, 8:1)

Melting Point: 192-193 °C

Optical rotation: $[\alpha]_D^{23} +84.2$ (c 0.06, CHCl₃)

CD: -

UV: -

IR: (thin film): ν_{\max} , cm⁻¹;
3323, 2917, 2866, 1639, 1462, 1369, 1111,
1087, 1040, 901 and 757

HRESIMS: m/z (relative intensity), 70 eV;
488.4462 [M+NH₄]⁺ (calcd. for C₃₂H₅₈NO₂,
488.4467)

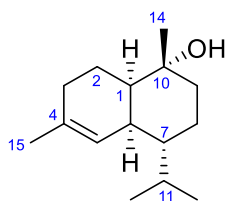
Chemical Formula: C₃₂H₅₄O₂

Exact Mass: 470.4124 g/mol

¹H NMR spectroscopic data δ ppm, 300 Hz in CDCl₃
see Table 2.18

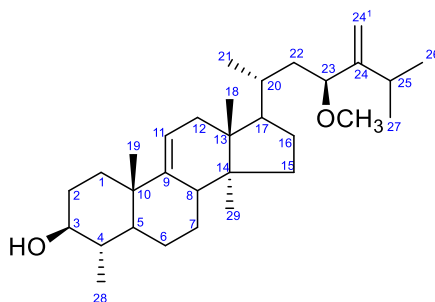
¹³C NMR spectroscopic data δ ppm, 75 Hz in CDCl₃
see Table 2.18

2.12.4 MS4



IUPAC name:	-
Common name:	T-muurolol
Appearance:	colorless viscous liquid;
Melting Point:	-
Optical rotation:	-
CD:	-
UV:	-
IR:	(thin film): ν_{\max} , cm^{-1} ; 3326, 2962, 1670, 1453, 1374, 1300, 1238, 1191, 1144 and 1028
HRESIMS:	m/z (relative intensity), 70 eV; 205.1957 $[\text{M}-\text{H}_2\text{O}+\text{H}]^+$ (calcd. for $\text{C}_{15}\text{H}_{25}$, 205.1956)
Chemical Formula:	$\text{C}_{15}\text{H}_{26}\text{O}$
Exact Mass:	222.1984 g/mol
^1H NMR spectroscopic data	δ ppm, 300 Hz in CDCl_3 see Table 2.19
^{13}C NMR spectroscopic data	δ ppm, 75 Hz in CDCl_3 see Table 19

2.12.5 MS5



IUPAC name: (3 β ,23 S)-23-methoxy-24-methylenenorlanost-9-en-3-ol

Common name: -

Appearance: colorless plate (ethanol:ethyl acetate, 8:1)

Melting Point: 140-142 °C

Optical rotation: $[\alpha]_D^{23} +88.5$ (c 0.15, CHCl₃)

CD: -

UV: -

IR: (thin film): ν_{\max} , cm⁻¹;
3371, 2935, 2870, 1647, 1456, 1373, 1108,
1085, 1041, 968, 904 and 758

HRESIMS: m/z (relative intensity), 70 eV;
474.4296 [M+NH₄]⁺ (calcd. for C₃₁H₅₆NO₂,
474.4310)

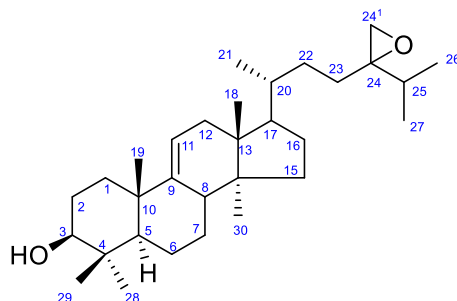
Chemical Formula: C₃₁H₅₂O₂

Exact Mass: 456.3967 g/mol

¹H NMR spectroscopic data δ ppm, 300 Hz in CDCl₃
see Table 2.20

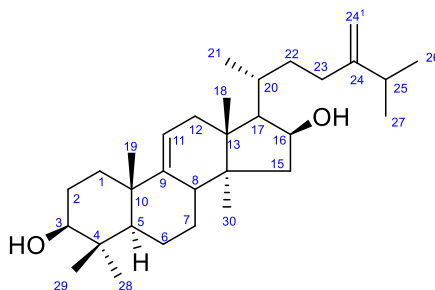
¹³C NMR spectroscopic data δ ppm, 75 Hz in CDCl₃
see Table 2.20

2.12.6 MS6



IUPAC name:	(3 β)-24,24 ¹ -epoxy-lanost-9-en-3-ol
Common name:	-
Appearance:	colorless plate (ethanol/ethyl acetate)
Melting Point:	-
Optical rotation:	$[\alpha]_D^{23} +48.6$ (c 0.04, CHCl ₃);
CD:	-
UV:	-
IR:	(thin film): ν_{\max} , cm ⁻¹ ; 3405, 2933, 2880, 1641, 1464, 1384, 1245, 1170, 1157, 1117, 1096, 1041, 980 and 885
HRESIMS:	m/z (relative intensity), 70 eV; 457.4023[M+H] ⁺ (calcd. for C ₃₁ H ₅₃ O ₂ , 457.4045)
Chemical Formula:	C ₃₁ H ₅₂ O ₂
Exact Mass:	456.3967 g/mol
¹ H NMR spectroscopic data	δ ppm, 300 Hz in CDCl ₃ see Table 2.21
¹³ C NMR spectroscopic data	δ ppm, 75 Hz in CDCl ₃ see Table 2.21

2.12.7 MS7



IUPAC name: (3 β ,16 β)-24-methylenelanost-9-en-3,16-diol

Common name: -

Appearance: colorless needle (ethanol:ethyl acetate, 8:1)

Melting Point: m.p. 164-165°C

Optical rotation: $[\alpha]_D^{23} +67.2$ (c 0.05, CHCl₃);

CD: -

UV: -

IR: (thin film): ν_{\max} , cm⁻¹;
3406, 2935, 2870, 1639, 1464, 1373, 1096,
1041, 980 and 885

HRESIMS: m/z (relative intensity), 70 eV;
474.4278 [M+NH₄]⁺ (calcd. for C₃₁H₅₆NO₂,
474.4310)

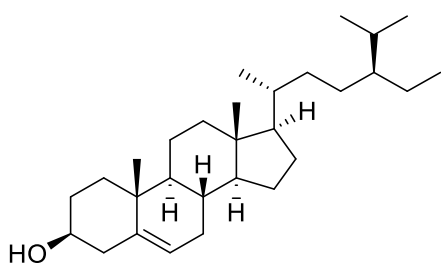
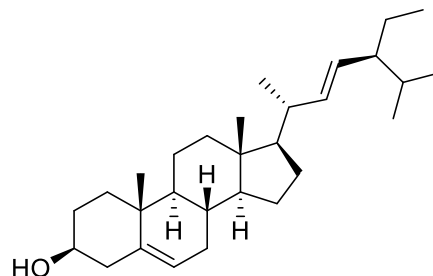
Chemical Formula C₃₁H₅₂O₂

Exact Mass 456.3967 g/mol

¹H NMR spectroscopic data δ ppm, 300 Hz in CDCl₃
see Table 2.22

¹³C NMR spectroscopic data δ ppm, 75 Hz in CDCl₃
see Table 2.22

2.12.8 a mixture of MS8 and MS9

 β -sitosterol

Stigmasterol

IUPAC name:

Common name: mixture of β -sitosterol and stigmasterol

Appearance: colorless needle (ethanol)

Melting Point: -

Optical rotation: -

CD: -

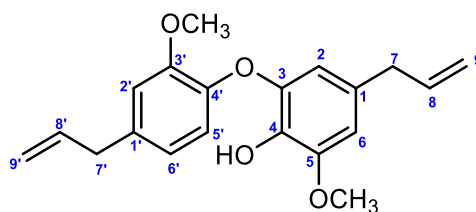
UV: -

IR: (thin film): ν_{\max} , cm^{-1} ;
3492, 2937, 2867, 1641, 1464, 1373, 1096 and
1041

HRESIMS: -

Chemical Formula $\text{C}_{29}\text{H}_{50}\text{O}$ for β -sitosterol, $\text{C}_{29}\text{H}_{48}\text{O}$ for
stigmasterolExact Mass 414.7180 g/mol for β -sitosterol,
412.7020 g/mol for stigmasterol ^1H NMR spectroscopic data δ ppm, 300 Hz in CDCl_3
see Table 2.23 ^{13}C NMR spectroscopic data δ ppm, 75 Hz in CDCl_3
see Table 2.23

2.12.9 MS10



IUPAC name: 4-hydroxy-3',5-dimethoxy-3,4'-oxyneolign-8,8'-dien

Common name: dehydrodieugenol B

Appearance: pale green-brown viscous liquid;

Melting Point: -

Optical rotation: -

CD: -

UV: (MeOH) λ_{\max} (log ϵ), nm;
205 (4.78), 230 (4.26), 277 (3.80)

IR: (thin film): ν_{\max} , cm^{-1} ;
3439, 1638, 1597, 1505, 1454, 1434, 1314,
1265, 1213, 1129, 1083, 1034, 994, 914 and 832

HRESIMS: m/z (relative intensity), 70 eV;
325.1442 $[\text{M}-\text{H}]^+$ (calcd. for $\text{C}_{20}\text{H}_{21}\text{O}_4$,
325.1440)

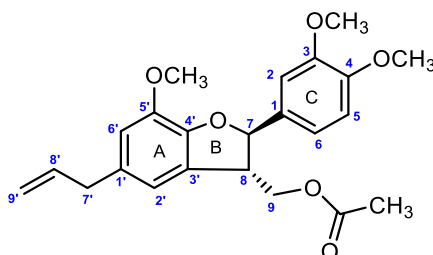
Chemical Formula $\text{C}_{20}\text{H}_{22}\text{O}_4$

Exact Mass 326.1518 g/mol

^1H NMR spectroscopic data δ ppm, 300 Hz in CDCl_3
see Table 2.24

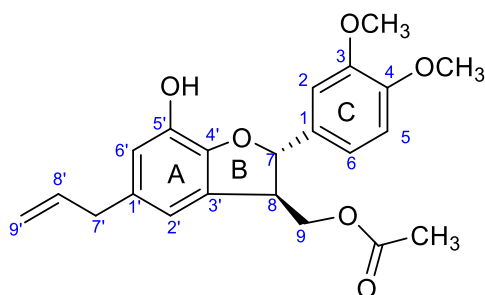
^{13}C NMR spectroscopic data δ ppm, 75 Hz in CDCl_3
see Table 2.24

2.12.10 MS11



IUPAC name:	(7 <i>R</i> ,8 <i>S</i>)-3,4,5'-trimethoxy-4',7-epoxy-8,3'-neolign-8'-en-9-acetate
Common name:	-
Appearance:	pale green-brown viscous liquid
Melting Point:	-
Optical rotation:	$[\alpha]_D^{28} -10.5$ (c 0.07, CHCl ₃);
CD	(c 3.73×10^{-4} M, MeOH) λ_{\max} ($\Delta\epsilon$), nm; 228 (+0.18), 242 (-2.44), 290 (-1.84)
UV:	(MeOH) λ_{\max} (log ϵ), nm; 204 (4.85), 230 (4.32), 277 (3.85)
IR:	(thin film): ν_{\max} , cm ⁻¹ ; 1726, 1605, 1516, 1498, 1464, 1329, 1252, 1218, 1143 and 1027
HRESIMS:	m/z (relative intensity), 70 eV; 421.1626 [M+Na] ⁺ (calcd. for C ₂₃ H ₂₆ O ₆ Na, 421.1627)
Chemical Formula	C ₂₃ H ₂₆ O ₆
Exact Mass	398.1729 g/mol
¹ H NMR spectroscopic data	δ ppm, 300 Hz in CDCl ₃ see Table 2.25
¹³ C NMR spectroscopic data	δ ppm, 75 Hz in CDCl ₃ see Table 2.25

2.12.11 MS12



IUPAC name: (7*S*,8*R*)-5'-hydroxy-3,4-dimethoxy-4',7-epoxy-8,3'-neolign-8'-en-9-acetate

Common name: -

Appearance: pale yellow crystals (EtOH)

Melting Point: 118-119 °C

Optical rotation: $[\alpha]_D^{28} +43.4$ (c 0.05, CHCl₃);

CD (c 3.73×10^{-4} M, MeOH) λ_{\max} ($\Delta\epsilon$), nm; 227 (-1.47), 241 (+1.02), 292 (+2.14)

UV: (MeOH) λ_{\max} (log ϵ), nm; 204 (4.91), 230 (4.38), 277 (3.98)

IR: (thin film): ν_{\max} , cm⁻¹; 3421, 1740, 1610, 1516, 1493, 1333, 1262, 1238, 1139 and 1028

HRESIMS: m/z (relative intensity), 70 eV; 407.1462 [M+Na]⁺ (calcd. for C₂₂H₂₄O₆Na, 407.1471)

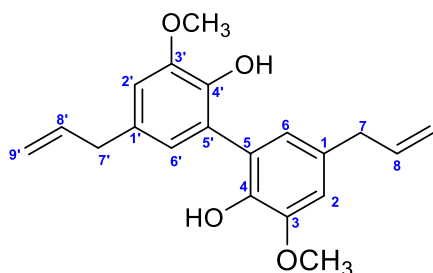
Chemical Formula C₂₂H₂₄O₆

Exact Mass 384.1573 g/mol

¹H NMR spectroscopic data δ ppm, 300 Hz in CDCl₃
see Table 2.26

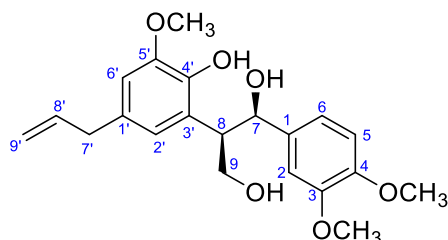
¹³C NMR spectroscopic data δ ppm, 75 Hz in CDCl₃
see Table 2.26

2.12.12 MS13



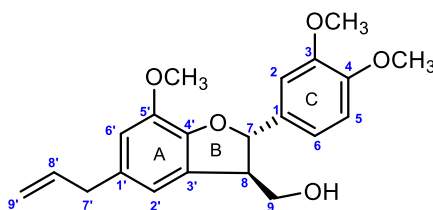
IUPAC name:	4,4'-dihydroxy-3,3'-dimethoxy-5,5'-neolign-8,8'-dien
Common name:	dehydrodieugenol A
Appearance:	pale yellow crystals (EtOH)
Melting Point:	118-119 °C
Optical rotation:	-
CD	-
UV:	(MeOH) λ_{\max} (log ϵ), nm; 219 (4.65), 253 (4.01), 290 (3.83)
IR:	(thin film): ν_{\max} , cm^{-1} ; 3252, 1639, 1599, 1490, 1467, 1454, 1424, 1327, 1257, 1229, 1145, 1047, 996, 907 and 852
HRESIMS:	m/z (relative intensity), 70 eV; 325.1447 [M-H] ⁺ (calcd. for C ₂₀ H ₂₂ O ₄ , 325.1440)
Chemical Formula	C ₂₀ H ₂₂ O ₄
Exact Mass	326.1518 g/mol
¹ H NMR spectroscopic data	δ ppm, 300 Hz in CDCl ₃ see Table 2.27
¹³ C NMR spectroscopic data	δ ppm, 75 Hz in CDCl ₃ see Table 2.27

2.12.13 MS14



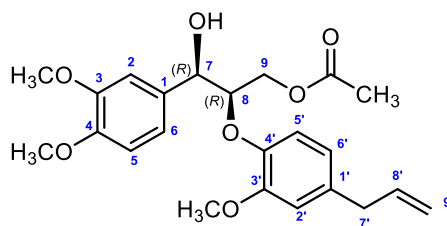
IUPAC name:	(7 <i>R</i> ,8 <i>R</i>)-4'-hydroxy-3,4,5'-trimethoxy-8,3'-neolign-8'-en-7,9-diol
Common name:	-
Appearance:	pale green-brown viscous liquid
Melting Point:	-
Optical rotation:	$[\alpha]_D^{28} -86.9$ (c 0.05, CHCl ₃);
CD	(c 4.06 × 10 ⁻⁴ M, MeOH) λ_{\max} ($\Delta\epsilon$), nm; 229 (-5.12), 248 (+1.15), 277 (-0.58), 295 (+0.17)
UV:	(MeOH) λ_{\max} (log ϵ), nm; 204 (4.87), 230 (4.31), 281 (3.81)
IR:	(thin film): ν_{\max} , cm ⁻¹ ; 3520, 1603, 1516, 1496, 1463, 1310, 1265, 1216, 1139 and 1027
HRESIMS:	m/z (relative intensity), 70 eV; 379.1513 [M+Na-H ₂ O] ⁺ (calcd. for C ₂₁ H ₂₄ O ₅ Na, 379.1522)
Chemical Formula	C ₂₁ H ₂₆ O ₅
Exact Mass	374.1729 g/mol
¹ H NMR spectroscopic data	δ ppm, 300 Hz in CDCl ₃ see Table 2.28
¹³ C NMR spectroscopic data	δ ppm, 75 Hz in CDCl ₃ see Table 2.28

2.12.14 MS15



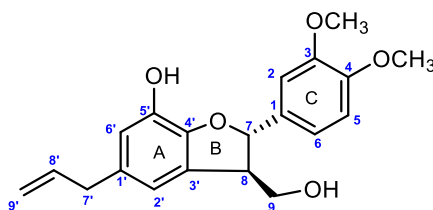
IUPAC name:	(7 <i>S</i> ,8 <i>R</i>)-3,4,5'-trimethoxy-4',7-epoxy-8,3'-neolign-8'-en-9-ol
Common name:	-
Appearance:	pale green-brown viscous liquid
Melting Point:	-
Optical rotation:	$[\alpha]_D^{28} +16.2$ (c 0.07, CHCl ₃);
CD	(c 3.78×10^{-4} M, MeOH) λ_{\max} ($\Delta\epsilon$), nm; 229 (-5.12), 248 (+1.15), 277 (-0.58), 295 (+0.17)
UV:	(MeOH) λ_{\max} (log ϵ), nm; 204 (4.86), 230 (4.32), 281 (3.84)
IR:	(thin film): ν_{\max} , cm ⁻¹ ; 3515, 1604, 1516, 1497, 1464, 1327, 1263, 1237, 1212, 1140 and 1027
HRESIMS:	m/z (relative intensity), 70 eV; 379.1526 [M+Na] ⁺ (calcd. for C ₂₁ H ₂₄ O ₅ Na, 379.1522)
Chemical Formula	C ₂₁ H ₂₄ O ₅
Exact Mass	356.1624 g/mol
¹ H NMR spectroscopic data	δ ppm, 300 Hz in CDCl ₃ see Table 2.29
¹³ C NMR spectroscopic data	δ ppm, 75 Hz in CDCl ₃ see Table 2.29

2.12.15 MS16



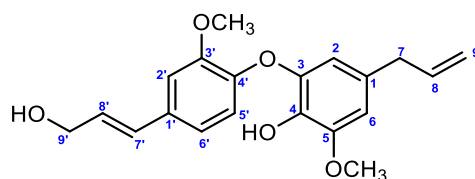
IUPAC name:	<i>threo</i> -(7 <i>R</i> ,8 <i>R</i>)-3,3',4-trimethoxy-8,4'-oxyneolign-8'-en-7-ol-9-acetate
Common name:	-
Appearance:	pale green-brown viscous liquid
Melting Point:	-
Optical rotation:	$[\alpha]_D^{28} -58.8$ (<i>c</i> 0.08, CHCl ₃);
CD	(<i>c</i> 4.70 × 10 ⁻⁴ M, MeOH) λ _{max} (Δε), nm; 208 (+3.09), 238 (-1.41)
UV:	(MeOH) λ _{max} (log ε), nm; 203 (4.94), 230 (4.34), 281 (3.91)
IR:	(thin film): ν _{max} , cm ⁻¹ ; 3486, 1740, 1591, 1511, 1464, 1419, 1264, 1234, 1140 and 1029
HRESIMS:	<i>m/z</i> (relative intensity), 70 eV; 439.1729 [M+Na] ⁺ (calcd. for C ₂₃ H ₂₈ O ₇ Na, 439.1733)
Chemical Formula	C ₂₃ H ₂₈ O ₇
Exact Mass	416.1835 g/mol
¹ H NMR spectroscopic data	δ ppm, 300 Hz in CDCl ₃ see Table 2.30
¹³ C NMR spectroscopic data	δ ppm, 75 Hz in CDCl ₃ see Table 2.30

2.12.16 MS17



IUPAC name:	(7 <i>S</i> ,8 <i>R</i>)-5'-hydroxy-3,4-dimethoxy-4',7-epoxy-8,3'-neolign-8'-en-9-ol
Common name:	-
Appearance:	pale green-brown viscous liquid
Melting Point:	-
Optical rotation:	$[\alpha]_D^{28} +9.1$ (c 0.09, CHCl ₃)
CD	(c 4.25 × 10 ⁻⁴ M, MeOH) λ_{\max} ($\Delta\epsilon$), nm; 227 (-2.13), 245 (+1.19), 292 (+1.85)
UV:	(MeOH) λ_{\max} (log ϵ), nm; 205 (4.82), 230 (4.34), 277 (3.89)
IR:	(thin film): ν_{\max} , cm ⁻¹ ; 3436, 1609, 1516, 1493, 1463, 1334, 1263, 1236, 1139 and 1025
HRESIMS:	m/z (relative intensity), 70 eV; 365.1364 [M+Na] ⁺ (calcd. for C ₂₀ H ₂₂ O ₅ Na, 365.1365)
Chemical Formula	C ₂₀ H ₂₂ O ₅
Exact Mass	342.1467 g/mol
¹ H NMR spectroscopic data	δ ppm, 300 Hz in CDCl ₃ see Table 2.31
¹³ C NMR spectroscopic data	δ ppm, 75 Hz in CDCl ₃ see Table 2.31

2.12.17 MS18



IUPAC name: 4-hydroxy-3',5-dimethoxy-3,4'-oxyneolign-7',8-dien-9'-ol

Common name: -

Appearance: pale green-brown viscous liquid

Melting Point: -

Optical rotation: -

CD: -

UV: (MeOH) λ_{\max} (log ϵ), nm;
205 (4.50), 230 (4.20), 299 (4.00)

IR: (thin film): ν_{\max} , cm^{-1} ;
3450, 1632, 1597, 1505, 1454, 1434, 1314,
1265, 1213, 1129, 1083, 1034, 994 and 914

HRESIMS: m/z (relative intensity), 70 eV;
341.1392 $[\text{M}-\text{H}]^+$ (calcd. for $\text{C}_{20}\text{H}_{21}\text{O}_5$,
341.1389)

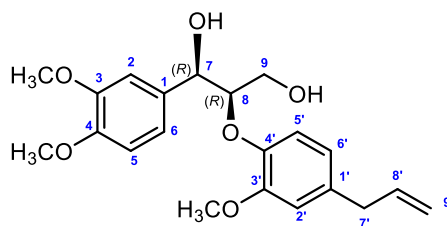
Chemical Formula $\text{C}_{20}\text{H}_{22}\text{O}_5$

Exact Mass 342.1467 g/mol

^1H NMR spectroscopic data δ ppm, 300 Hz in CDCl_3
see Table 2.32

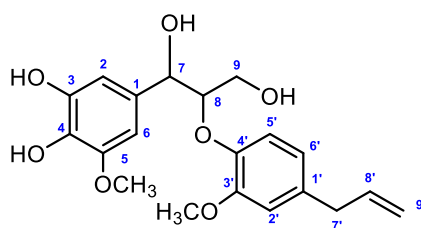
^{13}C NMR spectroscopic data δ ppm, 75 Hz in CDCl_3
see Table 2.32

2.12.18 MS19



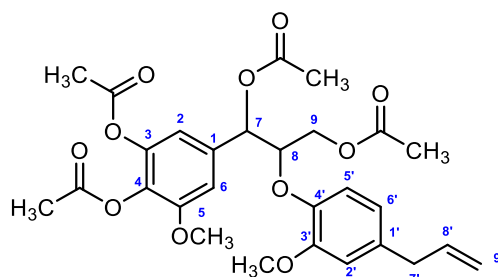
IUPAC name:	<i>threo</i> -(7 <i>R</i> ,8 <i>R</i>)-3,3',4-trimethoxy-8,4'-oxyneolign-8'-en-7,9-diol
Common name:	-
Appearance:	pale green-brown viscous liquid
Melting Point:	-
Optical rotation:	$[\alpha]_{\text{D}}^{28} -66.2$ (c 0.14, CHCl ₃);
CD	(c 4.69×10^{-4} M, MeOH) λ_{max} ($\Delta\epsilon$), nm; 208 (+5.89), 237 (-4.25)
UV:	(MeOH) λ_{max} (log ϵ), nm; 204 (4.93), 230 (4.32), 281 (3.84)
IR:	(thin film): ν_{max} , cm ⁻¹ ; 3473, 1592, 1511, 1464, 1419, 1263, 1228, 1139 and 1028
HRESIMS:	m/z (relative intensity), 70 eV; 397.1622 [M+Na] ⁺ (calcd. for C ₂₁ H ₂₆ O ₆ Na, 397.1627)
Chemical Formula	C ₂₁ H ₂₆ O ₆
Exact Mass	374.1729 g/mol
¹ H NMR spectroscopic data	δ ppm, 300 Hz in CDCl ₃ see Table 2.33
¹³ C NMR spectroscopic data	δ ppm, 75 Hz in CDCl ₃ see Table 2.33

2.12.19 MS20



IUPAC name:	<i>threo</i> -3,4-dihydroxy-3',5-dimethoxy-8,4'-oxyneolign-8'-en-7,9-diol
Common name:	-
Appearance:	pale green-brown viscous liquid
Melting Point:	-
Optical rotation:	$[\alpha]_D^{28}$ -27.0 (c 0.03, MeOH);
CD	(c 3.73×10^{-4} M, MeOH) λ_{\max} ($\Delta\epsilon$), nm; 208 (+0.90), 235 (-0.55)
UV:	(MeOH) λ_{\max} (log ϵ), nm; 205(4.84), 230(4.38), 276(3.88)
IR:	(thin film): ν_{\max} , cm^{-1} ; 3400, 1596, 1508, 1454, 1433, 1264, 1214, 1130 and 1086
HRESIMS:	m/z (relative intensity), 70 eV; 399.1411 $[\text{M}+\text{Na}]^+$ (calcd. for $\text{C}_{20}\text{H}_{24}\text{O}_7\text{Na}$, 399.1420)
Chemical Formula	$\text{C}_{20}\text{H}_{24}\text{O}_7$
Exact Mass	374.1729 g/mol
^1H NMR spectroscopic data	δ ppm, 300 Hz in CDCl_3 see Table 2.34
^{13}C NMR spectroscopic data	δ ppm, 75 Hz in CDCl_3 see Table 2.34

2.12.20 MS20a



IUPAC name: *threo*-3',5-dimethoxy-8,4'-neolign-8'-en-3,5,7,9-tetracetate

Common name: -

Appearance: pale green-brown viscous liquid

Melting Point: -

Optical rotation: -

CD: -

UV: (MeOH) λ_{\max} (log ϵ), nm;
206(4.79), 230(4.37), 276(3.67)

IR: (thin film): ν_{\max} , cm^{-1} ;
1748, 1612, 1507, 1430, 1371, 1217, 1152 and 1096,
1036

HRESIMS: m/z (relative intensity), 70 eV;
567.1840 $[\text{M}+\text{Na}]^+$ (calcd. for $\text{C}_{28}\text{H}_{32}\text{O}_{11}\text{Na}$,
567.1843)

Chemical Formula $\text{C}_{28}\text{H}_{32}\text{O}_{11}$

Exact Mass 544.1945 g/mol

^1H NMR spectroscopic data δ ppm, 300 Hz in CDCl_3
see Table 2.35

^{13}C NMR spectroscopic data δ ppm, 75 Hz in CDCl_3
see Table 2.35

Table 2.16 ^1H NMR (300 Hz), ^{13}C NMR (75 MHz) and HMBC NMR data for **MS1** in CDCl_3 (J in Hz in parentheses).

Position	MS1				δ_{H} (ppm)	δ_{C} (ppm)	HMBC ($\text{H} \rightarrow \text{C}$)		δ_{H} (ppm)	δ_{C} (ppm)
	δ_{H} (ppm)	δ_{C} (ppm)	2J	3J			δ_{H} (ppm)	δ_{C} (ppm)		
1	0.47 (1H, dd, 11.1, 9.9)	30.0	C-2, C-11	C-3, C-9, C-13	0.47 (1H, dd, 11.6, 9.6)	29.9				
2	0.71 (1H, ddd)	27.5	C-1, C-3, C-11	C-10	0.71	27.5				
3a	0.99 (1H, m)	24.7	C-4	C-5	1.01	24.8				
3b	1.94 (1H, m)				1.96					
4a	2.01 (1H, overlapped)	38.0	C-3, C-5	C-2, C-6, C-11	2.05	38.9				
4b	2.42 (1H, dd, 13.5, 6.3)				2.42 (1H, dd, 13.6, 5.2)					
5	-	153.4				153.5				
6	2.19 (1H, m)	53.4	C-5, C-10	C-1, C-4, C-14	2.20	53.4				
7a	1.61 (1H, m)	26.7	C-6, C-8	C-9, C-9, C-10	1.64					
7b	1.88 (1H, m)				1.91					
8a	1.56 (1H, m)	41.8	C-7, C-10	C-6, C-10, C-15	1.54	41.8				
8b	1.77 (1H, m)				1.77					
9	-	80.9				81.0				
10	1.29 (1H, overlapped)	54.3	C-1, C-6, C-9	C-5, C-11	1.31	54.4				
11	-	20.2				20.3				
12	1.04 (3H, s)	28.7	C-11	C-1, C-2, C-13	1.05	28.7				
13	1.05 (3H, s)	16.3	C-11	C-1, C-2, C-12	1.04	16.3				
14a	4.66 (1H, <i>br s</i>)	106.3	C-5	C-4, C-6	4.66	106.3				
14b	4.69 (1H, <i>br s</i>)				4.68					
15	1.28 (3H, <i>br s</i>)	26.1	C-9,	C-8, C-10,	1.28	26.1				

^a [29]

Table 2.17 ^1H NMR (300 Hz) and ^{13}C NMR (75 MHz) data for **MS2** in CDCl_3 (J in Hz in parentheses).

Position	MS2		phytol ^a	
	δ_{H} (ppm)	δ_{C} (ppm)	δ_{H} (ppm)	δ_{C} (ppm)
1	4.15 (d, 6.8)	59.4	4.16 (d)	59.30
2	5.41 (tq, 7.0, 1.3)	123.1	5.39 (t)	123.09
3	-	140.2		140.23
4	1.99 (m)	39.8	1.97 (m)	39.85
5	1.42 (m), 1.37 (m)	25.1	1.40 (m), 1.36 (m)	25.12
6	1.26 (m), 1.07 (m)	36.6	1.24 (m), 1.05 (m)	36.65
7	1.37 (m)	32.7	1.35 (m)	32.67
8	1.25 (m), 1.06 (m)	37.3	1.23 (m), 1.03 (m)	37.65
9	1.31 (m), 1.17 (m)	24.4	1.29 (m), 1.15 (m)	24.45
10	1.25 (m), 1.06 (m)	37.4	1.23 (m), 1.03 (m)	37.41
11	1.37 (m)	32.8	1.35 (m)	32.77
12	1.25 (m), 1.06 (m)	37.3	1.23 (m), 1.03 (m)	37.28
13	1.27 (m)	24.8	1.25 (m)	24.78
14	1.13 (m), 1.06(m)	39.4	1.11 (m), 1.03 (m)	39.35
15	1.52 (hp)	28.0	1.50 (hp)	27.95
16	0.87 (d, 6.6)	22.6	0.84 (d)	22.60
17	0.87 (d, 6.6)	22.7	0.84 (d)	22.69
18	0.85 (d, 6.5)	19.7	0.83 (d)	19.69
19	0.84 (d, 6.5)	19.7	0.82 (d)	19.72
20	1.67 (<i>b s</i>)	16.2	1.65 (s)	16.14

^a [30]

Table 2.18 ^1H NMR (300 Hz), ^{13}C NMR (75 MHz) and HMBC NMR data for **MS3** in CDCl_3 (J in Hz in parentheses).

Position	δ_{H} (ppm)	δ_{C} (ppm)	HMBC (H \rightarrow C)	
			2J	3J
1	1.45 (m), 1.78(m)	36.2	C-10	C-19
2	1.33 (m), 1.65 (m)	28.1	C-1	
3	3.21, (overlapped)	78.9	C-2	C-28, C-29
4	-	39.1		
5	0.87 (m)	52.5	C-10, C-4	C-1, C-7, C-28, C-29
6	1.48 (m), 1.69 (m)	21.4	C-5, C-7	C-8, C-10
7	1.65 (m), 1.77 (m)	27.8	C-6	C-5, C-9
8	2.14 (m)	41.8	C-9	C-11, C-13, C-30
9	-	148.6		
10	-	39.4		
11	5.23, (<i>br</i> d, 5.9)	114.9	C-12	C-8, C-10, C-13
12	1.93 (m), 2.08 (m)	37.3	C-11	C-9, C-14
13	-	44.6		
14	-	47.1		
15	1.34 (m)	33.8	C-14, C-16	C-13
16	1.33 (m), 1.87 (m)	28.1	C-17	C-13, C-14
17	1.56 (m)	51.7	C-13, C-16, C-20	C-12, C-15, C18
18	0.68 (s)	14.5	C-13	C-12, C-14, C-17
19	1.05 (s)	22.3	C-10	C-1, C-5, C-9
20	1.67 (m)	33.0	C-17	C-16
21	0.92 (d, 6.3)	18.3	C-20	C-17, C-22
22	1.01 (m), 1.66 (m)	43.2	C-23	C-24
23	3.59 (dd, 9.3, 1.0)	81.7	C-22, C-24	C-20, C-24 ¹ , C-25, 23-OCH ₃
24	-	156.6		
24 ¹	4.92 (s), 4.98 (s)	107.4	C-24	C-23, C-25
25	2.17 (m)	29.9	C-24, C-26, C-27	C-23, C-24 ¹
26	1.05 (d, 7.1)	23.5	C-25	C-24
27	1.07 (d, 7.1)	22.5	C-25	C-24
28	0.82 (s)	15.7	C-4	C-3, C-5
29	0.99 (s)	28.3	C-4	C-3, C-5
30	0.73 (s)	18.5	C-14	C-8, C-13, C-15
23-OMe	3.22 (s)	56.3		C-23

Table 2.19 ^1H NMR (300 Hz), ^{13}C NMR (75 MHz) and HMBC NMR data for **MS4**

Position	MS-4			T-muurolool ^a			T-cardinol ^b			α -cardinol ^b		
	δ_{H} (ppm)	δ_{C} (ppm)	HMBC (H \rightarrow C)			δ_{H} (ppm)	δ_{C} (ppm)	δ_{H} (ppm)	δ_{C} (ppm)	δ_{H} (ppm)	δ_{C} (ppm)	
			² J	³ J	³ J							
1	1.58 (m)	45.8	C-2, C-10	C-7	1.47 (1H, m)	46.4	47.9	50.0				
2a	1.11 (m)	21.6	C-1,	C-6, C-10	1.43 (2H, m)	21.3	22.6	22.0				
2b	1.51 (m)											
3a	2.00 (m)	31.1	C-1		1.87 (2H, m)	31.6	30.9	31.0				
3b												
4	-	134.4				133.5	134.4	134.9				
5	5.52 (dd, 5.4, 1.5)	124.6	C-4, C-6	C-1, C-3, C-15	5.68 (1H, d, 5.6)	125.8	5.52 (s)	122.4				
6	2.01 (m)	36.8	C-1, C-5, C-7	C-3, C-8	2.46 (1H, m)	34.8	37.7	39.9				
7	1.30 (m)	44.1	C-8	C-1, C-9, C-12	1.29 (1H, m)	44.5	46.6	46.7				
8a	1.56 (m)	18.3	C-6	C-1, C-9, C-12	1.28 (1H, m)	19.8	19.8	22.7				
8b	1.91 (m)		C-3		1.50 (1H, m)							
9a	1.51 (m)	35.3	C-8, C-10	C-1, C-7, C-14	1.28 (1Hm)	35.0	40.3	42.2				
9b	1.56 (m)				1.43 (1H, m)							
10	-	72.5				72.4	70.7	72.5				
11	1.97 (m)	26.4	C-6, C-7, C-12, C-13		2.08	27.1	2.16 (m)	26.0				
12	0.89 (d, 7.0)	21.7	C-11	C-7, C-13	(1H, dsept, J = 6.9, 2.7)	21.9	0.88 (d, 7.0)	21.5				
13	0.81 (d, 7.0)	15.3	C-11	C-7, C-12	0.91 (3H, d, 6.8)	15.4	0.76 (d, 7.0)	15.1				
14	1.30 (s)	28.0	C-10	C-1, C-9	0.90 (3H, d, 6.7)	29.6	1.19 (s)	20.8				
15	1.66 (s)	23.6	C-4	C-3, C-5	1.05 (3H, s)	23.9	1.70 (s)	23.8				

^a [31]; ^b [32]

Table 2.20 ^1H NMR (300 Hz), ^{13}C NMR (75 MHz) and HMBC NMR data for **MS5** in CDCl_3 (J in Hz in parentheses).

Position	δ_{H} (ppm)	δ_{C} (ppm)	HMBC (H \rightarrow C)	
			2J	3J
1	1.40 (m), 1.83 (m)	35.4	C-10	C-3, C-5, C-19
2	1.56 (m), 1.91 (m)	31.2	C-1, C-3	
3	3.08, (td, 11.5, 3.0)	76.5	C-2, C-4	C-5, C-28
4	1.32 (m)	39.4	C-3, C-5	C-10
5	0.80 (m)	49.3	C-4, C-6, C-10	C-1, C-3, C-7
6	1.21 (m), 1.79 (m)	24.0	C-5, C-7	C-4, C-8, C-10
7	1.31 (m), 1.63 (m)	27.4	C-6, C-8	C-5, C-9
8	2.17 (m)	41.3	C-7, C-9, C-14	C-11, C-13
9	-	146.5		
10	-	38.7		
11	5.23, (dd, 3.6, 2.8)	116.4	C-9, C-12	C-8, C-10, C-13
12	1.97 (m), 2.07(m)	37.5	C-11, C-13	C-9, C-14, C-18
13	-	44.4		
14	-	47.2		
15	1.37(m)	33.9	C-14, C-16	C-8, C-13, C-17
16	1.36 (m), 1.90 (m)	28.1	C-15, C-17	C-13, C-14, C-20
17	1.55 (m)	51.7	C-13, C-16, C-20	C-12, C-15
18	0.69 (s)	14.6	C-13	C-12, C-14, C-17
19	0.99 (s)	20.5	C-10	C-1, C-5, C-9
20	1.67 (m)	33.0	C-17, C-22	C-21
21	0.92 (d, 6.4)	18.2	C-20	C-17, C-22
22	1.02 (m), 1.68 (m)	43.2	C-23	C-24
23	3.60 (dd, 10.3, 1.4)	81.7	C-22, C-24,	C-20, C-24 ¹ , C-25, 23-OCH ₃
24	-	156.6		
24 ¹	4.92 (s), 4.98 (s)	107.4	C-24	C-23, C-25
25	2.17 (m)	29.9	C-24, C-26, C-27	C-23, C-24 ¹
26	1.05 (d, 7.0)	23.5	C-25	C-24
27	1.07 (d, 7.4)	22.5	C-25	C-24
28	0.97 (d, 6.3)	15.3	C-4	C-3, C-5
29	0.73 (s)	18.3	C-14	C-8, C-13, C-15,
23-OMe	3.21 (s)	56.4	C-23	

Table 2.21 ^1H NMR (300 Hz), ^{13}C NMR (75 MHz) and HMBC NMR data for **MS6** in CDCl_3 (J in Hz in parentheses).

Position	δ_{H} (ppm)	δ_{C} (ppm)	HMBC (H \rightarrow C)	
			2J	3J
1	1.44 (m), 1.79 (m)	36.1	C-10, C-2	C-3, C-5, C-19
2	1.65 (m), 1.75 (m)	28.0	C-1, C-3	C-4, C-10
3	3.21, (m)	78.9	C-2, C-4	C-1, C-5, C-28, C-29
4		39.2		
5	0.88 (m)	52.5	C-4, C-6, C-10	C-1, C-7
6	1.49 (m), 1.69 (m)	21.4	C-5, C-7	C-4, C-8, C-10
7	1.65 (m), 1.92 (m)	27.8	C-6, C-8	C-5, C-9
8	1.92 (m)	41.8	C-9, C-14	C-11, C-13, C-15
9	-	148.6		
10	-	39.4		
11	5.21, (bd, 6.03)	114.9	C-9, C-12	C-8, C-10, C-13
12	1.89 (m), 2.07(m)	37.2	C-11, C-13	C-9, C-14, C-18
13	-	44.3		
14	-	47.0		
15	1.34 (m), 1.39 (m)	33.9	C-14, C-16	C-8, C-13, C-17
16	1.32 (m), 1.65 (m)	28.1	C-15, C-17	C-13, C-14, C-20
17	1.62 (m)	50.8	C-20	
18	0.64 (s)	14.4	C-13	C-12, C-14, C-17
19	1.04 (s)	22.3	C-10	C-1, C-5, C-9
20	1.45 (m)	36.2	C-17, C-22	C-21
21	0.89 (d, 6.9)	18.3	C-20	C-17, C-22
22	1.04 (m), 1.47 (m)	30.7	C-20, C-23	C-24
23	1.46 (m), 1.68 (m)	28.5	C-22, C-24,	C-20, C-24 ¹
24	-	62.8		
24 ¹	2.54 (d, 4.6) 2.59 (d, 4.6)	50.5	C-24	C-23, C-25
25	1.79 (m)	31.7	C-24, C-26, C-27	C-23, C-24 ¹
26	0.96 (d, 6.8)	18.4	C-25	C-24, C-27
27	0.90 (d, 6.8)	17.7	C-25	C-24, C-26
28	0.82 (s)	15.7	C-4	C-3, C-5, C-29
29	0.99 (s)	28.3	C-4	C-3, C-5, C-28
30	0.73 (s)	18.5	C-14	C-8, C-13, C-15

Table 2.22 ^1H NMR (300 Hz), ^{13}C NMR (75 MHz) and HMBC NMR data for **MS7** in CDCl_3 (J in Hz in parentheses).

Position	δ_{H} (ppm)	δ_{C} (ppm)	HMBC (H→C)	
			2J	3J
1	1.44 (m), 1.79 (m)	36.1	C-10	C-3, C-5,
2	1.30 (m), 1.60 (m)	28.0	C-3,	
3	3.21, (td, 11.0, 4.3)	78.9	C-2, C-4	C-1, C-28, C-29
4	-	38.9		
5	0.87 (m)	52.4		C-3
6	1.50 (m), 1.70 (m)	21.3	C-5, C-7	C-4, C-8
7	1.67 (m), 1.77 (m)	27.8		C-5, C-8
8	2.25 (m)	41.7		C-30
9	-	148.6		
10	-	39.4		
11	5.21, (bd, 3.9, 2.0)	114.7	C-12	C-8, C-10, C-13
12	1.88 (m), 2.05 (m)	37.1	C-11, C-13	C-9, C-14
13	-	44.3		
14	-	44.9		
15	1.43 (m), 2.05 (m)	46.4	C-14, C-16	C-8, C-13, C-17
16	4.43 (dd, 12.4, 2.8)	72.7		C-13, C-14
17	1.70 (m)	55.0	C-13, C-16, C-20	C-12, C-15, C-22
18	0.83 (s)	15.3	C-13	C-12, C-14, C-17
19	1.06 (s)	22.3	C-10	C-1, C-5, C-9
20	1.78 (m)	30.2	C-17	
21	0.98 (d, 6.2)	18.0	C-20	C-17, C-22
22	1.18 (m), 1.73 (m)	35.4	C-20, C-23	C-17
23	1.97 (m), 2.19 (m)	31.6	C-22	C-20, C-25
24	-	157.0		
24 ¹	4.70 (s), 4.75 (s)	106.2	C-24	C-23, C-25
25	2.23 (m)	34.0	C-24	C-23, C-24 ¹
26	1.03 (d, 6.8)	21.9	C-25, C-27	C-24, C-24 ¹
27	1.03 (d, 6.8)	21.8	C-25, C-26	C-24, C-24 ¹
28	0.82 (s)	15.7	C-4	C-3, C-5, C-29
29	0.99 (s)	28.2	C-4	C-3, C-5, C-28
30	0.72 (s)	19.1	C-14	C-8, C-13

Table 2.23 ^1H NMR (300 Hz) data for a mixture of **MS8** and **MS9** in CDCl_3 (J in Hz in parentheses).

Position	a mixture of MS8 and MS9		β -sitosterol ^a		stigmasterol ^b	
	δ_{H} (ppm)	δ_{C} (ppm)	δ_{H} (ppm)	δ_{C} (ppm)	δ_{H} (ppm)	δ_{C} (ppm)
1	-	37.6	-	37.5	-	37.4
2	-	32.0	-	31.9	-	28.4
3	3.53 (m)	72.1	3.49 (, m)	72.0	3.54 (m)	72.0
4	-	42.6	-	42.6	-	39.0
5	-	140.9	-	140.9	-	140.9
6	5.35 (m)	121.9	5.31 (, d, 5.2)	121.9	5.36(t)	121.9
7	-	32.3	-	32.2	-	31.9
8	-	32.3	-	32.2	-	32.1
9	-	50.5	-	50.4	-	50.3
10	-	36.9	-	36.8	-	36.7
11	-	21.4	-	21.4	-	21.3
12	-	40.0	-	40.0	-	40.1
13	-	42.7	-	42.6	-	39.8
14	-	57.1	-	57.0	-	57.0
15	-	24.6	-	24.6	-	24.5
16	-	28.6	-	28.5	-	29.2
17	-	56.4	-	56.3	-	56.1
18	0.68 (s)	12.3	0.64 (s)	12.2	0.63 (s)	12.1
19	1.01(s)	19.8	0.97 (s)	19.7	1.06 (s)	19.1
20	-	36.5	-	36.4	-	40.7
21	0.92 (d, 6.3), 1.02 (d, 6.6)	19.2	0.88 (d, 6.4)	19.1	0.97 (d)	21.4
22	5.16 (dd, 15.3, 8.4)	138.6, 34.3	-	34.2	5.15 (m)	138.5
23	5.01 (dd, 15.3, 8.4)	129.6, 26.4	-	26.3	5.01 (m)	129.5
24	-	46.2	-	46.1	-	51.4
25	-	29.5	-	29.4	-	30.1
26	0.83 (m)	20.3	0.80 (d, 7.2)	20.1	0.88 (d)	19.9
27	0.80 (d, 6.6)	19.4	0.77 (d, 6.8)	19.3	0.78 (d)	22.3
28	-	23.6	-	23.6	-	25.6
29	0.82 (m)	12.4	0.81 (t, 7.2)	12.3	0.81 (t,)	12.1

^a [33]; ^b [34], [35]

Table 2.24 ^1H NMR (300 Hz), ^{13}C NMR (75 MHz) and HMBC NMR data for **MS10** in CDCl_3 (J in Hz in parentheses).

Position	δ_{H} (ppm)	δ_{C} (ppm)	HMBC (H \rightarrow C)	
			2J	3J
1	-	131.0		
2	6.42 (1H, d, 1.5)	111.8	C-1, C-3	C-4, C-6, C-7
3	-	144.4		
4	-	135.2		
5	-	147.9		
6	6.51 (1H, d, 1.5)	107.3	C-1, C-5	C-2, C-4, C-7
7	3.24 (2H, d, 6.6)	39.9	C-1, C-8	C-2, C-6, C-9
8	5.93 (1H, ddt, 16.1, 9.4, 6.6)	137.4	C-7	
9a	5.05 (1H, dd, 16.1, 1.4)			
9b	5.04 (1H, dd, 9.4, 1.4)	115.7	C-8	C-7
1'	-	136.4		
2'	6.81 (1H, d, 1.8)	113.0	C-3'	C-4', C-6', C-7'
3'	-	150.4		
4'	-	144.2		
5'	6.91 (1H, d, 8.1)	119.5	C-4', C-6'	C-1', C-3'
6'	6.72 (1H, dd, 8.1, 1.8)	120.8		C-2', C-4', C-7'
7'	3.38 (1H, d, 6.6)	39.9	C-1', C-8'	C-2', C-6', C-9'
8'	5.99 (1H, ddt, 17.0, 10.4, 6.6)	137.3	C-7'	
9'a	5.11 (1H, dd, 17.0, 1.5)			
9'b	5.10 (1H, dd, 10.4, 1.5)	115.9	C-7'	C-8'
OCH ₃ -5	3.89 (3H, s)	56.2		C-5
OCH ₃ -3'	3.86 (3H, s)	56.0		C-3'

Table 2.25 ^1H NMR (300 Hz), ^{13}C NMR (75 MHz) and HMBC NMR data for **MS11** in CDCl_3 (J in Hz in parentheses).

Position	δ_{H} (ppm)	δ_{C} (ppm)	HMBC (H \rightarrow C)	
			2J	3J
1	-	133.2		
2	6.93 (1H, d, 1.8)	109.3	C-1, C-3	C-6, C-7
3	-	149.1		
4	-	149.1		
5	6.83 (1H, d, 8.8)	111.0	C-4	C-1
6	6.94 (1H, dd, 8.8, 1.8)	118.8	C-1	C-2, C-4, C-7
7	5.46 (1H, d, 7.4)	88.4	C-1, C-8	C-2, C-6, C-9, C-4', C-3'
8	3.78 (1H, pq, 5.6)	50.5	C-7, C-9	C-1, C-4', C-2'
9a	4.45 (1H, dd, 11.1, 5.5)	65.5	C-8	C-7, C-3', OC(O)CH ₃ -9
9b	4.29 (1H, dd, 11.1, 7.7)			
1'	-	133.7		
2'	6.66 (1H, s)	112.7	C-1', C-3'	C-8, C-6', C-4', C-7'
3'	-	127.3		
4'	-	146.4		
5'	-	144.2		
6'	6.66 (1H, s)	116.4	C-1', C-5'	C-2', C-7'
7'	3.35 (2H, br d, 6.7)	40.1	C-1', C-8'	C-2', C-6', C-9'
8'	5.96 (1H, ddt, 16.9, 10.1, 6.7)	137.7	C-7'	C-1'
9'a	5.10 (1H, dd, 16.9, 1.8)	115.7	C-8'	C-7'
9'b	5.06 (1H, dd, 10.1, 1.8)			
OCH ₃ -3	3.86 (3H, s)	55.9		C-3
OCH ₃ -4	3.86 (3H, s)	55.9		C-4
OCH ₃ -5'	3.89 (3H, s)	56.0		C-5'
OC(O)CH ₃ -9	-	170.8		
OC(O)CH ₃ -9	2.03 (3H, s)	20.8	OC(O)CH ₃ -9	

Table 2.26 ^1H NMR (300 Hz), ^{13}C NMR (75 MHz) and HMBC NMR data for **MS12** in CDCl_3 (J in Hz in parentheses).

Position	δ_{H} (ppm)	δ_{C} (ppm)	HMBC (H \rightarrow C)	
			2J	3J
1	-	132.9		
2	6.92 (1H, d, 1.8)	109.1	C-1, C-3	C-6, C-7
3	-	149.3		
4	-	149.3		
5	6.85 (1H, d, 8.1)	111.1	C-4, C-6,	
6	6.94 (1H, dd, 8.1, 1.8)	118.8	C-1	C-2, C-4, C-7
7	5.43 (1H, d, 7.8)	88.7	C-1, C-8	C-2, C-6, C-9, C-3'
8	3.80 (1H, pq, 5.7)	50.8	C-9, C-3', C-7	C-1, C-2', C-4'
9a	4.45 (1H, dd, 11.1, 5.7)			
9b	4.30 (1H, dd, 11.1, 7.5)	65.4	C-8,	C-7, OC(O)CH ₃ -9
1'	-	134.2		
2'	6.68 (1H, <i>br s</i>)	116.3	C-3'	C-8, C-4', C-6', C-7'
3'	-	139.9		
4'	-	144.8		
5'	-	127.2		
6'	6.61 (1H, <i>br s</i>)	116.1	C-5'	C-4', C-2', C-3'
7'	3.30 (2H, d, 6.6)	39.8	C-1', C-8'	C-2', C-6', C-9'
8'	5.94 (1H, ddt, 16.8, 9.9, 6.6)	137.7	C-1', C-7'	
9'a	5.08 (1H, dd, 16.8, 1.8)			
9'b	5.06 (1H, dd, 9.9, 1.8)	115.7	C-8'	C-7'
OCH ₃ -3	3.86 (3H, s)	56.0		C-3
OCH ₃ -4	3.88 (3H, s)	56.0		C-4
OC(O)CH ₃ -9	-	170.9		
OC(O)CH ₃ -9	2.02 (3H, s)	20.8	OC(O)CH ₃ -9	C-9

Table 2.27 ^1H NMR (300 Hz), ^{13}C NMR (75 MHz) and HMBC NMR data for **MS13** in CDCl_3 (J in Hz in parentheses).

Position	δ_{H} (ppm)	δ_{C} (ppm)	HMBC (H \rightarrow C)	
			2J	3J
1	-	131.2		
2	6.78 (1H, d, 1.8)	110.7	C-1, C-3,	C-4, C-6, C-7
3	-	147.2		
4	-	140.9		
5	-	124.4		
6	6.75 (1H, d, 1.8)	123.4	C-5	C-2, C-7, C-5'
7	3.35 (2H, d, 6.6)	40.0	C-1, C-8	C-2, C-6, C-9
8	6.01 (1H, ddt, 16.8, 9.9, 6.6)	137.7		C-1
9a	5.14 (1H, dd, 16.8, 1.6)			
9b	5.10 (1H, dd, 9.9, 1.6)	115.7	C-8	C-7
1'	-	131.9		
2'	6.78 (1H, d, 1.8)	110.7	C-1', C-3'	C-4', C-6', C-7'
3'	-	147.2		
4'	-	140.9		
5'	-	124.4		
6'	6.75 (1H, d, 1.8)	123.4	C-5'	C-5, C-2', C-7'
7'	3.35 (2H, d, 6.6)	40.0	C-1', C-8'	C-2', C-6', C-9'
8'	6.01 (1H, ddt, 16.8, 9.9, 6.6)	137.7		C-1'
9'a	5.14 (1H, dd, 16.8, 1.6)			
9'b	5.10 (1H, dd, 9.9, 1.6)	115.7	C-8'	C-7'
OCH ₃ -3	3.94 (3H, s)	56.1		C-3
OCH ₃ -3'	3.94 (3H, s)	56.1		C-3'
OH-4	6.08 (1H, <i>br s</i>)		C-4	C-3, C-5
OH-4'	6.08 (1H, <i>br s</i>)		C-4'	C-3', C-5'

Table 2.28 ^1H NMR (300 Hz), ^{13}C NMR (75 MHz) and HMBC NMR data for **MS14** in CDCl_3 (J in Hz in parentheses).

Position	δ_{H} (ppm)	δ_{C} (ppm)	HMBC (H \rightarrow C)	
			2J	3J
1	-	129.2		
2	7.20 (1H, <i>br s</i>)	109.5	C-1, C-3	C-4, C-6, C-7
3	-	149.1		
4	-	148.9		
5	6.87 (1H, d, 8.4)	111.1	C-4, C-6	C-1, C-3,
6	7.01 (1H, dd, 8.4, 1.7)	118.7	C-1, C-5	C-2, C-4, C-7
7	5.83 (1H, d, 8.4)	87.0	C-1, C-8	C-2, C-6, C-9, C-3'
8	3.67 (1H, <i>pq</i> , 5.8)	49.6	C-9, C-3'	C-1, C-2', C-4'
9a	3.53 (1H, dd, 11.5, 7.0)			
9b	3.82 (1H, dd, 11.5, 5.8)	63.0	C-8	C-7, C-3'
1'	-	133.8		
2'	6.67 (1H, <i>br s</i>)	112.6	C-3'	C-8, C-4', C-6', C-7'
3'	-	129.2		
4'	-	146.4		
5'	-	144.3		
6'	6.72 (1H, <i>br s</i>)	117.1	C-1', C-5'	C-2', C-4', C-7'
7'	3.35 (1H, d, 6.7)	40.0	C-1', C-8'	C-2', C-6', C-9'
8'	5.97 (1H, <i>ddt</i> , 16.8, 10.0, 6.7)	137.7	C-7'	C-1'
9'a	5.11 (1H, dd, 16.8, 1.7)			
9'b	5.08 (1H, dd, 10.0, 1.7)	115.7	C-8'	C-7'
OCH ₃ -3	3.88 (3H, <i>s</i>)	55.9		C-3
OCH ₃ -4	3.89 (3H, <i>s</i>)	56.0		C-4
OCH ₃ -5'	3.91 (1H, <i>s</i>)	56.1		C-5'

Table 2.29 ^1H NMR (300 Hz), ^{13}C NMR (75 MHz) and HMBC NMR data for **MS15** in CDCl_3 (J in Hz in parentheses).

Position	δ_{H} (ppm)	δ_{C} (ppm)	HMBC (H \rightarrow C)	
			2J	3J
1	-	133.6		
2	6.95 (1H, <i>br s</i>)	109.4	C-1, C-3	C-4, C-6, C-7
3	-	149.2		
4	-	149.0		
5	6.83 (1H, d, 8.8)	111.1	C-4, C-6	C-1, C-3,
6	6.96 (1H, dd, 8.8, 1.9)	118.7	C-1, C-5	C-2, C-4, C-7
7	5.58 (1H, d, 7.4)	87.8	C-1, C-8	C-2, C-6, C-9, C-3', C-4'
8	3.62 (1H, pq, 5.6)	53.8	C-9, C-3'	C-1, C-4', C2'
9a	3.98 (1H, dd, 11.0, 6.0)			
9b	3.91 (1H, dd, 11.0, 5.2)	64.0	C-8	C-7, C-3'
1'	-	133.8		
2'	6.66 (1H, <i>br s</i>)	112.7	C-1', C-3'	C-8, C-6', C-4', C-7'
3'	-	127.7		
4'	-	146.8		
5'	-	144.3		
6'	6.66 (1H, <i>br s</i>)	116.1	C-1', C-5'	C-4', C-2', C-7'
7'	3.35 (1H, <i>br d</i> , 6.8)	40.1	C-1', C-8'	C-2', C-6', C-9'
8'	5.97 (1H, ddt, 16.8, 10.0, 6.8)	137.8	C-7'	C-1'
9'a	5.11 (1H, dd, 16.8, 1.8)			
9'b	5.07 (1H, dd, 10.0, 1.8)	115.7	C-8'	C-7'
OCH ₃ -3	3.85 (3H, s)	55.9		C-3
OCH ₃ -4	3.87 (3H, s)	55.9		C-4
OCH ₃ -5'	3.89 (3H, s)	56.0		C-5'

Table 2.30 ^1H NMR (300 Hz), ^{13}C NMR (75 MHz) and HMBC NMR data for **MS16** in CDCl_3 (J in Hz in parentheses).

Position	δ_{H} (ppm)	δ_{C} (ppm)	HMBC (H \rightarrow C)	
			2J	3J
1	-	131.8		
2	6.92 (1H, d, 1.8)	109.8	C-1, C-3	C-4, C-6, C-7
3	-	149.2		
4	-	149.1		
5	6.82 (1H, d, 7.7)	111.0	C-4	C-1, C-3,
6	6.90 (1H, dd, 7.7, 1.8)	119.8	C-1	C-2, C-4, C-7
7	4.86 (1H, d, 8.2)	74.3	C-1, C-8	C-2, C-6, C-9
8	4.16 (1H, ddd, 8.2, 5.3, 3.3)	86.4	C-7	C-4'
9a	3.99 (1H, dd, 11.9, 5.3)			
9b	4.24 (1H, dd, 11.9, 3.3)	63.3	C-8	C-7, <u>C</u> (O)CH ₃ -9
1'	-	136.2		
2'	6.76 (1H, d, 1.9)	112.5	C-3'	C-4', C-6', C-7'
3'	-	150.7		
4'	-	146.3		
5'	7.06 (1H, d, 7.9)	120.5	C-4'	C-1', C-3'
6'	6.74 (1H, dd, 7.9, 1.9)	121.2	C-5'	C-2', C-4', C-7'
7'	3.35 (2H, d, 6.7)	40.0	C-1', C-8'	C-9'
8'	5.96 (1H, ddt, 16.0, 10.8, 6.7)	137.2	C-7'	
9'a	5.11 (1H, dd, 16.0, 1.7)			
9'b	5.09 (1H, dd, 10.8, 1.7)	116.0	C-8'	C-7'
OCH ₃ -3	3.86 (3H, s)	55.9		C-3
OCH ₃ -4	3.86 (3H, s)	55.9		C-4
OCH ₃ -3'	3.90 (3H, s)	55.8		C-3'
C(O) <u>C</u> H ₃ -9	2.04 (3H, s)	20.8	<u>C</u> (O)CH ₃ -9	
<u>C</u> (O)CH ₃ -9	-	170.6		

Table 2.31 ^1H NMR (300 Hz), ^{13}C NMR (75 MHz) and HMBC NMR data for **MS17** in CDCl_3 (J in Hz in parentheses).

Position	δ_{H} (ppm)	δ_{C} (ppm)	HMBC (H→C)	
			2J	3J
1	-	133.6		
2	6.88 (1H, d 1.2)	109.2	C-1, C-3	C-4, C-6, C-7
3	-	149.2		
4	-	149.0		
5	6.78 (1H, d, 8.8)	111.2	C-4, C-6	C-1, C-3
6	6.90 (1H, dd, 8.8, 1.2)	118.6	C-1, C-5	C-2, C-4, C-7
7	5.49 (1H, d, 7.1)	87.9	C-1, C-8	C-2, C-6, C-9, C-3', C-4'
8	3.54 (1H, pq, 5.7)	54.0	C-7, C-9, C-3'	C-1, C-2' C-4'
9	3.87 (2H, m)	63.8	C-8	C-7, C-3'
1'	-	134.1		
2'	6.64 (1H, d, 1.1)	116.4	C-3'	C-8, C-4', C-6', C-7'
3'	-	127.5		
4'	-	145.1		
5'	-	140.1		
6'	6.56 (1H, <i>br s</i>)	115.8	C-5'	C-2', C-4', C-7'
7'	3.26 (1H, <i>br d</i> , 6.8)	39.8	C-1', C-8'	C-2', C-6', C-9'
8'	5.91 (1H, ddt, 16.8, 10.0, 6.8)	137.7	C-7'	C-1'
9'a	5.06 (1H, dd, 16.8, 1.8)	115.6	C-8'	C-7'
9'b	5.02 (1H, dd, 10.0, 1.8)			
OCH ₃ -3	3.79 (3H, s)	55.9		C-3
OCH ₃ -4	3.83 (3H, s)	55.9		C-4

Table 2.32 ^1H NMR (300 Hz), ^{13}C NMR (75 MHz) and HMBC NMR data for **MS18** in CDCl_3 (J in Hz in parentheses).

Position	δ_{H} (ppm)	δ_{C} (ppm)	HMBC (H \rightarrow C)	
			2J	3J
1	-	131.2		
2	6.41 (1H, d, 1.8)	112.2	C-1, C-3	C-4, C-6, C-7
3	-	143.8		
4	-	135.3		
5	-	147.9		C-2, C-4,
6	6.51 (1H, d, 1.8)	107.5	C-1, C-5	C-7, C-2, C-4
7	3.25 (2H, d, 6.6)	39.9	C-1, C-8	C-2, C-6, C-9
8	5.89 (1H, ddt, 16.2, 9.5, 6.6)	137.4		
9a	5.05 (1H, dd, 16.2, 1.3)			
9b	5.02 (1H, dd, 9.5, 1.3)	115.8	C-7	
1'	-	133.0		
2'	7.01 (1H, d, 1.6)	110.3	C-3'	C-4', C-6', C-7'
3'	-	150.4		
4'	-	145.9		
5'	6.87 (1H, d, 5.4)	118.9	C-4',	C-1', C-3'
6'	6.88 (1H, dd, 5.4, 1.6)	119.5	C-1'	C-2', C-4', C-7'
7'	6.57 (1H, d, 15.8)	130.8	C-1', C-8'	C-2', C-6', C-9'
8'	6.29 (1H, dt, 15.8, 5.8)	127.9	C-7', C-9'	C-1'
9'	4.32 (2H, d, 5.8)	63.7	C-8'	C-7'
OCH ₃ -5	3.89 (3H, s)	56.3		C-5
OCH ₃ -3'	3.89 (3H, s)	56.0		C-3'

Table 2.33 ^1H NMR (300 Hz), ^{13}C NMR (75 MHz) and HMBC NMR data for **MS19** in CDCl_3 (J in Hz in parentheses).

Position	δ_{H} (ppm)	δ_{C} (ppm)	HMBC (H \rightarrow C)	
			2J	3J
1	-	132.2		
2	6.99 (1H, <i>br s</i>)	110.0	C-1, C-3	C-4, C-6, C-7
3	-	149.1		
4	-	148.9		
5	6.84 (1H, d, 8.4)	111.1	C-4	C-1, C-3
6	6.98 (1H, dd, 8.4, 1.9)	119.6	C-1	C-2, C-4, C-7
7	4.98 (1H, d, 8.1)	73.9	C-1, C-8	C-2, C-6, C-9
8	3.98 (1H, <i>br dt</i> , 8.1, 3.5)	89.6	C-7	C-4'
9a	3.62 (1H, dd, 12.5, 3.1)			
9b	3.46 (1H, dd, 12.5, 3.5)	61.0	C-8	C-7
1'	-	136.2		
2'	6.76 (1H, <i>br s</i>)	112.5	C-3', C-1'	C-4', C-6', C-7'
3'	-	151.1		
4'	-	145.8		
5'	7.04 (1H, d, 7.9)	121.0	C-4'	C-1', C-3'
6'	6.75 (1H, dd, 7.9, 2.0)	121.5	C-1', C-5'	C-2', C-4', C-7'
7'	3.35 (2H, d, 6.7)	40.0	C-1', C-8'	C-2', C-6', C-9'
8'	5.95 (1H, ddt, 16.0, 11.4, 6.7)	137.2	C-7'	C-1'
9'a	5.10 (1H, dd, 16.0, 1.7)			
9'b	5.09 (1H, dd, 11.4, 1.7)	116.1	C-8'	C-7'
OCH ₃ -3	3.88 (3H, s)	55.9		C-3
OCH ₃ -4	3.87 (3H, s)	55.9		C-4
OCH ₃ -3'	3.90 (3H, s)	55.9		C-3'

Table 2.34 ^1H NMR (300 Hz), ^{13}C NMR (75 MHz) and HMBC NMR data for **MS20** in CDCl_3 (J in Hz in parentheses).

Position	δ_{H} (ppm)	δ_{C} (ppm)	HMBC (H \rightarrow C)	
			2J	3J
1	-	131.8		
2	6.48 (1H, <i>br s</i>)	110.2	C-1, C-3	C-4, C-6, C-7
3	-	144.3		
4	-	136.7		
5	-	148.2		
6	6.64 (1H, <i>br s</i>)	105.3	C-1, C-5	C-2, C-4, C-7
7	4.40 (1H, d, 6.5)	74.6	C-1, C-8	C-2, C-6, C-9
8	3.60 (1H, m)	75.9	C-7, C-9	
9a	3.34 (1H, overlapped)			
9b	3.43 (1H, <i>br d</i>)	63.2	C-8	C-7
1'	-	136.5		
2'	6.73 (1H, d, 1.1)	113.0	C-1', C-3'	C-4', C-6', C-7'
3'	-	150.1		
4'	-	143.9		
5'	6.78 (1H, d, 8.1)	119.1	C-4', C-6'	C-1', C-3'
6'	6.62 (1H, dd, 8.1, 1.1)	121.0	C-1'	C-2', C-4', C-7'
7'	3.30 (1H, d, 6.5)	40.0	C-1', C-8'	C-2', C-6', C-9'
8'	5.91 (1H, ddt, 16.9, 10.3, 6.7)	137.2	C-7'	C-1'
9'a	5.06 (1H, dd, 16.9, 1.4)			
9'b	5.05 (1H, dd, 10.3, 1.4)	116.1	C-8'	C-7'
OCH ₃ -5	3.75 (3H, s)	55.9		C-5
OCH ₃ -3'	3.75 (3H, s)	56.3		C-3'

Table 2.35 ^1H NMR (300 Hz), ^{13}C NMR (75 MHz) and HMBC NMR data for **MS20a** in CDCl_3 (J in Hz in parentheses).

Position	δ_{H} (ppm)	δ_{C} (ppm)	HMBC (H \rightarrow C)	
			2J	3J
1	-	134.0		
2	6.38 (1H, d, 1.7)	109.0	C-1, C-3	C-4, C-6, C-7
3	-	150.8		
4	-	150.8		
5	-	152.8		
6	6.60 (1H, d, 1.7)	104.8	C-1, C-5	C-2, C-4, C-7
7	5.83 (2H, d, 7.4)	73.4	C-1, C-8	C-2, C-6, C-9, <u>C</u> (O)CH ₃ -7
8	5.29 (1H, ddd, 7.4, 5.3, 3.6)	72.2		
9a	3.75 (1H, dd, 12.2, 5.3)			
9b	4.23 (1H, dd, 12.3, 3.61)	62.0	C-8	C-7, <u>C</u> (O)CH ₃ -9
1'	-	137.4		
2'	6.79 (1H, d, 1.8)	113.2	C-3'	C-4', C-6', C-7'
3'	-	151.0		
4'	-	142.8		
5'	6.87 (1H, d, 8.1)	121.1	C-4', C-6'	C-1', C-3'
6'	6.73 (1H, dd, 8.1, 1.8)	121.1	C-1'	C-2', C-4', C-7'
7'	3.38 (1H, d, 6.7)	40.0	C-1', C-8'	C-2', C-6', C-9'
8'	5.97 (1H, ddt, 16.7, 10.0, 6.7)	137.1	C-7', C-9'	C-1'
9'a	5.11 (1H, dd, 17.1, 1.7)			
9'b	5.10 (1H, dd, 9.6, 1.7)	116.1	C-8'	C-7'
OCH ₃ -5	3.85 (3H, s)	56.3		C-4
OCH ₃ -3'	3.78 (3H, s)	55.9		C-3'
OCO <u>C</u> H ₃ -3	2.26 (3H, s)	20.4		OCOCH ₃ -3
OCO <u>C</u> H ₃ -4	2.00 (3H, s)	20.7		OCOCH ₃ -4
OCO <u>C</u> H ₃ -7	2.05 (3H, s)	20.9		OCOCH ₃ -7
OCO <u>C</u> H ₃ -9	1.97 (3H, s)	20.6		OCOCH ₃ -9
OCOCH ₃ -3	-	168.2		
OCOCH ₃ -4	-	170.0		
OCOCH ₃ -7	-	169.5		
OCOCH ₃ -9	-	170.3		

Table 2.36 ^1H NMR (300 Hz) and $\Delta\delta$ values [$\Delta\delta$ (in ppm) = $\Delta\delta_S - \Delta\delta_R$] for *S*-(-)-MTPA ester MS16 and *R*-(+)-MTPA ester MS16 in CDCl_3 (J in Hz in parentheses).

Position	δ_{H} (ppm)		$\Delta\delta = \Delta\delta_S - \Delta\delta_R$
	<i>S</i> -(-)-MTPA ester MS16	<i>R</i> -(+)-MTPA ester MS16	
1	-	-	
2	6.96 (1H, d, 1.7)	6.71 (2H, <i>br s</i>)	+0.25
3	-	-	
4	-	-	
5	6.85 (1H, d, 8.1)	6.80 (1H, d, 8.3)	+0.05
6	7.00 (1H, dd, 8.1, 1.7)	6.90 (1H, dd, 8.3, 1.8)	+0.10
7	6.35 (1H, d, 7.2)	6.28 (1H, d, 8.2)	+0.07
8	4.59 (1H, m)	4.61 (1H, ddd, 3.8, 4.6, 8.2)	-0.02
9a	4.14 (1H, dd, 12.9, 4.0)	4.18 (1H, dd, 12.3, 3.8)	-0.04
9b	3.84 (1H, overlapped)	3.77 (1H, dd, 12.3, 4.6)	+0.07
1'	-	-	
2'	6.67 (1H, d, 1.6)	6.71 (2H, <i>br s</i>)	-0.04
3'	-	-	
4'	-	-	
5'	6.72 (1H, d, 8.1)	6.91 (1H, d, 8.1)	-0.19
6'	6.60 (1H, dd, 8.1, 1.6)	6.68 (1H, dd, 8.1, 1.8)	-0.08
7'	3.31 (1H, d, 6.4)	3.33 (1H, d, 6.6)	-0.02
8'	5.93 (1H, ddt, 16.4, 9.6, 6.4)	5.94 (1H, ddt, 16.1, 9.5, 6.5)	-0.01
9'	5.08 (2H, m)	5.08 (2H, m)	0.00
OCH ₃ -3	3.89 (3H, s)	3.88 (3H, s)	+0.01
OCH ₃ -4	3.84 (3H, s)	3.77 (3H, s)	+0.07
OCH ₃ -3'	3.75 (3H, s)	3.71 (3H, s)	+0.04
C(O)CH ₃ -9	1.94 (3H, s)	2.01 (3H, s)	-0.07

CHAPTER 3

RESULTS AND DISCUSSION

3.1 Structure elucidation and identification

The air-dried leaves of *M. sessilis* were ground into small particles and extracted at room temperature with hexane followed by EtOAc, CH₂Cl₂ and EtOH, respectively. The EtOAc extract and the CH₂Cl₂ extracts were combined and partitioned successively with hexane and EtOAc. The hexane and EtOAc extracts prepared from the leaves of this plant were test at the concentration of 50 µg/ml, showed cytotoxicity against MCF7 (93.52 and 82.15% inhibition, respectively) and NCI-H187 (98.82 and 98.37% inhibition, respectively). The bioactive hexane and EtOAc extracts were purified using a combination of various chromatographic separations led to the isolation of nine new neolignans including four dihydro[*b*]benzofuran neolignans: **MS12**, **MS15**, **MS17** and **MS11**, three 8-*O*-4' neolignans: **MS16**, **MS19** and **MS20**, one dineolignan: **MS14** and one phenylpropanoid dimer: **MS18**, and four new triterpens: **MS3**, **MS5**, **MS6** and **MS7**, together with seven other known compounds including, two neolignans: dehydrodieugenol A (**MS13**) [36] and dehydrodieugenol B (**MS10**) [36, 37], two sesquiterpenes: (+)-spathulenol (**MS1**) [29] and T-muurolol (**MS4**) [31, 32], phytol (**MS2**) [30] and a mixture of stigmasterol (**MS8**) [35, 38] and β-sitosterol (**MS9**) [33].

3.1.1 Neolignans

3.1.1.1 (7S,8R)-5'-Hydroxy-3,4-dimethoxy-4',7-epoxy-8,3'-neolign-8'-en-9-acetate (MS12)

MS12 was obtained as an optically active pale yellow crystalline, $[\alpha_D^{28}] +43.4^\circ$ (c 0.05, CHCl_3). The molecular formula of **MS12** was determined to be $\text{C}_{22}\text{H}_{24}\text{O}_6$ by HRESIMS, consistent with the molecular ion peak at m/z 407.1462 $[\text{M}+\text{Na}]^+$ (calcd. for $\text{C}_{22}\text{H}_{24}\text{O}_6\text{Na}$, 407.1471). The UV spectrum of **MS12** showed absorption bands at λ_{max} 277, 230 and 204 nm and the IR spectrum showed absorption bands at 3421, 1740, 1610, 1516, 1238, 1139 and 1028 cm^{-1} , suggesting the presence of hydroxyl, ester carbonyl, aromatic and ether functionalities. The ^{13}C NMR, DEPT and HMQC spectra revealed 22 carbons (Table 2.26), including a carbonyl carbon (δ_{C} 170.9), twelve aromatic carbons [δ_{C} 149.3 (C-3), 149.3 (C-4), 144.8 (C-4'), 139.9 (C-3'), 134.2 (C-1'), 132.9 (C-1), 127.2 (C-5'), 118.8 (C-6), 116.3 (C-2'), 116.1 (C-6'), 111.1 (C-5) and 109.1 (C-2), two methoxy groups [δ_{C} 56.0 (2 \times)], three methylenes [δ_{C} 115.7 (C-9'), 65.4 (C-9), 39.8 (C-7')], three methines (δ_{C} 137.7 (C-8'), 88.7 (C-7) and 50.8 (C-8)] and a methyl group (δ_{C} 20.8). The ^1H NMR spectrum of **MS12** (Table 2.26) exhibited two set of aromatic rings. The aromatic ring A showed two broad singlets at δ_{H} 6.68 (1H, H-2') and 6.61 (1H, H-6') indicated the presence of two *meta* aromatic hydrogens (Figure 3.1). For the aromatic ring C, the appearance of a typical ABX system at δ_{H} 6.85 (1H, d, $J = 8.1\text{ Hz}$, H-5), 6.94 (1H, dd, $J = 8.1, 1.8\text{ Hz}$, H-6) and 6.92 (1H, *br s*, H-2) corresponded to a 1,3,4-trisubstituted phenyl moiety. In addition, the ^1H NMR

signals reviewed the presence of an allylic group [δ_{H} 3.30 (2H, d, $J = 6.6$ Hz, H-7'), 5.94 (1H, ddt, $J = 16.8, 9.9, 6.6$ Hz, H-8') and δ_{H} 5.08 (1H, dd, $J = 16.8, 1.8$ Hz, H-9'a) and 5.06 (1H, dd, $J = 9.9, 1.8$ Hz, H-9'b)], two methoxy groups [δ_{H} 3.86 (3H, s, $\times 2$ OMe)] and an acetoxy methyl group [δ_{H} 2.02 (3H, s, OCOMe)]. The remaining $^1\text{H-NMR}$ signals also showed O-CH-CH-CH₂-O spin systems at δ 5.43 (1H, d, $J = 7.8$ Hz, H-7), 3.80 (1H, pq, $J = 5.7$ Hz, H-8), δ 4.45 (1H, dd, $J = 11.1, 5.7$ Hz, H-9a) and 4.30 (1H, dd, $J = 11.1, 7.5$ Hz, H-9b), which was supported by the $^1\text{H-}^1\text{H}$ COSY correlation (Figure 3.1), indicating a characteristic of dihydrobenzofuran-type neolignans. Our assumption was supported by important long-rang HMBC correlations which were observed between H-7 (δ_{H} 5.43) and C-1 (δ_{C} 132.9), C-2 (δ_{C} 109.1), C-6 (δ_{C} 118.8), C-8 (δ_{C} 50.8), C-9 (δ_{C} 65.4) and C-5' (δ_{C} 127.2); H-8 (δ_{H} 3.80) and C-1 (δ_{C} 132.9), C-9 (δ_{C} 65.4), C-4' (δ_{C} 144.8), C-5' (δ_{C} 127.2) and C-6' (δ_{C} 116.1) and H-9 (δ 4.30 and 4.45) and C-7 (δ_{C} 88.7) and C-8 (δ_{C} 50.8). The methyl singlet at δ 2.02, showed HMBC correlation to carbonyl carbon (δ_{C} 170.9), confirming the presence of an acetyl group. Additionally, the HMBC correlation between oxygenated methylene proton at δ_{H} 4.30 and 4.45 (H-9) and carbonyl carbon at δ_{C} 170.9 suggested that the acetyl group was linked to C-9. In ring C, the long range HMBC correlations were observed signals of the methoxy groups at δ_{H} 3.86 to δ_{C} 149.3 and at δ_{H} 3.88 to δ_{C} 149.3 (Figure 3.1 and Table 2.26), indicating that these methoxy groups should be placed at C-3 and C-4, respectively in the ring C.

In ring A, the key HMBC correlations of allylic methylene group at δ_{H} 3.30 (H-7') and C-1' (δ_{C} 134.2), C-2' (δ_{C} 116.3) and C-6' (δ_{C} 116.1) and olefinic methine group at δ_{H} 5.94 (H-8') and C-1' (δ_{C} 134.2) suggested that the allyl moiety was linked to C-1'. Moreover, the HMBC correlation between H-6' and C-5' (δ_{C} 139.9) suggested the location of a hydroxyl group at C-5'. The relative configuration at C-7 and C-8 was elucidated as *trans* by the large vicinal coupling constant ($J_{7,8} = 7.5$ Hz) [39, 40]. In addition, the X-ray analysis of **MS12** (Figure 3.2) confirmed its structure and relative configuration. The absolute configurations of **MS12** were determined by CD analysis. The CD spectrum showed a positive Cotton effect at 292 nm ($\Delta\epsilon +2.14$, Figure 3.3), indicating *7S* configuration [41, 42]. Thus, the absolute configurations of **M12** at C-7 and C-8 were assigned as *7S* and *8R* which was in accordance with its positive optical rotation ($[\alpha_{\text{D}}^{28}] +43.4^\circ$) [43]. Thus, **MS12** was characterized as (*7S,8R*)-5'-hydroxy-3,4-dimethoxy-4',7-epoxy-8,3'-neolign-8'-en-9-acetate.

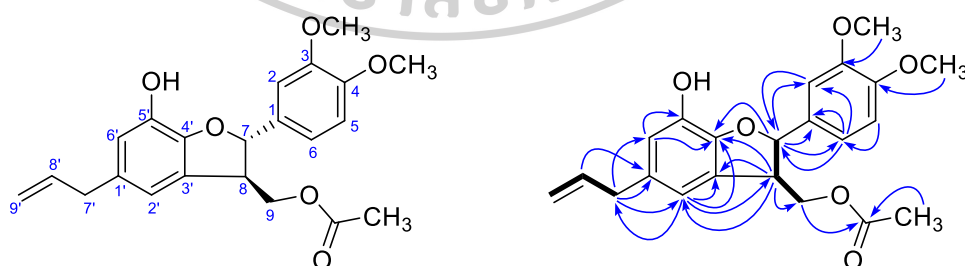


Figure 3.1 Structure, ^1H - ^1H COSY (bold line) and of HMBC (H→C) correlation of **MS12**.

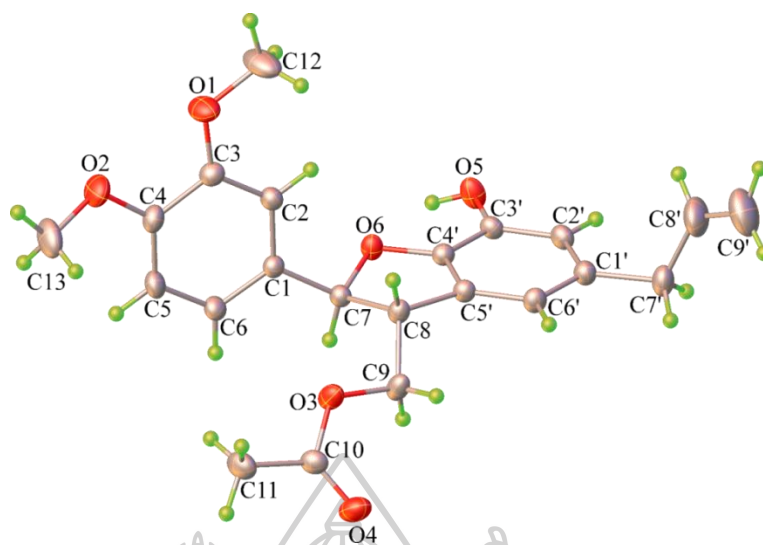


Figure 3.2 X-ray ORTEP diagram of MS12.

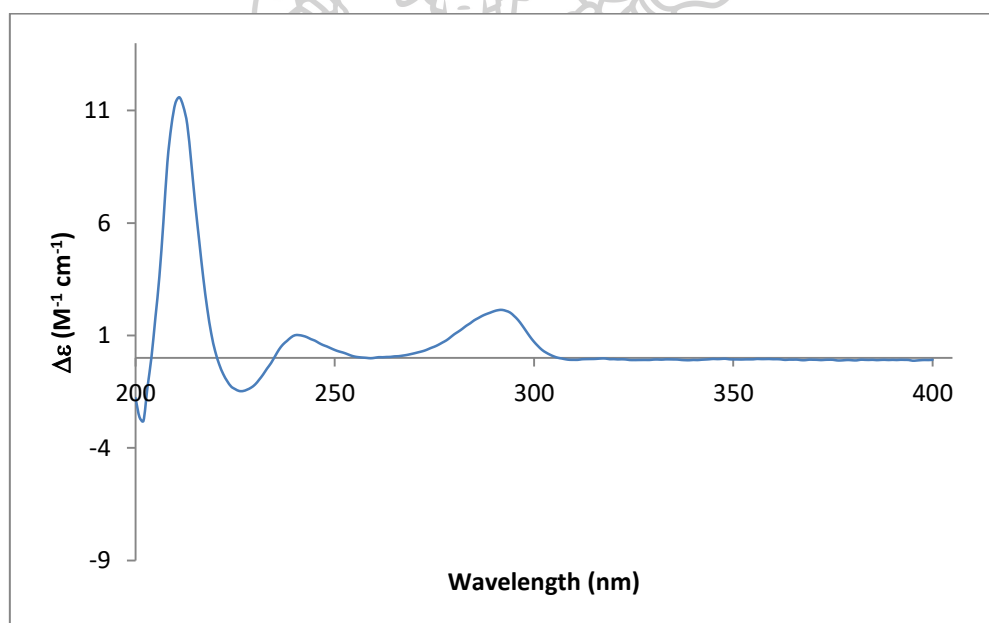


Figure 3.3 Circular dichroism (CD) spectra of MS12.

3.1.1.2 (7*S*,8*R*)-5'-Hydroxy-3,4-dimethoxy-4',7-epoxy-8,3'-neolign-8'-en-9-ol (MS17)

MS17 was obtained as a colorless viscous liquid with positive specific rotation ($[\alpha_D^{28}] +9.14^\circ$ (c 0.09, CHCl₃)). The HRESIMS of **MS17** showed a molecular ion peak at m/z 365.1634 $[M+Na]^+$ (calcd for C₂₀H₂₂O₅Na, 365.1365) and the molecular formula of **MS17** was determined as C₂₀H₂₂O₅. The UV spectrum of **MS17** supported aromatic ring functionalities, which showed absorption bands at λ_{max} 277, 230 and 205 nm. The IR spectrum showed strong bands of hydroxyl (3436 cm⁻¹), aromatic (1609, 1516, 1334, and 1025 cm⁻¹) and ether (1263, 1139cm⁻¹) functionalities. From the ¹H NMR, ¹³C NMR and HMBC spectroscopic data (Table 2.31 and Figure 3.4), indicated that **MS17** was a neolignan containing a dihydrobenzofuran skeleton, resembled closely those of **MS12** (Table 2.26 and Figure 3.1), except for the lack of an acetyl group. The placement of a hydroxyl moiety at C-9 was based upon the observation of upfield shifts assigned to H-9 [δ_H 3.87 (2H, m)] and C-9 (δ_C 63.8) while comparing the ¹H NMR and ¹³C NMR spectra of **M17** with those of **M12**. The absolute configuration of **MS17** was established as 7*S* and 8*R* based on its positive optical rotation and the CD spectrum (positive Cotton effect at 292 nm ($\Delta\epsilon$ +1.85), Figure 3.5). Our conclusion was confirmed by hydrolysis of **MS12** under mild acid condition to obtain compound **MS12** ($[\alpha_D^{28}] +13.6^\circ$ in CHCl₃). Consequently, the absolute stereostructure of **MS17** was elucidated as (7*S*,8*R*)-5'-hydroxy-3,4-dimethoxy-4',7-epoxy-8,3'-neolign-8'-en-9-ol.

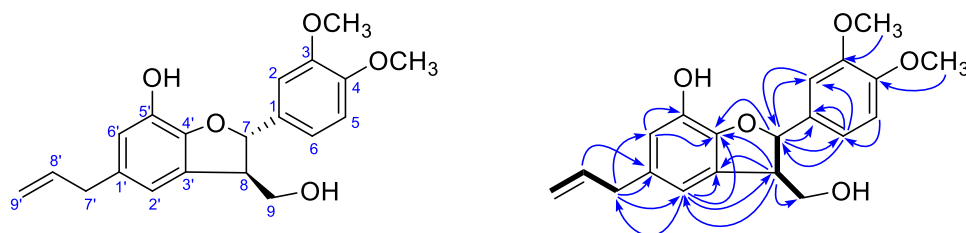


Figure 3.4 Structure, ^1H - ^1H COSY (bold line) and of HMBC (H \rightarrow C) correlation of MS17.

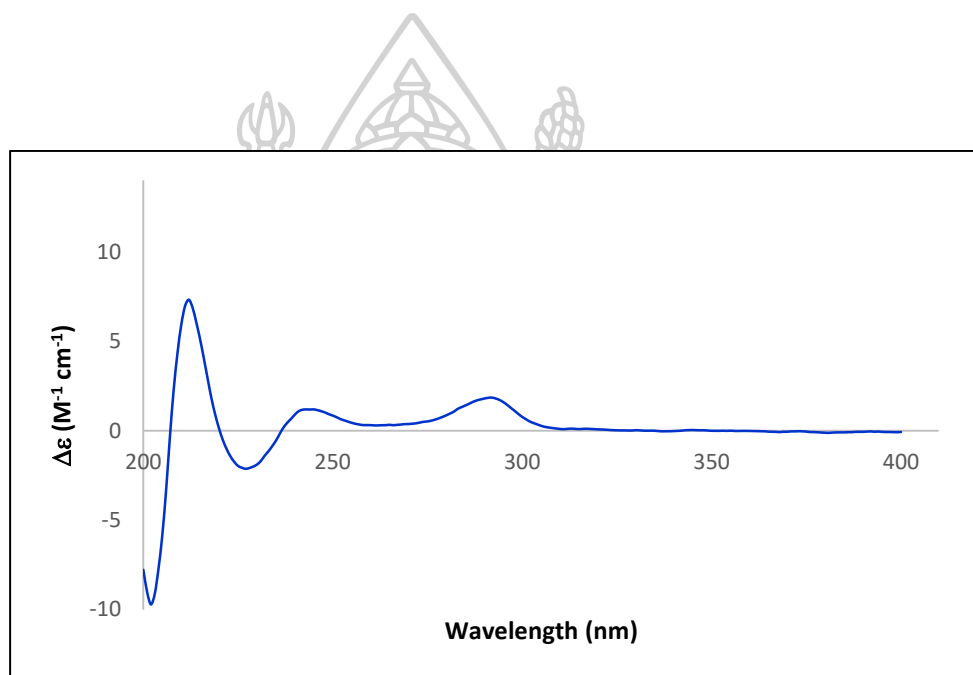


Figure 3.5 CD spectra of MS17.

3.1.1.3 (7*S*,8*R*)-3,4,5'-Trimethoxy-4',7-epoxy-8,3'-neolign-8'-en-9-ol (**MS15**)

MS15 was isolated as a colorless viscous liquid with positive specific optical rotation ($[\alpha_D^{28}] +16.2^\circ$ (c 0.07, CHCl₃)). The molecular formula was determined to be C₂₁H₂₄O₅ from its molecular ion peak at m/z 379.1526 [M+Na]⁺ (calcd for C₂₁H₂₄NaO₅, 379.1522) in the HRESIMS. The ¹H NMR and ¹³C NMR spectroscopic data (Table 2.29) of **MS15** were identical to those of dihydrocarinatinol, 5-allyl-7-methoxy-3-hydroxymethyl-2-(3',4'-dimethoxyphenyl) dihydrobenzofuran, previously isolated from *Virola carinata* (Kawanishi et al., 1982). The relative configuration and the absolute configuration were determined as those in **M12** and **M17** by the same experiments. The relative configuration of C-7 and C-8 was determined to be *threo* by its large coupling constant at H-7 and H-8 ($J_{7,8} = 7.4$ Hz). The absolute configurations were assigned as 7*S*,8*R* based upon the positive Cotton effect at 293 nm ($\Delta\epsilon +1.10$, Figure 3.7). However, the absolute configurations of dihydrocarinatinol have not been reported. **MS15** has a positive optical rotation, which was the opposite sign as that of dihydrocarinatinol ($[\alpha_D^{25}] -12.3^\circ$ in CHCl₃) [44]. Therefore, **MS15** was elucidated as an enantiomer of dihydrocarinatinol. Thus, compound **MS15** was identified as (7*S*,8*R*)-3,4,5'-trimethoxy-4',7-epoxy-8,3'-neolign-8'-en-9-ol. In addition, the absolute configurations of dihydrocarinatinol should be assigned as 7*R*,8*S*.

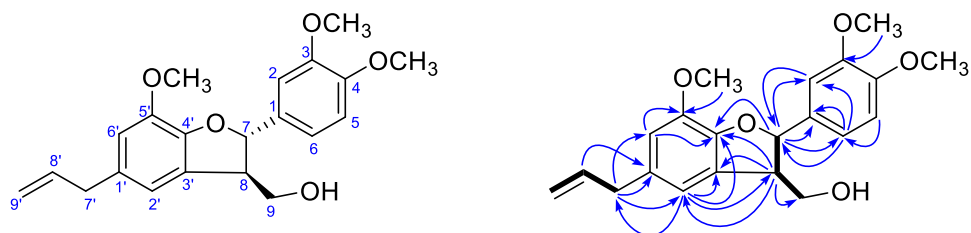


Figure 3.6 Structure, ^1H - ^1H COSY (bold line) and of HMBC ($\text{H} \rightarrow \text{C}$) correlation of **MS15**.

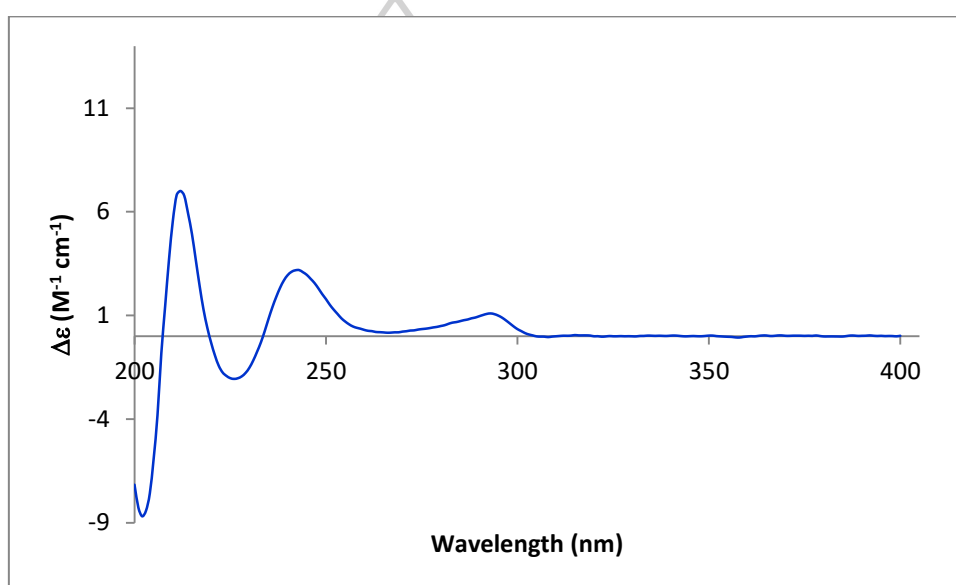


Figure 3.7 CD spectra of **MS15**.

3.1.1.4 (7*R*,8*S*)-3,4,5'-Trimethoxy-4',7-epoxy-8,3'-neolign-8'-en-9-acetate (MS11)

MS11 was isolated as a colorless viscous liquid with negative specific rotation ($[\alpha_D^{28}] -10.5^\circ$ (c 0.07, CHCl₃)). The molecular formula was determined to be C₂₃H₂₆O₆ from its molecular ion peak at m/z 421.1626 [M+Na]⁺ (calcd for C₂₃H₂₆NaO₆, 421.1627) in the HRESIMS. The IR spectrum of **MS11** also showed strong bands of ester carbonyl (1726 cm⁻¹), aromatic (1605 and 1516 cm⁻¹) and ether (1252, 1218 and 1143 cm⁻¹) functionalities. The ¹H NMR and ¹³C NMR spectroscopic data of **MS11** (Table 2.25) were characterized as a dihydrobenzofuran lignan, closely similar to those of **MS12** (Table 2.26), except for the presence of an additional methoxy group in **MS11**. The ¹H NMR and ¹³C NMR spectra of **MS11** showed the methoxy signal at δ_H 3.89 (s) and (δ_C 144.2) which was located at C-5' based upon the HMBC correlation between the OCH₃-5' protons and C-5' (δ_C 144.2) (Figure 3.8). The coupling constant ($J_{7,8} = 7.4$ Hz) between H-7 and H-8 suggested the *trans*-configuration in this structure [40]. The CD spectrum of **MS11** (Figure 3.9) showed the opposite curve comparing those of **MS12**, **MS15** and **MS17** (Figure 3.3, 3.7 and 3.5, respectively), in turn, indicating the opposite absolute configuration. Therefore, the absolute stereochemistry of **MS11** was assigned as 7*R*,8*S*. Thus, **MS11** was proposed as (7*R*,8*S*)-3,4,5'-trimethoxy-4',7-epoxy-8,3'-neolign-8'-en-9-acetate.

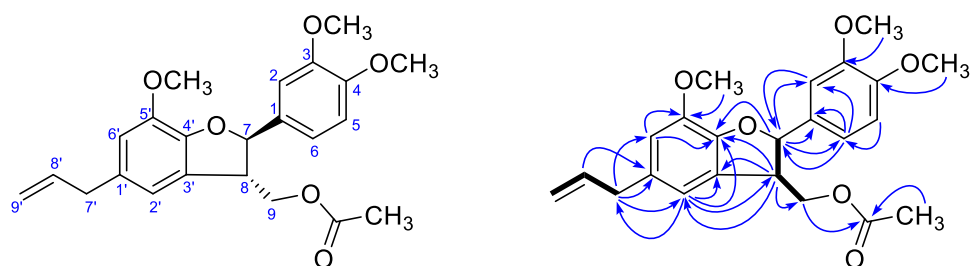


Figure 3.8 Structure, ^1H - ^1H COSY (bold line) and of HMBC (H \rightarrow C) correlation of MS11.

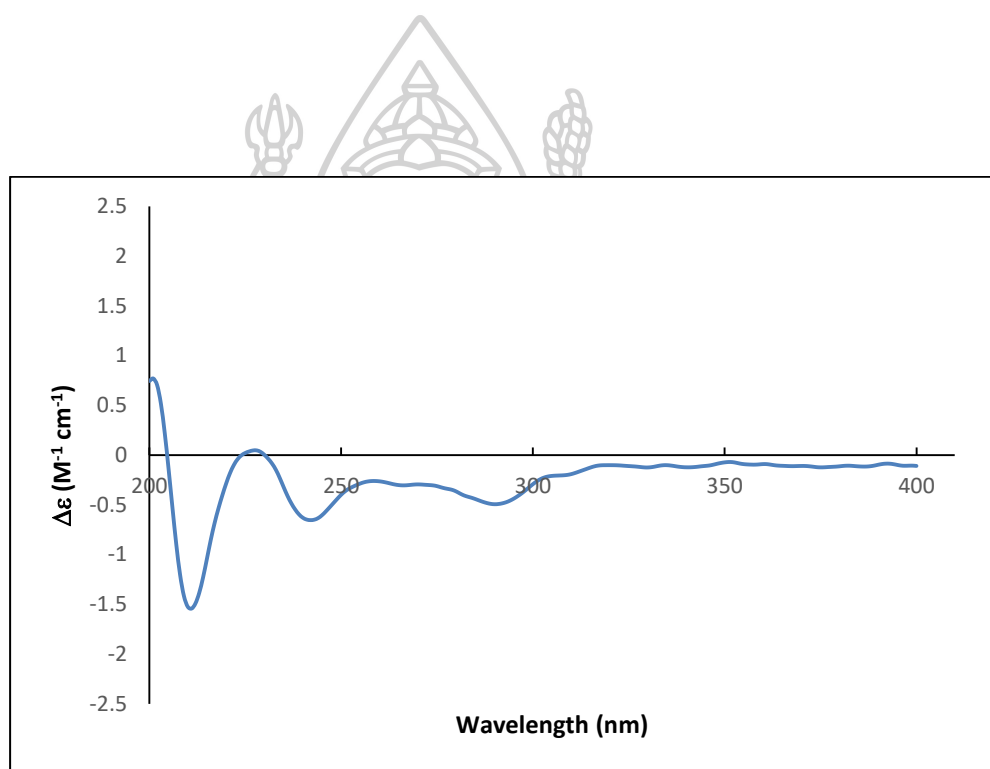


Figure 3.9 CD spectra of MS11.

3.1.1.5 (7R,8R)-4'-Hydroxy-3,4,5'-trimethoxy-8,3'-neolign-8'-en-7,9-diol (MS14)

MS14 was isolated as a pale yellow oil with negative optical rotation ($[\alpha]_D^{28}$ -86.9°, c 0.05, CHCl₃). The HRESIMS of **MS14** showed a molecular ion peak at m/z 379.1513 [M+Na-H₂O]⁺ (calcd for C₂₁H₂₄O₅Na, 379.1522) and the molecular formula of **MS14** was determined to be C₂₁H₂₆O₆. The ¹H NMR and ¹³C NMR data of **MS14** showed a lignan characteristic as deduced before for 7,8-dihydro[*b*]benzofuran (Table 2.28).

However, the CD spectrum pattern of **MS14** was different from those of compounds **MS11**, **MS12**, **MS15** and **MS17** (Figure 3.11), this suggested that **MS14** occupied 1,3-propane diol unit instead of dihydrobenzofuran skeleton. The presence of the propanoid moiety was observed in ¹H NMR spectrum at δ_H 5.83 (1H, d, *J* = 8.4 Hz, H-7), 3.67 (1H, pq, *J* = 5.8 Hz, H-8), 3.53 (1H, dd, *J* = 11.5, 7.0 Hz, H-9a) and 3.82 (1H, dd, *J* = 11.5, 5.8 Hz, H-9b), which in accordance with HMBC correlations between H-7 (δ_H 5.86) to C-1 (δ_C 129.2), C-6 (δ_C 118.7), C-9 (δ_C 63.0) and C-3' (δ_C 129.2) (Figure 3.10). From the above information indicated that **MS14** had a same planar structure to that of 2-(1-allyl-4-hydroxy-5-methoxyphenyl)-1-(3,4-dimethoxyphenyl)propane-1,3-diol which was a synthetic compound obtained from a reduction of carinatanol [44]. The relative stereochemistry of C-7 and C-8 of **MS14** was determined to be *threo* (*syn*) by a comparison of the coupling constant between H-7 and H-8 (*J*_{7,8} = 8.4 Hz) with those of the related *threo* and *erythro* isomers [45, 46]. The acid dehydration of compound **MS14** afforded a dihydrobenzofuran derivative, which was identical **MS15** by

means of the optical rotation value ($[\alpha_D^{28}] +21.8$, c 0.05, CHCl_3) and NMR spectroscopic data. This result encouraged us to conclude the absolute configurations of **MS14** as $7R,8R$. Accordingly, the structure of **MS14** was established as $(7R,8R)$ -4'-hydroxy-3,4,5'-trimethoxy-8,3'-neolign-8'-en-7,9-diol.

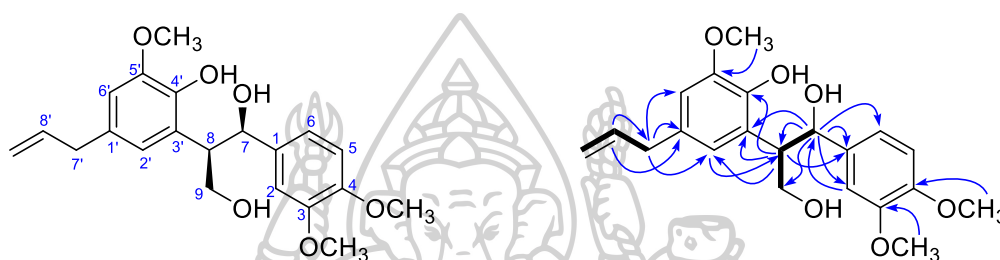


Figure 3.10 Structure, ^1H - ^1H COSY (bold line) and of HMBC ($\text{H}\rightarrow\text{C}$) correlation of **MS14**.

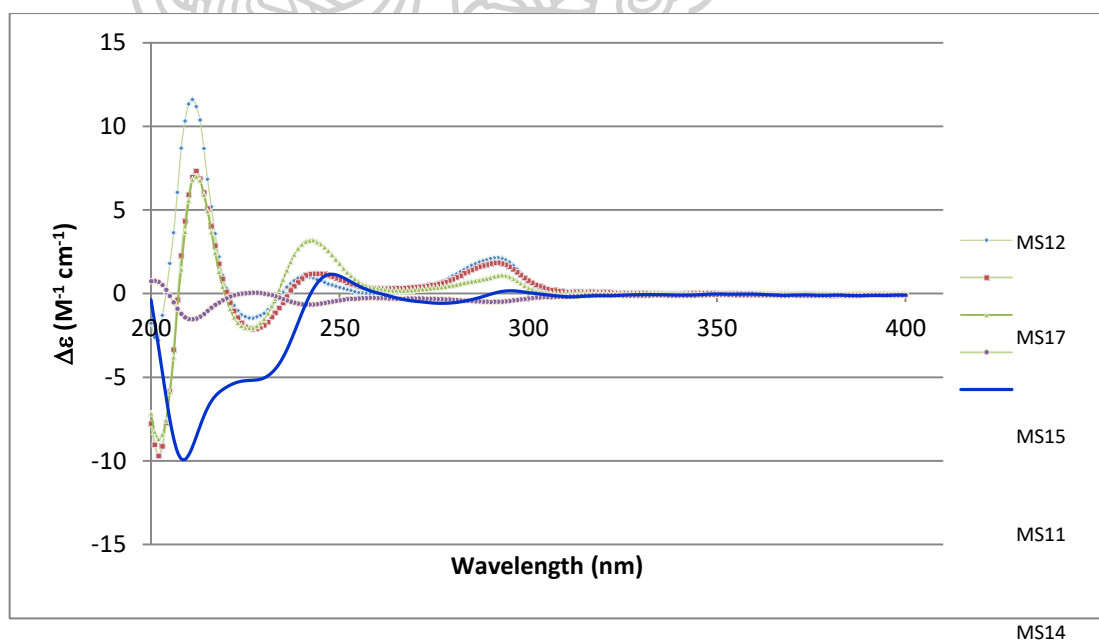


Figure 3.11 CD spectra of **MS14** compared with **MS11**, **MS12**, **MS15** and **MS17**.

3.1.1.6 *threo*-(7*R*,8*R*)-3,3',4-Trimethoxy-8,4'-oxyneolign-8'-en-7-ol-9-acetate (MS16)

MS16 was obtained as an optically active pale green-brown viscous liquid, $[\alpha_D^{28}] -58.8^\circ$ (c 0.08, CHCl₃) and its molecular formula was determined to be C₂₃H₂₈O₇ from its molecular ion peak at m/z 439.1729 [M+Na]⁺ (calcd for C₂₃H₂₈O₇Na, 439.1733) in HRESIMS. The IR spectrum showed absorption bands of hydroxyl (3486 cm⁻¹), ester carbonyl (1740 cm⁻¹), ether (1264, 1140 and 1029 cm⁻¹) and aromatic (1591 and 1464 cm⁻¹) moieties. The UV spectrum contained absorption bands at λ_{max} 281, 230 and 203 nm, suggesting the presence of aromatic ring. The ¹H NMR data revealed two sets of ABX aromatic rings at δ_H 6.92 (1H, *br s*, H-2), 6.82 (1H, *d*, *J* = 7.7 Hz, H-5) and 6.90 (1H, *dd*, *J* = 7.7, 1.8 Hz, H-6) and at δ_H 6.76 (1H, *br s*, H-2'), 7.06 (1H, *d*, *J* = 7.9 Hz, H-5') and 6.74 (1H, *dd*, *J* = 7.9, 1.9 Hz, H-6), represented two 1,3,4-trisubstituted phenyl moieties (Table 2.30). The ¹H NMR spectrum also showed three methoxy groups at δ_H 3.86 (3H, *s*, ×2 OMe) and 3.90 (3H, *s*). The ¹³C NMR (Table 2.30), DEPT and HMQC spectra exhibited resonances of twelve aromatic carbons including six methines [δ_C 109.8 (C-2), 111.0 (C-5), 119.8 (C-6), 112.5 (C-2'), 120.5 (C-5') and 121.3 (C-6')], two quaternary [131.8 (C-1) and 136.2 (C-1')] and four oxygenated quaternary carbons [δ_C 149.0 (C-3), 149.2 (C-4), 150.7 (C-3') and 146.3 (C-4')]. The ¹³C NMR and ¹H NMR spectra of **MS16** showed the signals at δ_C 40.0 (C-7'), 137.2 (C-8') and 116.2 (C-9') and allylic methylene protons at δ_H 3.35 (2H, *d*, *J* = 6.7 Hz, H-7'), olefinic methine proton at δ_H 5.96 (1H, *ddt*, *J* = 16.0, 10.8, 6.7 Hz, H-8') and

vinyllic methylene proton at δ_{H} 5.11 (1H, dd, $J = 16.0, 1.7$ Hz, H-9'a) and 5.09 (1H, dd, $J = 10.8, 1.7$ Hz, H-9'b), indicating the occurrence of allyl moiety, which was supported by ^1H - ^1H COSY experiment (Figure 3.12). Additionally, the ^{13}C NMR and ^1H NMR spectra exhibited the signals at δ_{C} 74.3 (C-7), 86.4 (C-8) and 63.3 (C-9) and an oxygenated methine proton at δ_{H} 4.86 (1H, d, $J = 8.2$ Hz, H-7), an oxygenated methine proton at δ_{H} 4.16 (1H, ddd, $J = 8.2, 5.3, 3.3$ Hz, H-8) and two oxygenated methylene protons at δ_{H} 4.24 (1H, dd, $J = 11.9, 3.3$ Hz, H-9b) and 3.99 (1H, dd, $J = 11.9, 5.3$ Hz, H-9a), indicating the occurrence of C3 unit, $-\text{OCHCHOHCH}_2\text{O}-$, which was supported by ^1H - ^1H COSY experiment (Figure 3.12). In addition, the ^1H NMR experiments of **MS16** exhibited a singlet at δ_{H} 2.04 (3H, s), which showed HMQC connectivity with the carbon at δ_{C} 20.8 and HMBC correlation with a carbonyl carbon at δ_{C} 170.6, confirming the presence of an acetyl group. From above mentioned NMR data indicated **MS16** was an 8-*O*-4' neolignan similar to *threo*-1-(3',4'-dimethoxyphenyl)-2-(2''-methoxy-4''-allylphenoxy)propane diol (carinatidiol) [47]. The main difference was an additional acetyl group in **MS16**. The HMBC correlation of the oxygenated protons at H-9 (δ_{H} 3.99, 4.24) to carbonyl carbon (δ_{C} 170.6) indicated that the acetyl group was attached to C-9. The relative configurations of **MS16** was verified to be 7,8-*threo* due to its large coupling constant between H-7 and H-8 ($J_{7,8} = 8.2$ Hz) [48]. The assignment of the absolute configuration was determined *via* the modified Mosher's ester method [49, 50]. **MS16** was then subsequently esterified by (*S*)- and (*R*)-MTPA-OH to yield the (*S*)- and (*R*)-MTPA esters,

respectively. Analysis of ^1H NMR chemical shift difference between (*S*)- and (*R*)-MTPA esters ($\Delta\delta_{\text{H}} = \delta_{\text{S}} - \delta_{\text{R}}$) of **MS16** is shown in figure 3.13 and table 2.36, indicating a 7*R* configuration. Thus, the absolute configuration of **MS16** was assigned as 7*R*,8*R*. Our conclusion was confirmed by CD spectrum of **MS16** which showed a cotton effect at 238 nm ($\Delta\epsilon$ -1.41, Figure 3.14) indicating an 8*R* configuration. This was also in accordance with its negative optical rotation by comparing with those of related 8-*O*-4'-neolignans reported in literature [48]. Therefore, the structure of **MS16** was elucidated as *threo*-(7*R*,8*R*)-3,3',4-trimethoxy-8,4'-oxyneolign-8'-en-7-ol-9-acetate.

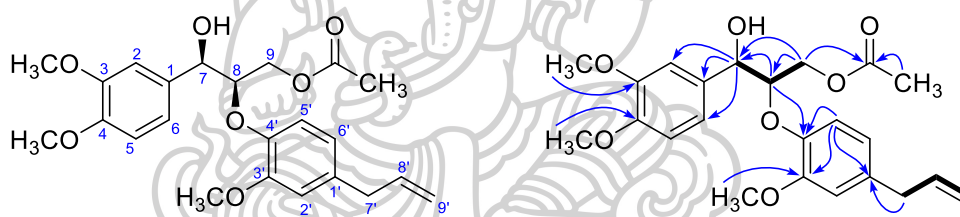


Figure 3.12 Structure, ^1H - ^1H COSY (bold line) and of HMBC (H \rightarrow C) correlation of **MS16**.

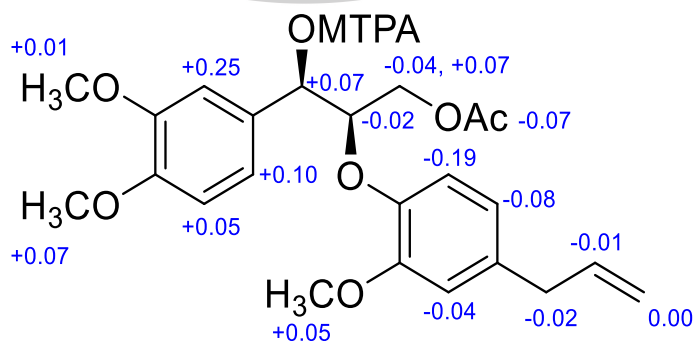


Figure 3.13 Difference in the $\Delta\delta$ values [$\Delta\delta$ (in ppm) = $\Delta\delta_{\text{S}} - \Delta\delta_{\text{R}}$] obtained from (*S*)- and (*R*)-MTPA esters of **MS16**.

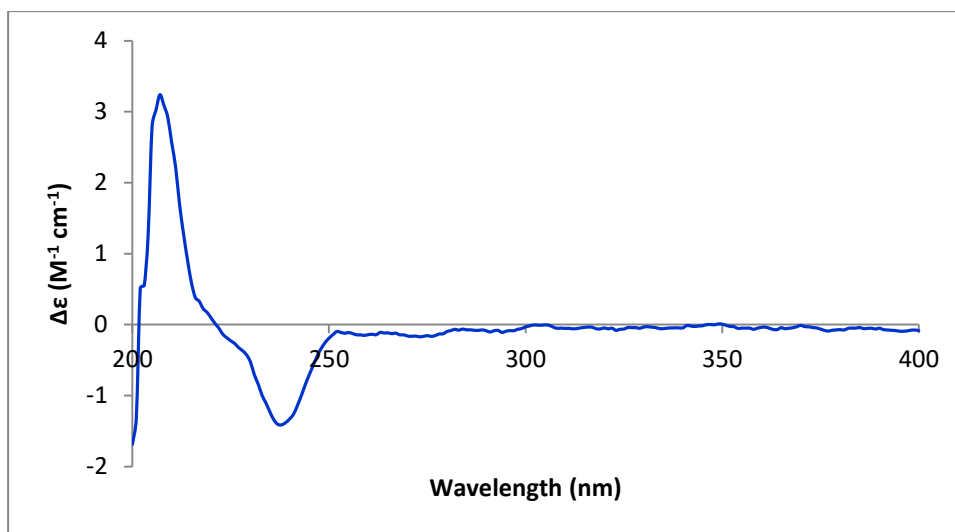


Figure 3.14 CD spectra of MS16.

3.1.1.7 *threo*-(7*R*,8*R*)-3,3',4-Trimethoxy-8,4'-oxyneolign-8'-en-7,9-diol (MS19)

MS19 was separated as an optically active pale green-brown viscous liquid, $[\alpha_D^{28}] -66.2^\circ$ (c 0.14, CHCl₃) with a molecular formula C₂₁H₂₆O₆ from the HRESTMS ion at m/z 397.1622 [M+Na]⁺ (calcd for C₂₁H₂₆O₆Na, 397.1627). The IR spectrum showed absorption bands of hydroxyl (3473 cm⁻¹), ether (1263, 1139 and 1028 cm⁻¹) and aromatic (1592 and 1464 cm⁻¹) moieties and the UV spectrum contained absorption band at λ_{\max} 281, 230 and 204 nm which supported the presence of aromatic ring. The ¹H NMR and ¹³C NMR data of **MS19** are similar to those of **MS16** except for disappearance of signals due to an acetyl group and the up field shift signals of an oxygenated methylene group at δ_H 3.62, 3.46 (2H, m, H-9) and δ_C 61.0 (C-9). The relative configuration of C-7 and C-8 was determine to be *threo* by its large coupling constant at H-7 and H-8 ($J_{7,8} = 7.4$ Hz). The absolute configurations were assigned as 8*R* based upon a negative cotton effect at 237 nm ($\Delta\varepsilon -4.25$, Figure

3.7). Furthermore, the comparison of the optical rotation values between **MS19** ($[\alpha_D^{23}] -66.2^\circ$) and *threo*-(7*R*,8*R*)-3,3',4-trimethoxy-8,4'-oxyneolign-8'-en-7-ol-9-acetate (**MS16**) ($[\alpha_D^{28}] -58.8^\circ$) suggested that **MS19** and **MS16** should have the same absolute configuration. Our conclusion was confirmed by hydrolysis of **MS16** under mild alkaline condition to provide hydrolyzed product which provided ^1H NMR, ^{13}C NMR spectral data and optical rotation value ($[\alpha_D^{23}] -52.5^\circ$ in CHCl_3) identical with **MS19**. Therefore, **MS19** was elucidated as *threo*-(7*R*,8*R*)-3,3',4-trimethoxy-8,4'-oxyneolign-8'-en-7,9-diol. The planar structure of **MS19** was identical to carinatidiol [47]. However, **MS19** had a negative optical rotation which was opposite to that of carinatidiol ($[\alpha]_D +97.2$ in CHCl_3). Thus **MS19** was defined as an enantiomer of carinatidiol.

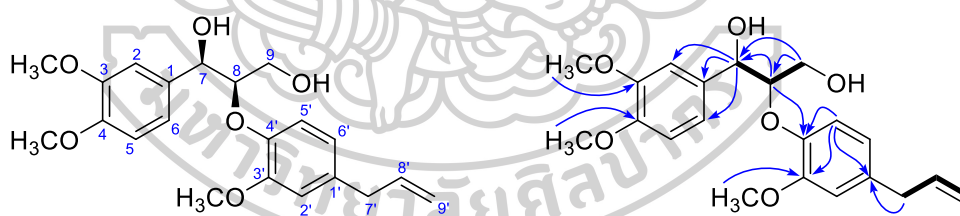


Figure 3.15 Structure, ^1H - ^1H COSY (bold line) and of HMBC (H→C) correlation of **MS19**.

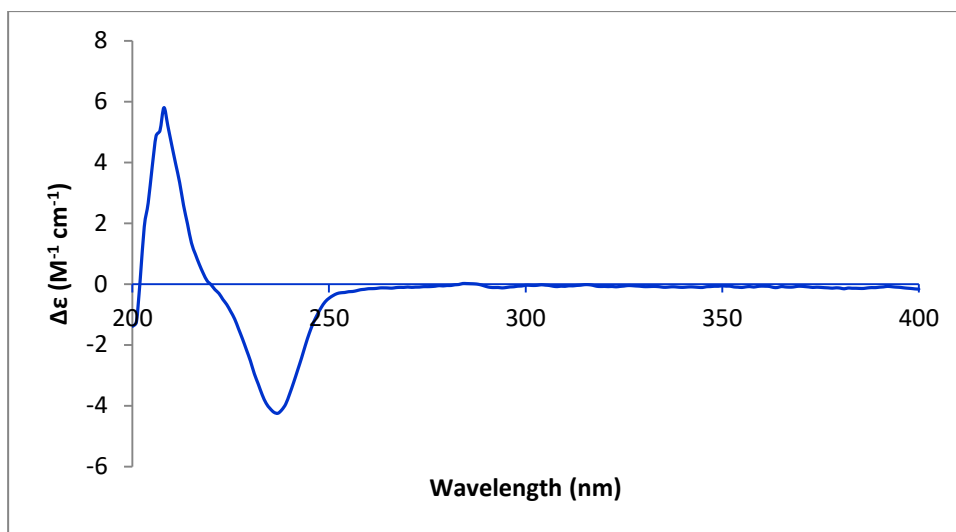
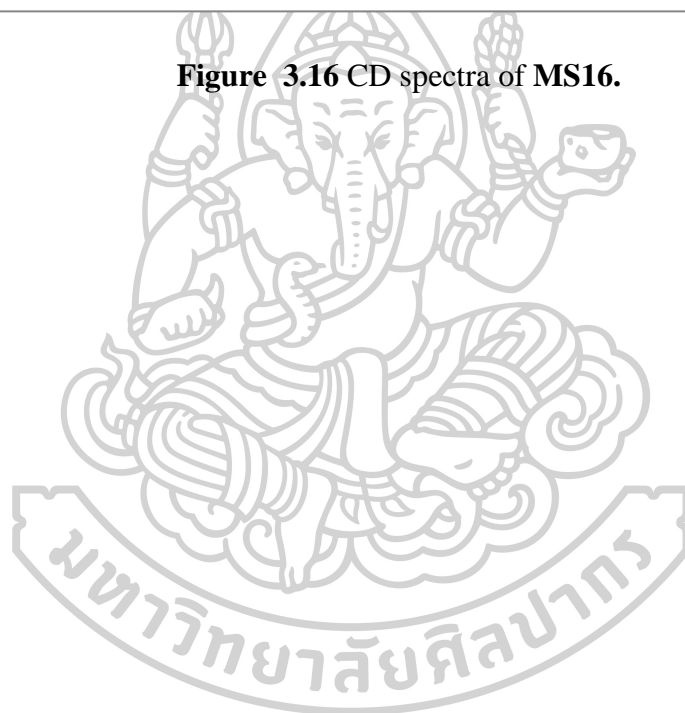


Figure 3.16 CD spectra of MS16.



3.1.1.8 *threo*-3,4-Dihydroxy-3',5-dimethoxy-8,4'-oxyneolign-8'-en-7,9-diol (MS20)

MS20 was separated as a colorless viscous liquid, $[\alpha_D^{28}] +1.5^\circ$ (c 0.13, CHCl₃) with a molecular formula C₂₀H₂₄O₇ from the HRESIMS ion at m/z 399.1411 [M+Na]⁺ (calcd for C₂₀H₂₄O₇Na, 399.1420). The IR spectrum showed absorption bands of hydroxyl (3400 cm⁻¹), ether (1264, 1130 and 1086 cm⁻¹) and aromatic (1596 and 1454 cm⁻¹) moieties. The ¹H NMR spectra (Table 2.34) of **MS20** showed the signals of one 1,3,4,5-tetrasubstituted aromatic ring [δ 6.48 (1H, *br s*, H-2) and 6.64 (1H, *br s*, H-6)], one 1,3,5-trisubstituted aromatic ring [6.73 (1H, *d*, $J = 1.1$ Hz, H-2'), 6.78 (1H, *d*, $J = 8.1$ Hz, H-5'), and 6.62 (1H, *dd*, $J = 8.1, 1.1$ Hz, H-6')], one 1,2,3-propane-triol moiety [δ 4.40 (1H, *d*, $J = 6.5$ Hz, H-7), 3.60 (1H, *m*, H-8), 3.34 (1H, overlapped, H-9b) and 3.43 (1H, *br d*, H-9a)] and one allyl moiety [3.30 (1H, *d*, $J = 6.5$ Hz, H-7'), 5.91 (1H, *ddt*, $J = 16.9, 10.3, 6.7$ Hz, H-8'), 5.06 (1H, *dd*, $J = 16.9, 1.4$ Hz, H-9'a) and 5.05 (1H, *dd*, $J = 10.3, 1.4$ Hz, H-9'b)]. Additionally, two methoxyl groups attached to aromatic ring at δ 3.75 (3H, *s*, $\times 2$ OMe) were observed. The ¹³C NMR spectrum of **MS20** showed twenty carbon signals. Aside from the two methoxy carbon signals the remaining eighteen carbon signals, including twelve aromatic and six aliphatic carbons. The HMBC correlations (Figure 3.17 and Table 2.34) of H-7 at δ_H 4.40 to C-1 (δ_C 131.8), C-2 (δ_C 110.2), C-6 (δ_C 105.3) C-8 (δ_C 74.6) and C-9 (δ_C 63.2) and of H-7' at δ_H 3.30 to C-1' (δ_C 136.5), C-2' (δ_C 113.0), C-6' (δ_C 121.0), C-8' (δ_C 137.2) and C-9' (δ_C 116.1) confirmed that the presence of two phenyl

propanoid units. These NMR spectroscopic data indicated **MS20** was an 8-*O*-4' neolignan. The position of two methoxyl groups at C-5 (δ_C 148.2) and C-3' (δ_C 150.1) were confirmed by HMBC correlations (Figure 3.15, Table 2.34). The substituents at C-3 (δ_C 144.3), C-4 (δ_C 136.7), C-7 (δ_C 74.6) and C-9 (δ_C 63.2) were identified as hydroxyl groups due to its relatively downfield ^{13}C NMR chemical shifts. The four hydroxyl groups were further confirmed by acetylation of **MS20** by treatment with acetic anhydride and pyridine at room temperature to obtain an acetated product (**MS20a**). The ^1H NMR and ^{13}C NMR of **MS20a** (Table 2.35) exhibited four acetate signal groups at δ_H 2.26, 2.00, 2.05 and 1.97, which showed one bond $^1\text{H}/^{13}\text{C}$ connectivity with the carbon at δ_C 20.4, 20.7, 20.9 and 20.6, respectively and HMBC correlation with carbonyl signals at δ_C 168.2, 170.0, 169.5 and 170.3, respectively, confirmed the presence of four acetyl groups. For the **MS20a**, the HMBC correlation of H-7 (δ_H 5.83) to carbonyl carbon (δ_C 169.5) and of H-9 (δ_H 4.23, 3.75) to carbonyl carbon (δ_C 170.3) indicated that two acetyl groups were placed on C-7 and C-9, respectively. The HMBC correlation of H-2 to C-1 (δ_C 133.9), C-3 (δ_C 150.8), C-4 (δ_C 150.8) and C-7 (δ_C 73.4) and of H-6 to C-1 (δ_C 134.0), C-5 (δ_C 152.8) and C-7 (δ_C 73.4) (Table 2.35) indicated that two aromatic acetyl groups were located at C-3 and C-4, respectively. The *threo* configuration between two chiral centers at C-7 and C-8 was determined by its large coupling constant ($J_{7,8} = 6.5$ Hz). Since the specific rotation of **MS20** was nearly zero comparing to those of optically pure compounds **MS16** and **MS19**. In addition, there was no cotton effect on the CD spectrum (Figure

3.18), indicating that compound **MS20** was obtained as a racemic mixture. Therefore, the structure of **MS20** was defined as *threo*-3,4-dihydroxy-3',5-dimethoxy-8,4'-oxyneolign-8'-en-7,9-diol.

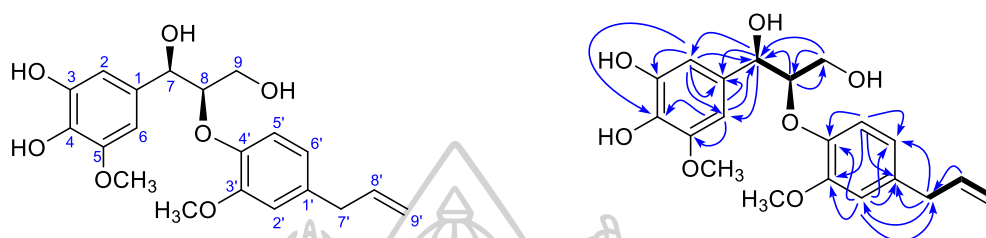


Figure 3.17 Structure, ^1H - ^1H COSY (bold line) and of HMBC (H \rightarrow C) correlation of **MS20**.

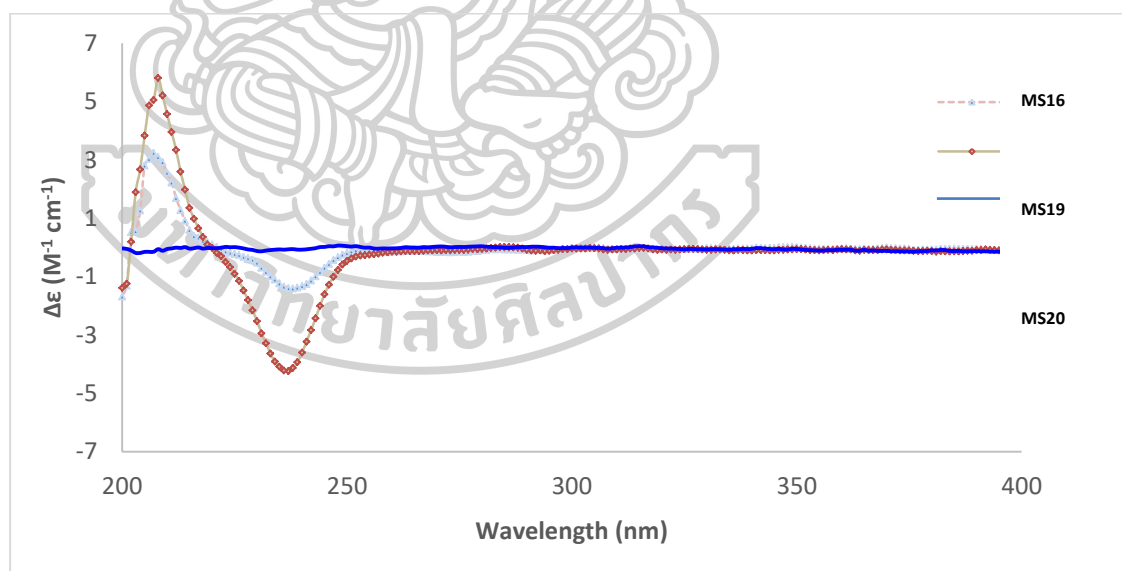


Figure 3.18 CD spectra of **MS20** compared with **MS16** and **MS19**.

3.1.2 Phenylpropanoid dimers

3.1.2.1 4-Hydroxy-3',5-dimethoxy-3,4'-oxyneolign-8,8'-dien

(dehydrodieugenol B) (MS10)

MS10 was obtained as pale green-brown viscous liquid and its molecular formula was determined to be $C_{20}H_{22}O_4$ from its molecular ion peak at m/z 325.1442 $[M-H]^+$ (calcd for 325.1440, $C_{20}H_{21}O_4$) in the HRESIMS. The IR spectrum showed the presence of a hydroxyl (3439 cm^{-1}), aromatic (1597 and 1454 cm^{-1}), alkene (1638 cm^{-1}) and ether (1129 and 1083 cm^{-1}) moieties. The ^1H NMR, ^{13}C NMR and HMBC spectra (Table 2.24 and Figure 3.19) of **MS10** showed the signals of one 1,3,4,5-tetrasubstituted aromatic ring [δ_{H} 6.42 (1H, d, $J = 1.5$ Hz, H-2), δ_{C} 111.8 (C-2) and 6.51 (1H, d, $J = 1.5$ Hz, H-6), 107.3 (C-6)], one 1,3,5-trisubstituted aromatic ring [6.81 (1H, d, $J = 1.8$ Hz, H-2'), 113.0 (C-2'); 6.91 (1H, d, $J = 8.1$ Hz, H-5'), 119.5 (C-5') and 6.72 (1H, dd, $J = 8.1, 1.8$ Hz, H-6'), 120.8, C-6'] and two allylic groups [δ_{H} 3.24 (2H, d, $J = 6.6$ Hz, H-7), 39.9 (C-7); 5.93 (1H, ddt, $J = 16.1, 9.4, 6.6$ Hz, H-8), 137.4 (C-8); 5.05 (1H, dd, $J = 16.1, 1.4$ Hz, H-9a) and 5.04 (1H, dd, $J = 9.4, 1.4$ Hz, H-9b), 115.7 (C-9) and 3.38 (2H, d, $J = 6.6$ Hz, H-7'), 39.9 (C-7'); 5.99 (1H, ddt, $J = 17.0, 10.4, 6.6$ Hz, H-8'), 137.3 (C-8); 5.11 (1H, dd, $J = 17.0, 1.5$ Hz, H-9'a) and 5.10 (1H, dd, $J = 10.4, 1.5$ Hz, H-9b), 115.9 (C-9)]. In addition, The ^1H NMR spectroscopic data showed two methoxyl groups at δ_{H} 3.89 (3H, s, $\times 2$ OMe) were observed. From the information above indicated that **MS10** was dehydrodieugenol B (1-(8-propenyl)-3-[1'-(8'-propenyl)-3'-methoxyphenoxy]-4-hydroxy-5-methoxybenzene or 4-hydroxy-3',5-dimethoxy-3,4'-oxyneolign-8,8'-dien) [36, 37].

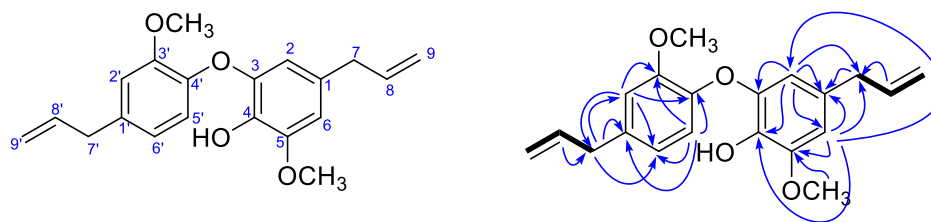


Figure 3.19 Structure, ^1H - ^1H COSY (bold line) and of HMBC (H \rightarrow C) correlation of **MS10**.

3.1.2.2 4,4'-Dihydroxy-3,3'-dimethoxy-5,5'-neolign-8,8'-dien, (dehydrodieugenol A) (MS13)

MS13 was isolated as pale yellow crystals and its molecular formula was determined to be $\text{C}_{20}\text{H}_{22}\text{O}_4$ from its molecular ion peak at m/z 325.1447 $[\text{M}-\text{H}]^+$ (calcd for 325.1440, $\text{C}_{20}\text{H}_{21}\text{O}_4$) in the HRESIMS. The IR spectrum showed the presence of hydroxyl (3452 cm^{-1}), aromatic (1599 and 1467 cm^{-1}), alkene (1639 cm^{-1}) and ether (1145 and 1047 cm^{-1}) moieties. The ^1H NMR and ^{13}C NMR spectra (Table 2.27) of **MS13** showed the signals of one 1,3,4,5-tetrasubstituted aromatic ring [δ_{H} 6.78 (1H, d, $J = 1.8\text{ Hz}$, H-2), δ_{C} 110.7 (C-2) and 6.75 (1H, d, $J = 1.8\text{ Hz}$, H-6), 123.4 (C-6)] and one allyl moiety [3.35 (2H, d, $J = 6.6\text{ Hz}$, H-7), 40.0 (C-7); 6.01 (1H, ddt, $J = 16.8, 9.9, 6.7\text{ Hz}$, H-8), 137.7 (C-8); 5.14 (1H, dd, $J = 16.8, 1.6\text{ Hz}$, H-9a) and 5.10 (1H, dd, $J = 9.9, 1.6\text{ Hz}$, H-9b), 115.7 (C-9). Additionally, ^1H NMR spectrum of **MS13** exhibited one methoxy group at δ 3.94 (3H, s, OMe) and one hydroxy group at δ 6.08 (1H, *br s*). The HMBC correlation of methoxy protons (δ_{H} 3.94) to C-3 (δ_{C} 147.2) and of hydroxy group (δ_{H} 6.08) to C-3 (δ_{C} 147.2), C-4 (δ_{C} 140.9) and C-5 (δ_{C} 148.2) indicated that methoxy and hydroxy groups were located

on C-3 and C-4, respectively. Up to now, a part of structure of **MS13** had been deduced as the ring A with the chemical formula of $C_{10}H_{11}O_2$. The exact molecule formula of **MS13** ($C_{20}H_{22}O_4$) suggested that **MS13** in fact a dimer. From the above evidence, the structure of **MS5** was defined as 4-hydroxy-3',5-dimethoxy-3,4'-oxyneolign-8,8'-dien (dehydrodieugenol B) [36].

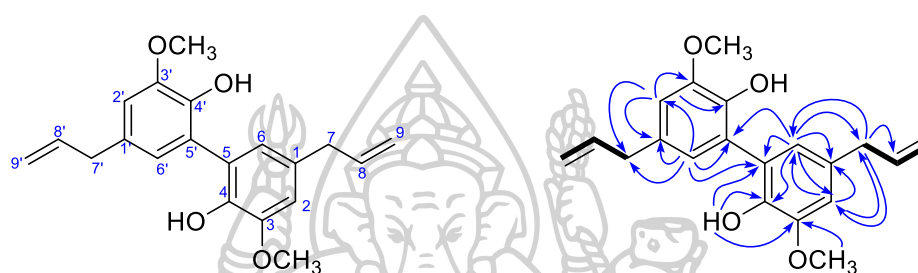


Figure 3.20 Structure, 1H - 1H COSY (bold line) and of HMBC (H→C) correlation of **MS13**.

3.1.2.3 4-Hydroxy-3',5-dimethoxy-3,4'-oxyneolign-7',8-dien-9'-ol

(MS18)

MS18 was obtained as pale yellow oil and its molecular formula was determined to be $C_{20}H_{22}O_5$ from its molecular ion peak at m/z 342.1467 $[M-H]^+$ (calcd for 341.1389, $C_{20}H_{21}O_5$) in the HRESIMS. The IR spectrum showed the presence of hydroxyl (3450 cm^{-1}), aromatic (1597 and 1454 cm^{-1}), alkene (1632 cm^{-1}) and ether (1129 and 1083 cm^{-1}) moieties. The ^1H NMR and ^{13}C NMR spectra (Table 2.32) of **MS18** showed the signals of one 1,3,4,5-tetrasubstituted aromatic ring [δ_{H} 6.41 (1H, d, $J = 1.8$ Hz, H-2), δ_{C} 112.2 (C-2) and 6.51 (1H, d, $J = 1.8$ Hz, H-6), 107.5 (C-6)], one 1,3,5-trisubstituted aromatic ring [7.01 (1H, d, $J = 1.6$ Hz, H-2'), 110.3 (C-2'); 6.87 (1H, d, $J = 5.4$ Hz, H-5'), 118.9 (C-5') and 6.88 (1H, dd, $J = 5.4, 1.6$ Hz, H-6'), 119.5, C-6'] and one allylic moiety [3.25 (2H, d, $J = 6.6$ Hz, H-7), 39.9 (C-7); 5.89 (1H, ddt, $J = 16.2, 9.5, 6.6$ Hz, H-8), 137.4 (C-8); 5.05 (1H, dd, $J = 16.2, 1.3$ Hz, H-9a) and 5.02 (1H, dd, $J = 9.5, 1.3$ Hz, H-9b), 115.8 (C-9)]. In addition, two methoxyl groups at δ 3.89 (3H, s, $\times 2$ OMe) were observed. The NMR spectra of **MS18** closely resembled those of the known dehydrodieugenol B (**MS10**) [36, 37], also isolated from this plant, established that they were closely related. The main difference was the observation of signal attributed of a -CH=CHCH₂OH in ^1H NMR of **MS18** at δ_{H} 6.57 (1H, d, $J = 15.8$ Hz, H-7'), 6.29 (1H, dt, $J = 15.8, 5.8$ Hz, H-8') and 4.32 (1H, d, $J = 5.8$ Hz, H-9'). The ^{13}C NMR data also displayed two olefinic methine carbons at δ_{C} 130.8 (C-7') and δ_{C} 127.9 (C-8') and an oxygenated methylene carbon at δ_{C} 63.7 (C-9')

confirming the presence of the $-\text{CH}=\text{CHCH}_2\text{OH}$ moiety which was supported by $^1\text{H}-^1\text{H}$ COSY data (Figure 3.21). The HMBC spectrum showed correlations between the signals at δ_{H} 6.29 (H-8') and C-1' (δ_{C} 133.0), C-7' and C-9' and at δ_{H} 6.57 (H-7') and C-1', C-2' (δ_{C} 110.3), C-6' (δ_{C} 119.5), C-8' and C-9' (Figure 3.21). This suggested that the 3-hydroxypropenyl moiety was placed at C-1'. Therefore, the structure of **MS18** was defined as 4-hydroxy-3',5-dimethoxy-3,4'-oxyneolign-7',8-dien-9'-ol.

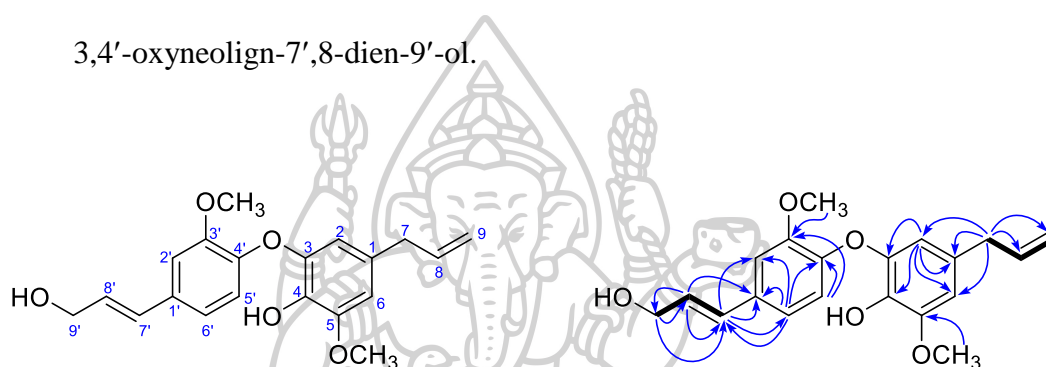


Figure 3.21 Structure, $^1\text{H}-^1\text{H}$ COSY (bold line) and of HMBC (H \rightarrow C) correlation of **MS18**.



3.1.3 Triterpenes

3.1.3.1 (3 β ,23*S*)-23-Methoxy-24-methylenenorlanost-9-en-3-ol

(MS5)

MS5 was obtained as a colorless crystalline from ethanol/ethyl acetate with a positive optical rotation, $[\alpha_D^{23}] +88.5^\circ$ (c 0.15, CHCl₃). The IR spectrum showed the presence of hydroxyl (3371 cm⁻¹), alkene (1647 cm⁻¹) and ether (1085 and 1108 cm⁻¹) functionalities. The molecular formula was established as C₃₁H₅₂O₂ from the pseudomolecular HRESIMS [M+NH₄]⁺ ion peak at 474.4296 (cald for C₃₁H₅₆NO₂, 474.4310). The ¹H NMR spectrum of **MS5** (Table 2.20) indicated the presence of three tertiary methyls [δ_H 0.69 (3H, s, Me-18), 0.73 (3H, s, Me-29) and 0.99 (3H, s, Me-19)], four secondary methyls [δ_H 0.92 (3H, d, $J = 6.4$ Hz, Me-21), 0.97 (3H, d, $J = 6.3$ Hz, Me-28), 1.05 (3H, d, $J = 7.0$ Hz, Me-26) and 1.07 (3H, d, $J = 7.4$ Hz, Me-27)], a methoxy group at δ_H 3.21 (3 H, s, OMe-23), two methylenes at δ_H 4.92 (1H, s, H-24¹) and 4.98 (1H, s, H-24¹), a vinyl methine at δ_H 5.23 (1H, dd, $J = 3.6, 2.8$ Hz, H-11) and two oxygenated methine protons [δ_H 3.08 (1H, td, $J = 11.5, 3.0$ Hz, H-3) and 3.60 (1H, dd, $J = 10.3, 1.4$ Hz, H-23)]. The ¹³C NMR spectral data (Table 2.20) indicated 31 carbons resonances which were classified by DEPT and HMQC experiments as one trisubstituted double bond [δ_C 146.5 (C-9) and 116.4 (C-11)] and one terminal double bond [δ_C 156.6 (C-24) and 107.4 (C-24¹)] carbons. The remaining 27 carbons were assigned to seven methyl carbons [δ_C 23.5 (C-26), 22.5 (C-27), 20.5 (C-19), 18.3 (C-29), 18.2 (C-21), 15.3 (C-28) and 14.6 (C-18)], an oxygenated methyl carbon (δ_C 56.4, C-23-

OMe), two oxygenated methine carbons [δ_C 81.7 (C-23) and 76.5 (C-3)], six methine carbons [δ_C 51.7 (C-17), 49.3 (C-5), 41.3 (C-8), 39.4 (C-4), 33.0 (C-20) and 29.9 (C-25)], three quaternary carbons [δ_C 47.2 (C-14), 44.4 (C-13) and 38.7 (C-10)] and eight methylene carbons [δ_C 43.2 (C-22), 37.5 (C-12), 35.4 (C-1), 33.9 (C-15), 31.2 (C-2), 28.1 (C-16), 27.4 (C-7) and 24.0 (C-6)]. From the molecular formula ($C_{31}H_{52}O_2$) of **MS5** indicated six degrees of unsaturation together with the above NMR data, suggesting **MS5** to be a tetracyclic triterpene with two olefinic groups. The structure of **MS5** was determined from HMBC and 1H - 1H COSY spectra (Figure 3.22). The HMBC spectrum of **MS5** indicated long-range correlations of CH_3 -19 (δ_H 0.99) to C-1, C-5, C-9 and C-10; CH_3 -18 (δ_H 0.69) to C-12, C-13, C-14 and C-17 and CH_3 -29 (δ_H 0.73) to C-8, C-13, C-14 and C-15. The HMBC correlations of olefinic methine proton at δ_H 5.23 (H-11) to C-8, C-9, C-10, C-12 and C-13 indicated that an olefinic group positioned on C-9 and C-11. Significant cross-peaks were observed from oxygenated methine proton at δ_H 3.08 to C-2, C-4, C-5 and methyl protons at δ_H 0.97 to C-3, C-4, and C-5 in the HMBC experiment, indicating a hydroxyl group and a methyl group placed on C-3 and C-4, respectively. The hydroxyl-bearing methine proton signal at δ_H 3.08 was assigned to H-3 and the β configuration of the C-3 hydroxyl group was confirmed by its large coupling constant (td, $J = 11.5, 3.0$ Hz) (Li et al., 1993). The spectroscopic data above suggested that the structure of **MS5** was a 29-nor-9(11)-en-lanost-3 β -ol skeleton [51-53]. The position of an exomethylene group was established by the observation of the HMBC correlations between

the exomethylene proton signals (δ_{H} 4.92 and 4.98) and C-22 (δ_{C} 43.2), C-23 (δ_{C} 81.7), C-25 (δ_{C} 29.9), C-26 (δ_{C} 23.5) and C-27 (δ_{C} 22.5). The position of a methoxy group was suggested on C-23 by the observation of the HMBC correlation from the methoxyl protons (δ_{H} 3.21) to C-23 (δ_{C} 81.7). The relative configuration of **MS5** was confirmed by X-ray crystallographic analysis, which was shown in figure 3.23. Thus, structure **MS5** was established as (3 β ,23*S*)-23-methoxy-24-methylenenorlanost-9-en-3-ol.

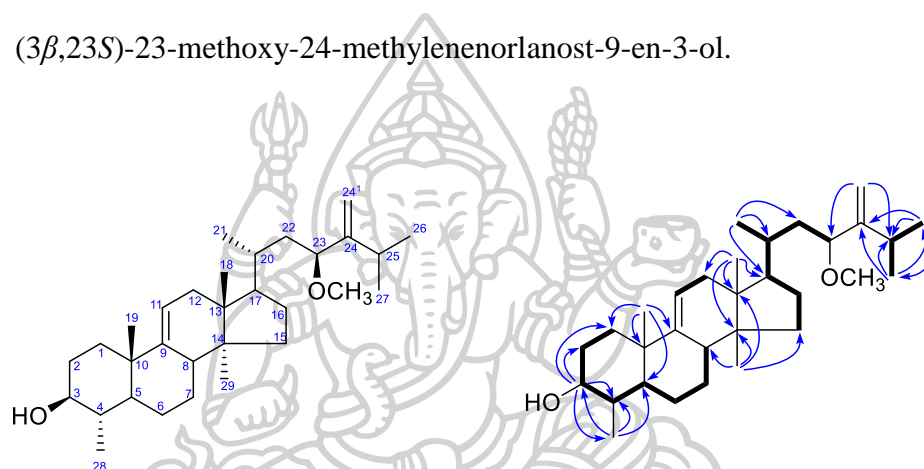


Figure 3.22 Structure, ^1H - ^1H COSY (bold line) and of HMBC (H \rightarrow C) correlation of **MS5**.

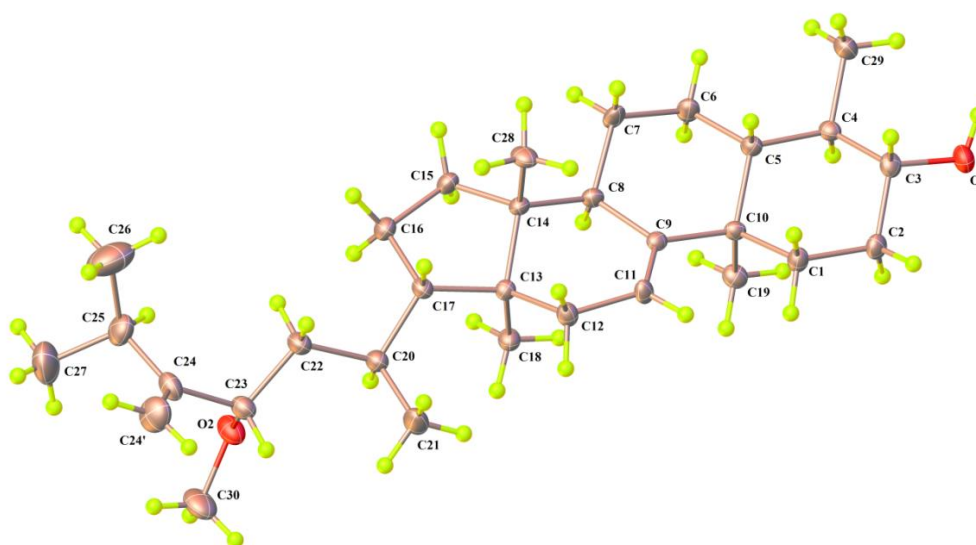


Figure 3.23 X-ray ORTEP diagram of **MS5**.

3.1.3.2 (3 β ,23S)-23-Methoxy-24-methylenelanost-9-en-3-ol (MS3)

MS3 was provided as a colorless needle from ethanol/ethyl acetate with a positive optical rotation, $[\alpha_D^{23}] +84.2^\circ$ (c 0.06, CHCl₃) and its IR spectrum presented of hydroxyl (3323 cm⁻¹), alkene (1639 cm⁻¹) and ether (1111 and 1087 cm⁻¹) groups. The molecular formula of **MS3** was determined to be C₃₂H₅₄O₂ from the pseudomolecular HRESIMS [M+NH₄]⁺ ion peak at 488.4462 (calcd for C₃₂H₅₈NO₂, 488.4467). The ¹H NMR, ¹³C NMR and HMBC spectra of **MS3** indicated the presence of five tertiary methyls [δ_H 1.05 (3H, s, H-19), δ_C 22.3 (C-19); 0.99 (3H, s, H-29), 28.3 (C-29); 0.82 (3H, s, H-28), 15.7 (C-28); 0.73 (3H, s, H-30), 18.5 (C-30) and 0.68 (3H, s, H-18), 14.5 (C-18);], three secondary methyls [δ_H 1.05 (3H, d, $J = 7.1$ Hz, H-26), δ_C 23.5 (C-26); 1.07 (3H, d, $J = 7.1$ Hz, H-27), 22.5 (C-27) and 0.92 (3H, d, $J = 6.3$ Hz, H-21), 18.3 (C-21)], a vinyl methylene [δ_H 4.92 (1H, s, H-24¹), 4.98 (1H, s, H-24¹) and δ_C 107.4 (C-24¹)] and two oxygenated methines [δ_H 3.21 (1H, overlapped, H-3), δ_C 78.9 (C-3) and 3.59 (dd, $J = 9.3, 1.0$ Hz, H-23), 81.7 (C-23)] (Table 2.18). The molecular formula indicated the presence of six degrees of unsaturation concomitant with the NMR spectral data, suggesting **MS3** to be a tetracyclic triterpene with two olefinic groups. The NMR spectroscopic data pattern of **MS3** resembled those of **MS5** except for the appearance of an additional methyl group in **MS3**. The ¹H NMR spectrum of **MS3** show two tertiary methyl singlets at δ_H 0.82 (3H, s, Me-28) and 0.99 (3H, s, Me-29) which showed one bond ¹H/¹³C connectivity with the carbons at δ_C 28.3 and 15.7, respectively. The HMBC spectrum showed long-range correlation from

Me-28 and Me-29 to C-3 (δ_C 78.9), C-4 and C-5 (δ_C 52.5) (Figure 3.24), indicating that both methyl groups were placed at C-4. The relative configuration of **MS3** was also confirmed by X-ray crystallographic analysis (Figure 3.25). Therefore, structure **MS3** was established as (3 β ,23*S*)-23-methoxy-24-methylenelanost-9-en-3-ol.

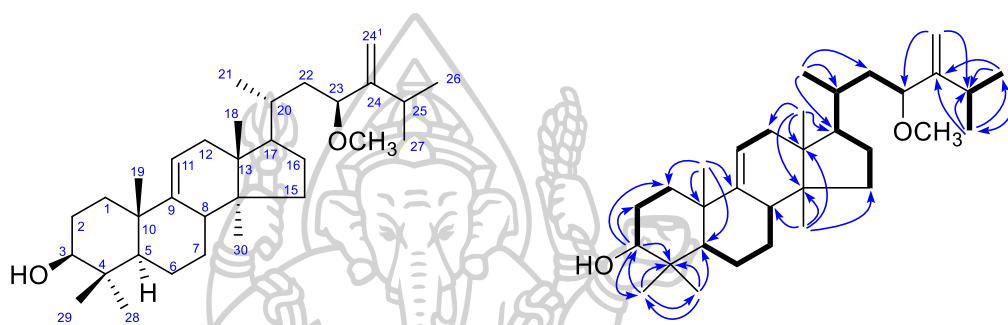


Figure 3.24 Structure, ^1H - ^1H COSY (bold line) and of HMBC (H \rightarrow C) correlation of **MS3**.

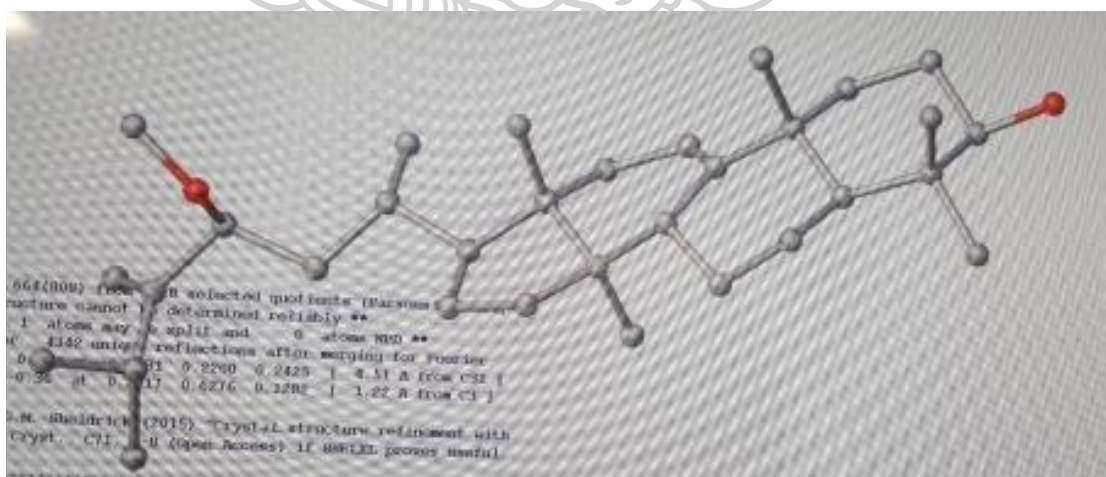


Figure 3.25 X-ray ORTEP diagram of **MS3**.

3.1.3.3 (3 β ,16 β)-24-Methylenelanost-9-en-3,16-diol (MS7)

MS7 was provided as a colorless needle from ethanol/ethyl acetate with a positive optical rotation, $[\alpha_D^{23}] +67.2^\circ$ (c 0.046, CHCl₃) and its IR spectrum presented of hydroxyl (3406 cm⁻¹) and alkene (1639 cm⁻¹) absorptions. The molecular of MS7 was determined to be C₃₁H₅₂O₂ from the pseudomolecular HRESIMS [M+NH₄]⁺ ion peak at 474.4278 (calcd for C₃₁H₅₆NO₂, 474.4310). The ¹H NMR and ¹³C NMR spectra of MS7 indicated the presence of five tertiary methyls [δ_H 1.06 (3H, s, H-19), δ_C 22.3 (C-19); 0.99 (3H, s, H-29), 28.2 (C-29); 0.83 (3H, s, H-18), 15.3 (C-18); 0.82 (3H, s, H-28), 15.7 (C-28) and 0.72 (3H, s, H-30), 19.1 (C-30)], three secondary methyls [δ_H 1.03 (3H, d, $J = 6.8$ Hz, H-26), δ_C 21.9 (C-26); 1.03 (3H, d, $J = 6.8$ Hz, H-27), 21.8 (C-27) and 0.98 (3H, d, $J = 6.2$ Hz, H-21), 18.0 (C-21)], a vinyl methylene [δ_H 4.70 (1H, s, H-24¹), 4.75 (1H, s, H-24¹) and δ_C 106.2 (C-24¹)] and two oxygenated methines [δ_H 3.21 (td, $J = 11.0, 4.3$ Hz, H-3), δ_C 78.9 (C-3) and 4.43 (dd, $J = 12.4, 2.8$ Hz, H-16), 72.7 (C-16)] (Table 2.22). From the above information suggested that the structure of MS7 similar to MS3. The main difference were the absence of the C-23 methoxy substituent and the observation of an additional oxygenated methine proton at δ_H 4.43 (dd, $J = 12.4, 2.8$ Hz) in the ¹H NMR spectrum of MS7. From the ¹H-¹H COSY spectrum and the HMBC correlations (Figure 3.26) from H-17 (δ_H 1.70, m) and H-15 (δ_H 1.43, m and δ_H 2.05, m) to the oxygenated methine carbon at δ_C 72.7 indicated that the hydroxyl group was located at C-16. Furthermore, the relative configuration was also confirmed by X-ray crystallographic analysis.

A 3-D structure of molecule **MS7** is shown in figure 3.24. On the basis of the spectroscopic evidence, the structure of **MS7** was characterized as (3 β ,16 β)-24-methylenelanost-9-en-3,16-diol.

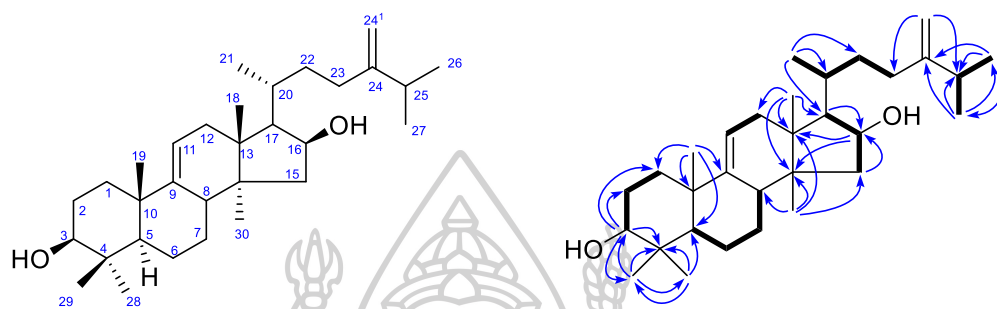


Figure 3.26 Structure, ^1H - ^1H COSY (bold line) and of HMBC (H \rightarrow C) correlation of **MS7**.

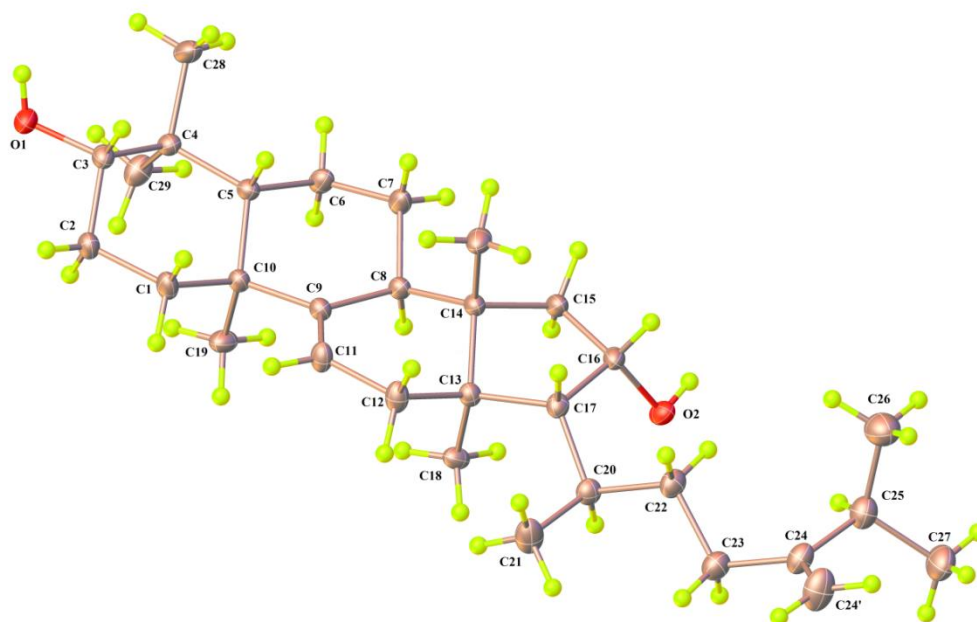


Figure 3.27 X-ray ORTEP diagram of **MS7**.

3.1.3.4 (3 β)-24,24¹-Epoxy- lanost-9-en-3-ol (MS6)

MS6 was provided as a colorless needle from ethanol/ethyl acetate with a positive optical rotation, $[\alpha]_D^{23} +48.6^\circ$ (c 0.046, CHCl₃) and its IR spectrum revealed absorptions for a hydroxyl group at 3405 cm⁻¹, an alkene group at 1639 cm⁻¹ and ether groups at 1245, 1157 and 980 cm⁻¹. The HRESIMS [M+H]⁺ ion peak at 457.4023 (cald for C₃₁H₅₃NO₂, 457.4045) suggested the molecular formula C₃₁H₅₂O₂. The ¹H NMR and ¹³C NMR spectra of **MS6** were similar to those of **MS3**, except for the side chain data which lack of methoxy group. Furthermore, the ¹H NMR and ¹³C NMR spectrum showed an oxirane group [δ_H 2.54 (1H, d, $J = 4.6$, H₂₄¹), 2.59 (1H, d, $J = 4.6$, H-24¹), δ_C 62.8 (C-24) and 50.5 (C-24¹)] was attributed to the side chain. The presence of HMBC correlation from H-26 (δ_H 0.96, d, $J = 6.8$) to C-24 (δ_C 62.8), H-27 (δ_H 0.90, d, $J = 6.8$) to C-24 (δ_C 62.8), H-25 (δ_H 1.79, m) to C24 and C-24¹ and also H-24¹ to C-23, C-24 and C-25, indicated the side chain of **MS6** to be 24,24¹-epoxyl substituted (figure 3.28). Thus, structure of **MS6** was established as (3 β)-24,24¹-Epoxy- lanost-9-en-3-ol.

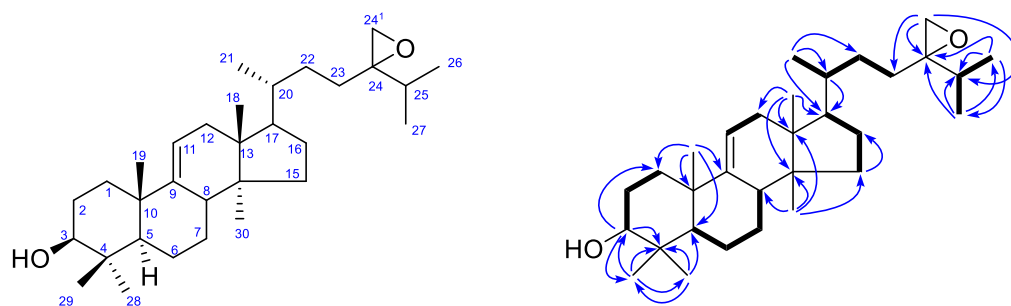


Figure 3.28 Structure, ¹H-¹H COSY (bold line) and of HMBC (H→C) correlation of **MS6**.

3.2 Biological evaluation

We measured the cytotoxicities of all the isolated compounds against four tumor cell lines, including HeLa (human cervical carcinoma), HN22 (head and neck cancer), HepG2 (Hepatocellular carcinoma) and HCT116 (colorectal cancer) cell lines, as well as a normal cell line (HaCaT, human immortalized keratinocyte cell line). The results of their cytotoxic activities and selective index (SI) compared with a normal cell line HaCaT are shown in Table 3.1. Four dihydro[*b*]benzofuran neolignans (**MS11**, **MS12**, **MS15** and **MS17**) exhibited significant cytotoxic activities against the HeLa cell line with IC_{50} values from 0.04 to 2.50 μM . Among them, **MS17** displayed the most promising cytotoxic activity with the lowest IC_{50} value of 0.04 μM and the highest SI value of 187.8. Compound **MS12** exhibited strong cytotoxicity against both the HN22 and HeLa cell lines with IC_{50} values of 0.18 and 0.23 μM , however, these compounds showed poor selectivity towards both tested cell lines (8.2 and 6.4, respectively). Two 8-*O*-4' neolignans **MS16** and **MS19** showed lower cytotoxic activities against the HeLa cell line than compounds **MS11**, **MS12**, **MS15** and **MS17** with IC_{50} (SI) values of 4.06 (75.3) and 2.86 (46.2) μM , respectively, whereas compound **MS20** was inactive toward four cancer cell lines. Phenylpropanoid dimer **MS10** had a strong cytotoxic effect against the HepG2 cell line with $IC_{50} = 2.17\mu\text{M}$ and $SI = 20.4$, while compound **MS18** exhibited moderate to weak cytotoxic activities against the four cell lines with the IC_{50} values ranging from 9.79 to 88.52 μM . On the other hand, dineolignan **MS14** and dehydrodieugenol A (**MS13**) were inactive toward all cancer cell lines ($IC_{50} > 150 \mu\text{M}$)

Table 3.1 Cytotoxic activity and selectivity index (SI) of compounds isolated from *M. sessilis* leaves.

Cpd.	Cell Lines											
	HaCaT		HeLa		HN22		HepG2		HCT116			
	IC ₅₀ ^a	IC ₅₀	SI ^b	IC ₅₀	IC ₅₀	SI	IC ₅₀	IC ₅₀	SI	IC ₅₀	IC ₅₀	SI
MS11	46.34 (22.08-97.42)	1.76 (0.95-3.26)	26.3	37.30 (19.94-67.83)	1.2	8.04 (5.42-11.85)	8.66 (6.25-11.98)	5.8	8.66 (6.25-11.98)	5.4		
MS12	1.48 (0.31-1.74)	0.23 (0.05-0.98)	6.4	0.18 (0.05-0.57)	8.2	2.92 (2.06-4.11)	4.53 (2.63-7.84)	0.5	4.53 (2.63-7.84)	0.3		
MS15	164.42 (144.82-186.63)	2.50 (1.57-3.93)	65.8	34.31 (15.05-78.25)	4.8	6.15 (2.86-13.11)	16.45 (11.48-23.61)	26.7	16.45 (11.48-23.61)	10.0		
MS17	7.51 (3.43-16.44)	0.04 (0.01-0.13)	187.8	35.25 (25.08-49.54)	0.2	12.92 (6.43-25.90)	102.68 (65.80-162.71)	0.6	102.68 (65.80-162.71)	0.1		
MS14	>500	>150	ND ^c	>150	ND	>150	>150	ND	>150	ND		
MS16	305.87 (255.90-365.46)	4.06 (3.20-5.17)	75.3	43.06 (25.42-72.92)	7.1	49.47 (32.17-76.12)	75.21 (48.54-116.51)	6.2	75.21 (48.54-116.51)	4.1		
MS19	132.16 (77.77-224.58)	2.86 (2.11-3.88)	46.2	40.28 (24.75-65.56)	3.3	9.59 (3.96-23.20)	107.46 (74.91-154.10)	13.8	107.46 (74.91-154.10)	1.2		
MS20	>500	>150	ND	>150	ND	>150	>150	ND	>150	ND		
MS10	55.16 (36.79-82.66)	11.31 (5.18-24.71)	4.9	15.45 (5.89-40.50)	3.6	2.71 (1.33-5.58)	52.66 (36.10-76.83)	20.4	52.66 (36.10-76.83)	1.0		
MS13	>500	>150	ND	>150	ND	>150	>150	ND	>150	ND		
MS18	276.87 (142.57-537.78)	18.09 (11.87-27.53)	15.3	9.79 (5.32-18.06)	28.3	88.52 (49.15-159.34)	40.20 (33.36-48.41)	3.1	40.20 (33.36-48.41)	6.9		
PC^d	6.14 (4.63-8.15)	97.25 (65.20-145.10)	0.1	13.23 (11.84-14.77)	0.5	6.96 (5.07-9.55)	6.30 (4.97-7.97)	0.9	6.30 (4.97-7.97)	0.1		

^a IC₅₀ (concentration inhibiting 50% growth) are expressed as μ M.^b Selectivity Index (SI) is the ratio of the treatments on HaCaT cells to those in the cancer cell lines.^c Not determine^d Positive control is irinotecan

CHAPTER 4

CONCLUSIONS

The first investigation of the leaves extracts of *Milium sessilis* yielded neolignans, triterpenes and sesquiterpenes. Neolignans were the main second metabolites which complemented previous reports of the occurrence of neolignans in the *Milium* genus. Nine new neolignans (**MS11**, **MS12**, **MS14-MS20**) were first isolated from this plant, together with two known neolignans (**MS10** and **MS13**) that were first isolated from this genus. Four new lanostane triterpenes (**MS3**, **MS5-MS7**) were isolated for the first time from this genus, together with two known sesquiterpenes (**MS1** and **MS4**). Neolignans were estimated for their cytotoxicity activity against four cancer cell lines. Of all these compounds isolated, **MS17** exhibited the most significant cytotoxic effect against HeLa cells with IC_{50} in the micromolar range and high selectivity index over 180 fold against HeLa cells compare to non-cancer cell line HaCaT. Thus, **MS17** may be a potential candidate for anticancer drug development.

REFERENCES

1. Mols, J.B. and P.J.A. Kessler, *The genus Miliusa (Annonaceae) in the austro-Malesian area*. Blumea, 2003. **48**(3): p. 421-462.
2. Chaowasku, T. and P.J.A. Kessler, *Seven new species of Miliusa (Annonaceae) from Thailand*. Nord. J. Bot., 2013. **31**(6): p. 680-699.
3. Chaowasku, T. and P.J.A. Kessler, *Miliusa lanceolata (Annonaceae), a new species from Papua New Guinea*. Blumea, 2006. **51**(3): p. 553-557.
4. Chaowasku, T. and P.J.A. Kessler, *Miliusa cambodgensis sp. nov. (Annonaceae) from Cambodia and M. astiana, M. ninhbinhensis spp. nov. from Vietnam*. Nord. J. Bot., 2014. **32**(3): p. 298-307.
5. Promchai, T., T. Saesong, K. Ingkaninan, S. Laphookhieo, S.G. Pyne, and T. Limtharakul, *Acetylcholinesterase inhibitory activity of chemical constituents isolated from Miliusa thorelii*. Phytochem Lett., 2018. **23**: p. 33-37.
6. Promchai, T., A. Jaidee, S. Cheenpracha, K. Trisuwan, R. Rattanajak, S. Kamchonwongpaisan, S. Laphookhieo, S.G. Pyne, and T. Ritthiwigrom, *Antimalarial oxoprotoberberine alkaloids from the leaves of Miliusa cuneata*. J. Nat. Prod., 2016. **79**(4): p. 978-983.
7. Jumana, S., C.M. Hasan, and M.A. Rashid, *Isocorydine- α -N-oxide: A new aporphine alkaloid from M. velutina*. Nat. Prod. Lett, 2000. **14**: p. 393-397.
8. Harrigan, G.G., A.L. Gunatilaka, D.G. Kingston, G.W. Chan, and R.K. Johnson, *Isolation of bioactive and other oxoaporphine alkaloids from two annonaceous plants, Xylopiya aethiopica and Miliusa cf. banacea*. J. Nat. Prod., 1994. **57**(1): p. 68-73.
9. Zhang, H.-J., C. Ma, N.V. Hung, N.M. Cuong, G.T. Tan, B.D. Santarsiero, A.D. Mesecar, D.D. Soejarto, J.M. Pezzuto, and H.H. Fong, *Miliusanes, a class of cytotoxic agents from Miliusa sinensis*. J. Med. Chem., 2006. **49**(2): p. 693-708.
10. Sawasdee, K., T. Chaowasku, V. Lipipun, T.-H. Dufat, S. Michel, V. Jongbunprasert, and K. Likhitwitayawuid, *Geranylated homogentisic acid derivatives and flavonols from Miliusa umpangensis*. Biochem. Syst. Ecol, 2014. **54**: p. 179-181.
11. Huong, D.T., C. Kamperdick, and T.V. Sung, *Homogentisic acid derivatives from Miliusa balansae*. J. Nat. Prod., 2004. **67**(3): p. 445-447.
12. Wongsas, N., K. Kanokmedhakul, J. Boonmak, S. Youngme, and S. Kanokmedhakul, *Bicyclic lactones and racemic mixtures of dimeric styrylpyrones from the leaves of Miliusa velutina*. RSC advances, 2017. **7**(41): p. 25285-25297.

13. Van, N.T.H., C. Kamperdick, N.T.H. Anh, and T. Van Sung, *Two new bis-styryl compounds from Miliusa balansae*. Z. Naturforsch. B, 2008. **63**(3): p. 335-338.
14. Kamperdick, C., N.H. Van, and T. Van Sung, *Constituents from Miliusa balansae (Annonaceae)*. Phytochemistry, 2002. **61**(8): p. 991-994.
15. Sawasdee, K., T. Chaowasku, V. Lipipun, T.-H. Dufat, S. Michel, and K. Likhitwitayawuid, *New neolignans and a lignan from Miliusa fragrans, and their anti-herpetic and cytotoxic activities*. Tetrahedron Lett., 2013. **54**(32): p. 4259-4263.
16. Sawasdee, K., T. Chaowasku, V. Lipipun, T.-H. Dufat, S. Michel, and K. Likhitwitayawuid, *Neolignans from leaves of Miliusa mollis*. Fitoterapia, 2013. **85**: p. 49-56.
17. Sawasdee, K., T. Chaowasku, and K. Likhitwitayawuid, *New neolignans and a phenylpropanoid glycoside from twigs of Miliusa mollis*. Molecules, 2010. **15**(2): p. 639-648.
18. Wongsas, N., S. Kanokmedhakul, and K. Kanokmedhakul, *Corrigendum to "Cananginones A–I, linear acetogenins from the stem bark of Cananga latifolia" [Phytochemistry 72 (14-15)(2011) 1859–1864]*. Phytochemistry, 2015. **109**: p. 154.
19. Wu, R., Q. Ye, N.Y. Chen, and G.L. Zhang, *A new norditerpene from Miliusa balansae Finet et Gagnep.* Chin Chem Lett., 2001. **12**(3): p. 247-248.
20. Thao, N.P., B.T.T. Luyen, B.H. Tai, N.M. Cuong, Y.C. Kim, C. Van Minh, and Y.H. Kim, *Chemical constituents of Miliusa balansae leaves and inhibition of nitric oxide production in lipopolysaccharide-induced RAW 264.7 cells*. Bioorg. Med. Chem. Lett., 2015. **25**(18): p. 3859-3863.
21. Lei, Y., L.J. Wu, H.M. Shi, and P.F. Tu, *Three new glycosides from the stems of Miliusa balansae*. Helv. Chim. Acta., 2008. **91**(3): p. 495-500.
22. Lei, Y., L.-j. WU, D. BI, J.-w. SUN, and P.-f. TU, *Isolation and identification of chemical constituents from stems of Miliusa balansae Fin. et Gag.[J]*. Shenyang Yaoke Daxue Xuebao, 2009. **2**.
23. Jumana, S., C.M. Hasan, and M.A. Rashid, *Alkaloids from the stem bark of Miliusa velutina*. Biochem. Syst. Ecol, 2000. **28**(5): p. 483-485.
24. Jumana, S., C.M. Hasan, and M.A. Rashid, *Antibacterial activity and cytotoxicity of Miliusa velutina*. Fitoterapia, 2000. **71**(5): p. 559-561.
25. Wongsas, N., S. Kanokmedhakul, and K. Kanokmedhakul, *Cananginones A–I, linear acetogenins from the stem bark of Cananga latifolia*. Phytochemistry, 2011. **72**(14-15): p. 1859-1864.

26. Promgool, T., K. Kanokmedhakul, S. Tontapha, V. Amornkitbamrung, S. Tongpim, W. Jamjan, and S. Kanokmedhakul, *Bioactive homogentisic acid derivatives from fruits and flowers of Miliusa velutina*. *Fitoterapia*, 2019. **134**: p. 65-72.
27. Huong, D.T., D.V. Luong, T.T.P. Thao, and T.V. Sung, *A new flavone and cytotoxic activity of flavonoid constituents isolated from Miliusa balansae (Annonaceae)*. *Pharmazie*, 2005. **60**(8): p. 627-629.
28. Thuy, T.T.T., T.D. Quan, N.T.H. Anh, and T. Van Sung, *A new hydrochalcone from Miliusa sinensis*. *Nat. Prod. Res.*, 2011. **25**(14): p. 1361-1365.
29. Ragasa, C.Y., J. Ganzon, J. Hofilena, B. Tamboong, and J.A. Rideout, *A new furanoid diterpene from Caesalpinia pulcherrima*. *Chem. Pharm. Bull.*, 2003. **51**(10): p. 1208-1210.
30. Arigoni, D., W. Eisenreich, C. Latzel, S. Sagner, T. Radykewicz, M.H. Zenk, and A. Bacher, *Dimethylallyl pyrophosphate is not the committed precursor of isopentenyl pyrophosphate during terpenoid biosynthesis from 1-deoxyxylulose in higher plants*. *Proceedings of the National Academy of Sciences*, 1999. **96**(4): p. 1309-1314.
31. Rabe, P., T. Schmitz, and J.S. Dickschat, *Mechanistic investigations on six bacterial terpene cyclases*. *Beilstein J. Org. Chem.*, 2016. **12**(1): p. 1839-1850.
32. Chang, S.-T., S.-Y. Wang, C.-L. Wu, P.-F. Chen, and Y.-H. Kuo, *Comparison of the antifungal activity of cadinane skeletal sesquiterpenoids from Taiwania (Taiwania cryptomerioides Hayata) heartwood*. *Holzforschung*, 2000. **54**(3): p. 241-245.
33. Kim, D.-H., M.-H. Bang, M.-C. Song, S.-U. Kim, Y.-J. Chang, and N.-I. Baek, *Isolation of β -sitosterol, Phytol and Zingerone 4-O- β -D-glucopyranoside from Chrysanthemum Boreale Makino*. *Korean J. Medicinal Crop Sci.*, 2005. **13**(5): p. 284-287.
34. Alam, M.S., N. Chopra, M. Ali, and M.J.P. Niwa, *Oleanen and stigmaterol derivatives from Ambroma augusta*. 1996. **41**(4): p. 1197-1200.
35. Govindarajan, P. and D. Sarada, *Isolation and characterization of stigmaterol and β -sitosterol from Acacia nilotica (L.) delile ssp indica (benth.) brenan*. *J. Pharm. Res*, 2011. **4**: p. 3601-3602.
36. de Diaz, A.M.P., H.E. Gottlieb, and O.R. Gottlieb, *Dehydrodieugenols from Ocotea cymbarum*. *Phytochemistry*, 1980. **19**(4): p. 681-682.
37. Da Costa-Silva, T.A., S.S. Grecco, F.S. De Sousa, J.H.G. Lago, E.G.A. Martins, C.A. Terrazas, S. Varikuti, K.L. Owens, S.M. Beverley, A.R. Satoskar, and A.G. Tempone, *Immunomodulatory and antileishmanial activity of phenylpropanoid dimers isolated from Nectandra leucantha*. *J. Nat. Prod.*, 2015.

- 78(4): p. 653-657.
38. Alam, M.S., N. Chopra, M. Ali, and M. Niwa, *Oleanen and stigmasterol derivatives from Ambroma augusta*. *Phytochemistry*, 1996. **41**(4): p. 1197-1200.
 39. Wang, Y.H., Q.Y. Sun, F.M. Yang, C.L. Long, F.W. Zhao, G.H. Tang, H.M. Niu, H. Wang, Q.Q. Huang, and J.J. Xu, *Neolignans and caffeoyl derivatives from Selaginella moellendorffii*. *Helv. Chim. Acta.*, 2010. **93**(12): p. 2467-2477.
 40. Pieters, L., T. De Bruyne, A. De Groot, G. Mei, R. Dommissse, G. Lemièrre, and A. Vlietinck, *NMR study of some dihydrobenzofuran lignans*. *Magn. Reson. Chem*, 1993. **31**(7): p. 692-693.
 41. Kim, T.H., H. Ito, K. Hayashi, T. Hasegawa, T. Machiguchi, and T. Yoshida, *Aromatic Constituents from the Heartwood of Santalum album L*. *Chem. Pharm. Bull.*, 2005. **53**(6): p. 641-644.
 42. Antus, S., T. Kurtan, L. Juhász, L. Kiss, M. Hollósi, and Z. Májer, *Chiroptical properties of 2, 3-dihydrobenzo [b] furan and chromane chromophores in naturally occurring O-heterocycles*. *Chirality*, 2001. **13**(8): p. 493-506.
 43. Yuen, M.S.M., F. Xue, T.C.W. Mak, and H.N.C. Wong, *On the absolute structure of optically active neolignans containing a dihydrobenzo [b] furan skeleton*. *Tetrahedron*, 1998. **54**(41): p. 12429-12444.
 44. Kawanishi, K., Y. Uhara, and Y. Hashimoto, *Neolignans of Virola carinata bark*. *Phytochemistry*, 1982. **21**(11): p. 2725-2728.
 45. Wang, C.Z. and Z.J. Jia, *Neolignan glycosides from Pedicularis longiflora*. *Planta Medica.*, 1997. **63**(03): p. 241-244.
 46. Park, S.Y., S.S. Hong, X.H. Han, J.S. Hwang, D. Lee, J.S. Ro, and B.Y. Hwang, *Lignans from Arctium lappa and their inhibition of LPS-induced nitric oxide production*. *Chem. Pharm. Bull.*, 2007. **55**(1): p. 150-152.
 47. Kawanishi, K., Y. Uhara, and Y. Hashimoto, *The neolignans, carinatidin, dihydrocarinatidin, carinatidiol and dehydrodieugenol B from virola carinata*. *Phytochemistry*, 1983. **22**(10): p. 2277-2280.
 48. Lu, Y., Y. Xue, J. Liu, G. Yao, D. Li, B. Sun, J. Zhang, Y. Liu, C. Qi, and M. Xiang, *(±)-Acortatarinowins A–F, norlignan, neolignan, and lignan enantiomers from Acorus tatarinowii*. *J. Nat. Prod.*, 2015. **78**(9): p. 2205-2214.
 49. Hoye, T.R., C.S. Jeffrey, and F. Shao, *Mosher ester analysis for the determination of absolute configuration of stereogenic (chiral) carbinol carbons*. *Nat. Protoc.*, 2007. **2**(10): p. 2451.
 50. Seco, J.M., E. Quinoá, and R. Riguera, *The assignment of absolute configuration*

by NMR. Chem. Rev., 2004. **104**(1): p. 17-118.

51. Akihisa, T., T. Yokota, N. Takahashi, T. Tamura, and T. Matsumoto, *25-Methylgramisterol and other 4 α -methylsterols from Phaseolus vulgaris seeds*. Phytochemistry, 1989. **28**(4): p. 1219-1224.
52. Hasan, C.M., S. Shahnaz, I. Muhammad, A.I. Gray, and P.G. Waterman, *Chemistry in the Annonaceae, XXIII. 24-Methylene-lanosta-7, 9 (11)-dien-3 β -ol from Artabotrys odorotissimus stem bark*. J. Nat. Prod., 1987. **50**(4): p. 762-763.
53. Liu, H.-K., T.-H. Tsai, T.-T. Chang, C.-J. Chou, and L.-C. Lin, *Lanostane-triterpenoids from the fungus Phellinus gilvus*. Phytochemistry, 2009. **70**(4): p. 558-563.



APPENDIX A
LIST OF ABBREVIATIONS

Å	angstrom sign, ångström
α	alpha
$[\alpha]_D^{28}$	specific rotation
β	beta
<i>br s</i>	broad singlet
<i>br d</i>	broad doublet
<i>br dt</i>	broad doublet of triplet
<i>n</i> -BuOH	normal butanol
¹³ C NMR	carbon-13 nuclear magnetic resonance
°C	degree celsius
CC	column chromatography
λ_{\max}	wavelength at maxima absorption
CD	circular dichroism
CDCl ₃	deuteriochloroform
CD ₃ OD	deuteromethanol
CeSO ₄	cerium sulfate
CHCl ₃	Chloroform
CH ₂ Cl ₂	Dichloromethane
cm	centimeter
cm ⁻¹	reciprocal centimeter (wave number)
CH ₃ CN	acetonitrile
COSY	correlated spectroscopy
d	doublet

LIST OF ABBREVIATIONS (CONTINUED)

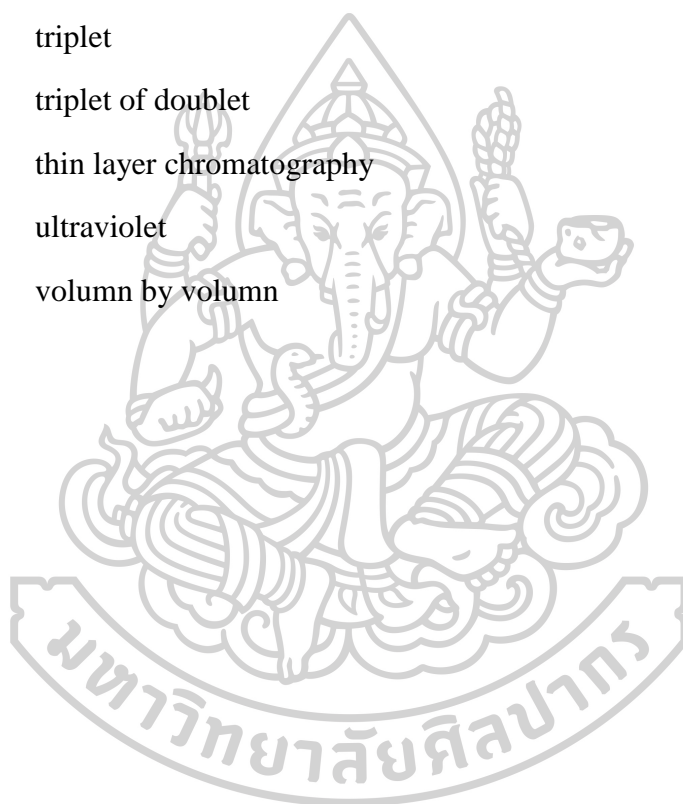
dd	doublet of doublet
ddd	doublet of doublet of doublet
ddt	doublet of doublet of triplet
δ	chemical shift relative to tetramethylsilane (TMS)
DEPT	Distortion Spectroscopy
DMF	dimethylformamide
DMSO	dimethyl sulfoxide
ϵ	epsilon
EtOAc	ethyl acetate
eq.	equivalent
g	gram
g/mol	gram per mole
h	hour
kg	kilogram
HaCaT	human immortalized keratinocyte cancer cell line
HCT116	colorectal cancer cell line
HeLa	cervical cancer cell line
HepG2	Hepatocellular carcinoma cell line
HN22	head-and-neck cancer-cell line
HMBC	Heteronuclear Multiple Bond Coherence
HMQC	Heteronuclear Multiple Quantum Coherence
$^1\text{H-NMR}$	Proton Nuclear Magnetic Resonance
H_3PO_4	phosphoric acid
H_2SO_4	sulfuric acid
HRESIMS	high resolution electrospray ionization mass spectrometry
Hz	hertz

LIST OF ABBREVIATIONS (CONTINUED)

IC ₅₀	50% Inhibition concentration
IR	Infrared absorption
IUPAC	International Union of Pure and Applied Chemistry
<i>J</i>	coupling constant
M	molar
Me ₂ CO	acetone
MeOH	methanol
m	meter
m	multiplet
mL	milliliter
mm	millimeter
m.p.	melting point
MTT	3-(4,5-dimethylthiazol-2-yl)-2,5-diphenyltetrazolium bromide
<i>m/z</i>	mass to charge ratio
MHz	Megahertz
μg	microgram
μL	microliter
μM	micromolar
μmol	micromole
ν _{max}	frequency of the wave at maxima absorption
N	normality
NaH	sodium hydride
NaOH	sodium hydroxide
NH ₄ Cl	ammonium chloride
nm	nanometer
NMR	nuclear magnetic resonance

LIST OF ABBREVIATIONS (CONTINUED)

<i>n</i> -hexane	normal hexane
PLC	preparative layer chromatography
ppm	part per million
pq	pseudo quartet
RP-18	octadecyl carbon chain (C18)-bonded silica reversed-phase
t	triplet
td	triplet of doublet
TLC	thin layer chromatography
UV	ultraviolet
v/v	volumn by volumn



APPENDIX B

LIST OF NMR SPECTRAL DATA OF ISOLATED COMPOUNDS

Figure content	Page
Neolignan	
S1 ^1H NMR spectrum of MS11 (300 MHz, CDCl_3)	157
S2 ^{13}C NMR spectrum of MS11 (75 MHz, CDCl_3)	158
S3 DEPT 135 spectrum of MS11 (75 MHz, CDCl_3)	159
S4 COSY spectrum of MS11 (300 MHz, CDCl_3)	160
S5 HMQC spectrum of MS11	161
S6 HMBC spectrum of MS11	162
S7 ^1H NMR spectrum of MS12 (300 MHz, CDCl_3)	163
S8 ^{13}C NMR spectrum of MS12 (75 MHz, CDCl_3)	164
S9 DEPT 135 spectrum of MS12 (75 MHz, CDCl_3)	165
S10 COSY spectrum of MS12 (300 MHz, CDCl_3)	166
S11 HMQC spectrum of MS12	167
S12 HMBC spectrum of MS12	168
S13 ^1H NMR spectrum of MS14 (300 MHz, CDCl_3)	169
S14 ^{13}C NMR spectrum of MS14 (75 MHz, CDCl_3)	170
S15 DEPT 135 spectrum of MS14 (75 MHz, CDCl_3)	171
S16 COSY spectrum of MS14 (300 MHz, CDCl_3)	172
S17 HMQC spectrum of MS14	173
S18 HMBC spectrum of MS14	174
S19 ^1H NMR spectrum of MS15 (300 MHz, CDCl_3)	175
S20 ^{13}C NMR spectrum of MS15 (75 MHz, CDCl_3)	176

LIST OF NMR SPECTRAL DATA OF ISOLATED COMPOUNDS

(CONTINUED)

Figure	content	Page
S21	DEPT 135 spectrum of MS15 (75 MHz, CDCl ₃)	177
S22	COSY spectrum of MS15 (300 MHz, CDCl ₃)	178
S23	HMQC spectrum of MS15	179
S24	HMBC spectrum of MS15	180
S25	¹ H NMR spectrum of MS16 (300 MHz, CDCl ₃)	181
S26	¹³ C NMR spectrum of MS16 (75 MHz, CDCl ₃)	182
S27	DEPT 135 spectrum of MS16 (75 MHz, CDCl ₃)	183
S28	COSY spectrum of MS16 (300 MHz, CDCl ₃)	184
S29	HMQC spectrum of MS16	185
S30	HMBC spectrum of MS16	186
S31	¹ H NMR spectrum of <i>S</i> -(-)-MTPS ester of MS16 (300 MHz, CDCl ₃)..	187
S32	¹ H NMR spectrum of <i>R</i> -(+)-MTPS ester of MS16 (300 MHz, CDCl ₃).	188
S33	¹ H NMR spectrum of MS17 (300 MHz, CDCl ₃)	189
S34	¹³ C NMR spectrum of MS17 (75 MHz, CDCl ₃)	190
S35	DEPT 135 spectrum of MS17 (75 MHz, CDCl ₃)	191
S36	COSY spectrum of MS17 (300 MHz, CDCl ₃)	192
S37	HMQC spectrum of MS17	193
S38	HMBC spectrum of MS17	194
S39	¹ H NMR spectrum of MS19 (300 MHz, CDCl ₃)	195
S40	¹³ C NMR spectrum of MS19 (75MHz, CDCl ₃)	196
S41	DEPT 135 spectrum of MS19 (75 MHz, CDCl ₃)	197

LIST OF NMR SPECTRAL DATA OF ISOLATED COMPOUNDS

(CONTINUED)

Figure	content	Page
S42	COSY spectrum of MS19 (300 MHz, CDCl ₃)	198
S43	HMQC spectrum of MS19	199
S44	HMBC spectrum of MS19	200
S45	¹ H NMR spectrum of MS20 (300 MHz, CDCl ₃)	201
S46	¹³ C NMR spectrum of MS20 (75 MHz, CDCl ₃)	202
S47	DEPT 135 spectrum of MS20 (75 MHz, CDCl ₃)	203
S48	COSY spectrum of MS20 (300MHz, CDCl ₃)	204
S49	HMQC spectrum of MS20	205
S50	HMBC spectrum of MS20	206
S51	¹ H NMR spectrum of MS20a (300 MHz, CDCl ₃)	207
S52	¹³ C NMR spectrum of MS20a (75 MHz, CDCl ₃)	208
S53	DEPT 135 spectrum of MS20a (75 MHz, CDCl ₃)	209
S54	COSY spectrum of MS20a (300MHz, CDCl ₃)	210
S55	HMQC spectrum of MS20a	211
S56	HMBC spectrum of MS20a	212
Phenylpropanoid dimer		
S57	¹ H NMR spectrum of MS18 (300 MHz, CDCl ₃)	214
S58	¹³ C NMR spectrum of MS18 (75 MHz, CDCl ₃)	215
S59	DEPT 135 spectrum of MS18 (75 MHz, CDCl ₃)	216
S60	COSY spectrum of MS18 (300 MHz, CDCl ₃)	217
S61	HMQC spectrum of MS18	218

LIST OF NMR SPECTRAL DATA OF ISOLATED COMPOUNDS

(CONTINUED)

Figure	content	Page
S62	HMBC spectrum of MS18	219
Triterpenes		
S63	¹ H NMR spectrum of MS3 (300 MHz, CDCl ₃).....	221
S64	Zoom of the ¹ H NMR spectrum of MS3	222
S65	¹³ C NMR spectrum of MS3 (75 MHz, CDCl ₃).....	223
S66	Zoom of the ¹³ C NMR spectrum of MS3	224
S67	DEPT 135 spectrum of MS3 (75 MHz, CDCl ₃).....	225
S68	Zoom of the DEPT 135 spectrum of MS3	226
S69	COSY spectrum of MS3 (300 MHz, CDCl ₃).....	227
S70	HMQC spectrum of MS3	228
S71	HMBC spectrum of MS3	229
S72	¹ H NMR spectrum of MS5 (300 MHz, CDCl ₃)	230
S73	Zoom of the ¹ H NMR spectrum of MS5	231
S74	¹³ C NMR spectrum of MS5 (75 MHz, CDCl ₃)	232
S75	DEPT 135 spectrum of MS5 (75 MHz, CDCl ₃)	233
S76	COSY spectrum of MS5 (300 MHz, CDCl ₃)	234
S77	HMQC spectrum of MS5	235
S78	HMBC spectrum of MS5	236
S79	¹ H NMR spectrum of MS6 (300 MHz, CDCl ₃)	237
S80	Zoom of the ¹ H NMR spectrum of M	238
S81	¹³ C NMR spectrum of MS6 (75 MHz, CDCl ₃)	239

LIST OF NMR SPECTRAL DATA OF ISOLATED COMPOUNDS

(CONTINUED)

Figure	content	Page
S82	Zoom of the ^{13}C NMR spectrum of MS6.....	240
S83	DEPT 135 spectrum of MS7 (75 MHz, CDCl_3)	241
S84	Zoom of the DEPT 135 spectrum of MS6.....	242
S85	COSY spectrum of MS6 (300 MHz, CDCl_3)	243
S86	HMQC spectrum of MS6	244
S87	HMBC spectrum of MS6	245
S88	^1H NMR spectrum of MS7 (300 MHz, CDCl_3)	246
S89	Zoom of the ^1H NMR spectrum of MS7.....	247
S90	^{13}C NMR spectrum of MS7 (75 MHz, CDCl_3)	248
S91	Zoom of the ^{13}C NMR spectrum of MS7.....	249
S92	DEPT 135 spectrum of MS7 (75 MHz, CDCl_3)	250
S93	Zoom of the DEPT 135 spectrum of MS7.....	251
S94	COSY spectrum of MS6 (300 MHz, CDCl_3)	252
S95	HMQC spectrum of MS6	253
S96	HMBC spectrum of MS6	254

APPENDIX B
LIST OF NMR SPECTRAL DATA OF ISOLATED COMPOUND



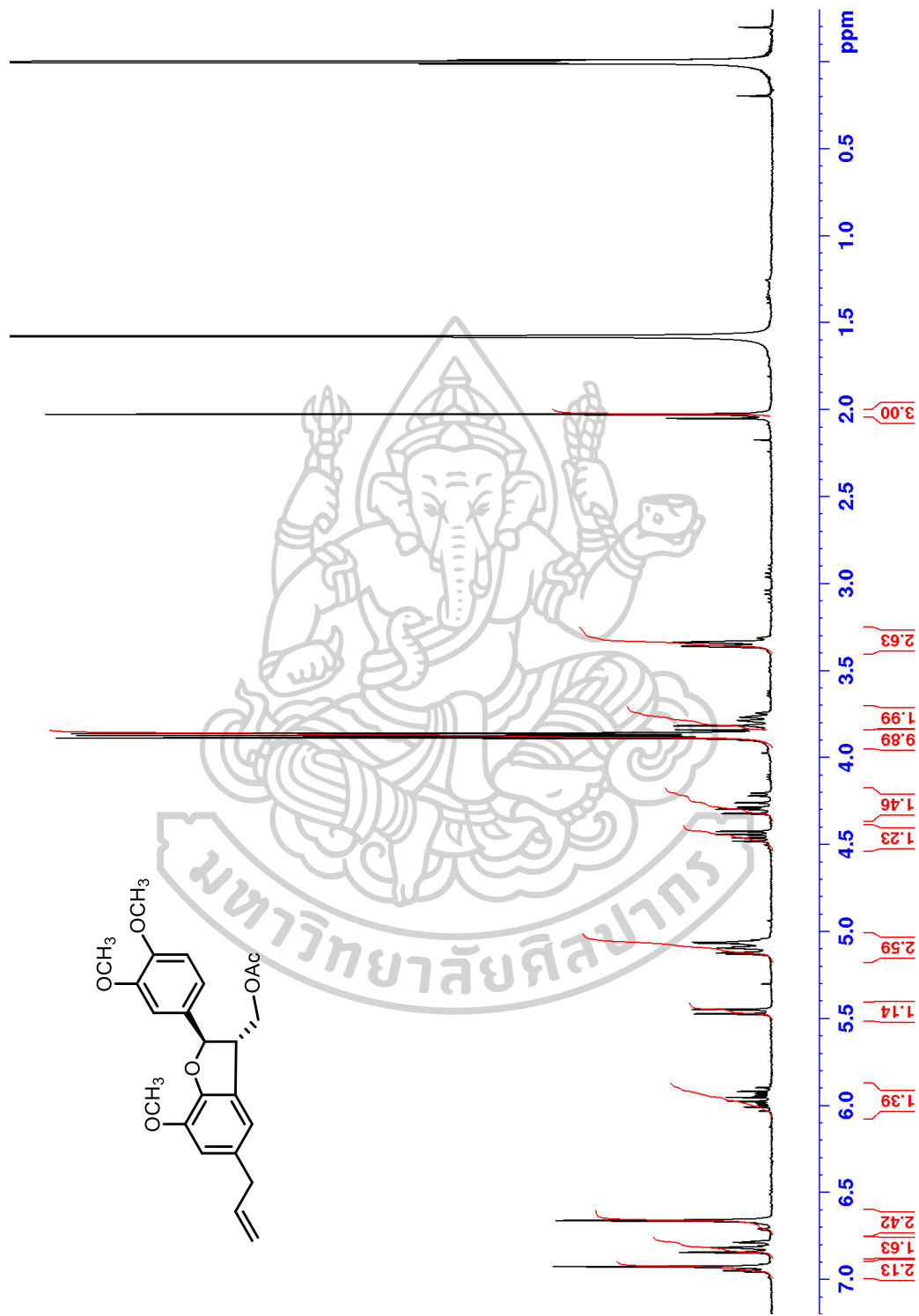


Figure S1 ^1H NMR spectrum of MS11 (300 MHz, CDCl_3)

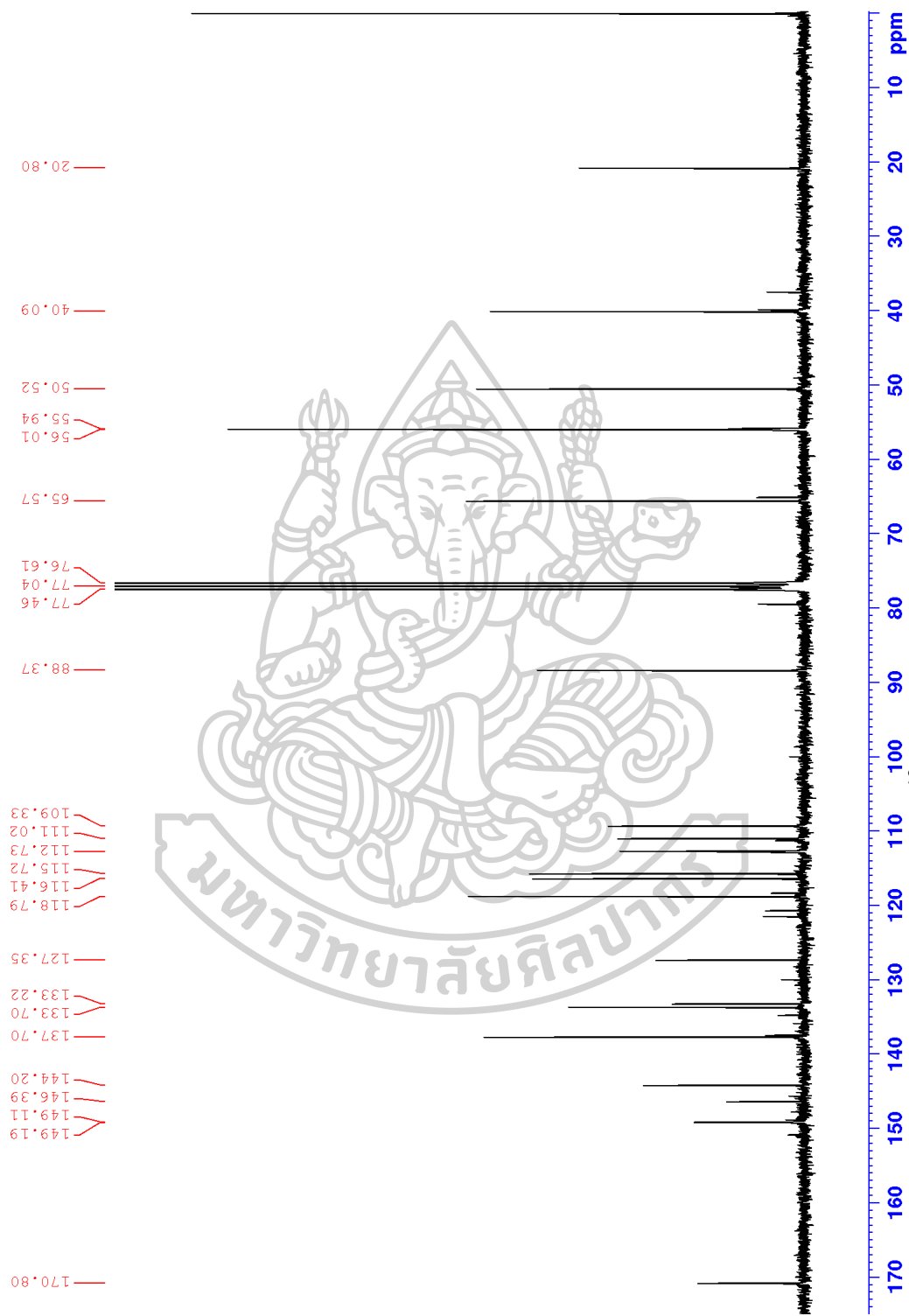


Figure S2 ^{13}C NMR spectrum of MS11 (75 MHz, CDCl_3)

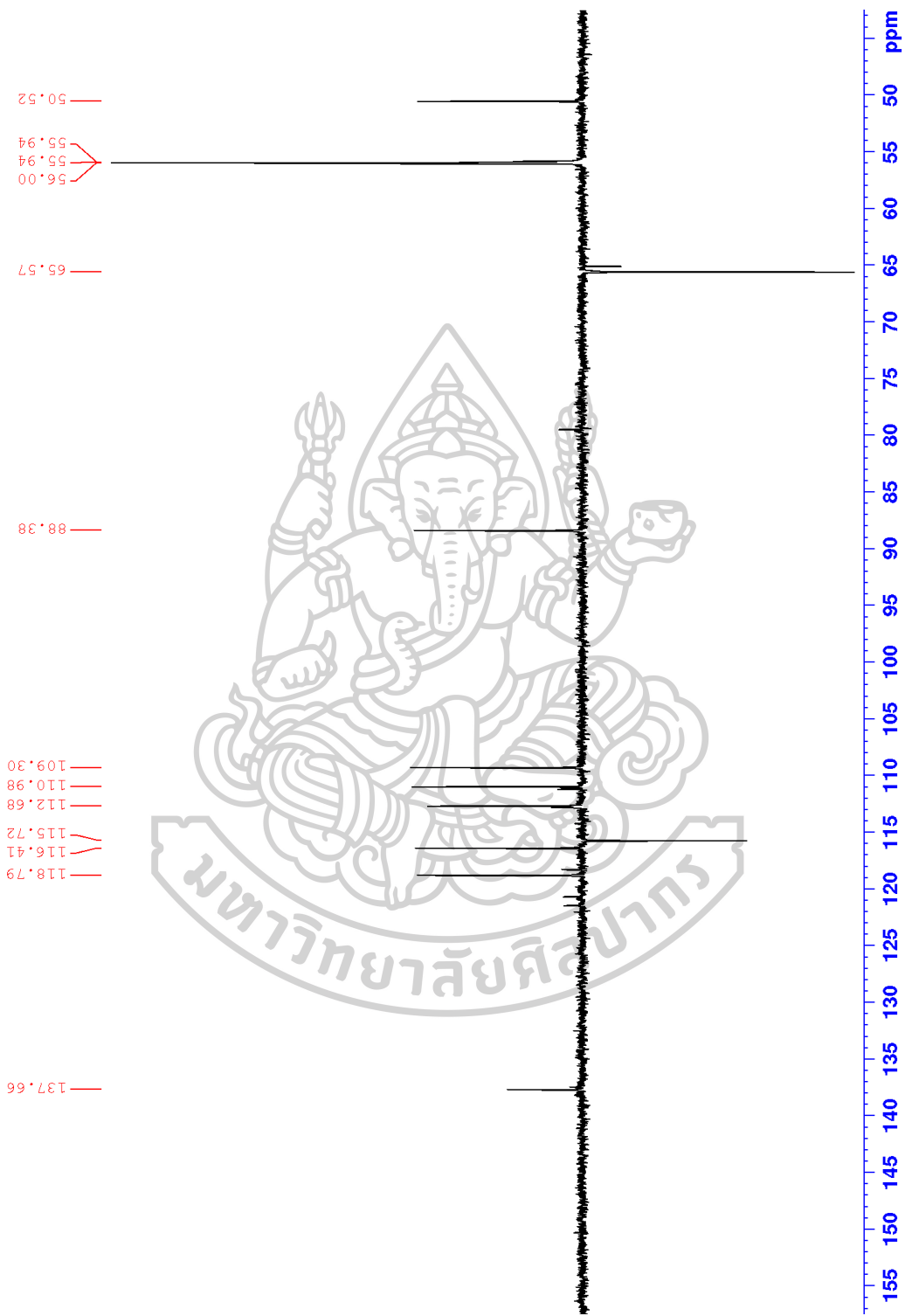


Figure S3 DEPT 135 spectrum of MS11 (75 MHz, CDCl₃)

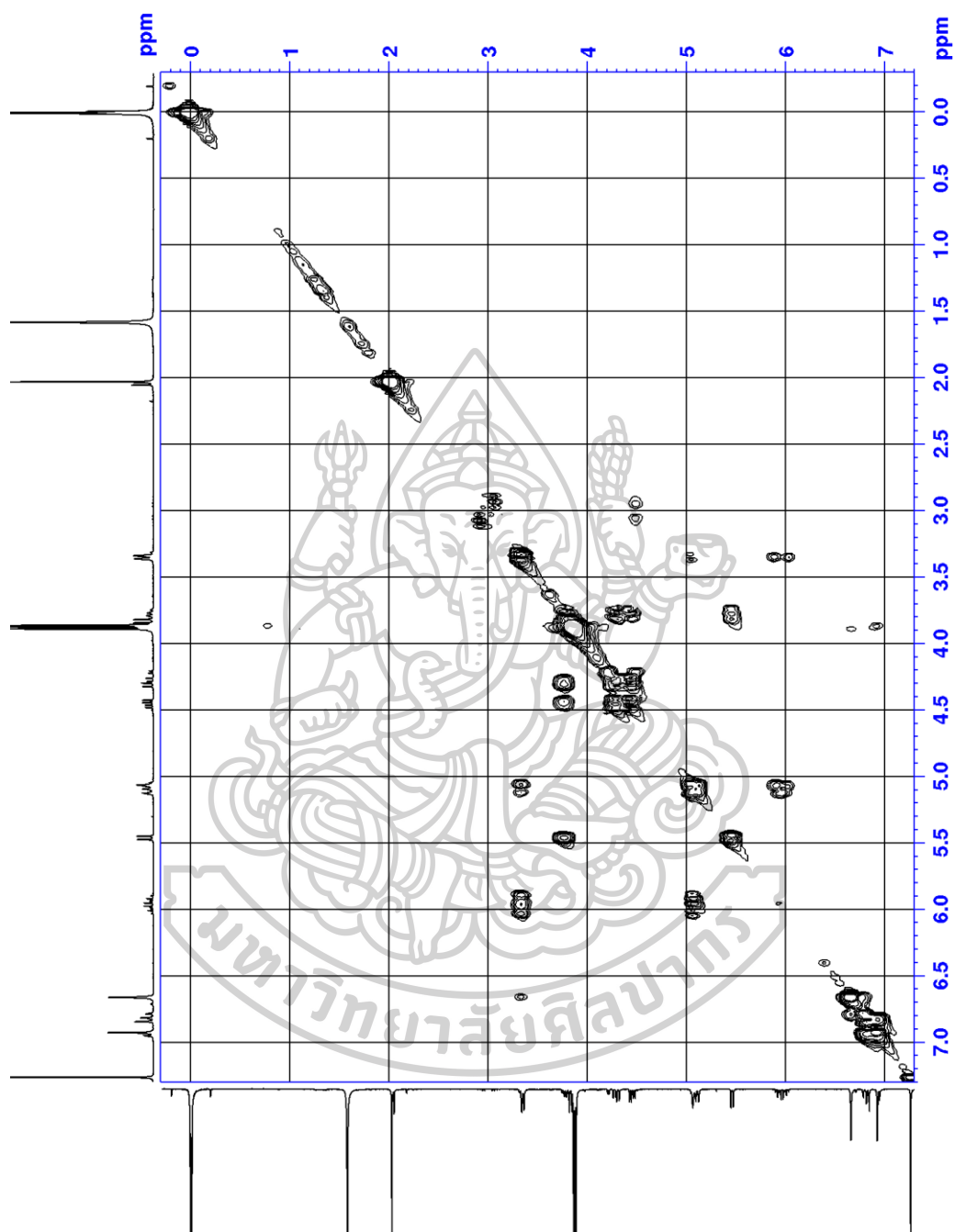


Figure S4 COSY spectrum of **MS11** (300 MHz, CDCl_3)

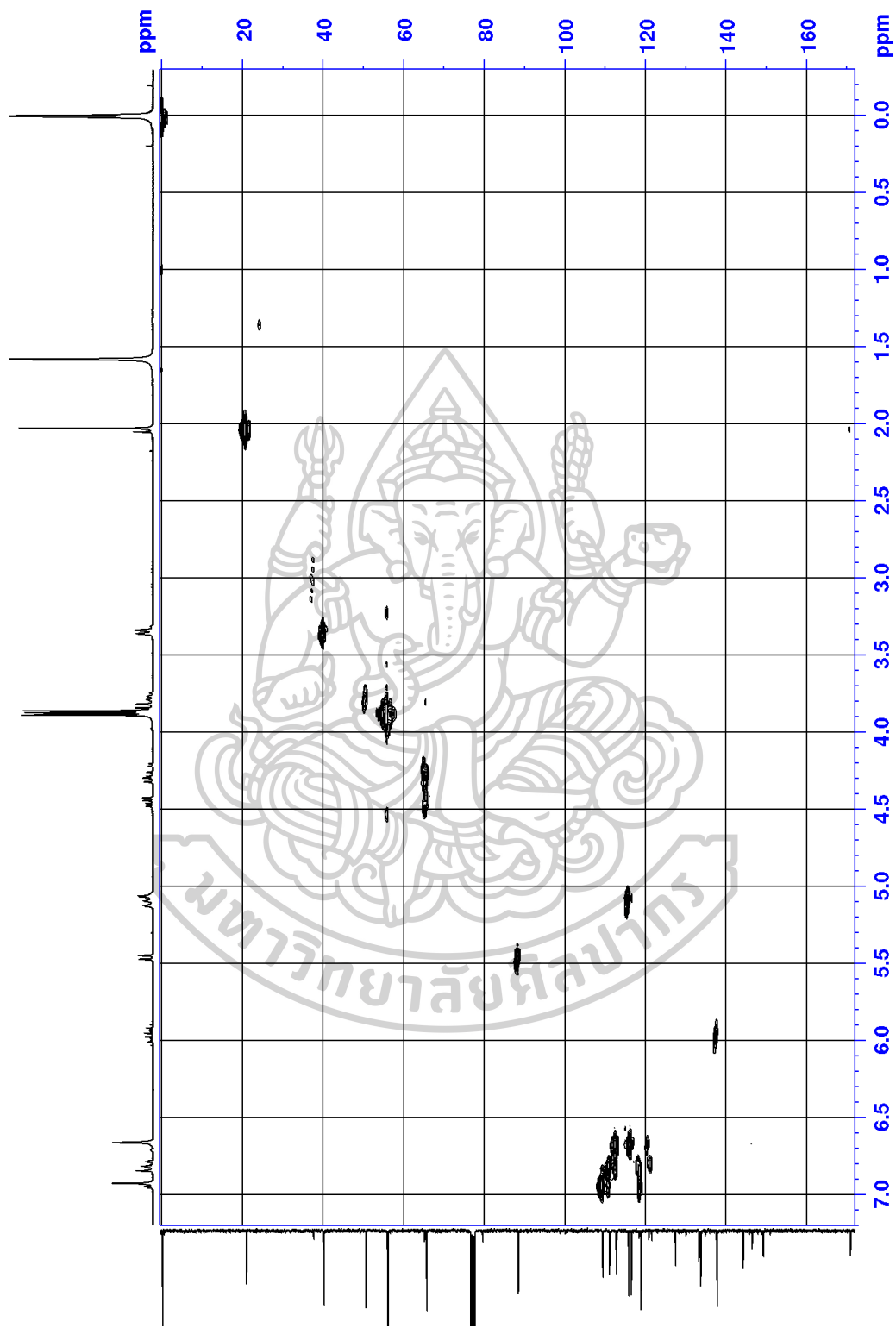


Figure S5 HMQC spectrum of MS11

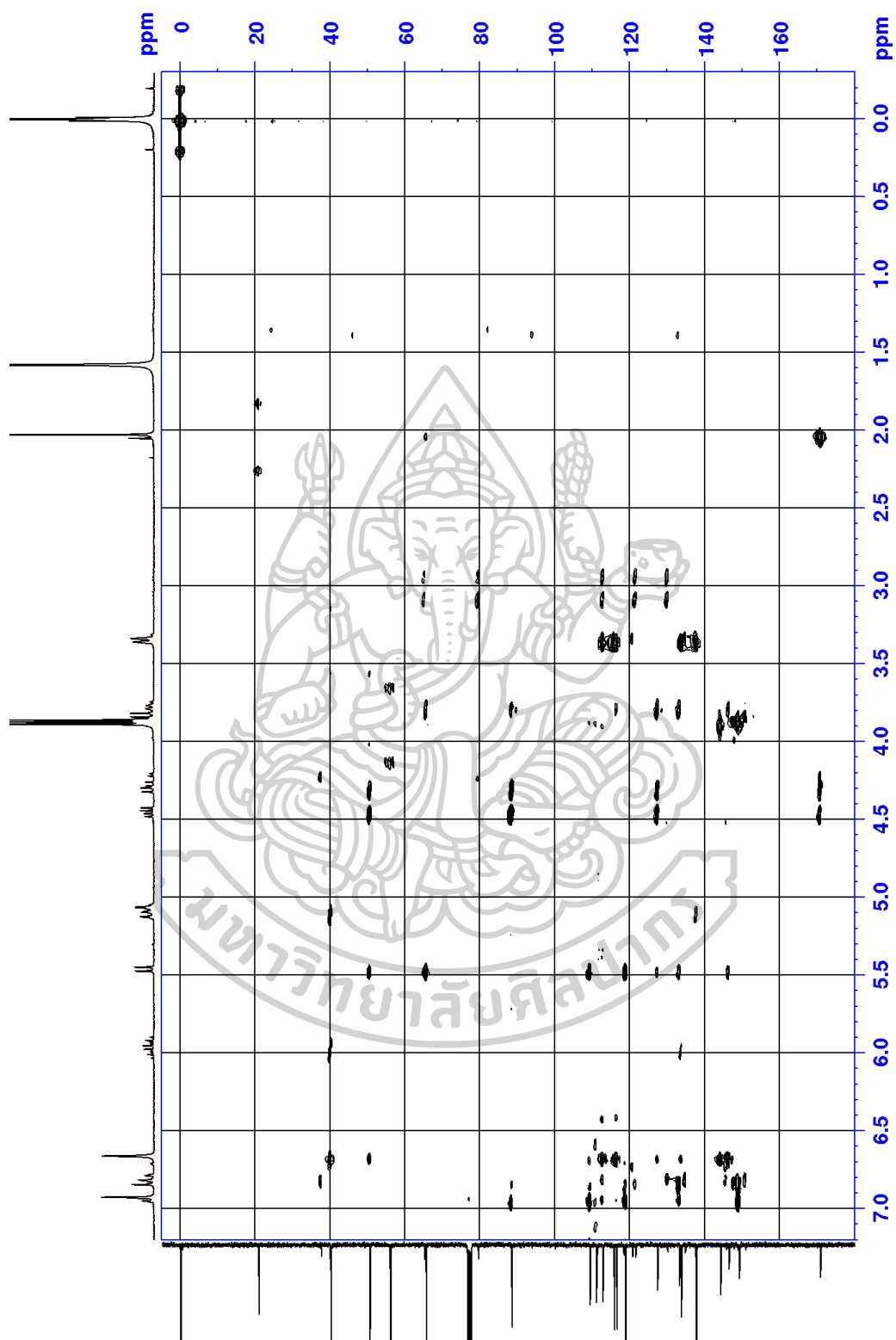


Figure S6 HMBC spectrum of MS11

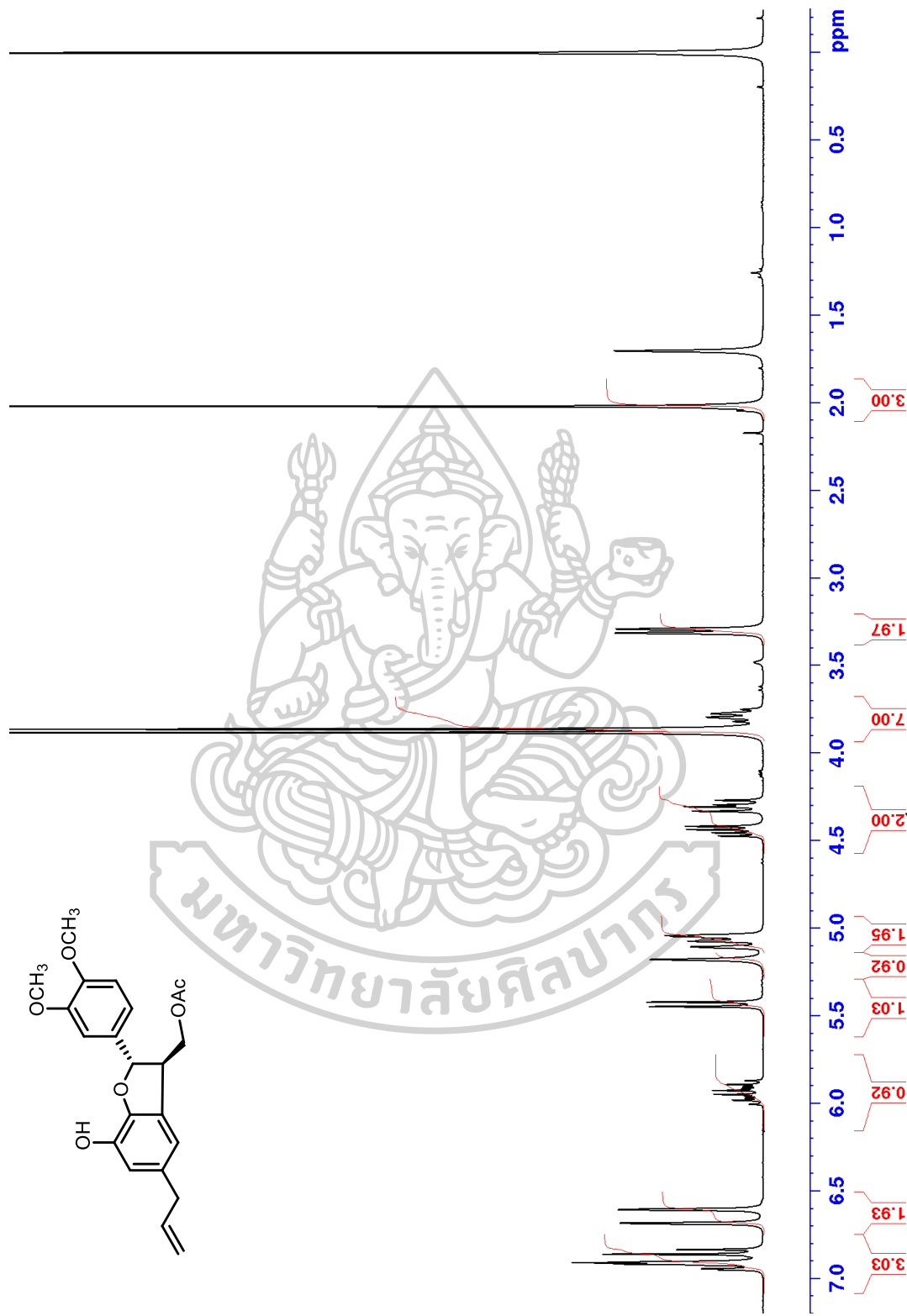


Figure S7 ^1H NMR spectrum of MS12 (300 MHz, CDCl_3)

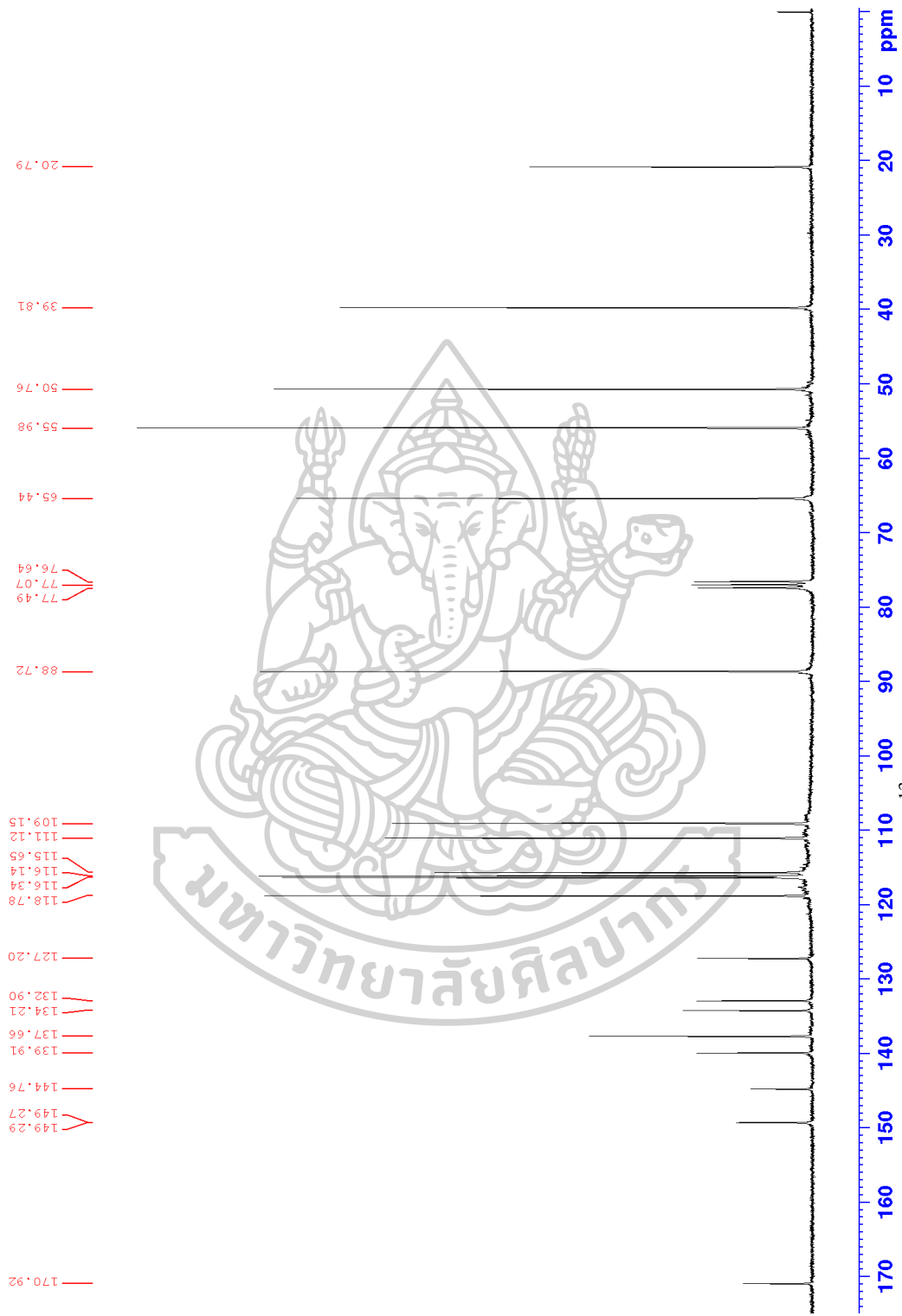


Figure S8 ^{13}C NMR spectrum of MS12 (75 MHz, CDCl_3)

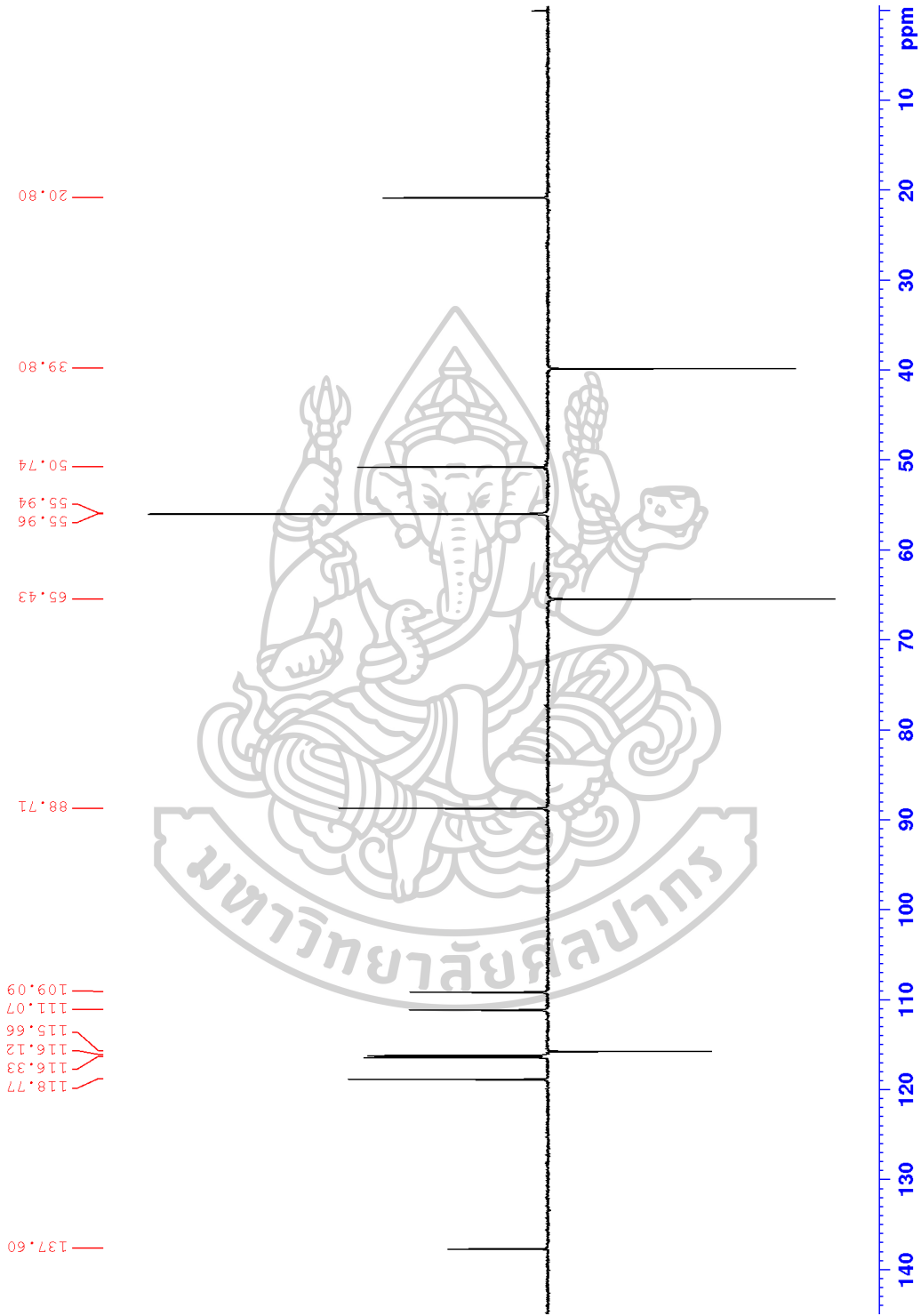


Figure S9 DEPT 135 spectrum of MS12 (75 MHz, CDCl₃)

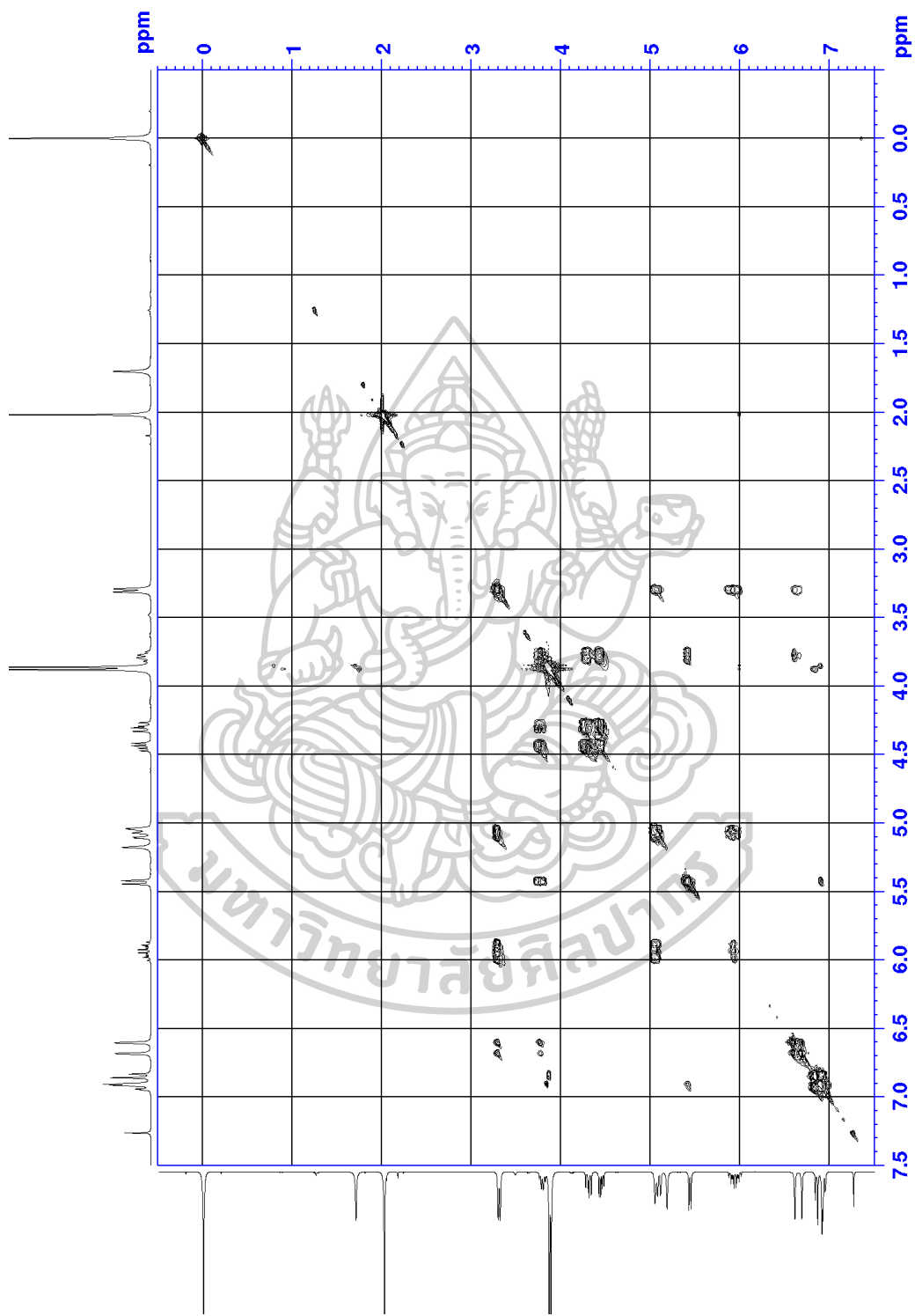


Figure S10 COSY spectrum of MS12 (300 MHz, CDCl₃)

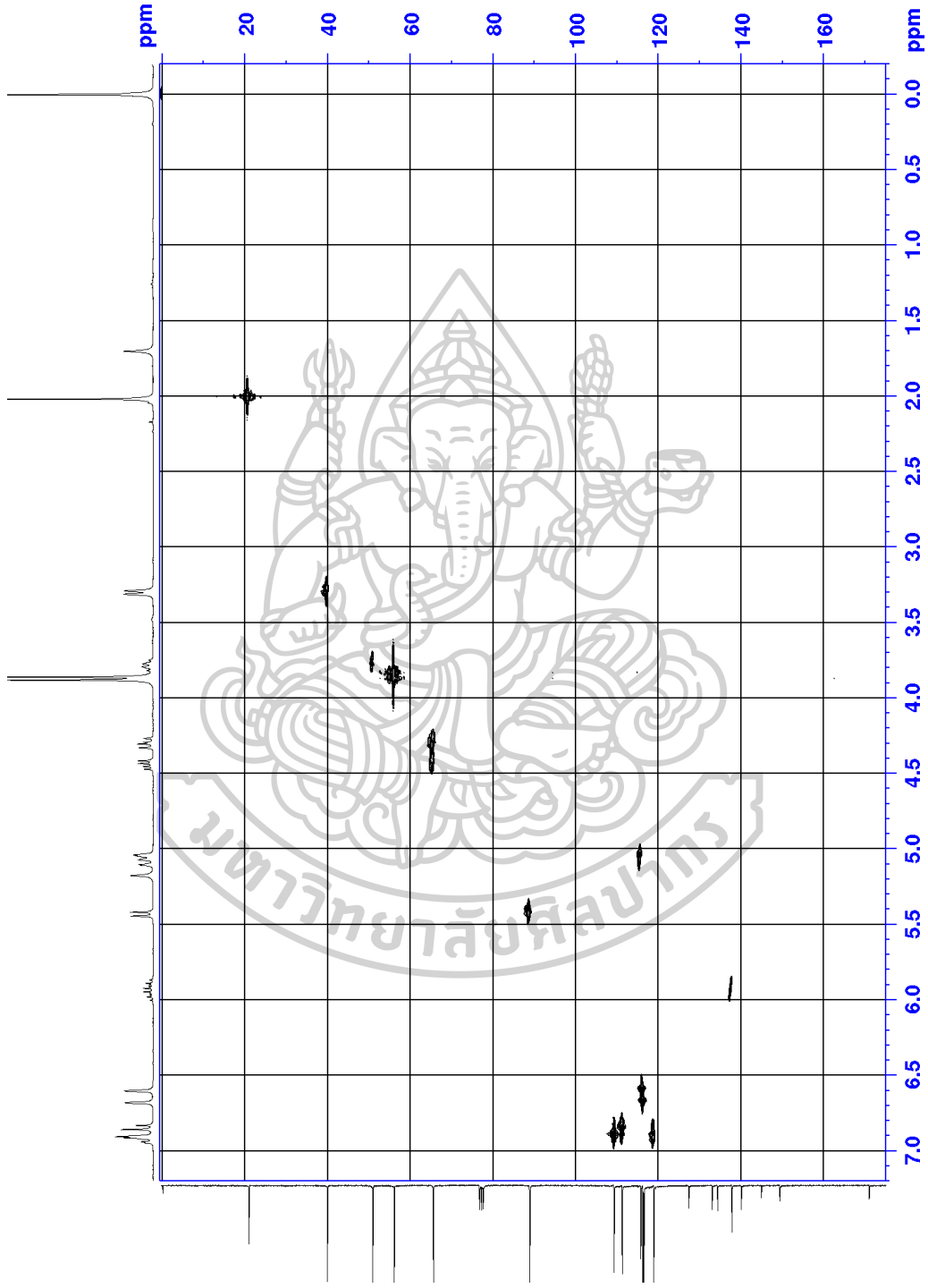


Figure S11 HMQC spectrum of MS12

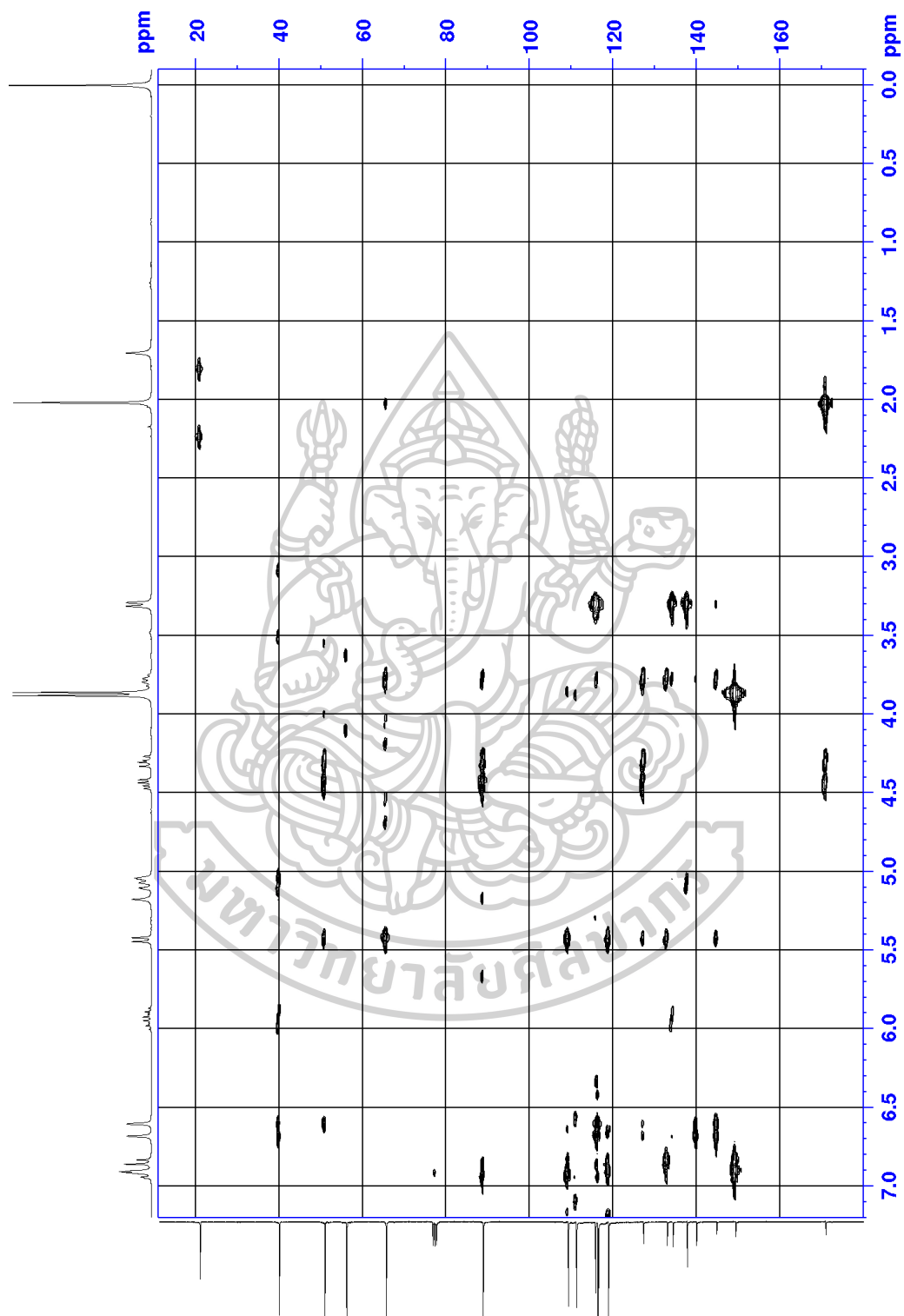


Figure S12 HMBC spectrum of MS12

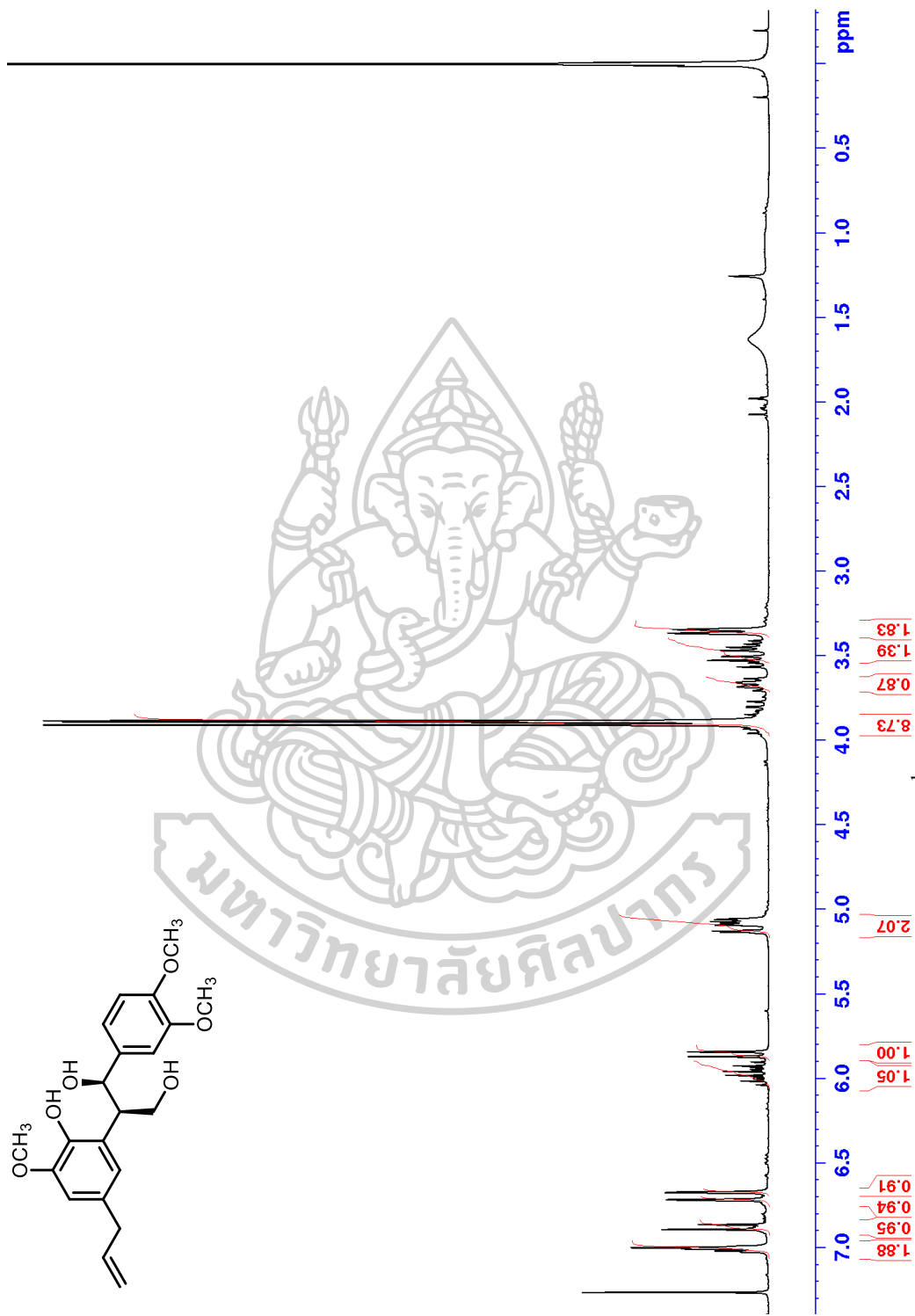
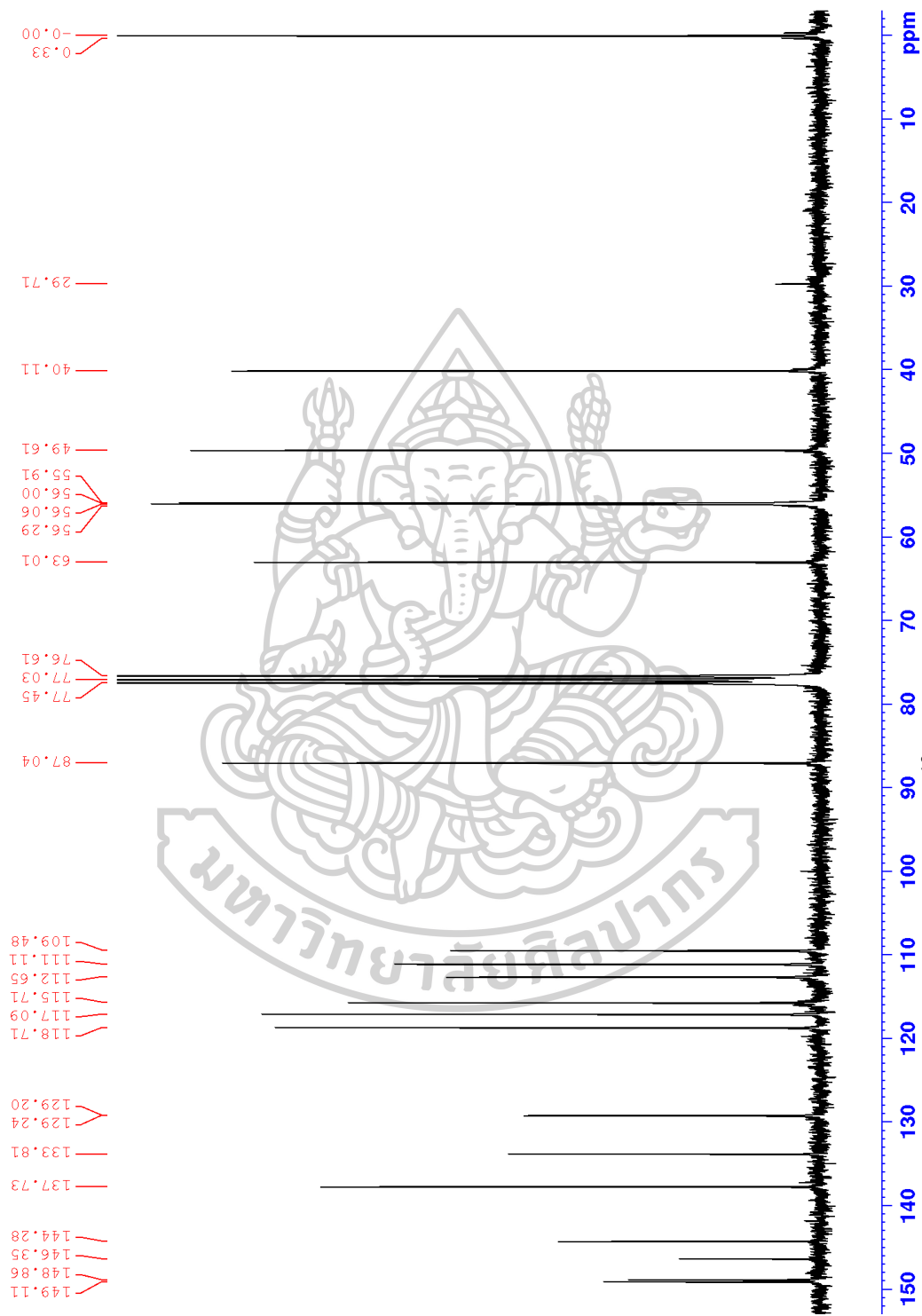
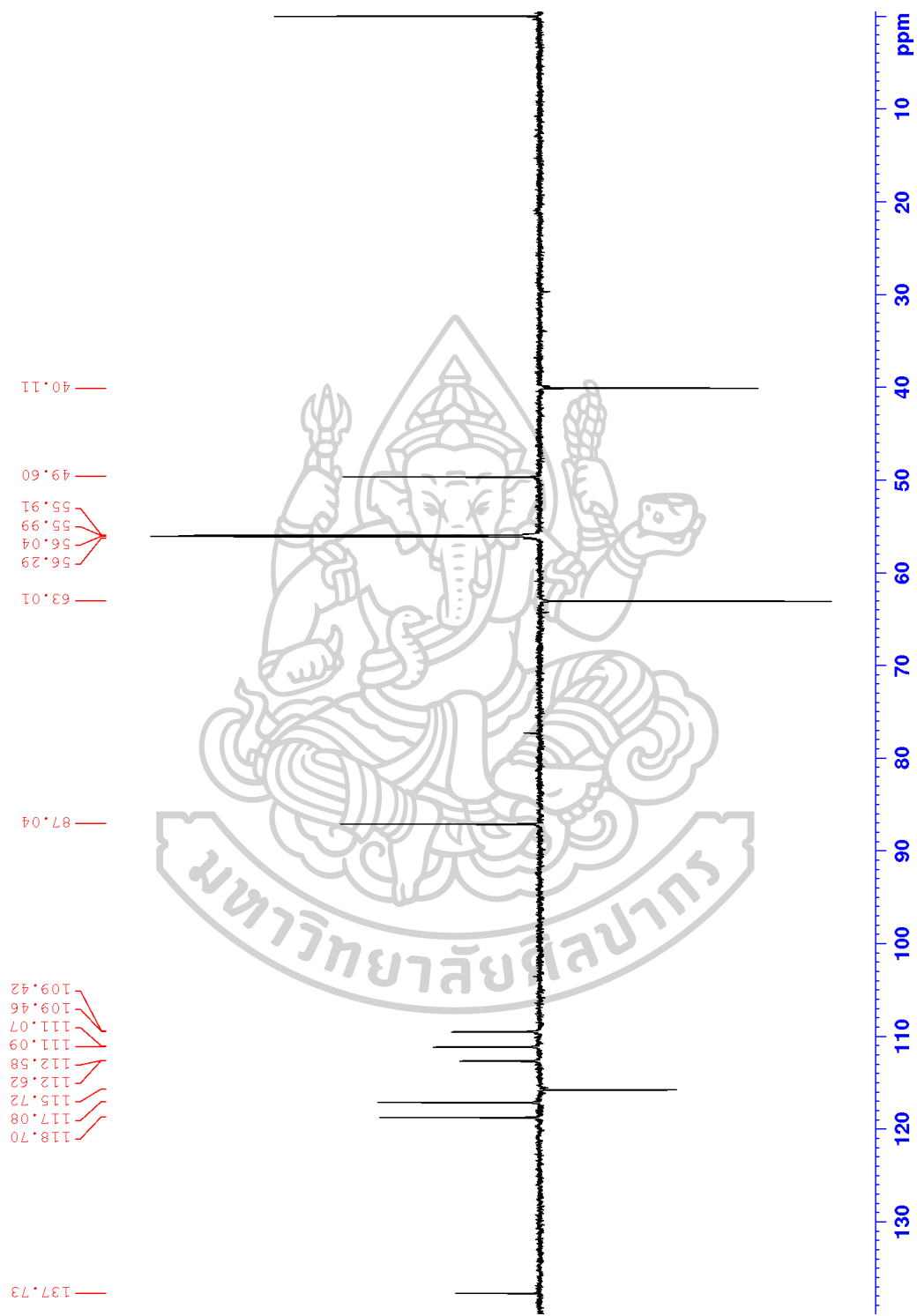


Figure S13 ¹H NMR spectrum of MS14 (300 MHz, CDCl₃)

Figure S14 ^{13}C NMR spectrum of MS14 (75 MHz, CDCl_3)

Figure S15 DEPT 135 spectrum of MS14 (75 MHz, CDCl₃)

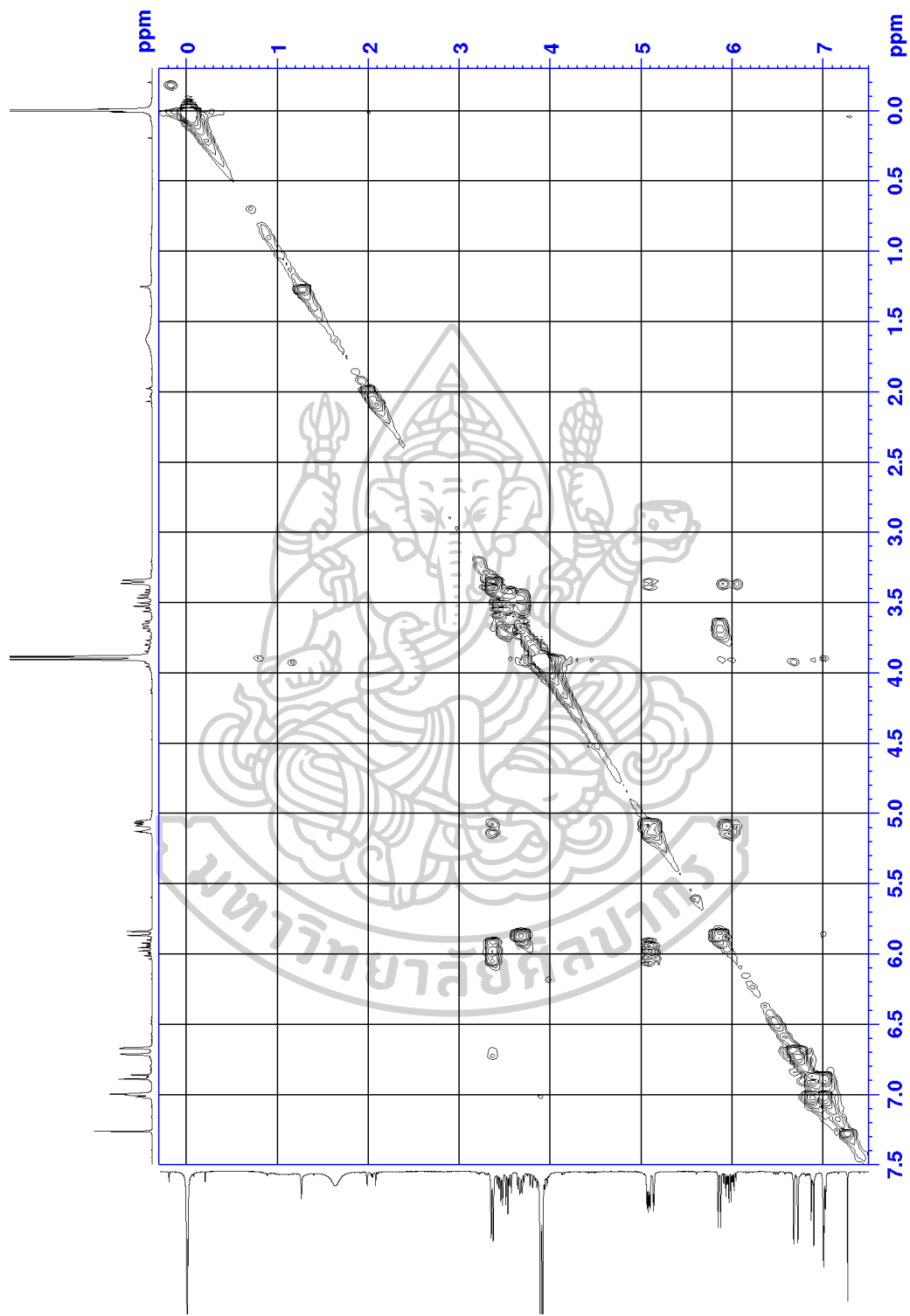


Figure S16 COSY spectrum of MS14 (300 MHz, CDCl₃)

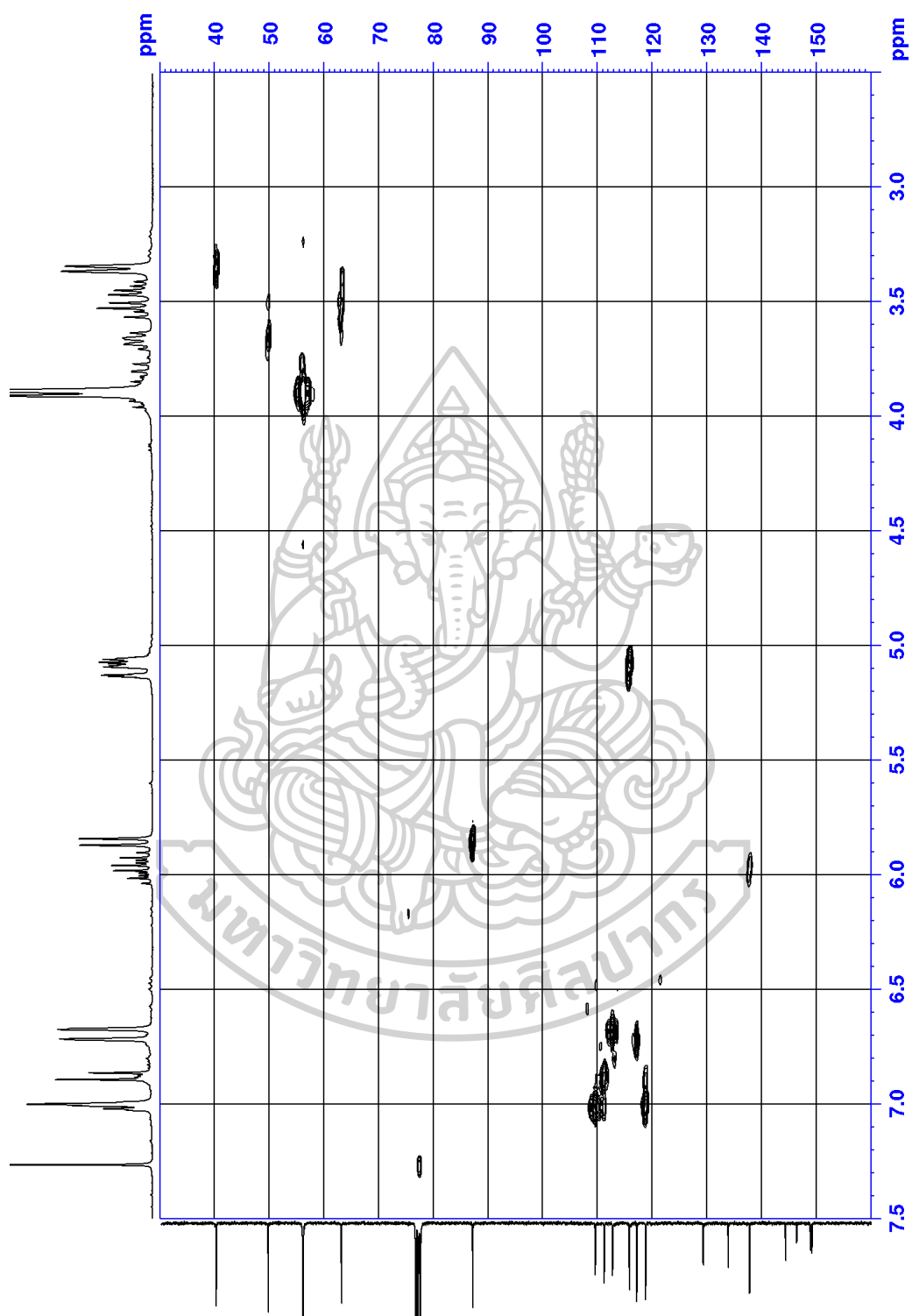


Figure S17 HMQC spectrum of MS14

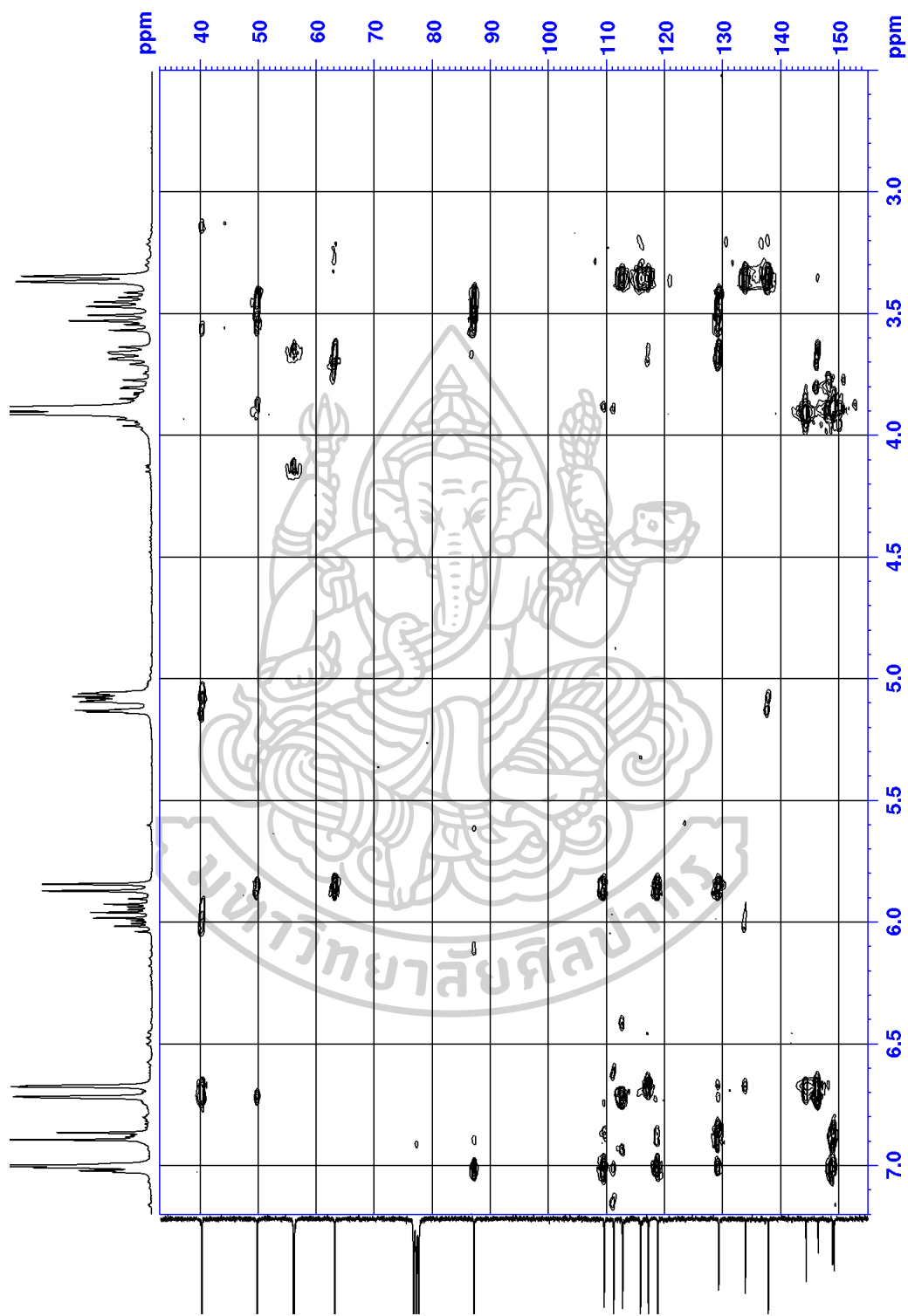


Figure S18 HMBC spectrum of MS14

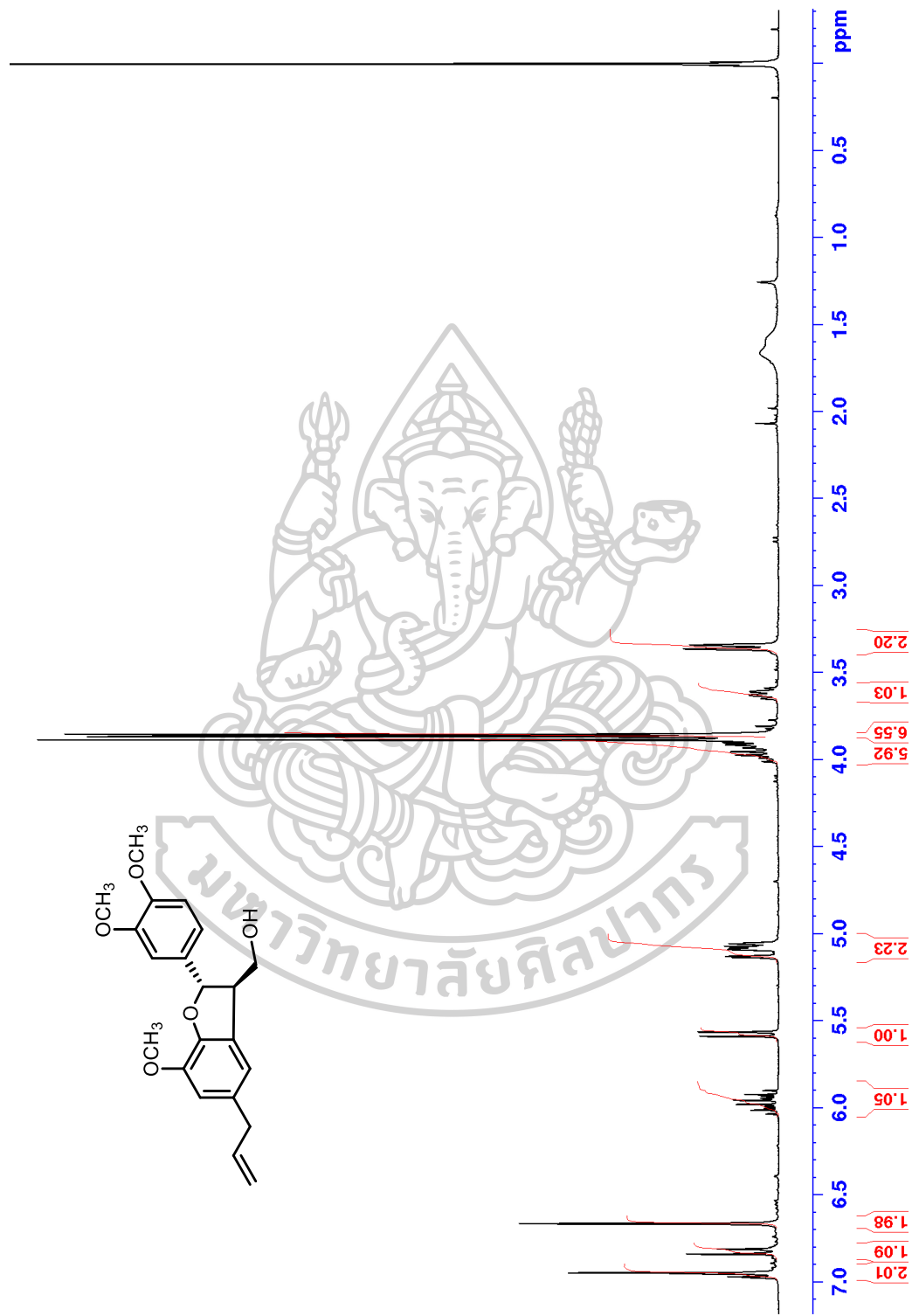


Figure S19 ^1H NMR spectrum of MS15 (300 MHz, CDCl_3)

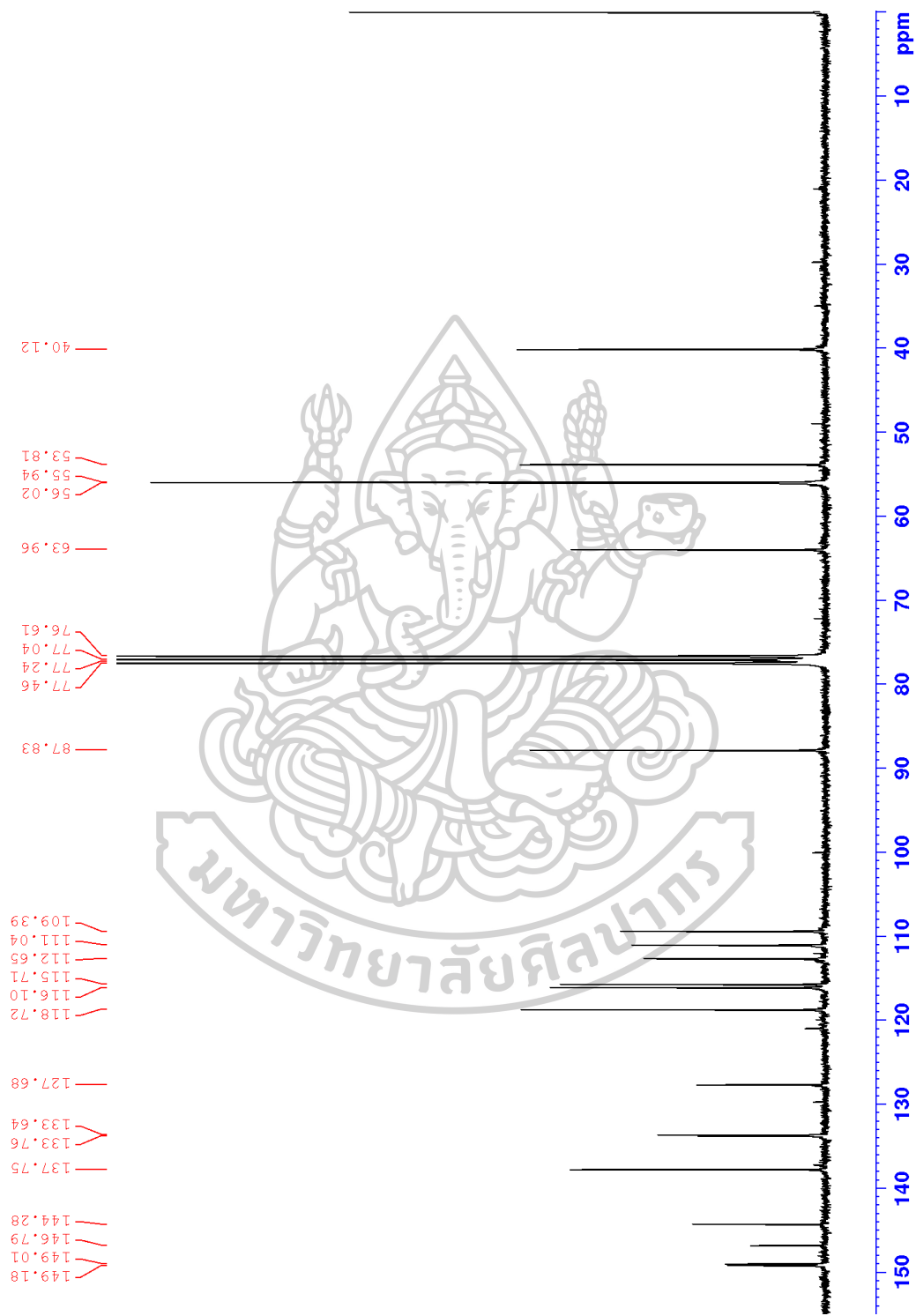


Figure S20 ^{13}C NMR spectrum of MS15 (75 MHz, CDCl_3)

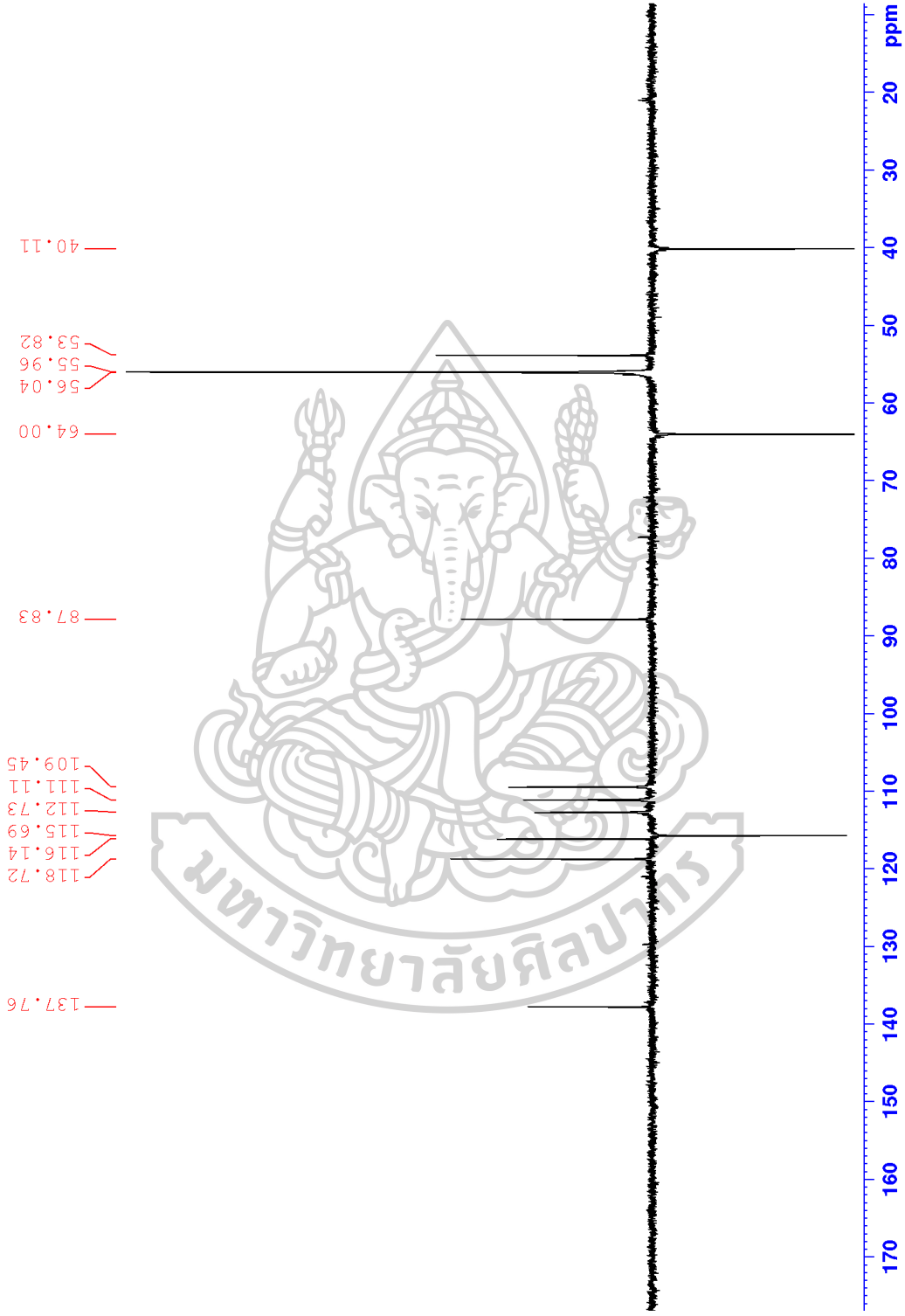


Figure S21 DEPT 135 spectrum of MS15 (75 MHz, CDCl₃)

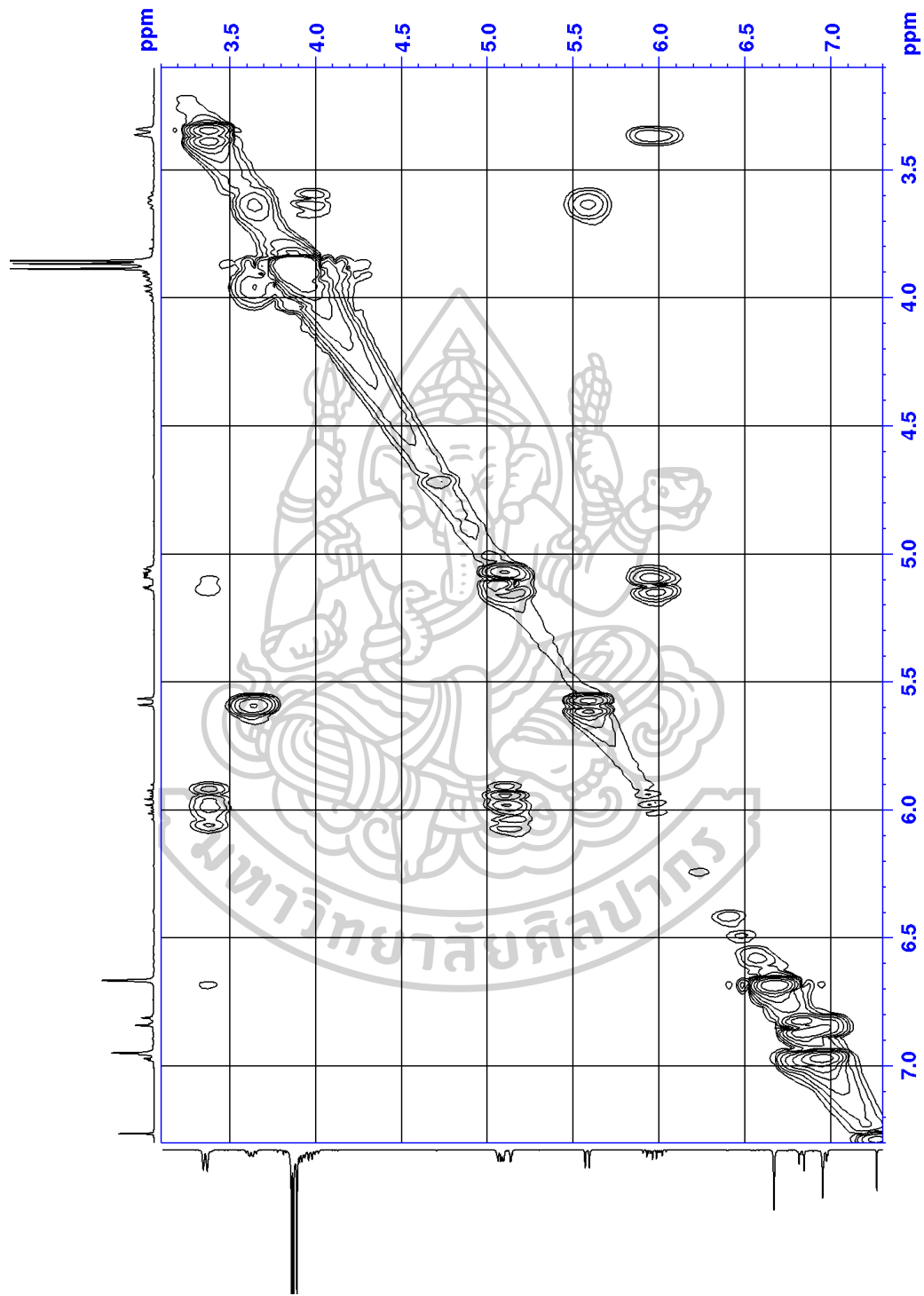


Figure S22 COSY spectrum of MS15 (300 MHz, CDCl₃)

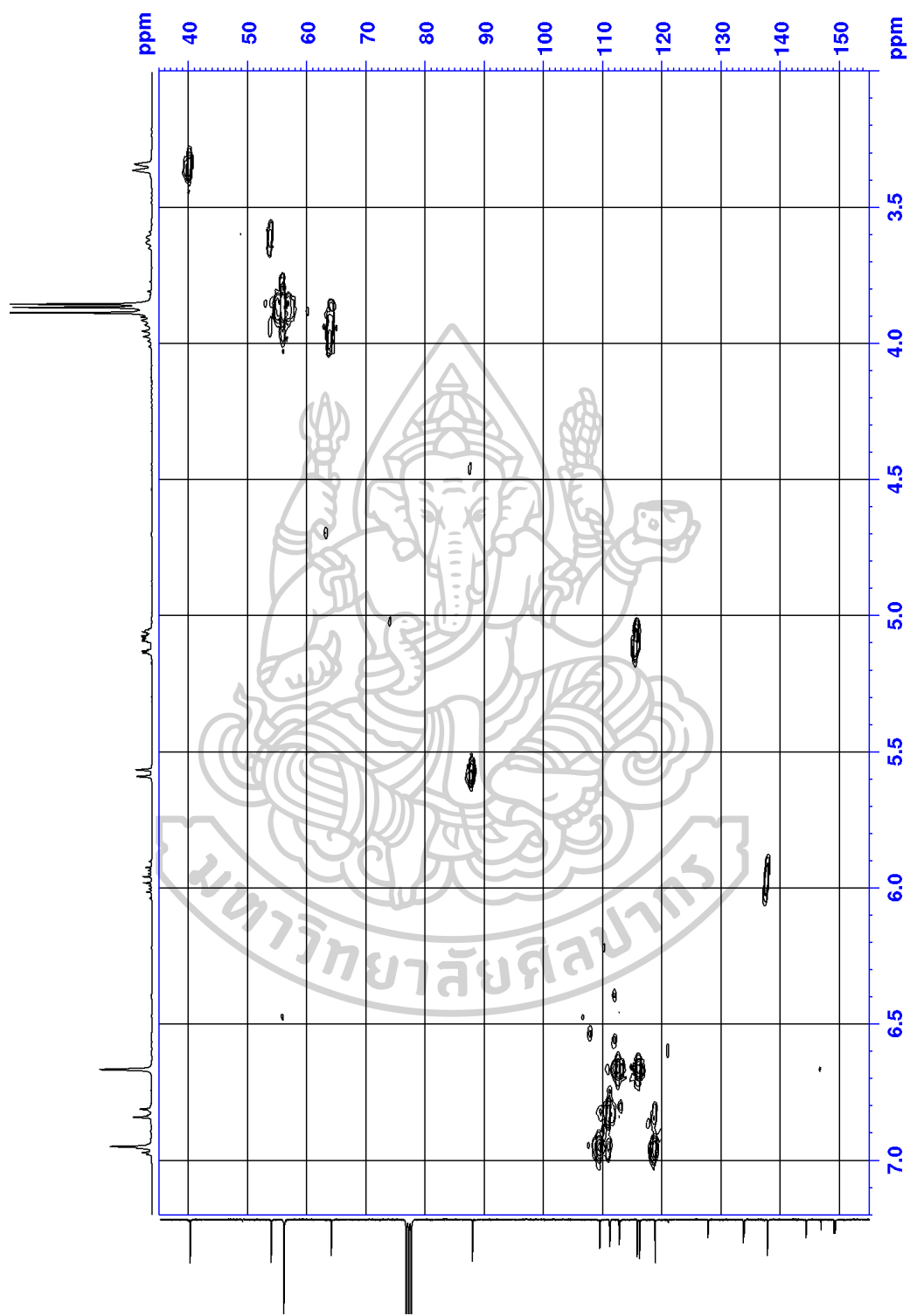


Figure S23 HMQC spectrum of MS15

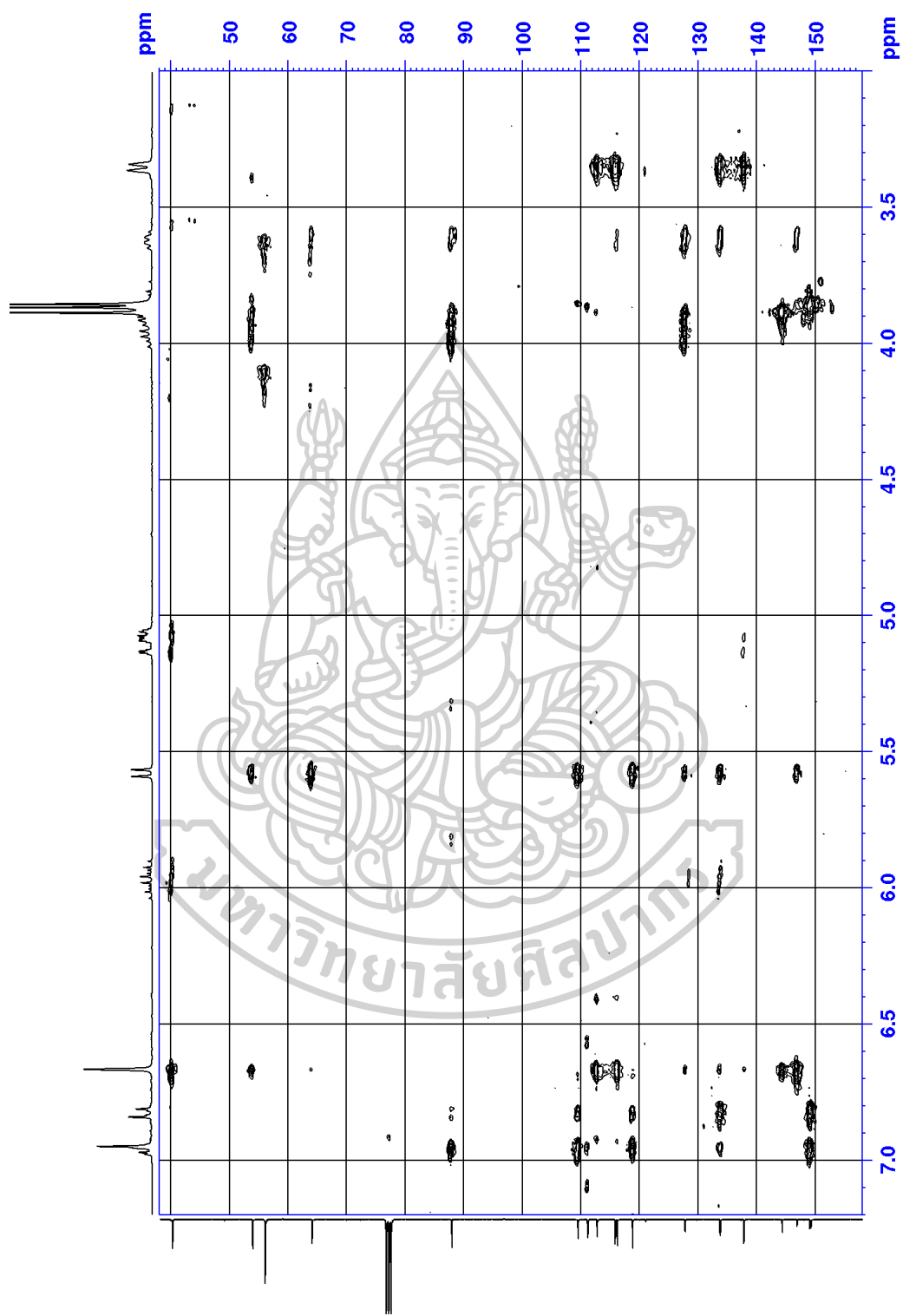
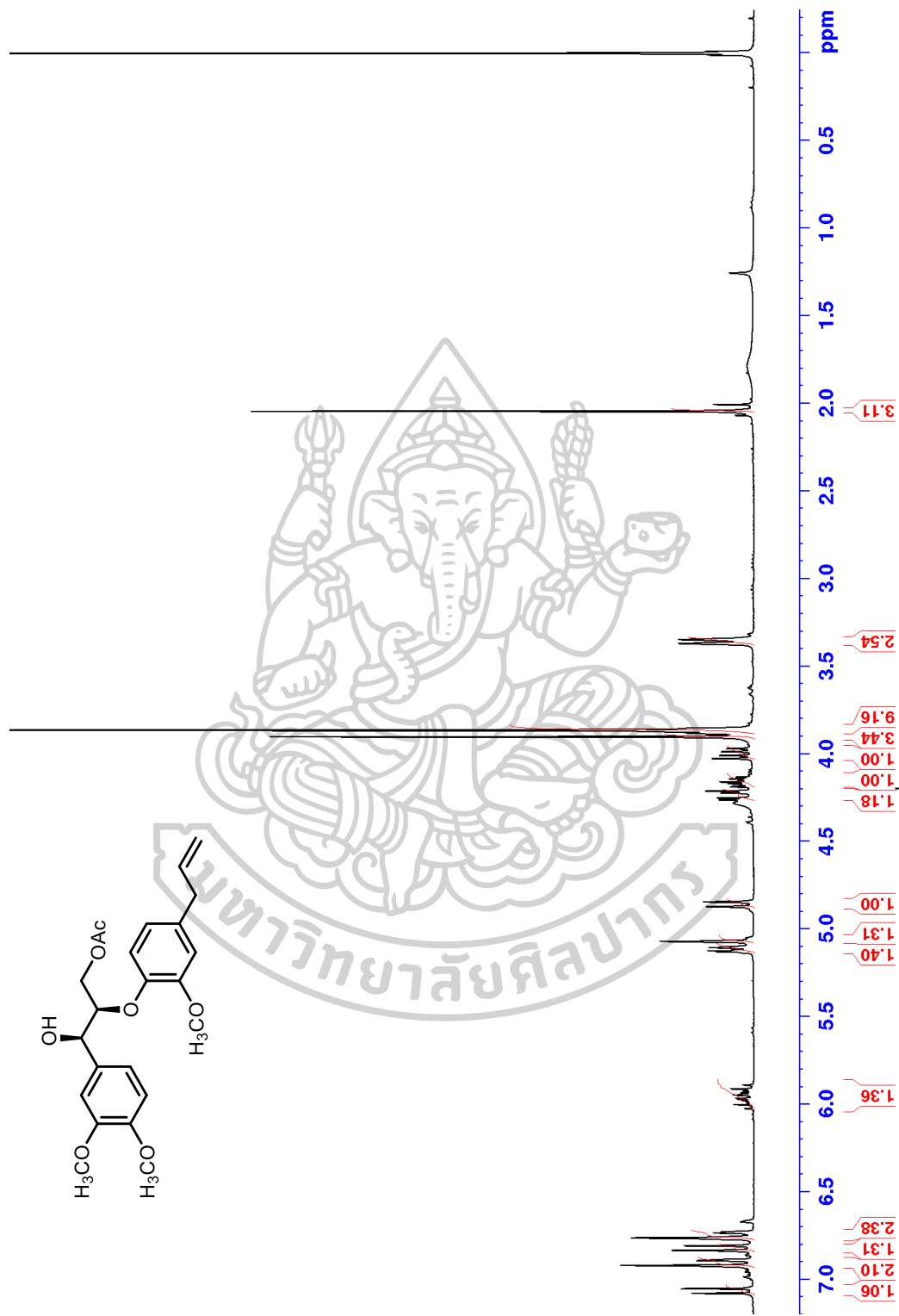


Figure S24 HMBC spectrum of MS15

Figure S25 ¹H NMR spectrum of MS16 (300 MHz, CDCl₃)

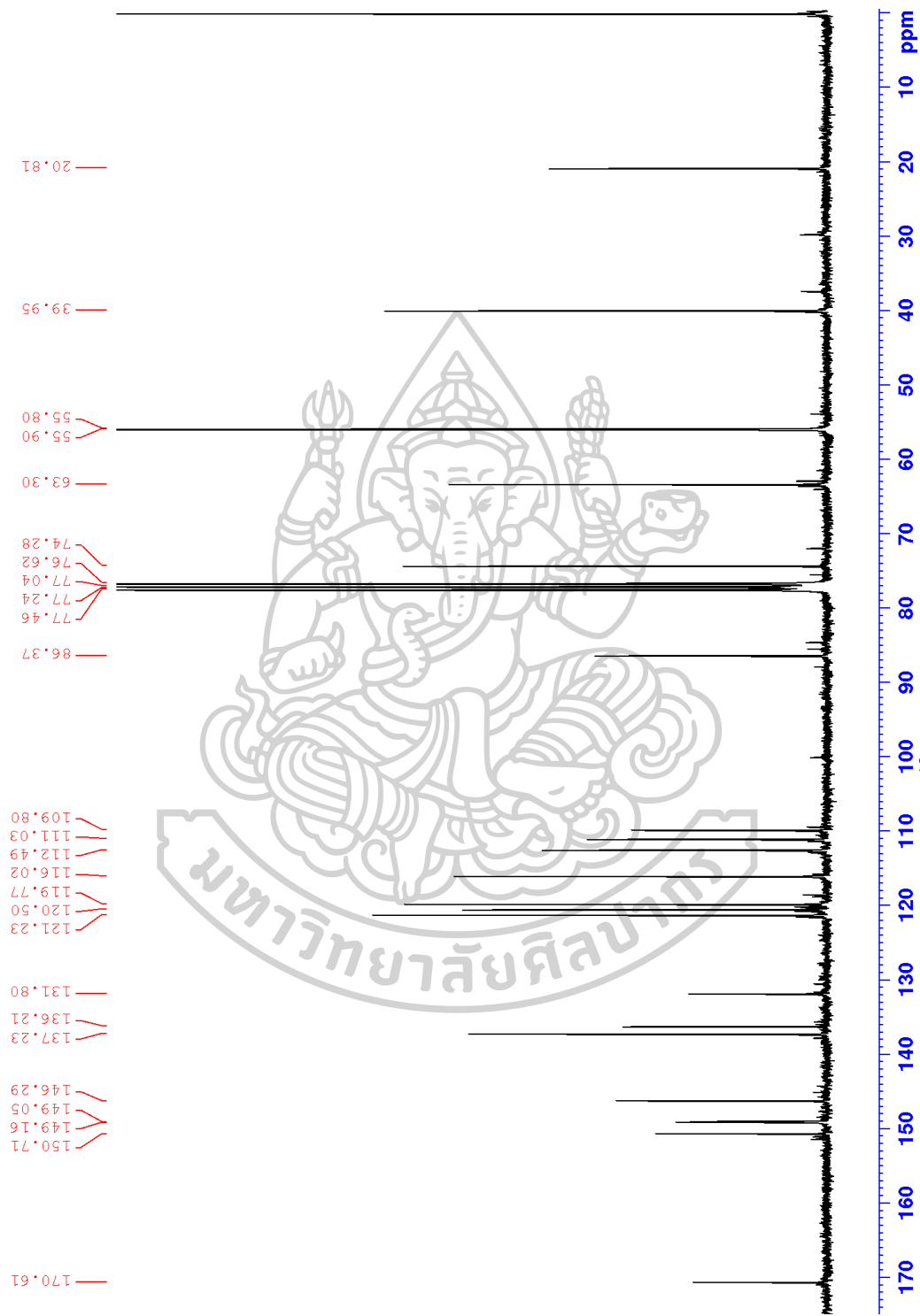
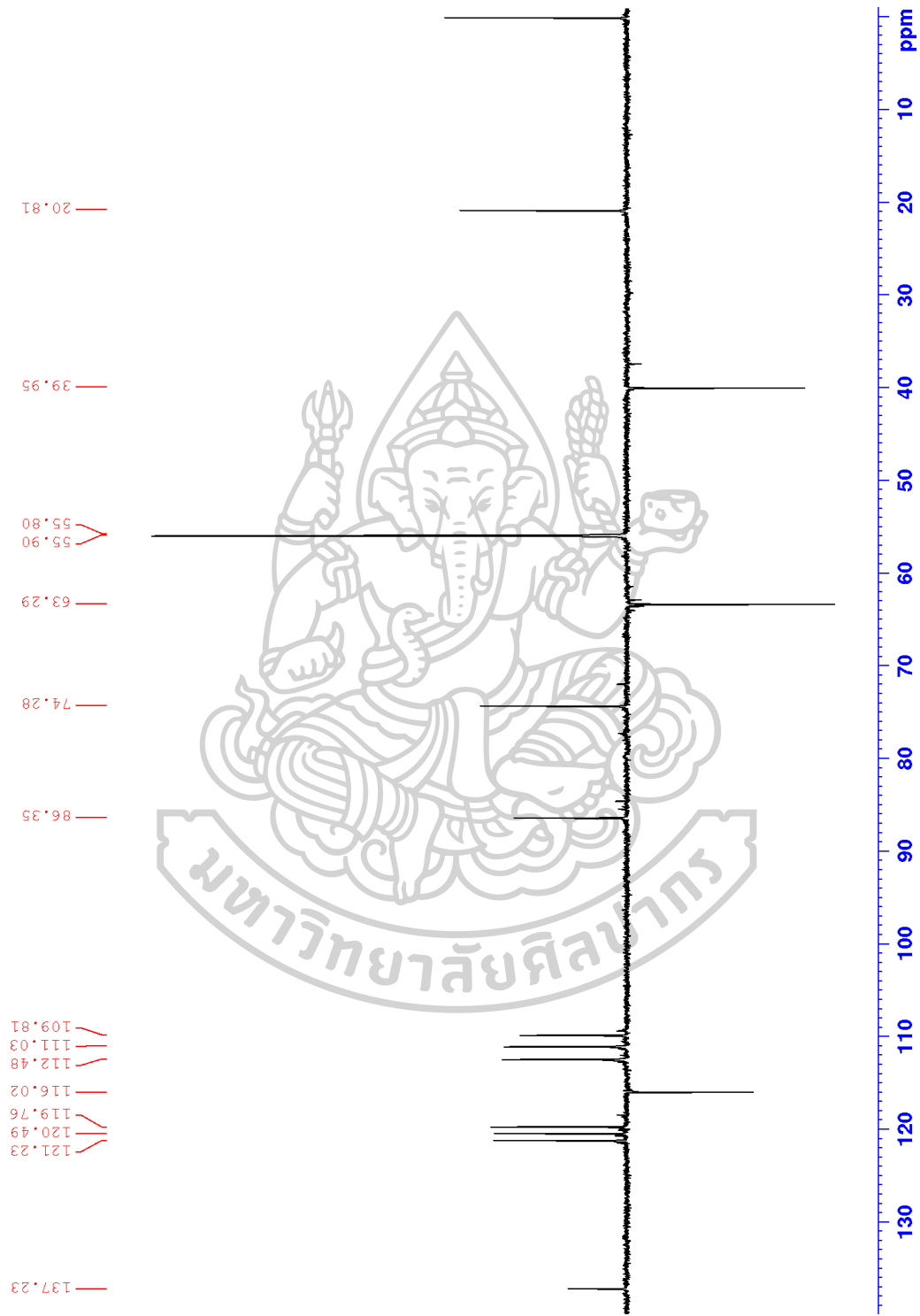


Figure S26 ^{13}C NMR spectrum of MS16 (75 MHz, CDCl_3)

Figure S27 DEPT 135 spectrum of MS16 (75 MHz, CDCl₃)

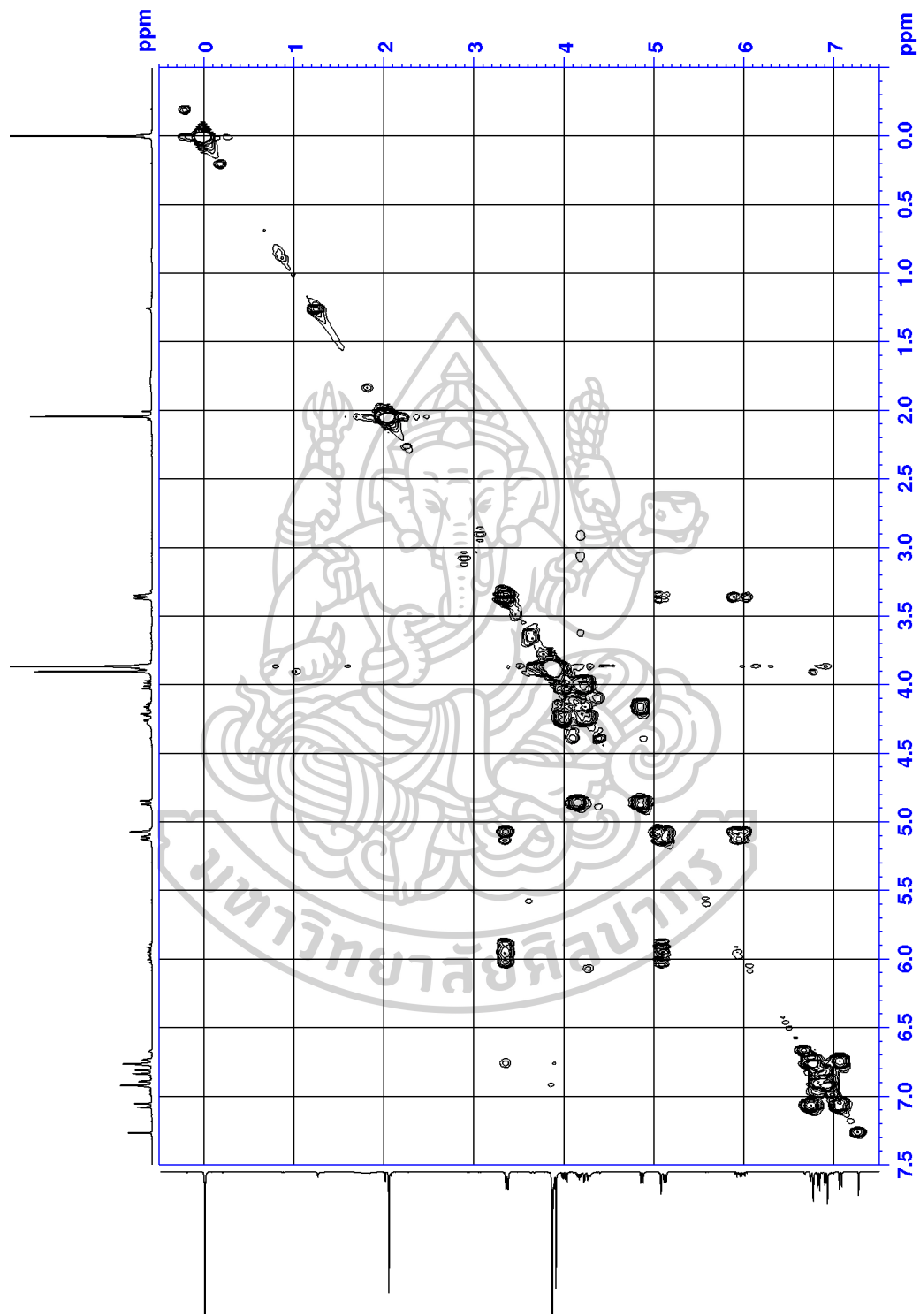


Figure S28 COSY spectrum of MS16 (300 MHz, CDCl₃)

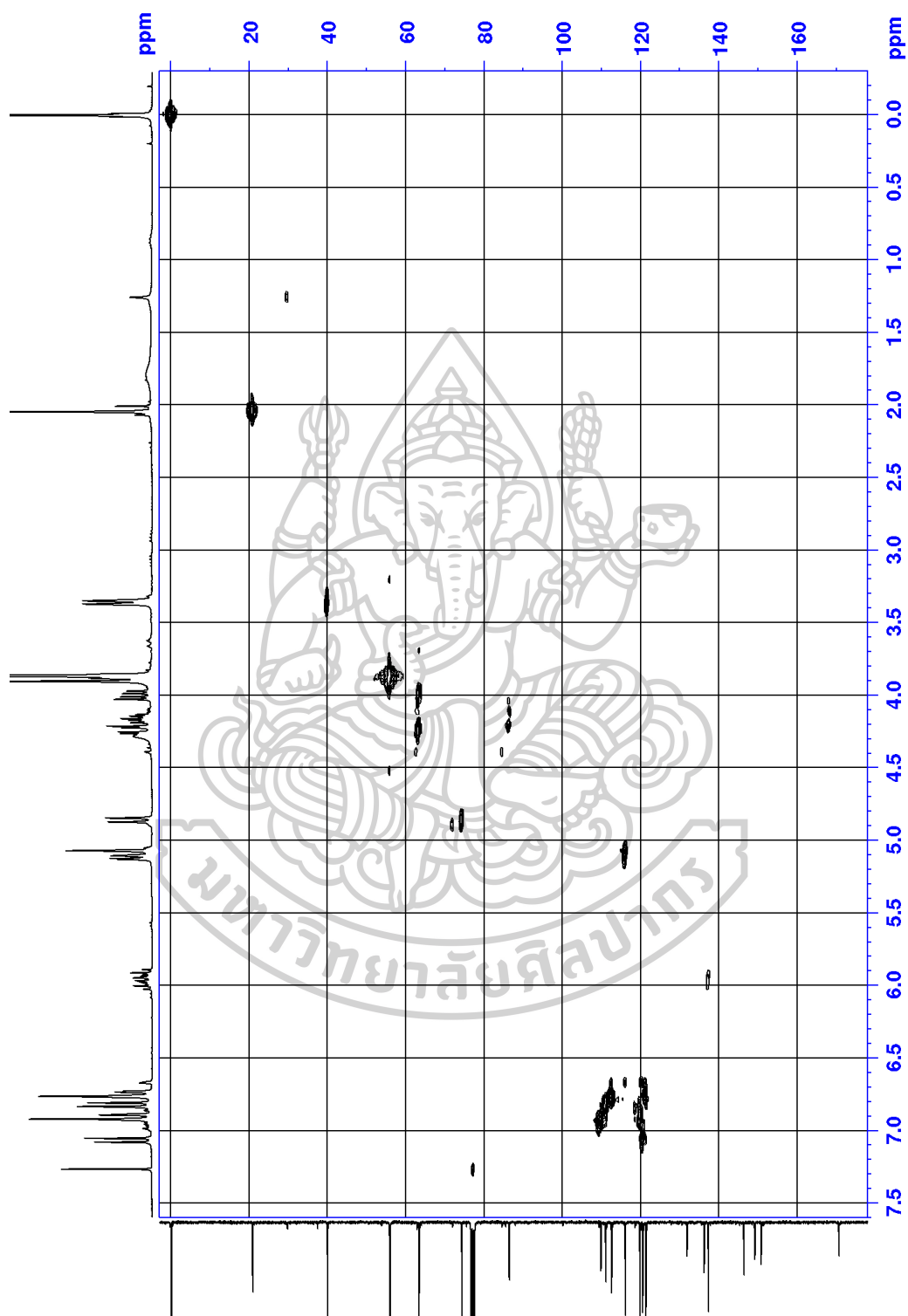


Figure S29 HMQC spectrum of MS16

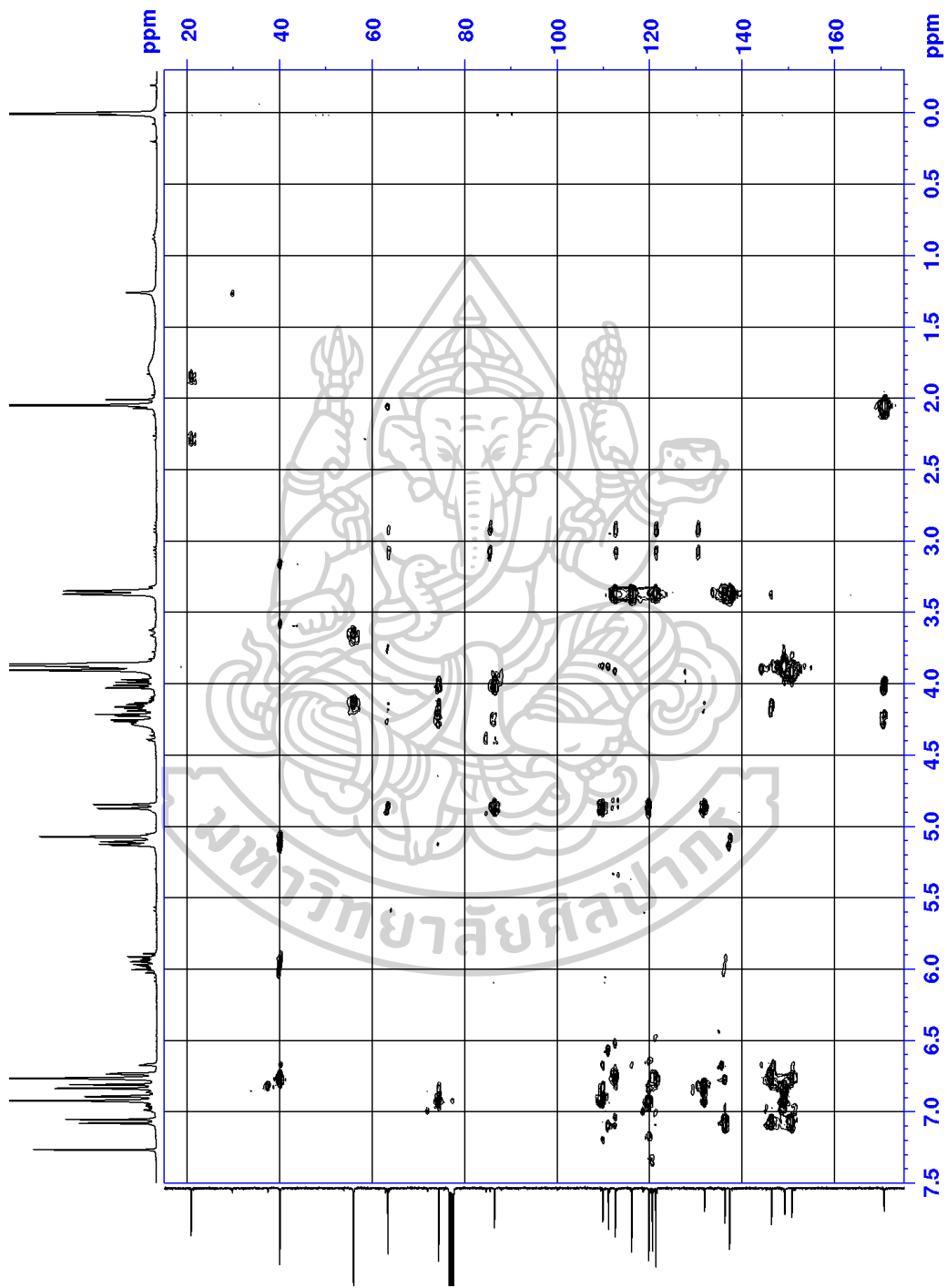


Figure S30 HMB spectrum of MS16

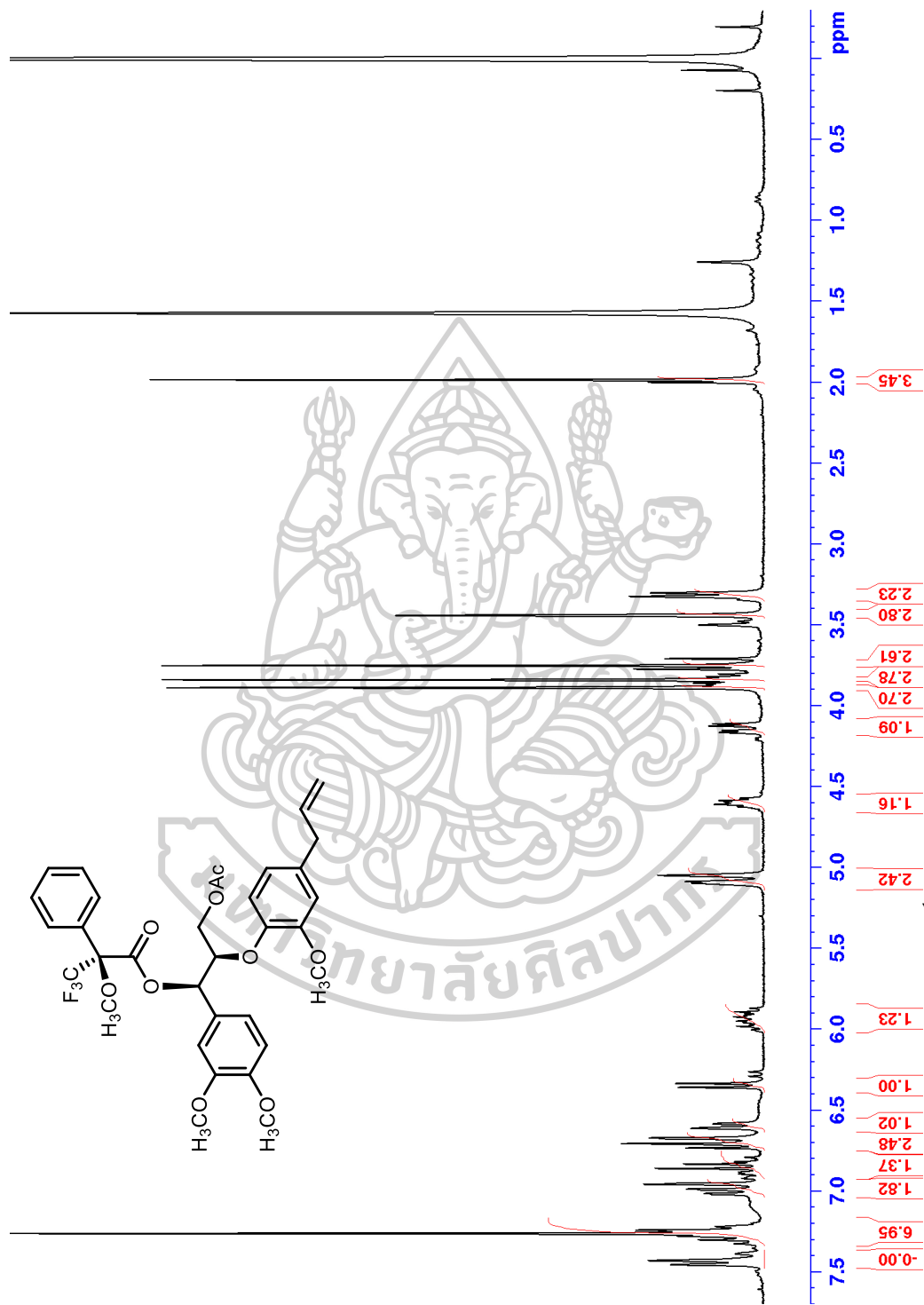


Figure S31 ^1H NMR spectrum of S-(-)-MTPS ester of MS16 (300 MHz, CDCl_3)

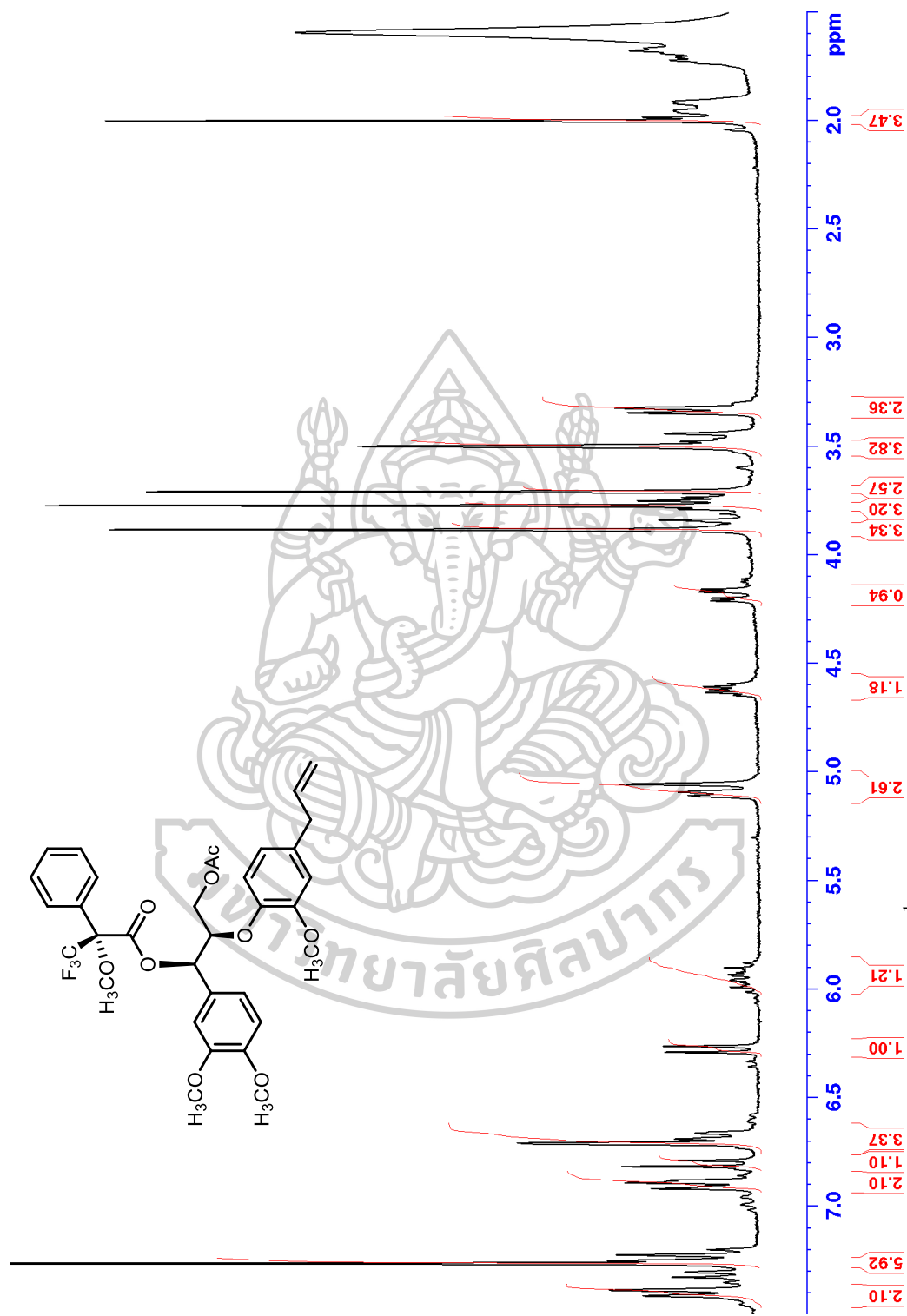


Figure S32 ^1H NMR spectrum of *R*-(+)-MTPS ester of MS16 (300 MHz, CDCl_3)

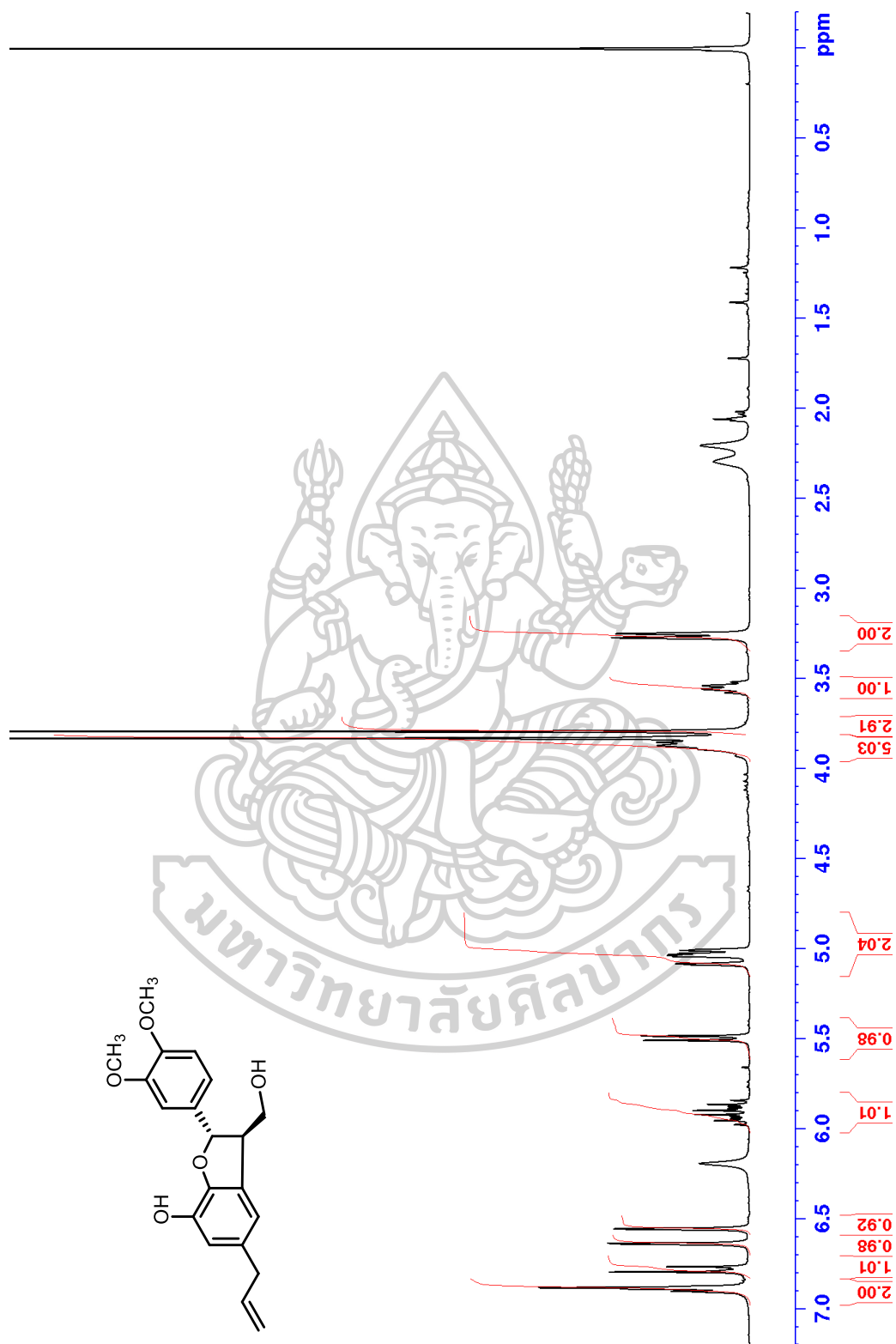


Figure S33 ^1H NMR spectrum of MS17 (300 MHz, CDCl_3)

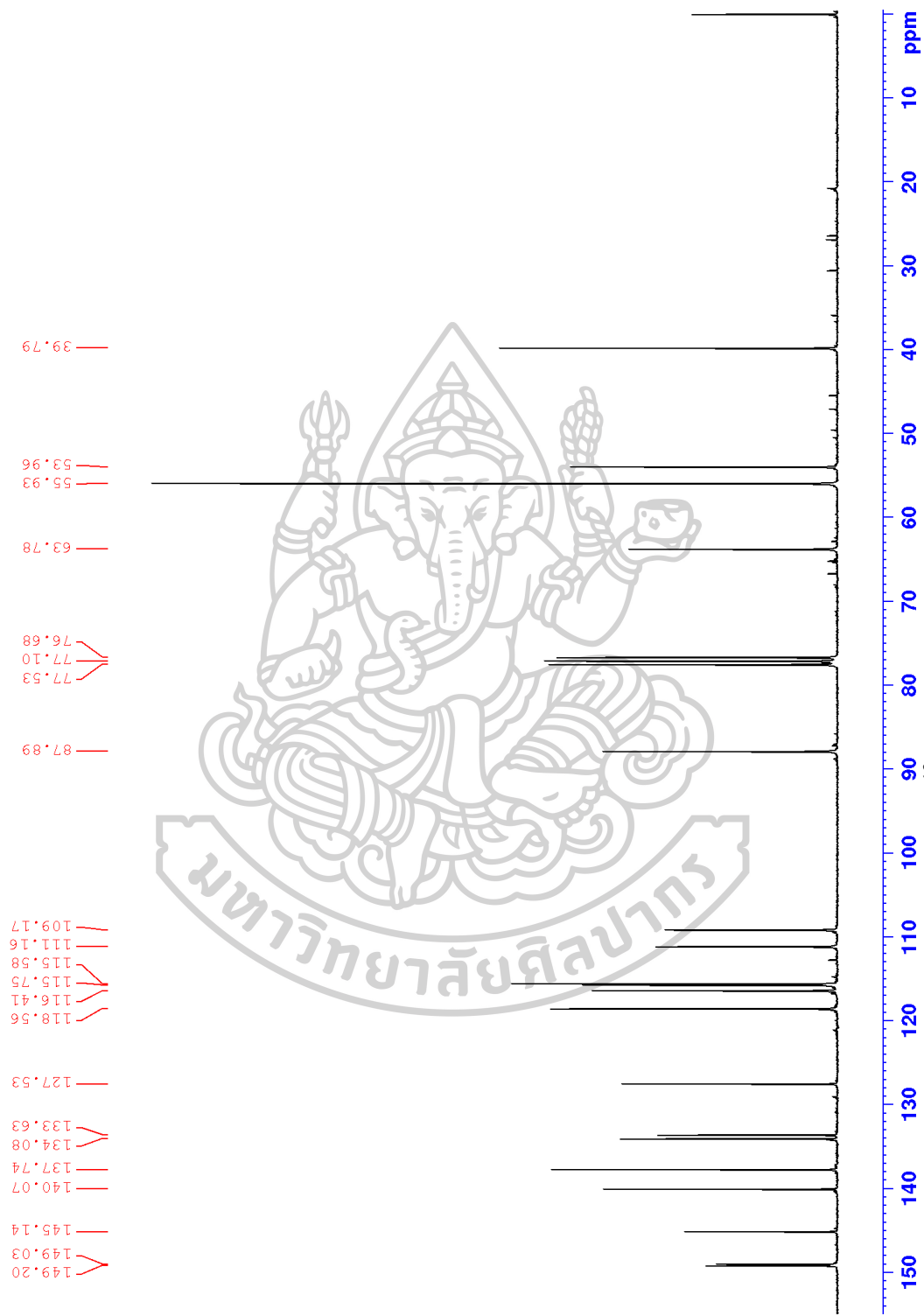
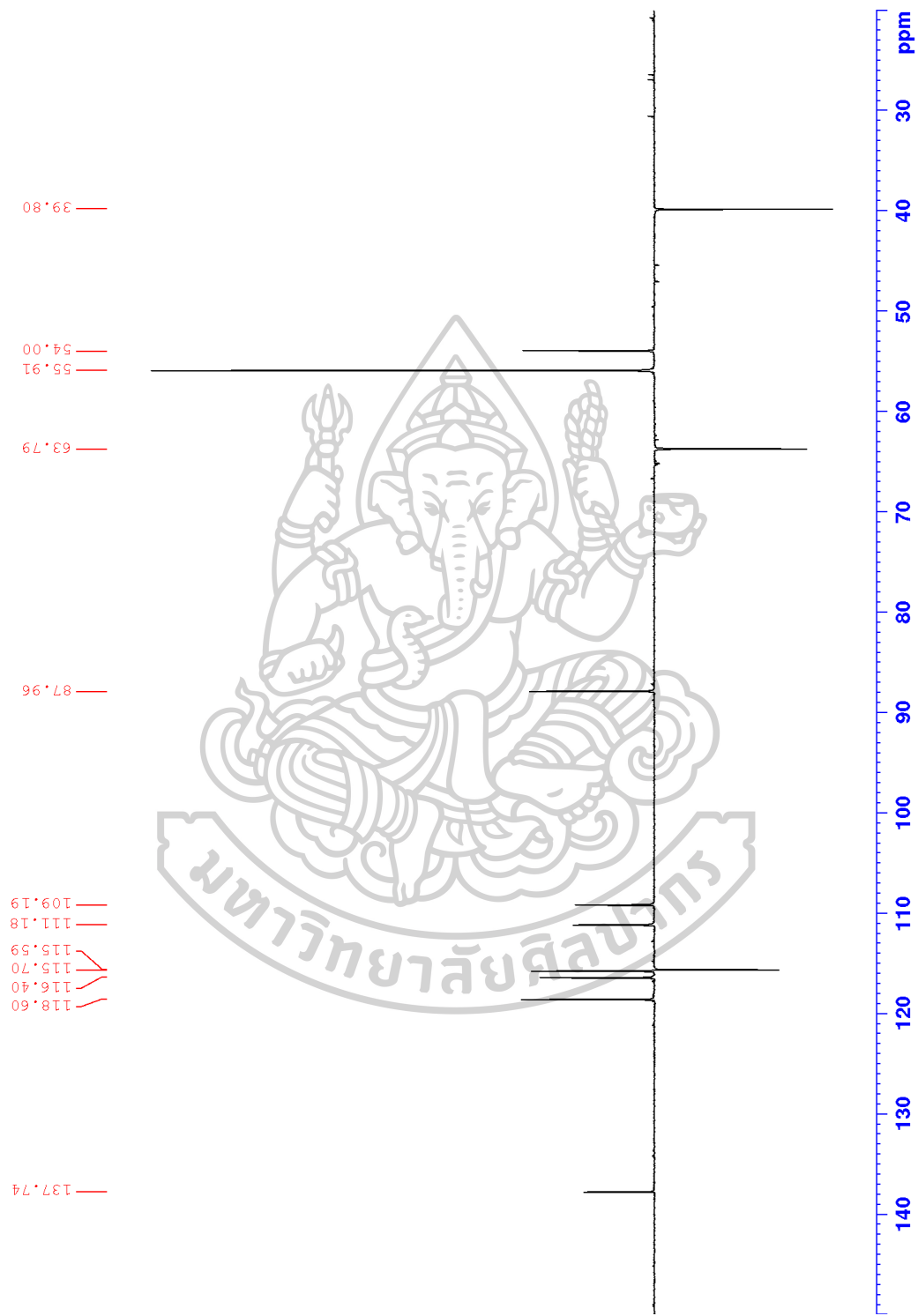


Figure S34 ^{13}C NMR spectrum of MS17 (75 MHz, CDCl_3)

Figure S35 DEPT ^{135}M spectrum of MS17 (75 MHz, CDCl_3)

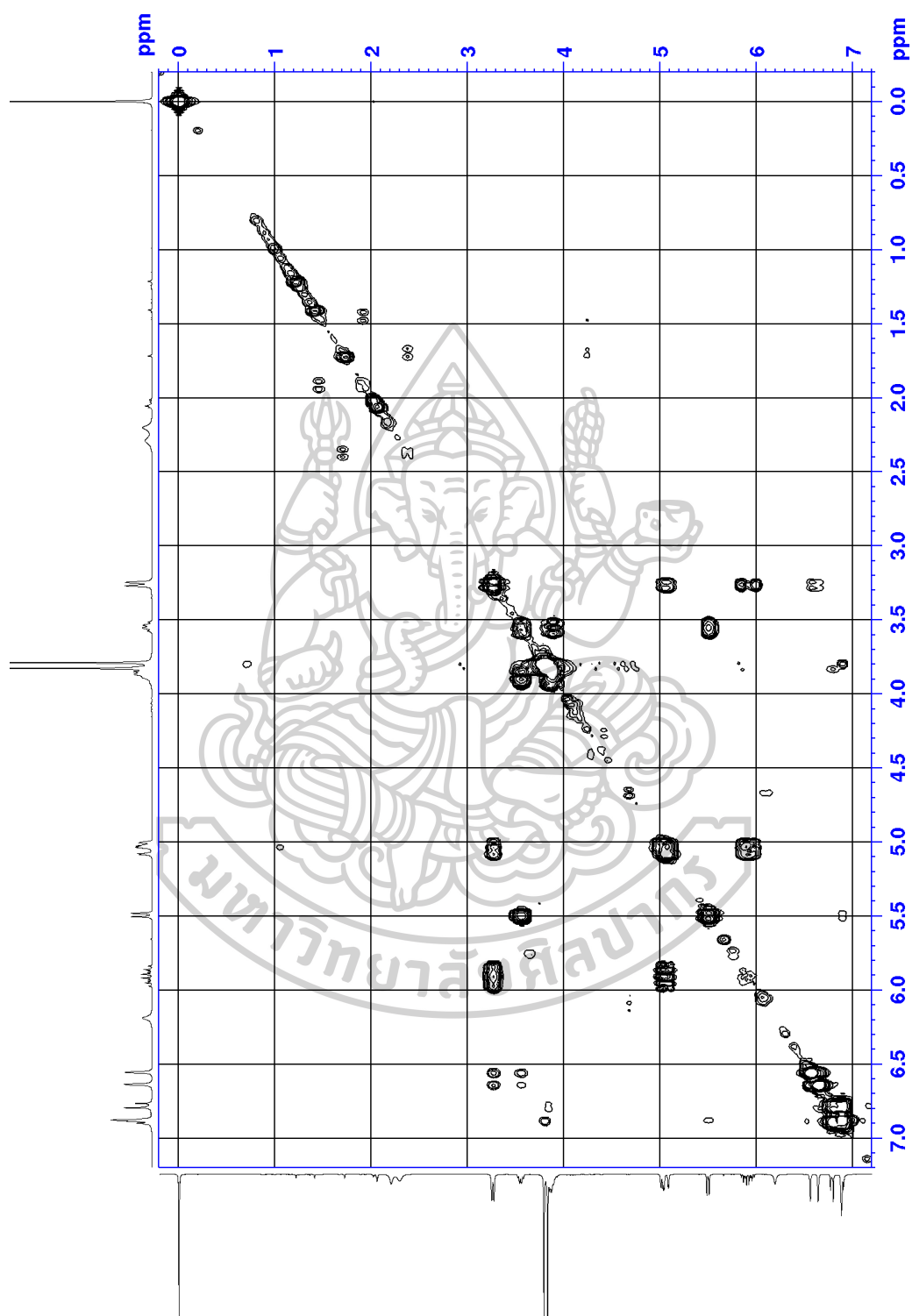


Figure S36 COSY spectrum of MS17 (300 MHz, CDCl_3)

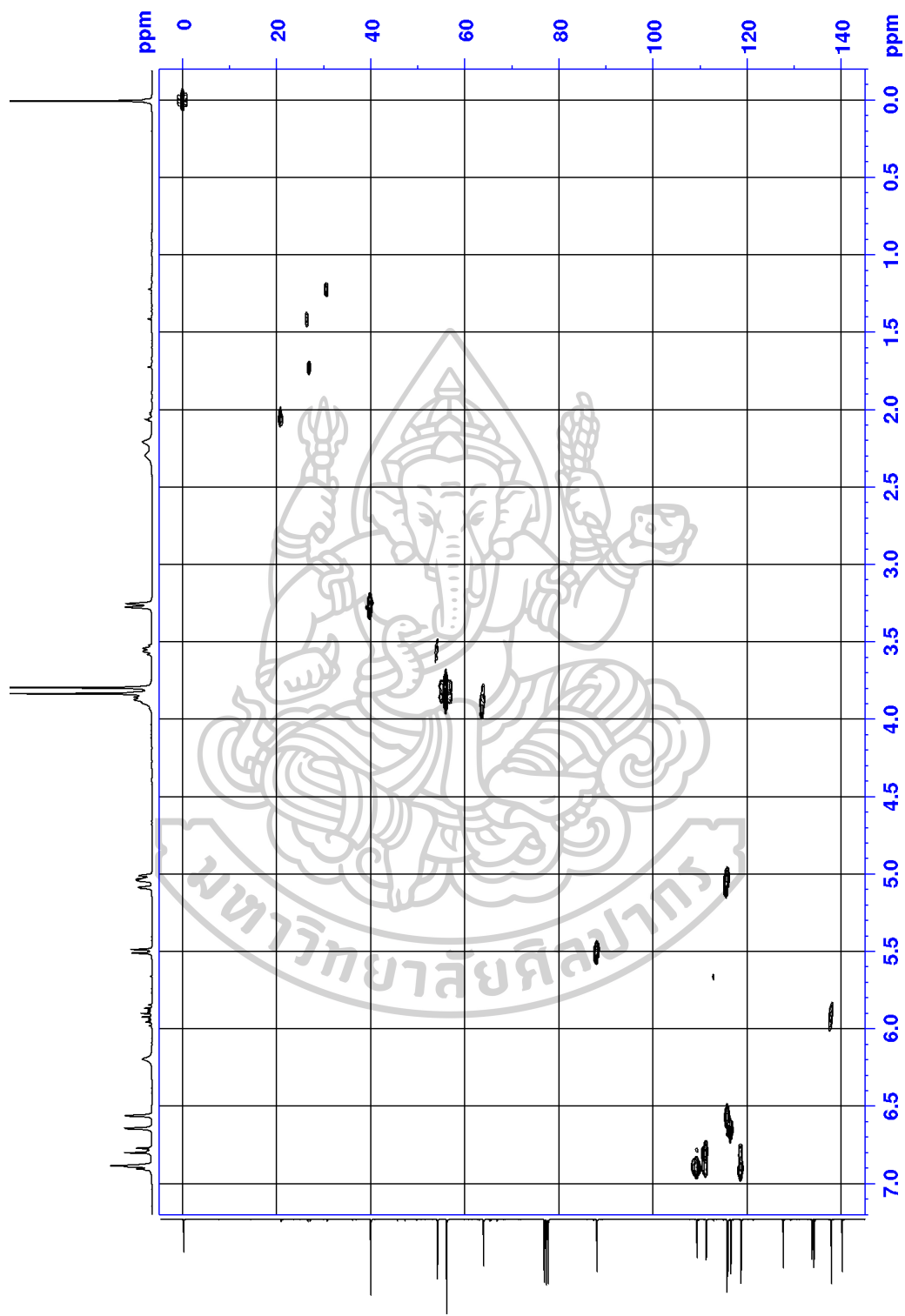


Figure S37 HMQC spectrum of MS17

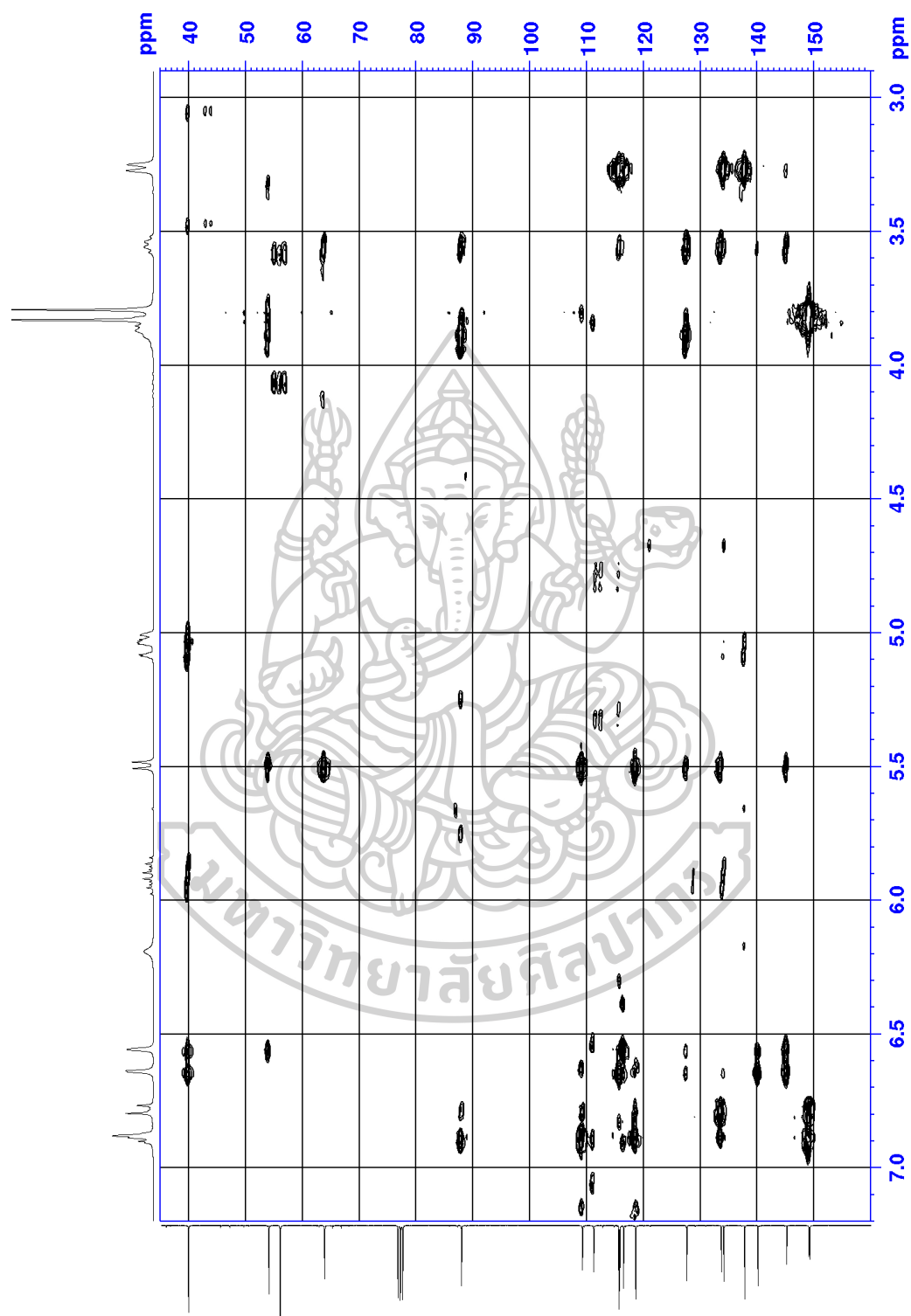


Figure S38 HMBC spectrum of MS17

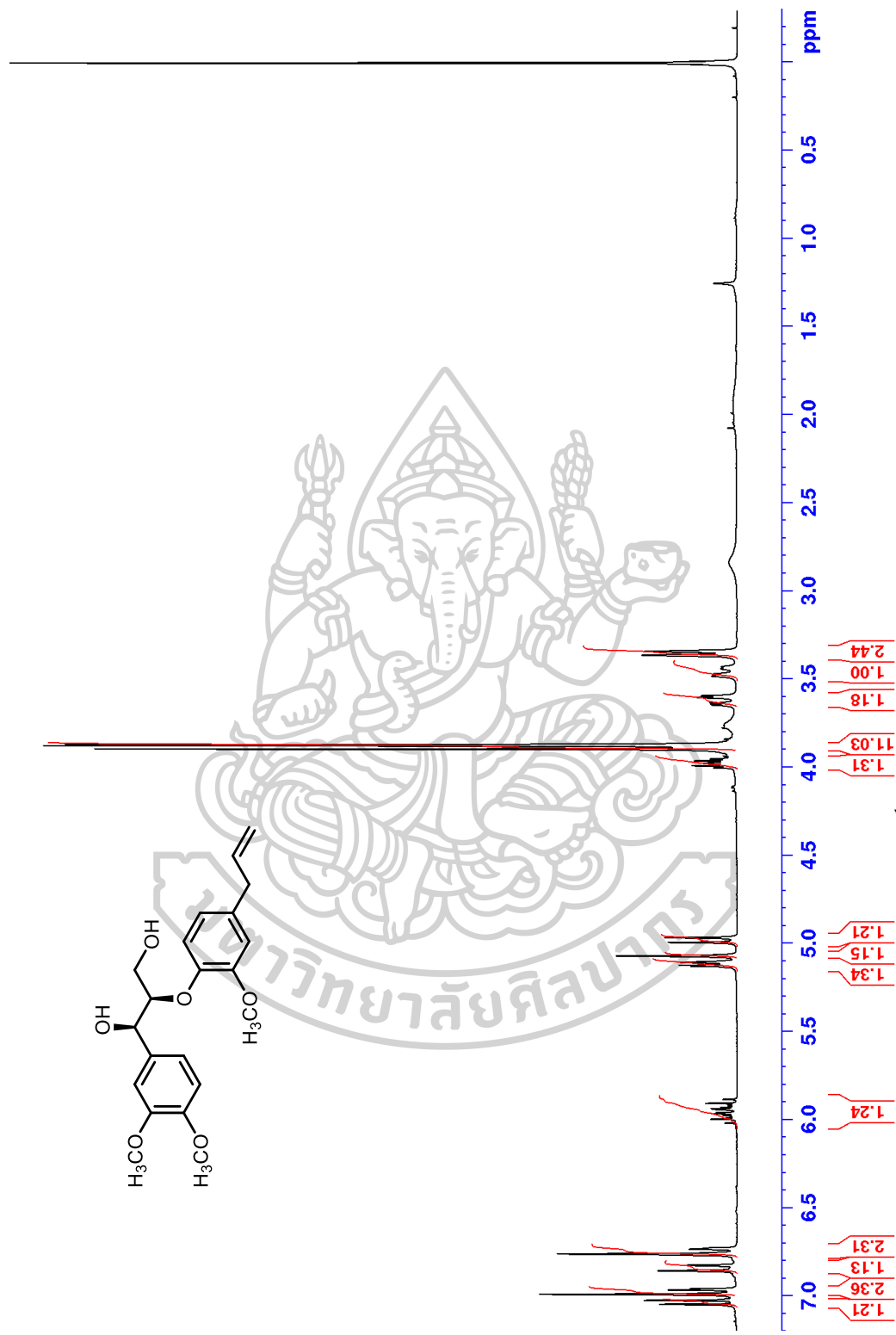


Figure S39 ^1H NMR spectrum of MS19 (300 MHz, CDCl_3)

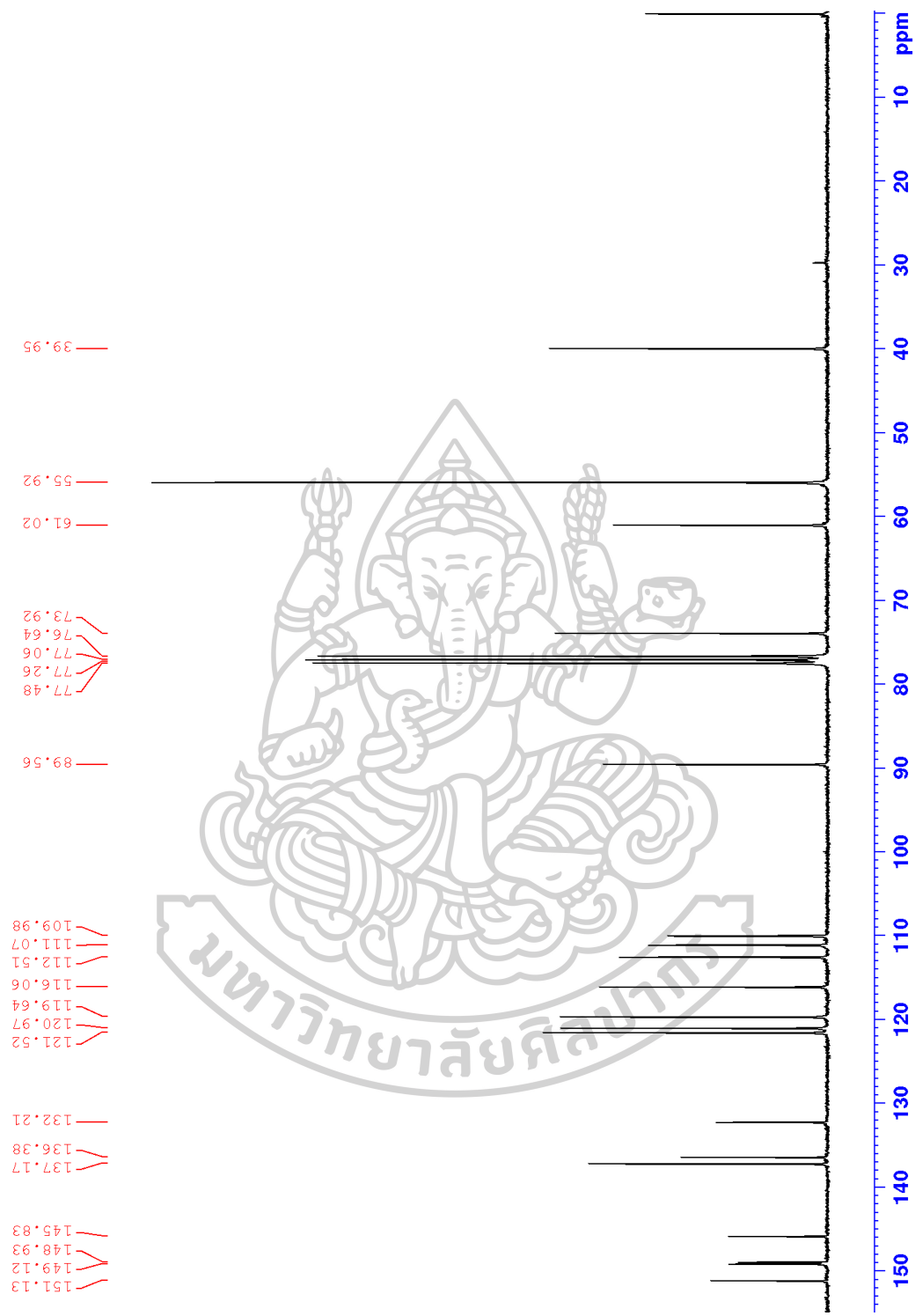


Figure S40 ^{13}C NMR spectrum of MS19 (75 MHz, CDCl_3)

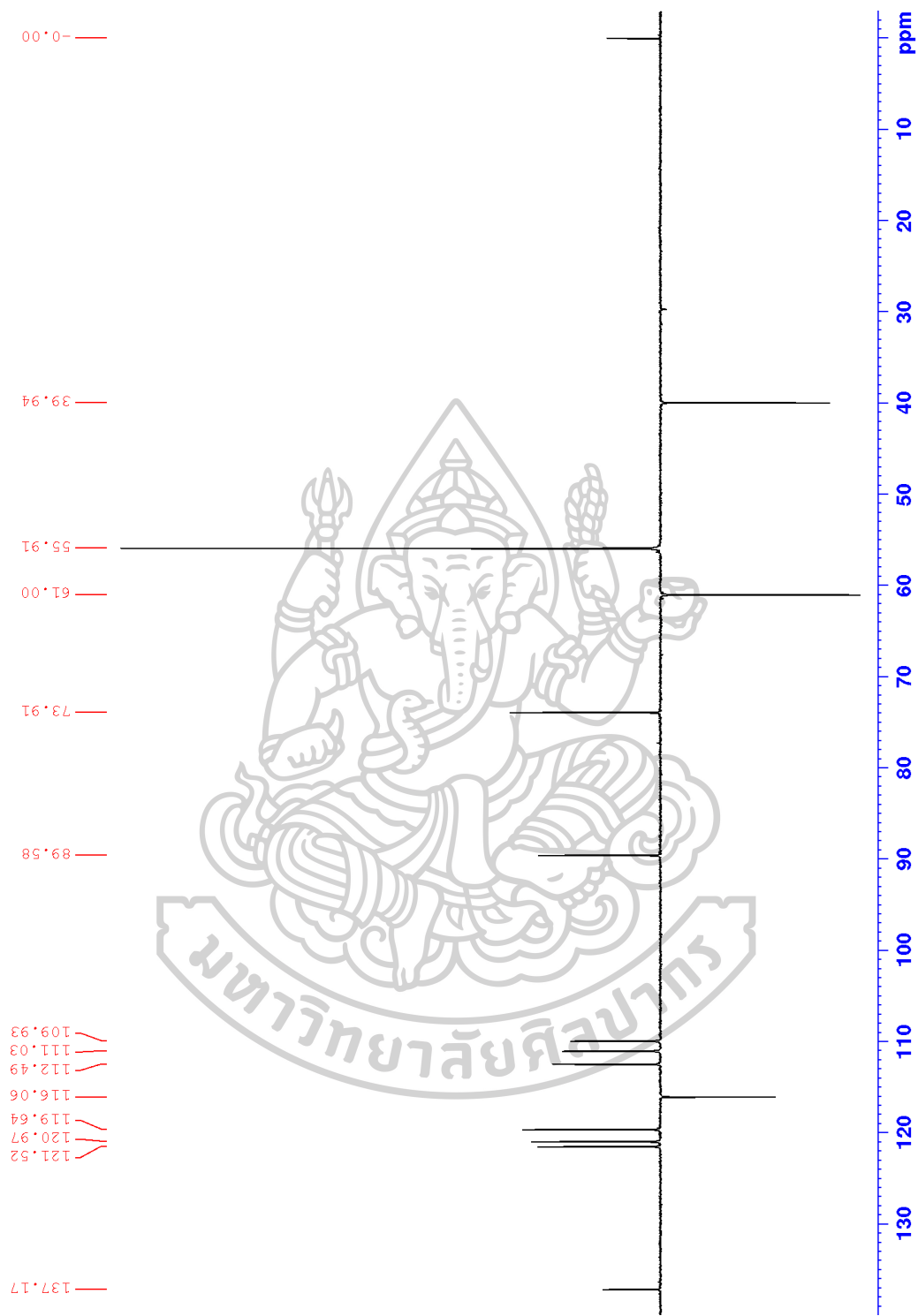


Figure S41 DEPT 135 spectrum of MS19 (75 MHz, CDCl₃)

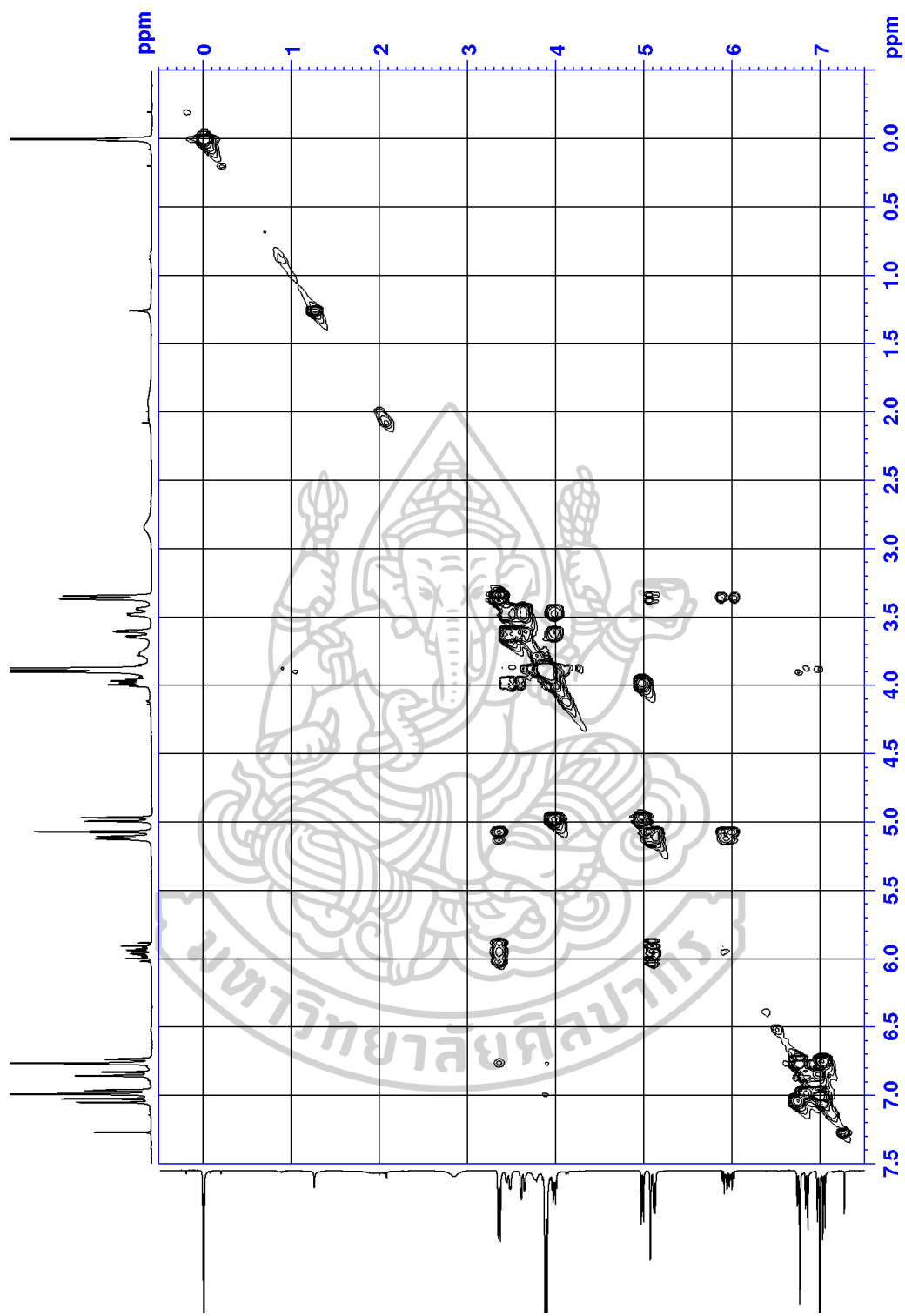


Figure S42 COSY spectrum of MS19 (300 MHz, CDCl₃)

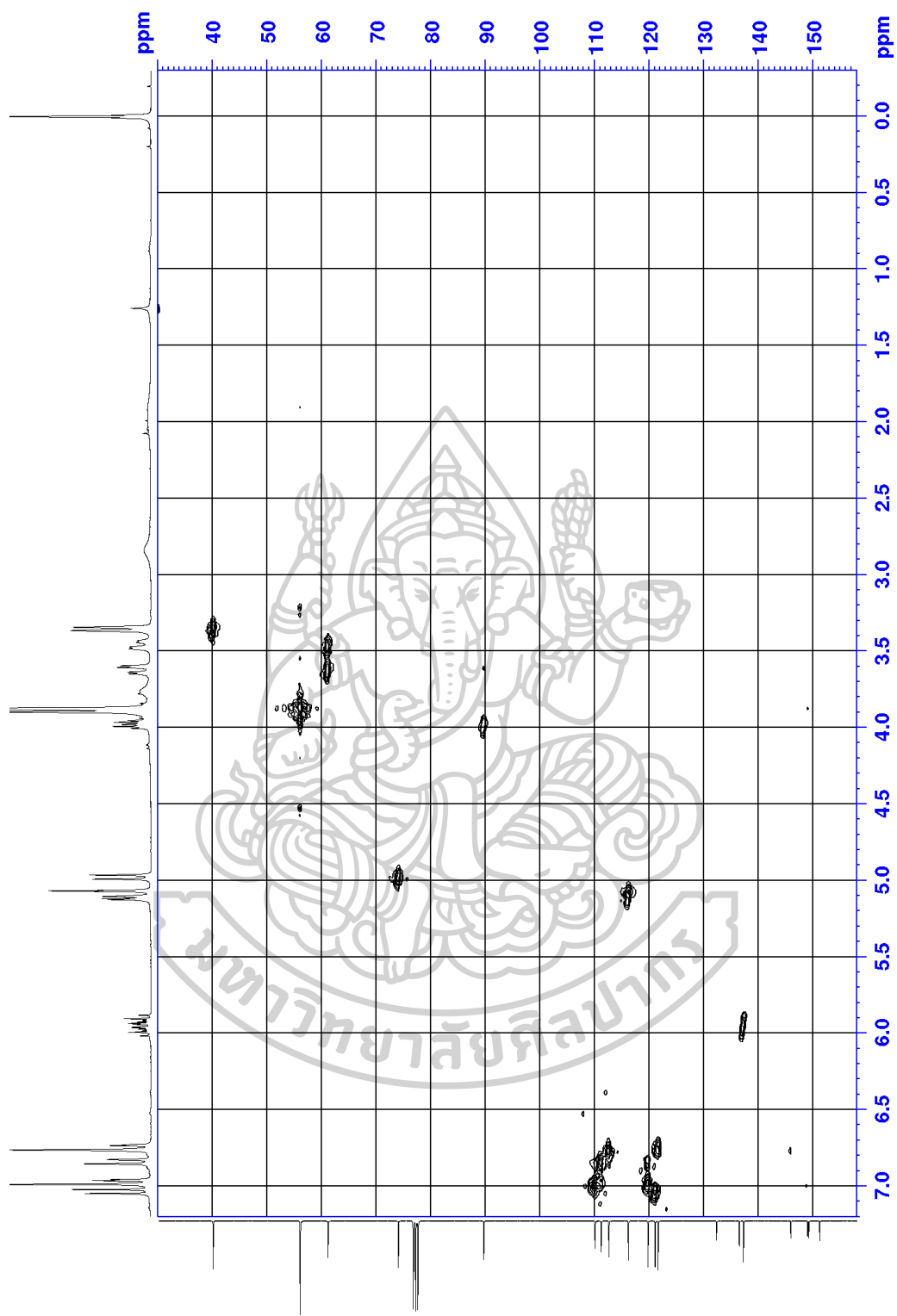


Figure S43 HMQC spectrum of MS19

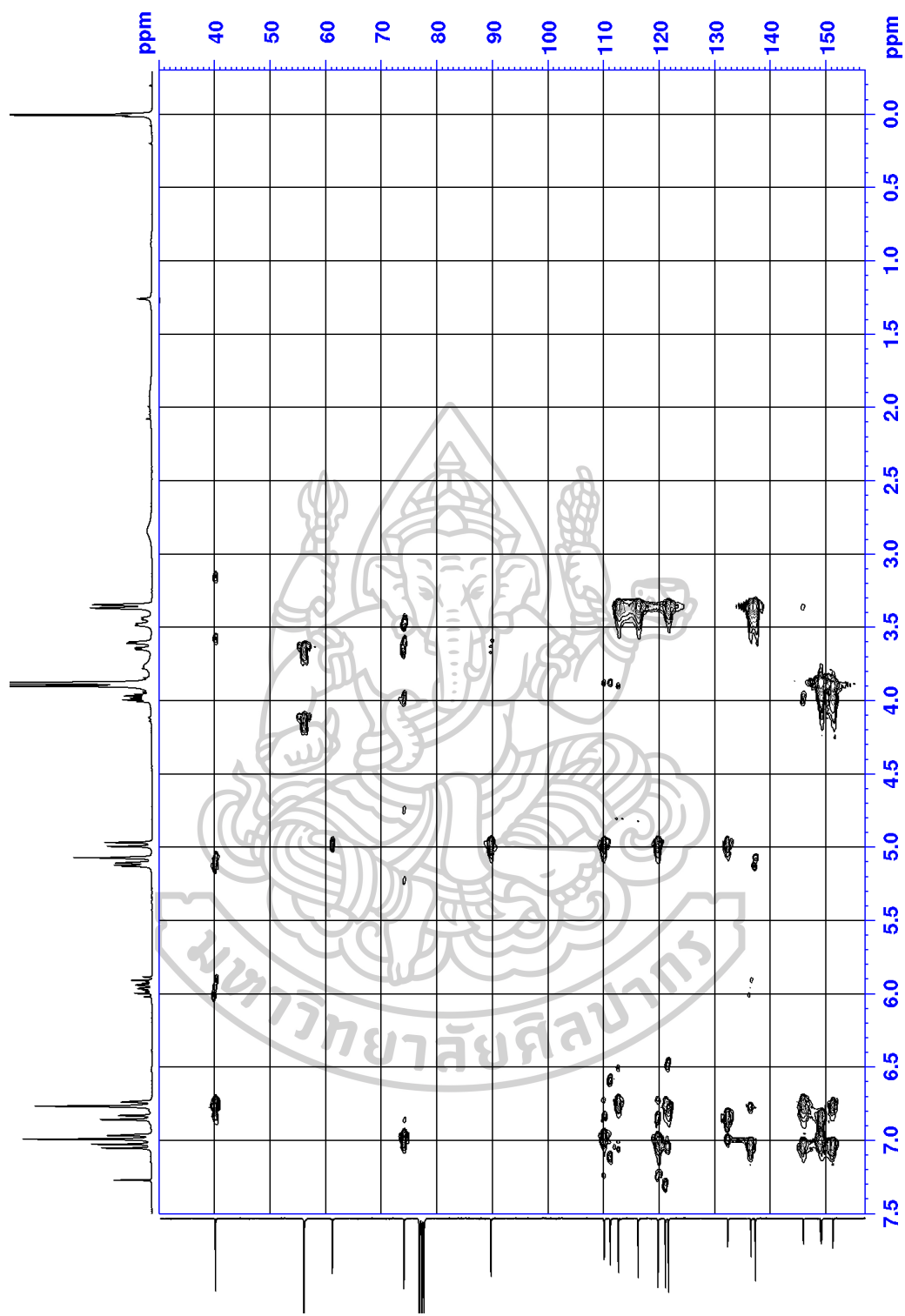
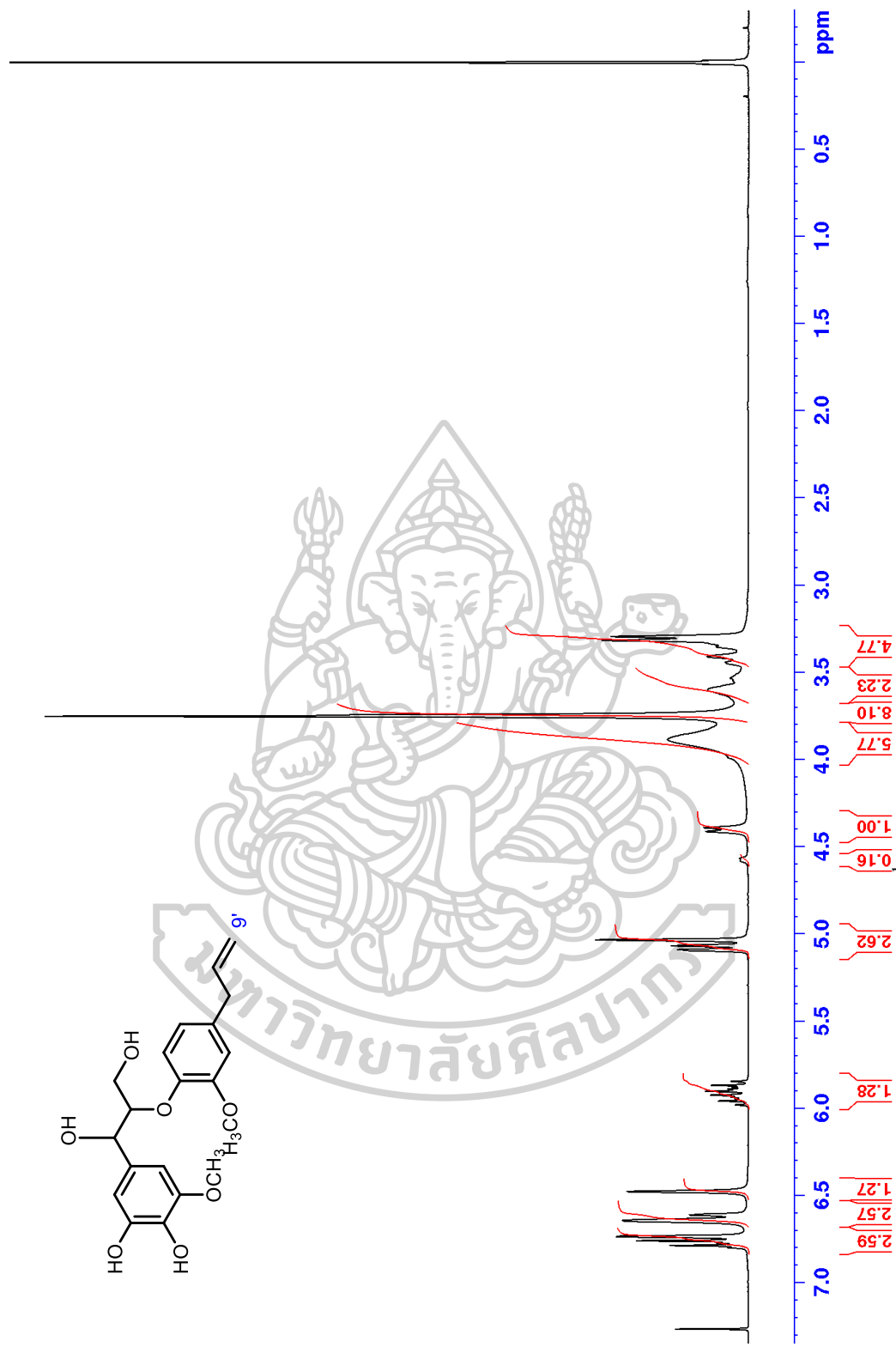


Figure S44 HMB spectrum of MS19

Figure S45 ^1H NMR spectrum of MS20 (300 MHz, CDCl_3)

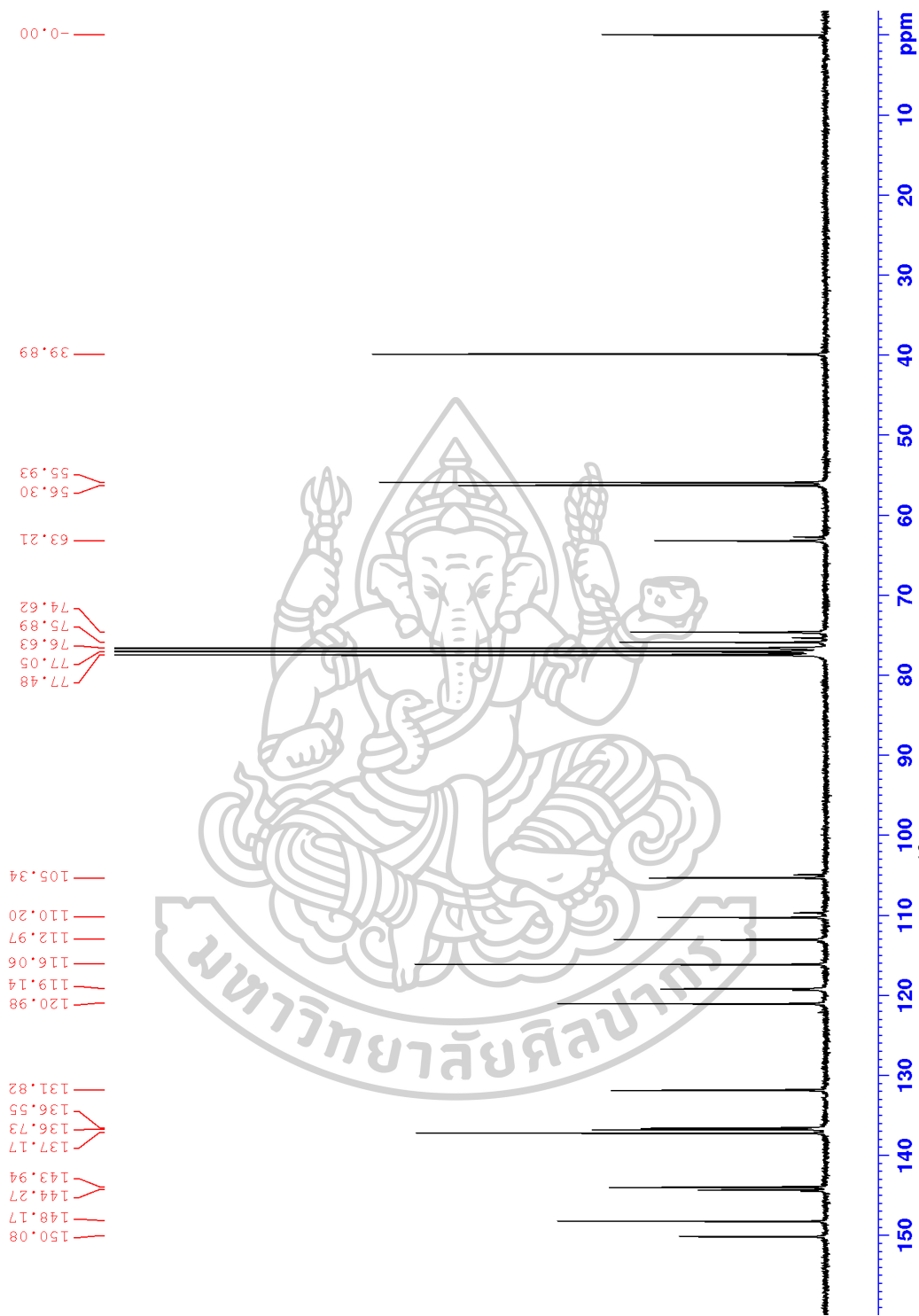


Figure S46 ^{13}C NMR spectrum of MS20 (75 MHz, CDCl_3)

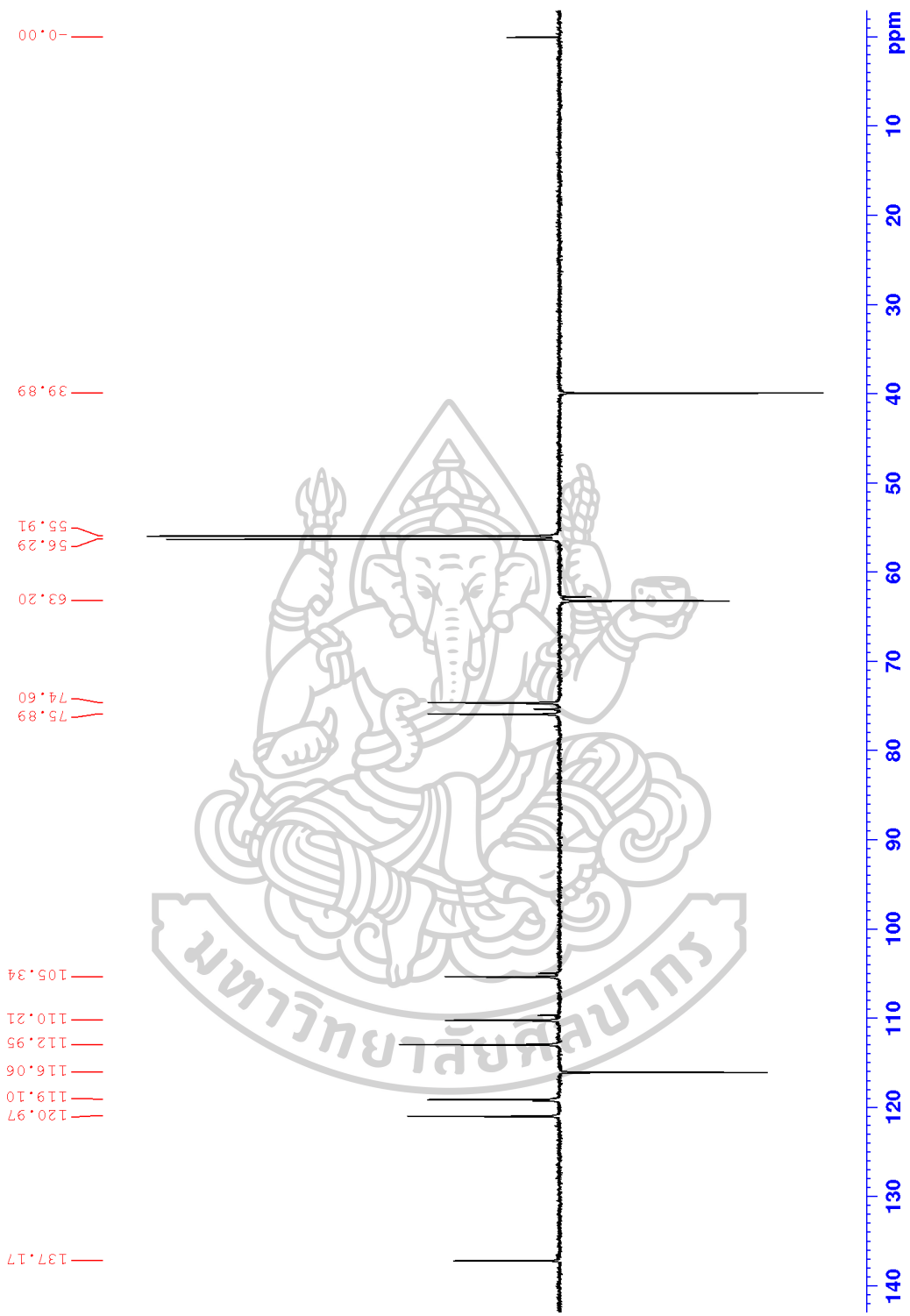


Figure S47 DEPT 135 spectrum of MS20 (75 MHz, CDCl₃)

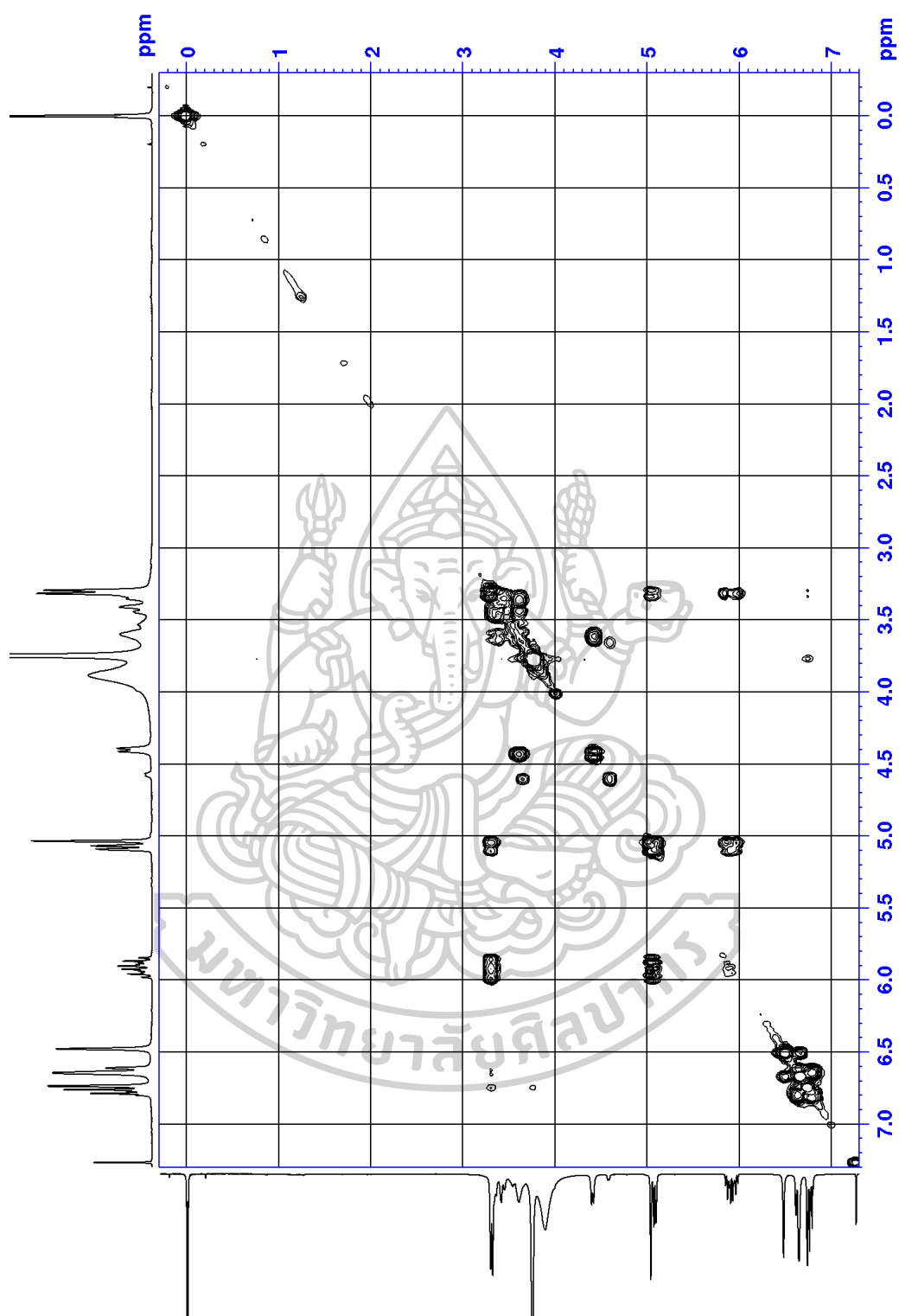


Figure S48 COSY spectrum of MS20 (300MHz, CDCl₃)

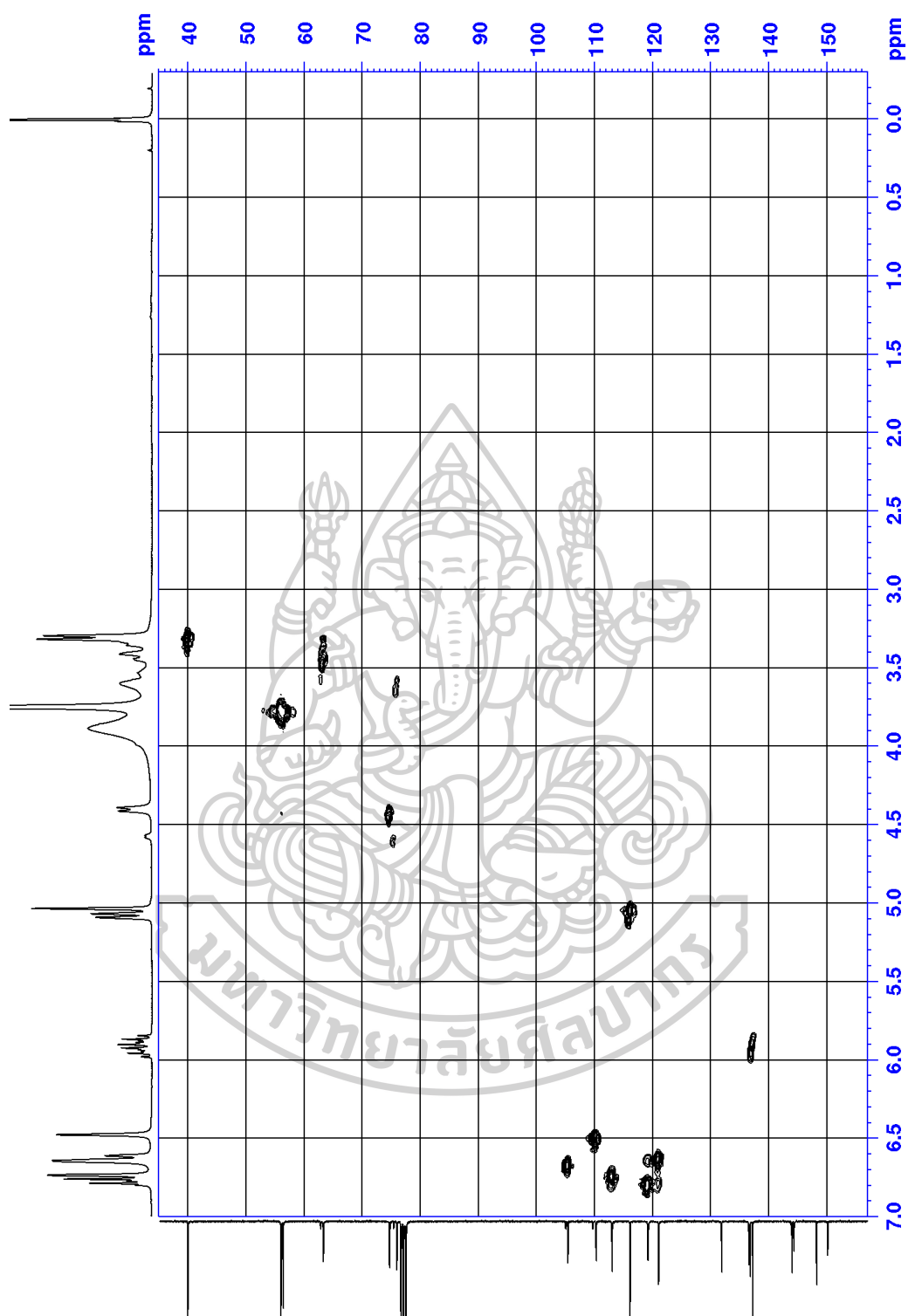


Figure S49 HMQC spectrum of MS20

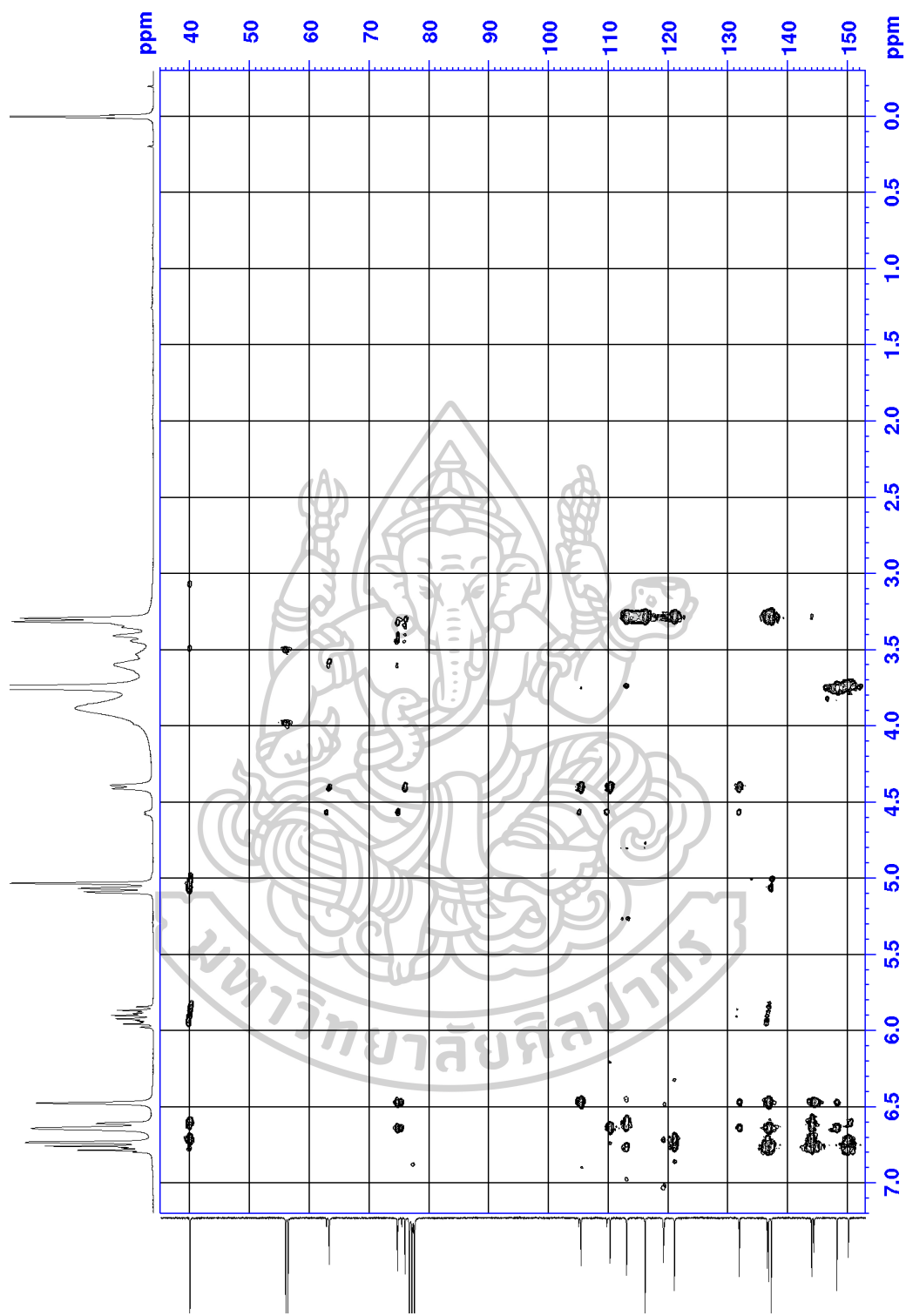


Figure S50 HMBN spectrum of MS20

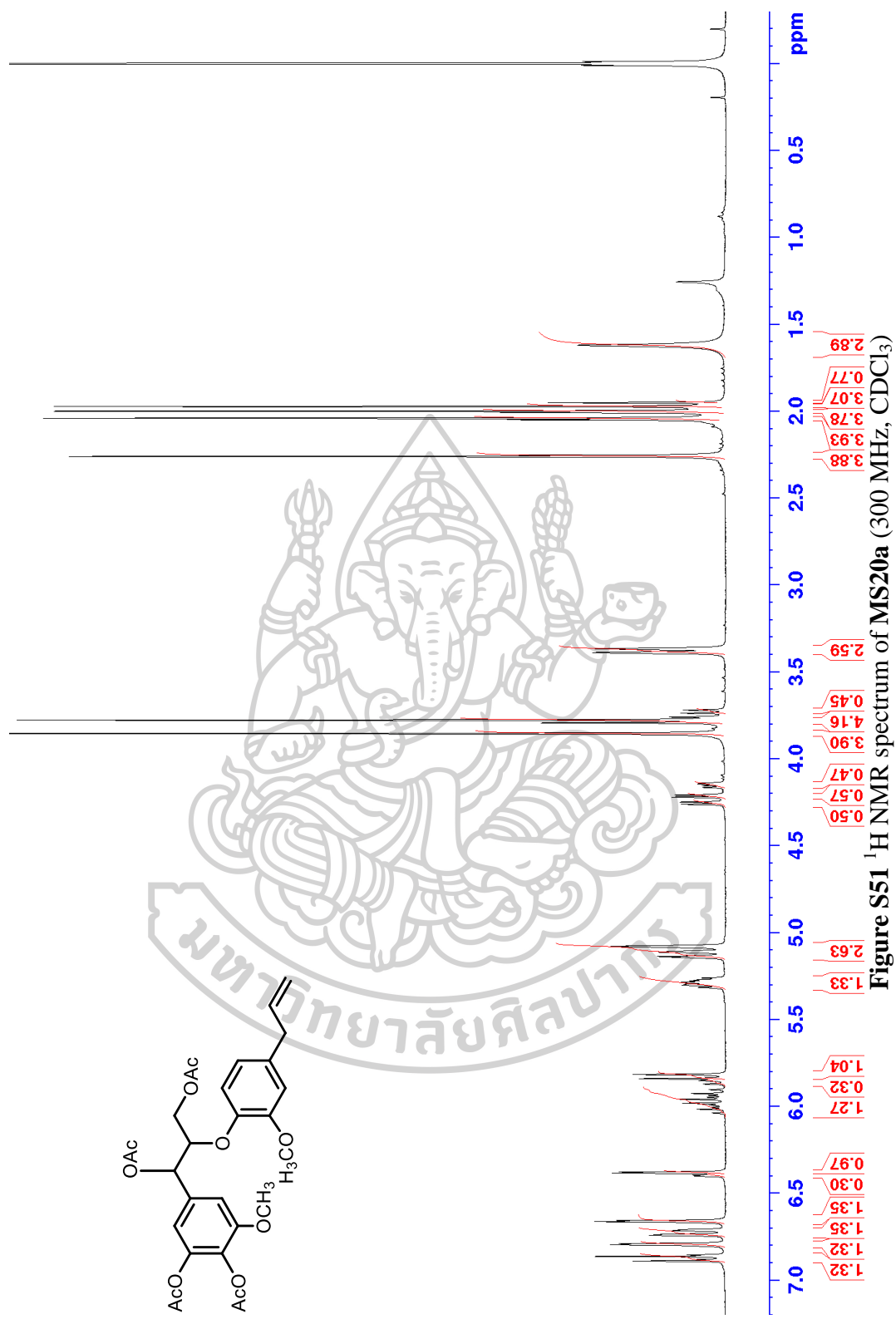
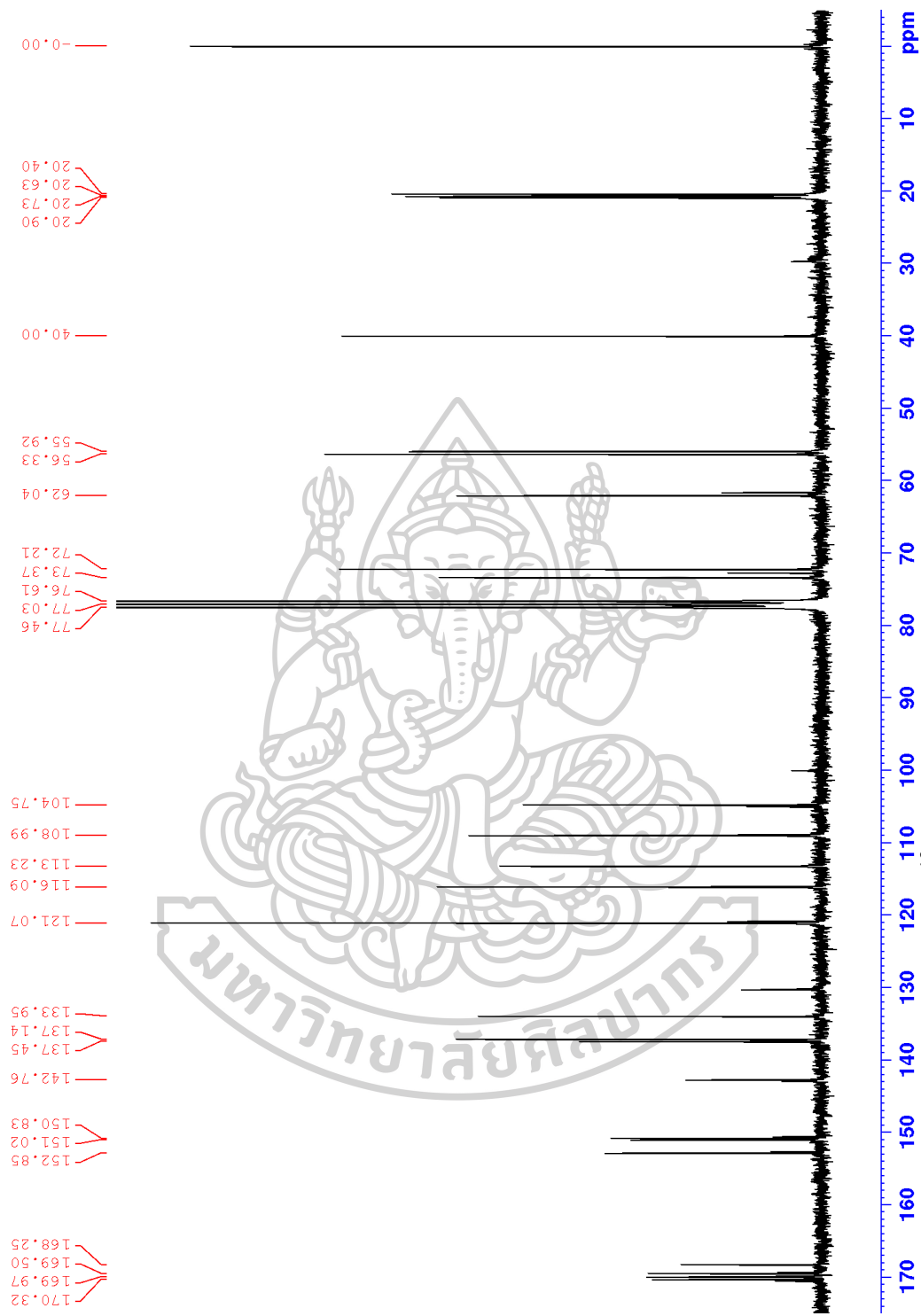


Figure S51 ¹H NMR spectrum of MS20a (300 MHz, CDCl₃)



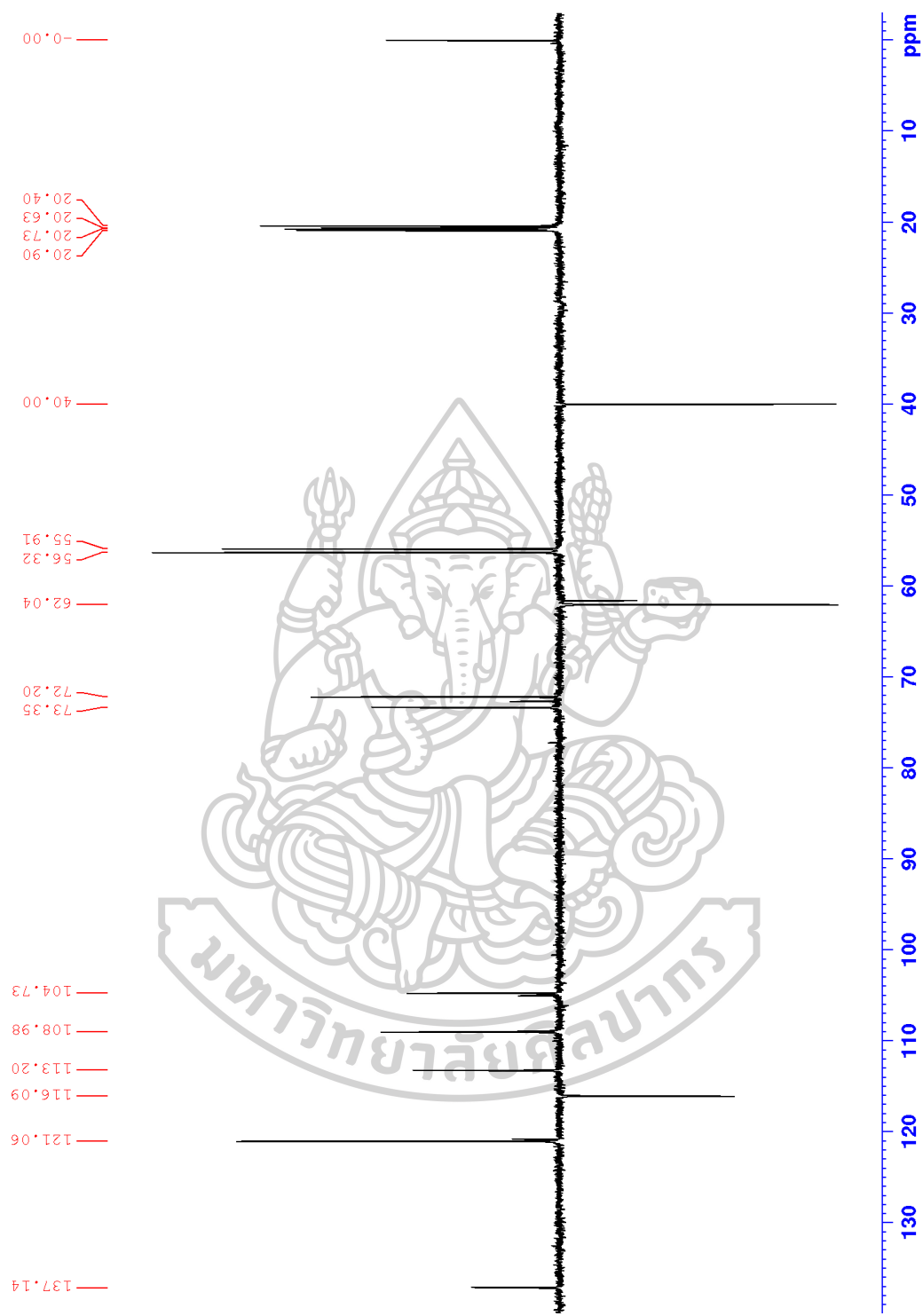


Figure S53 DEPT 135 spectrum of MS20a (75 MHz, CDCl₃)

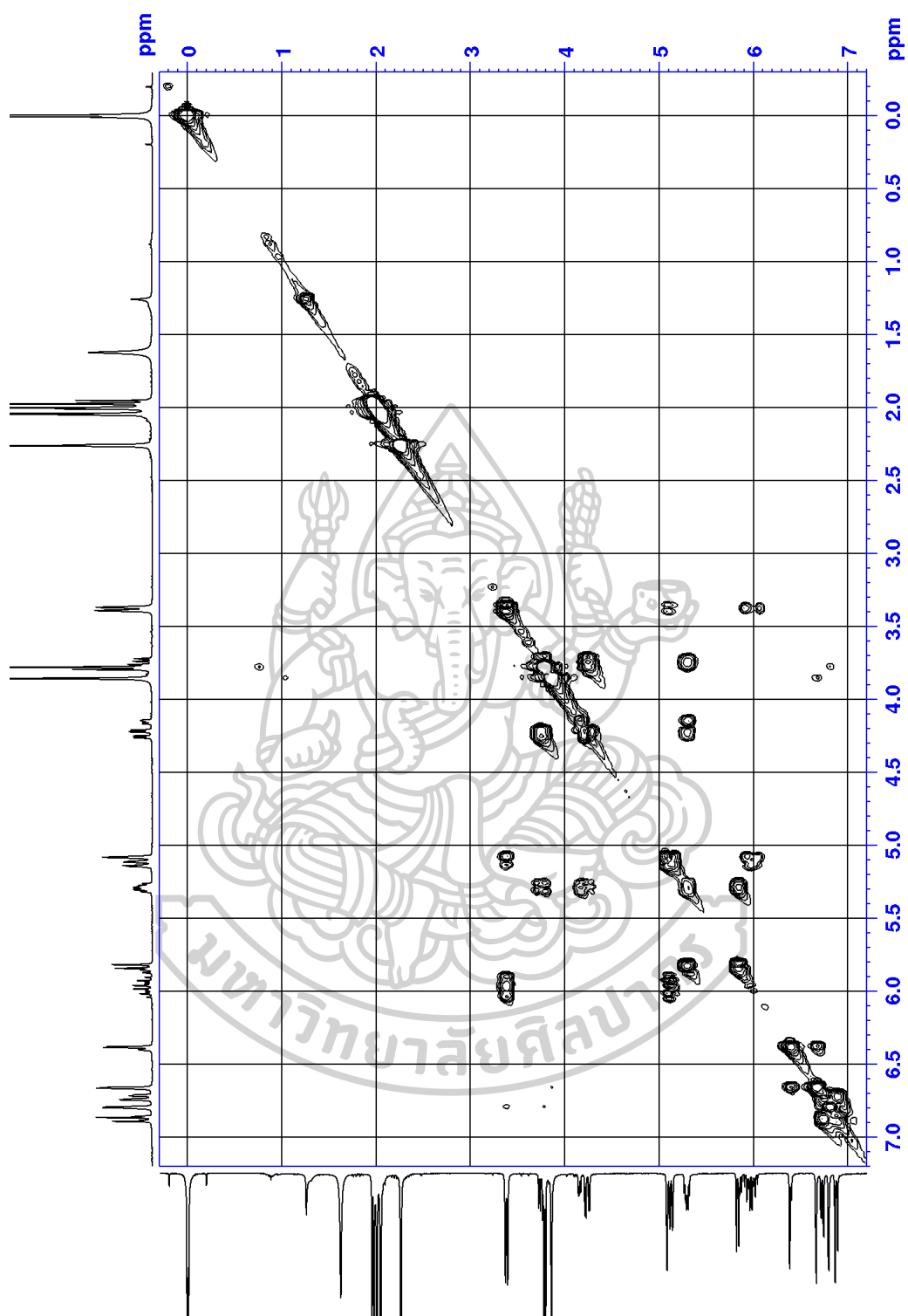


Figure S54 COSY spectrum of MS20a (300MHz, CDCl₃)

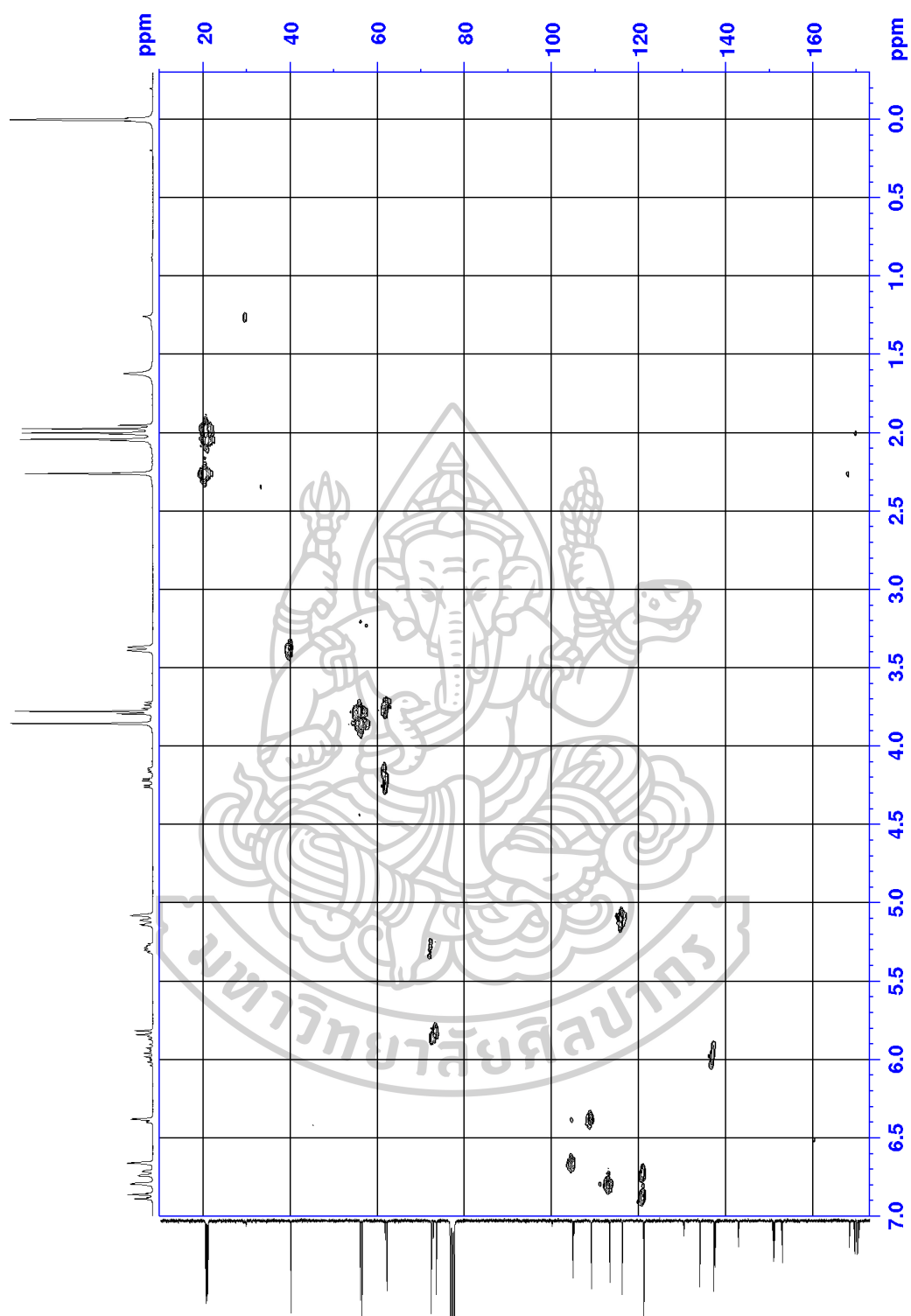


Figure S55 HMQC spectrum of MS20a

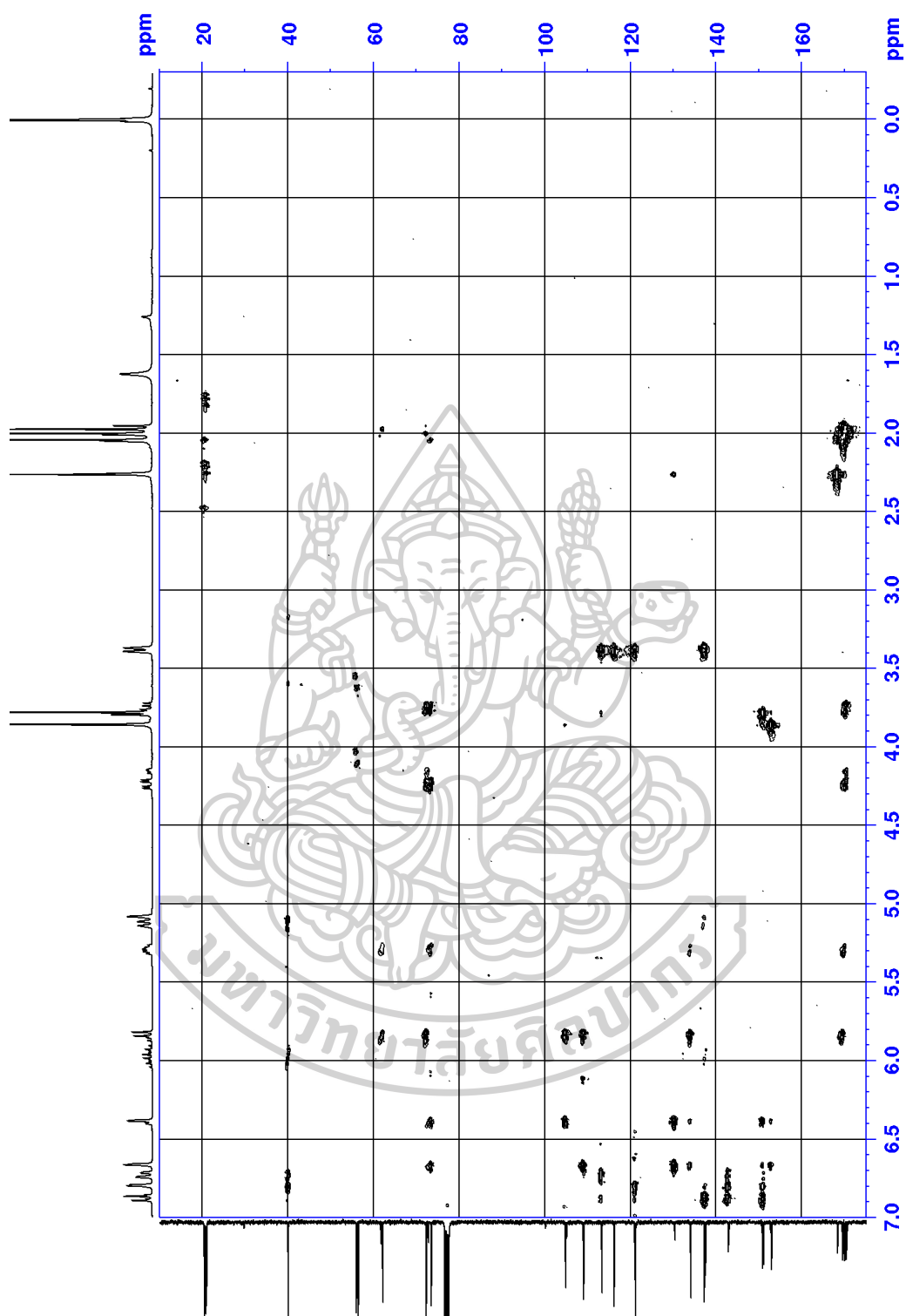
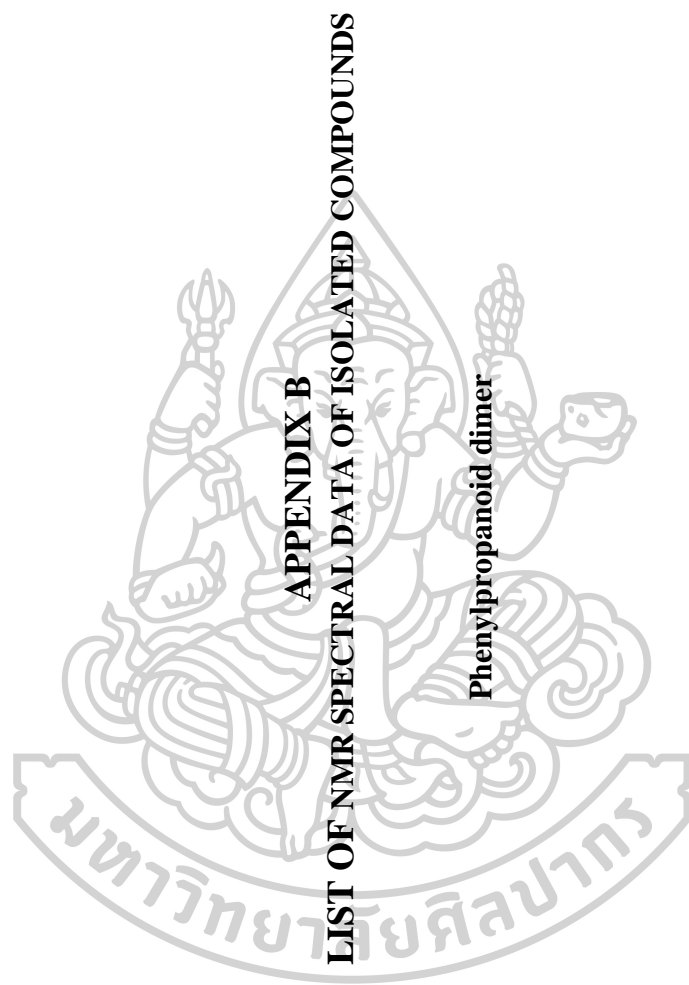


Figure S56 HMBC spectrum of MS20a



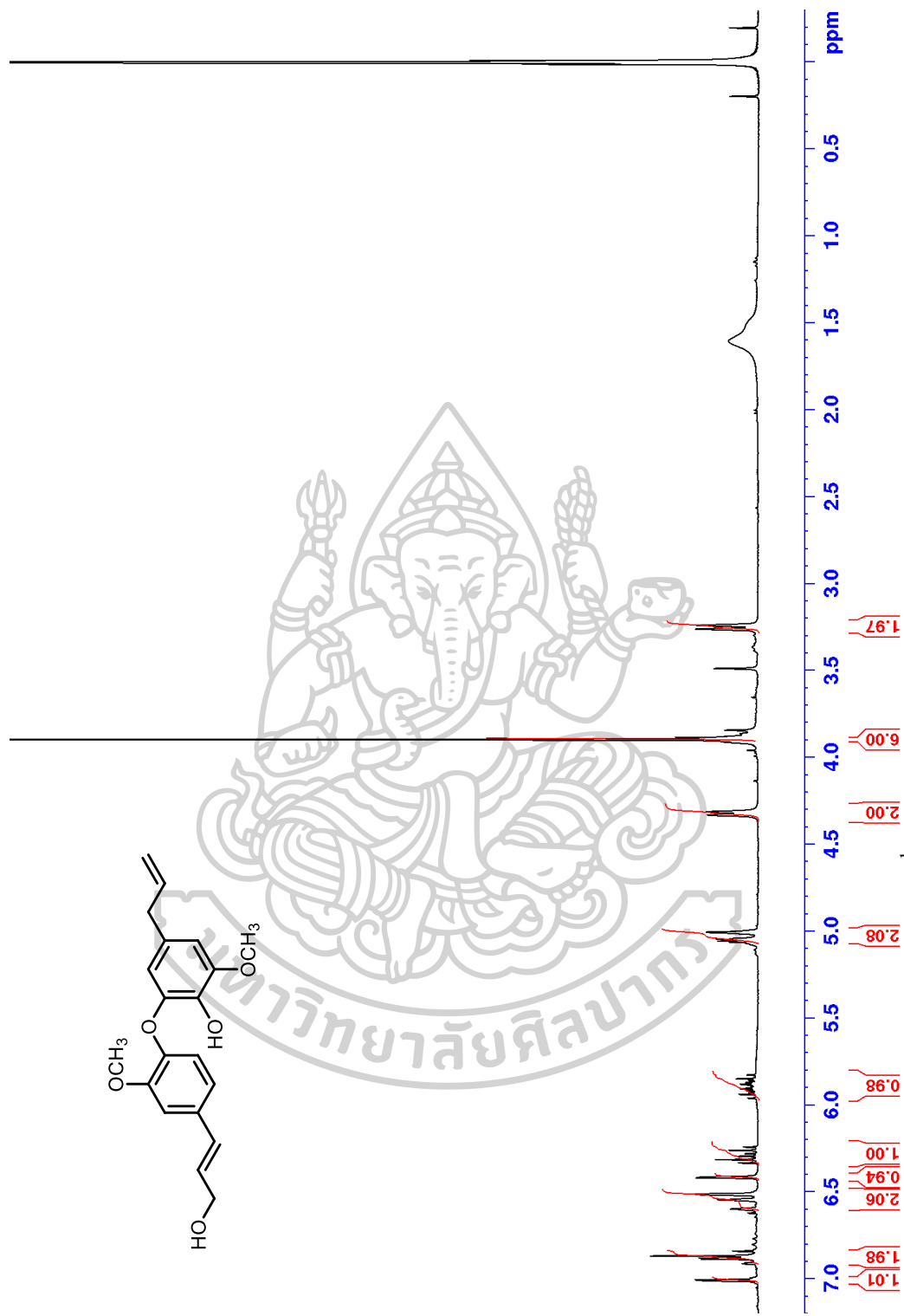


Figure S57 ^1H NMR spectrum of MS18 (300 MHz, CDCl_3)

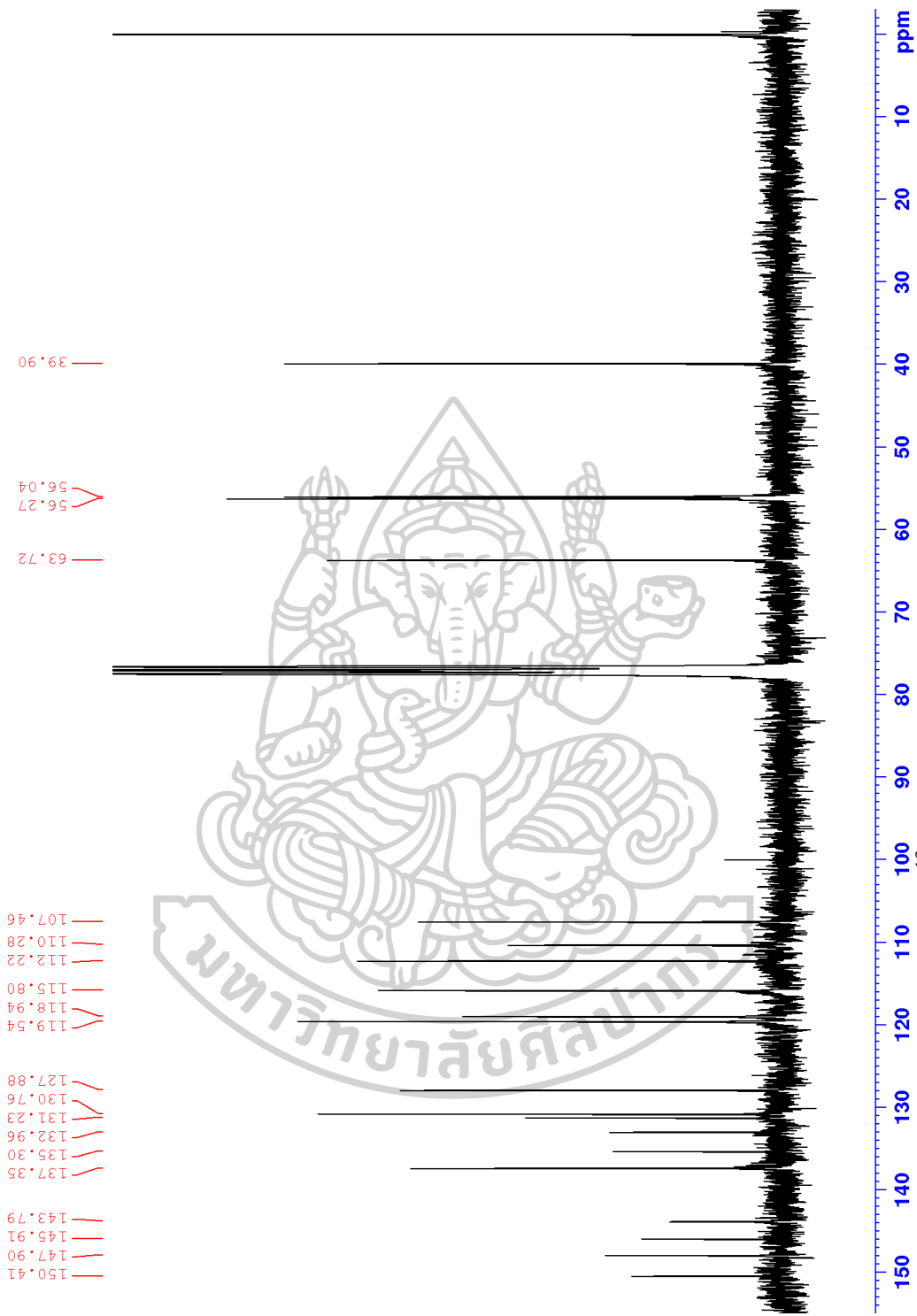


Figure 58 ^{13}C NMR spectrum of MS18 (75 MHz, CDCl_3)

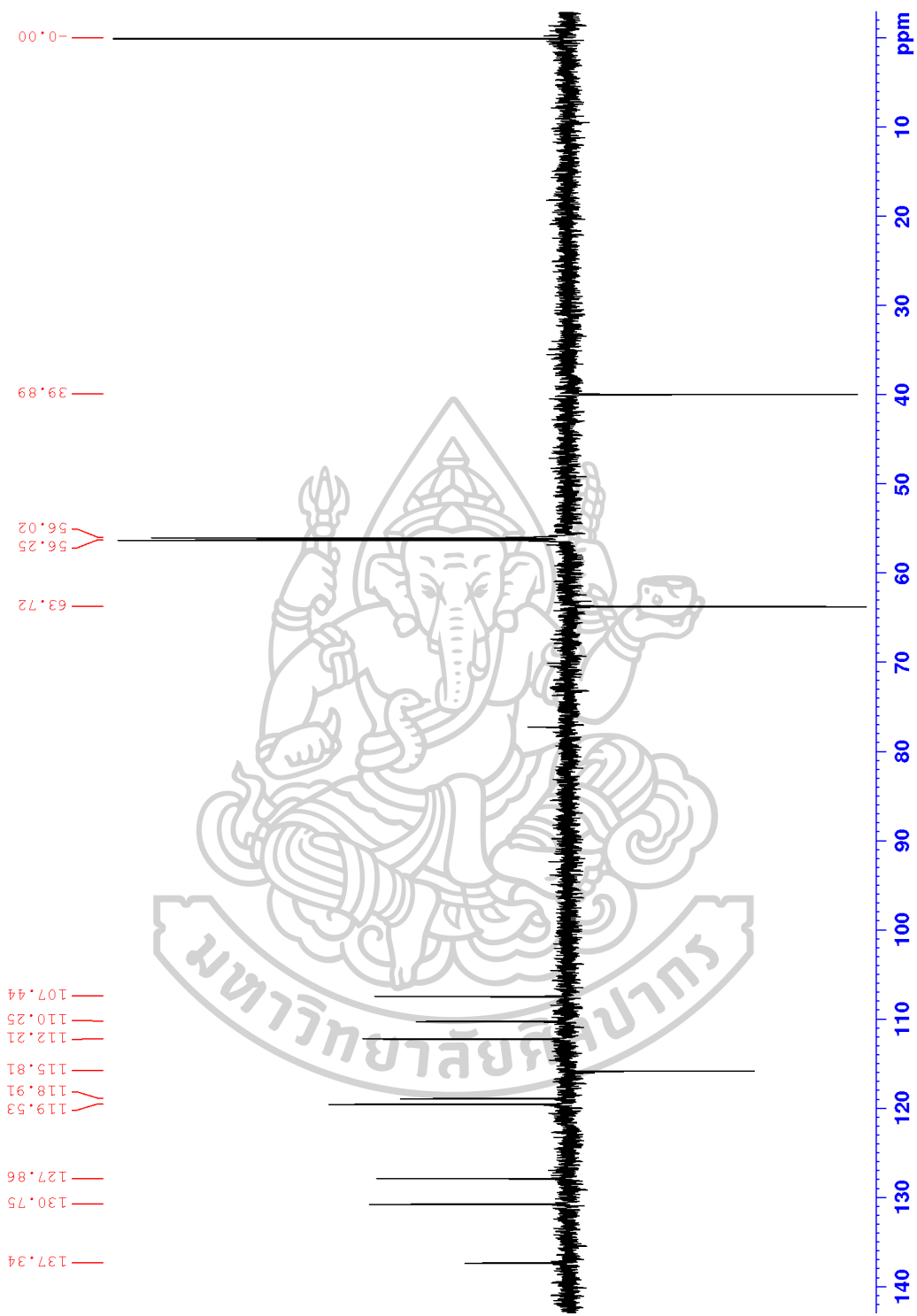


Figure 59 DEPT 135 spectrum of MS18 (75 MHz, CDCl₃)

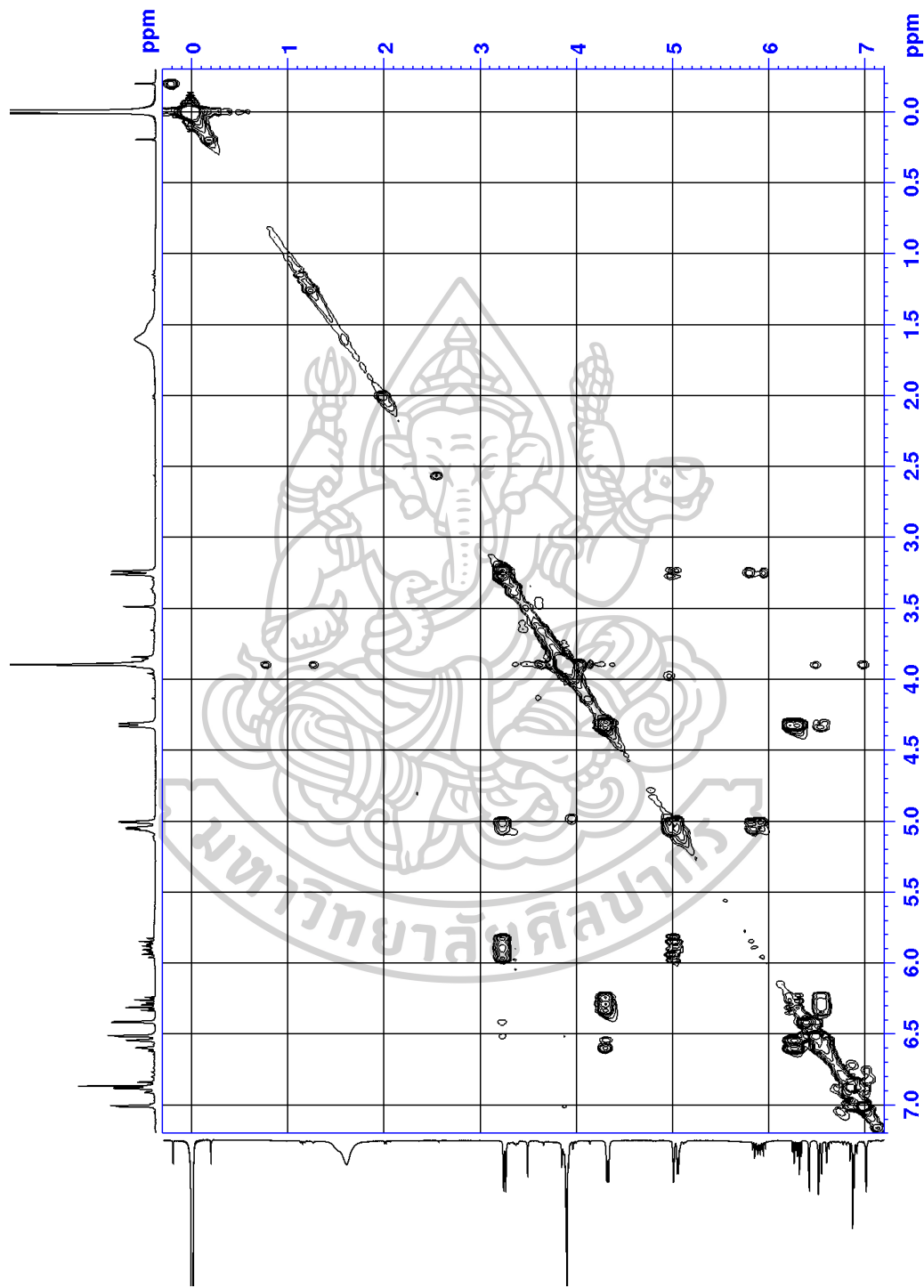


Figure S60 COSY spectrum of MS18 (300 MHz, CDCl₃)

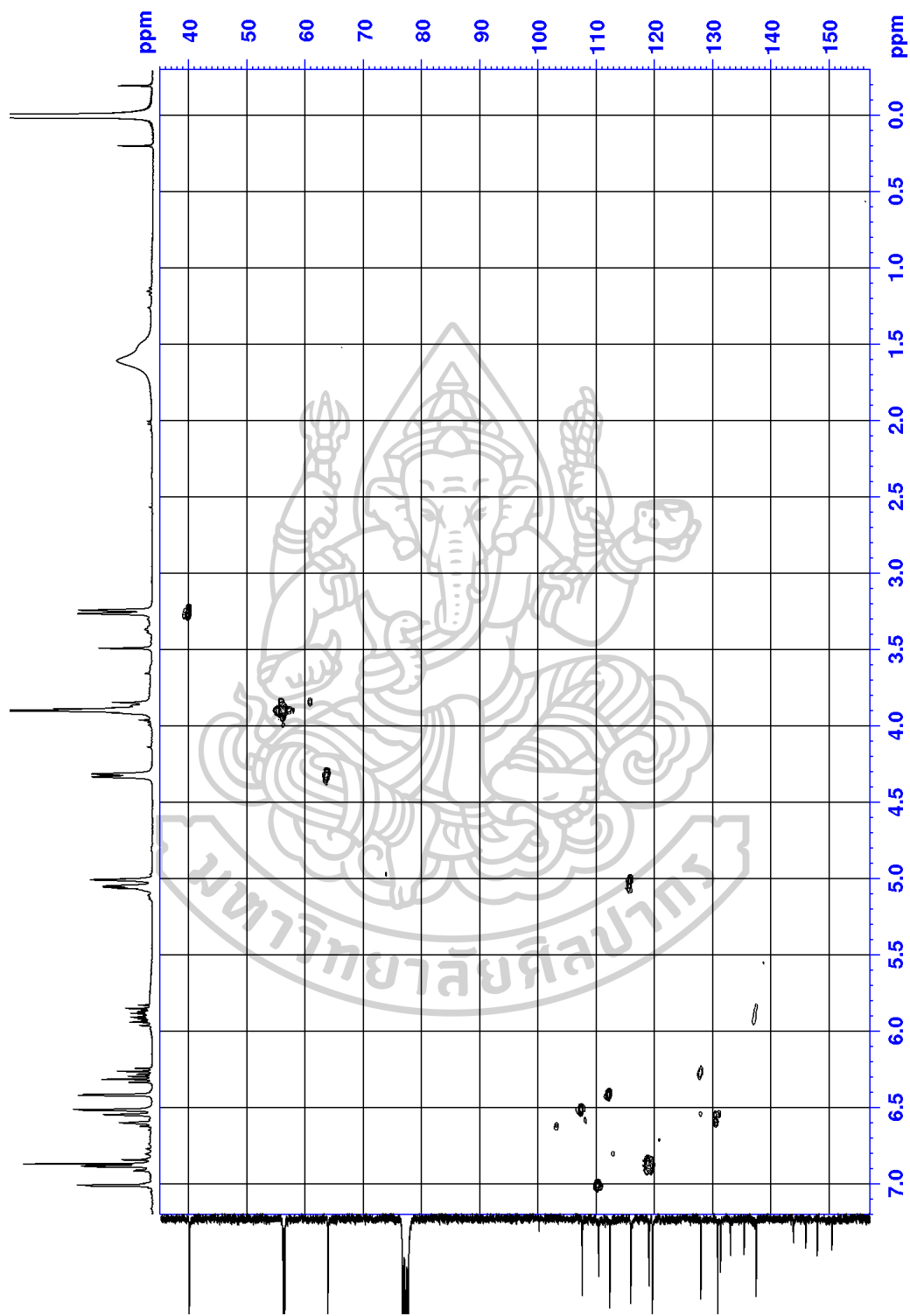


Figure S61 HMQC spectrum of MS18

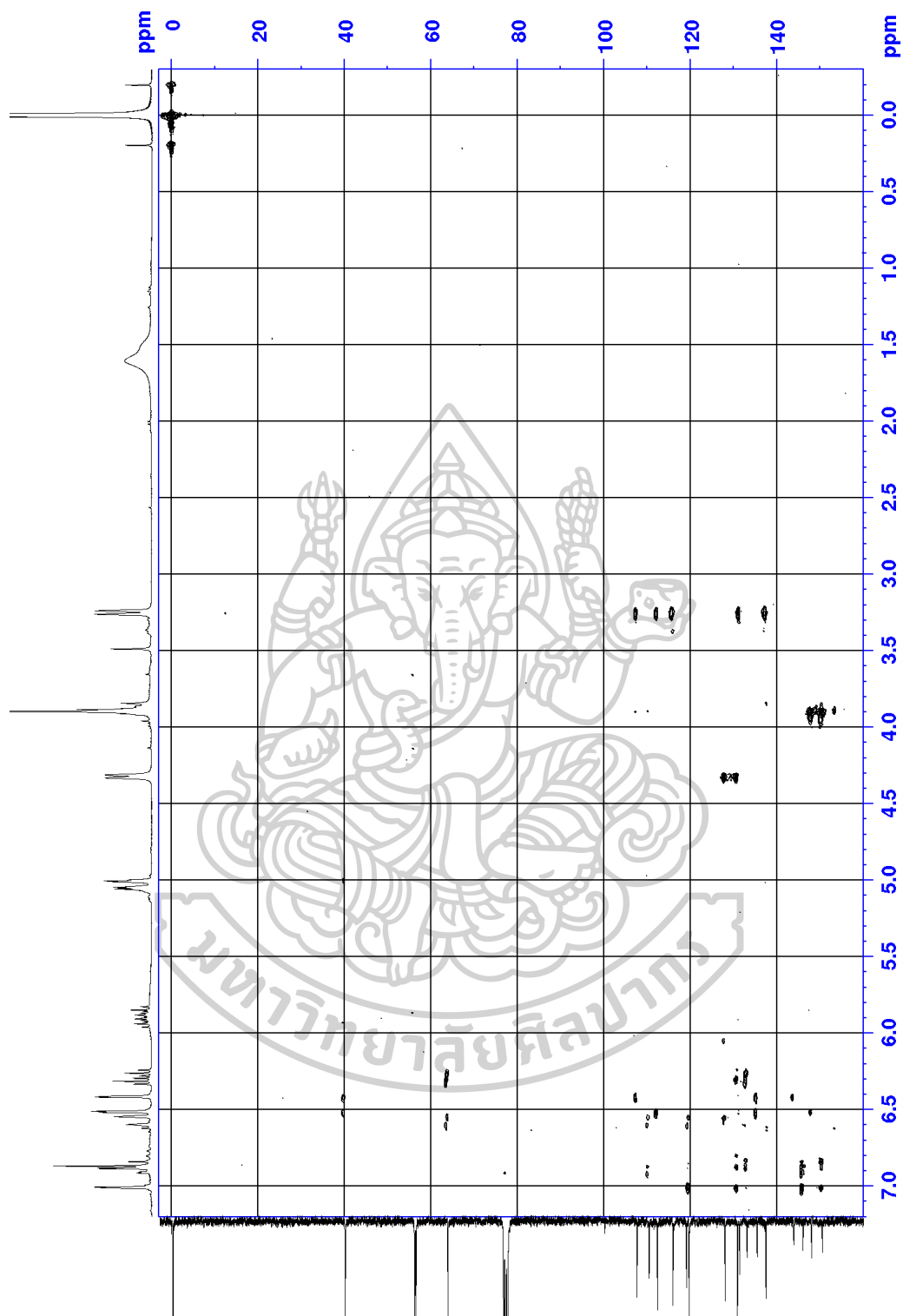
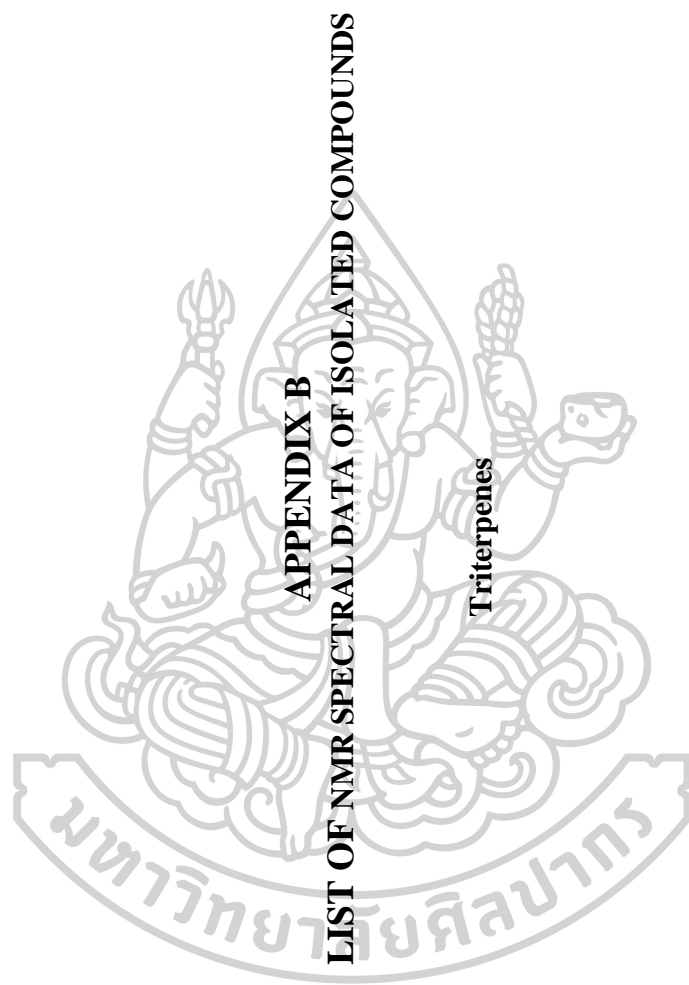


Figure S62 HMBC spectrum of MS18



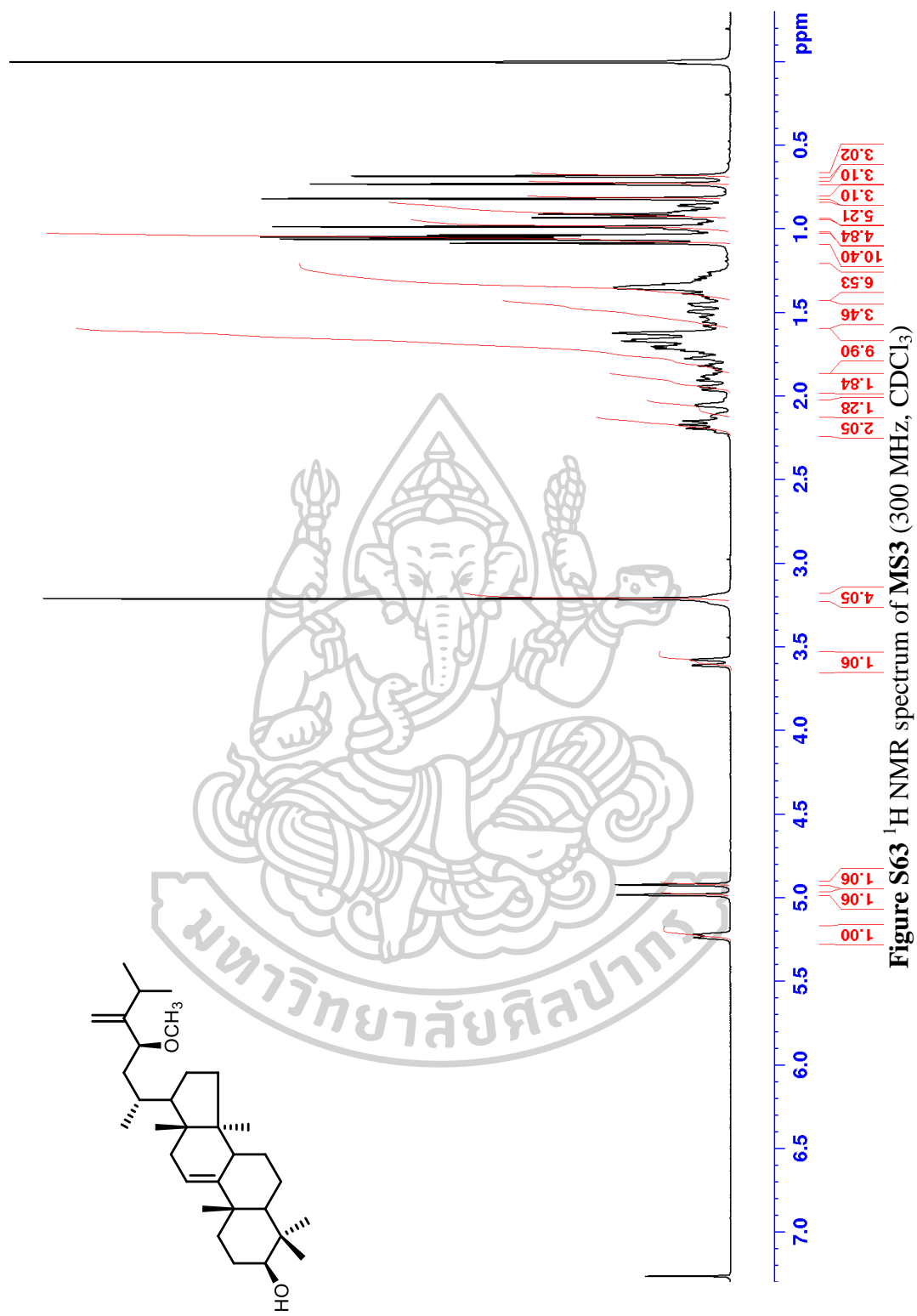


Figure S63 ^1H NMR spectrum of MS3 (300 MHz, CDCl_3)

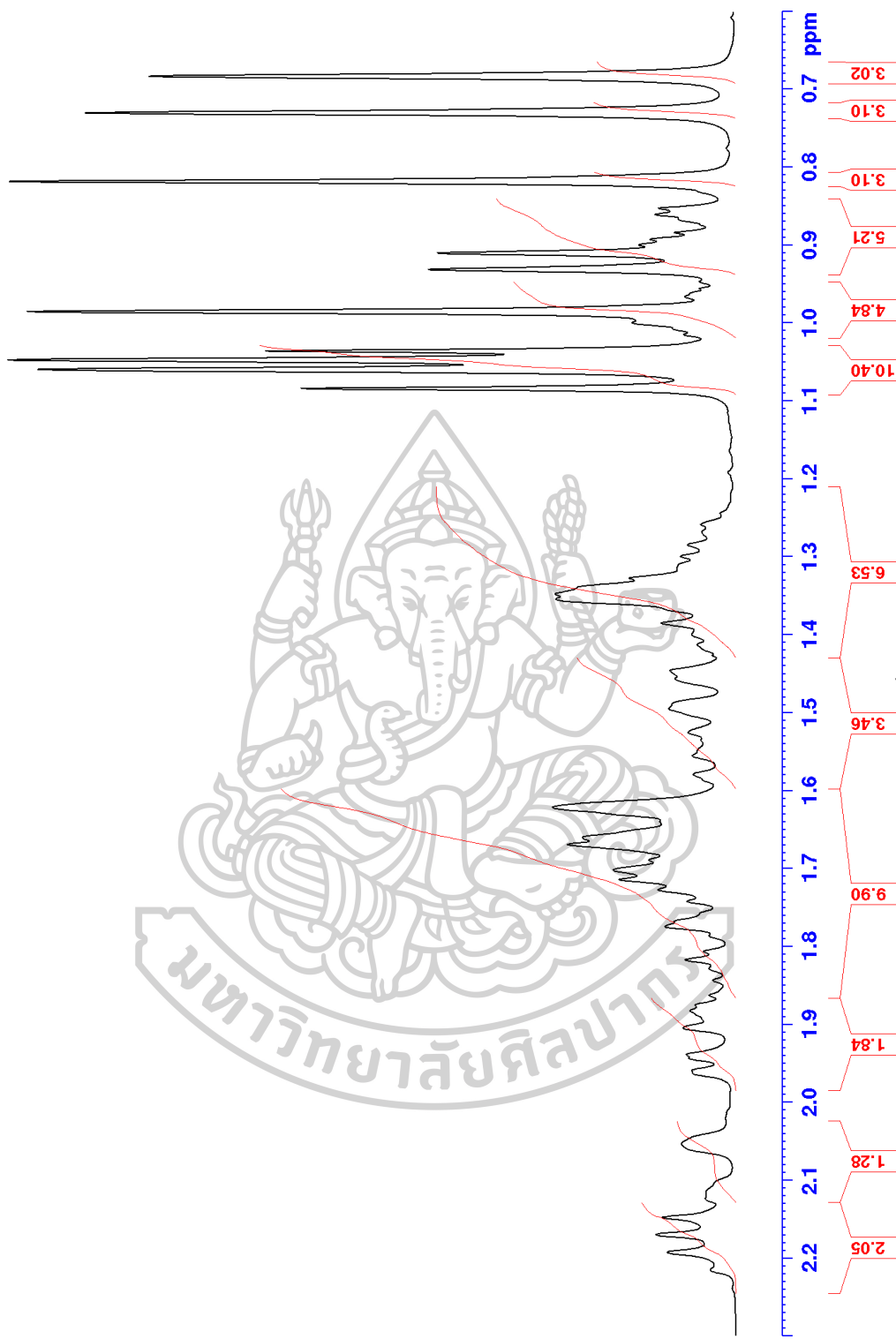


Figure S64 Zoom of the ¹H NMR spectrum of MS3

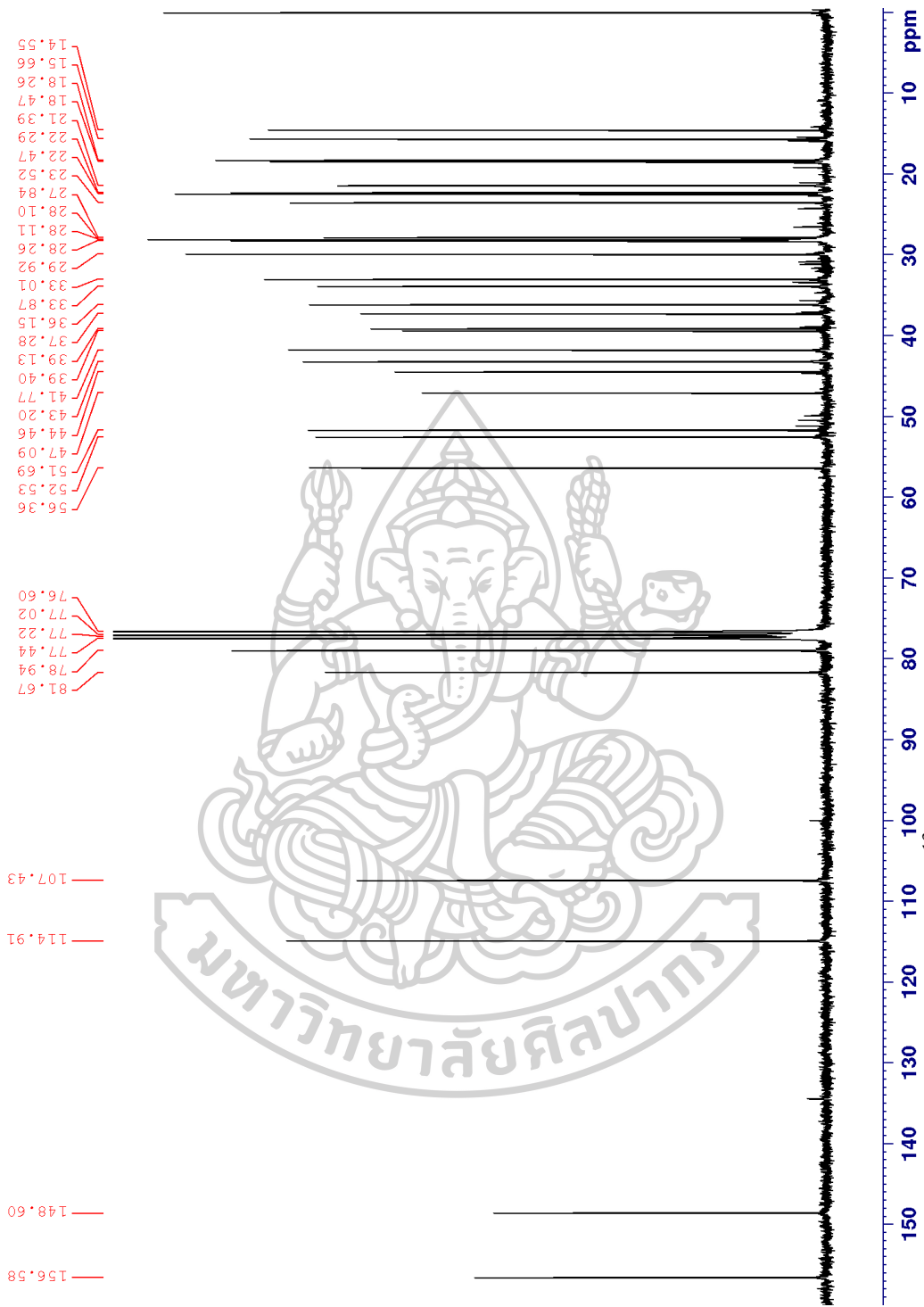


Figure S65 ^{13}C NMR spectrum of MS3 (75 MHz, CDCl_3)

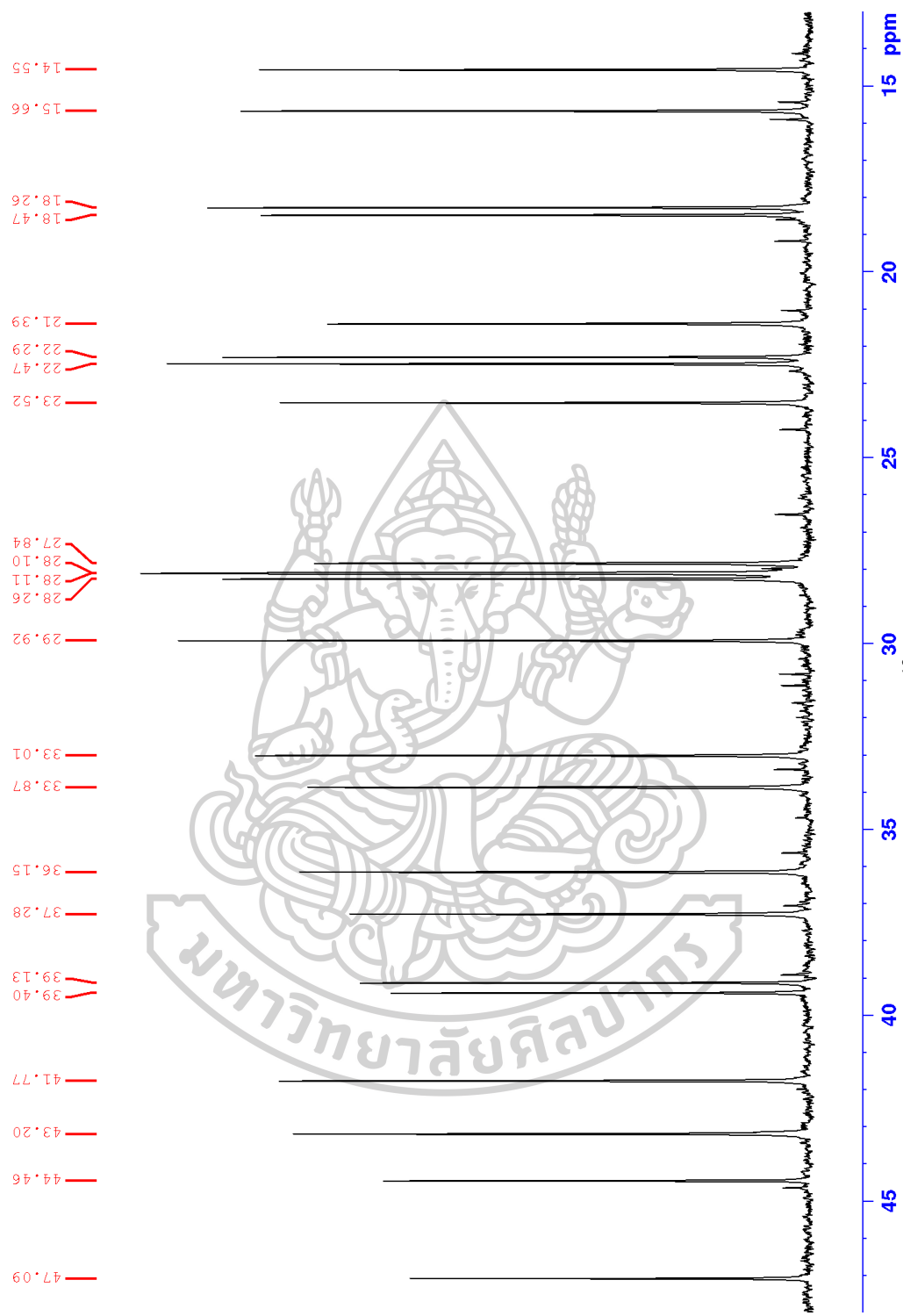


Figure S66 Zoom of the ^{13}C NMR spectrum of MS3

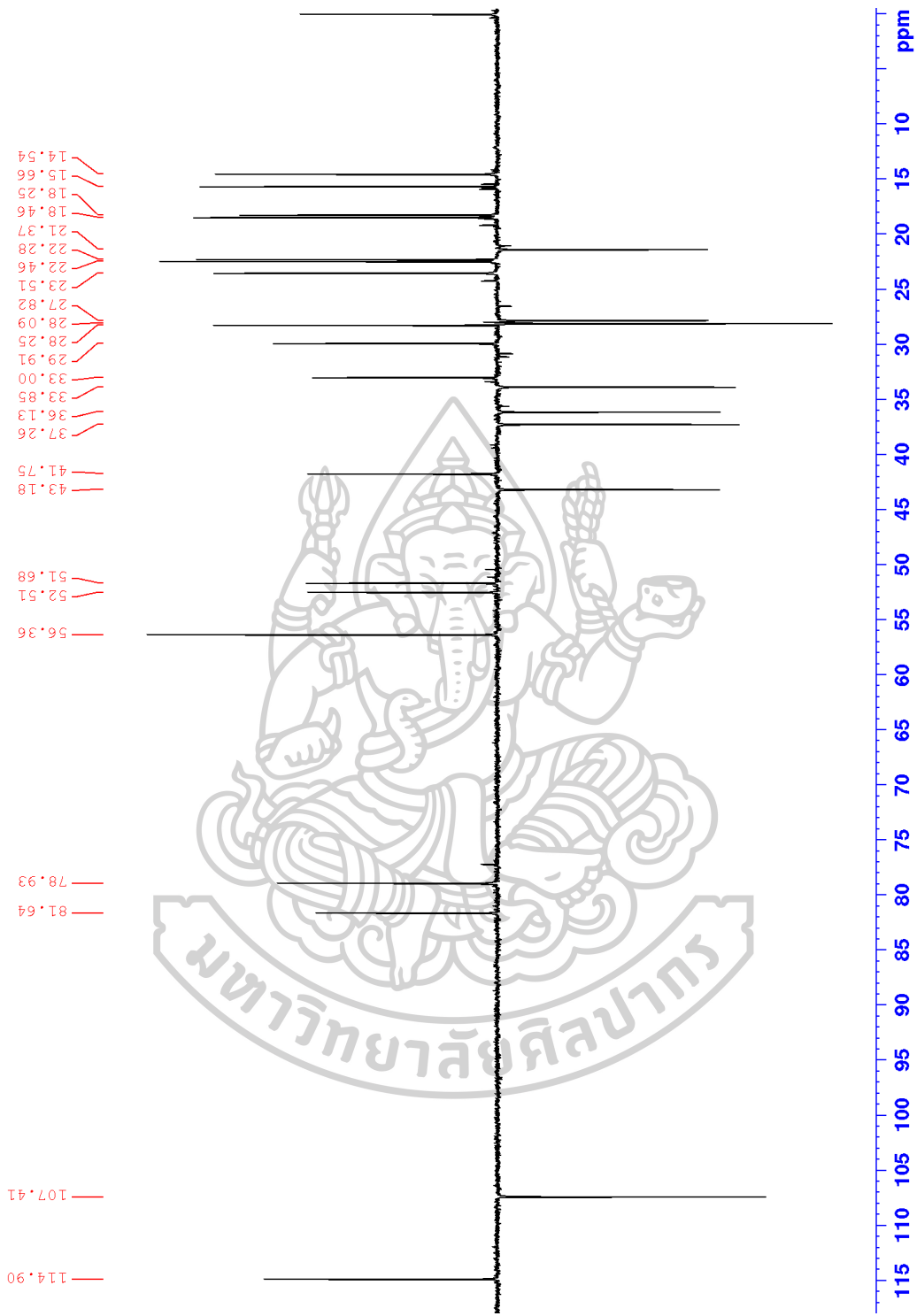


Figure S67 DEPT 135 spectrum of MS3 (75 MHz, CDCl₃)

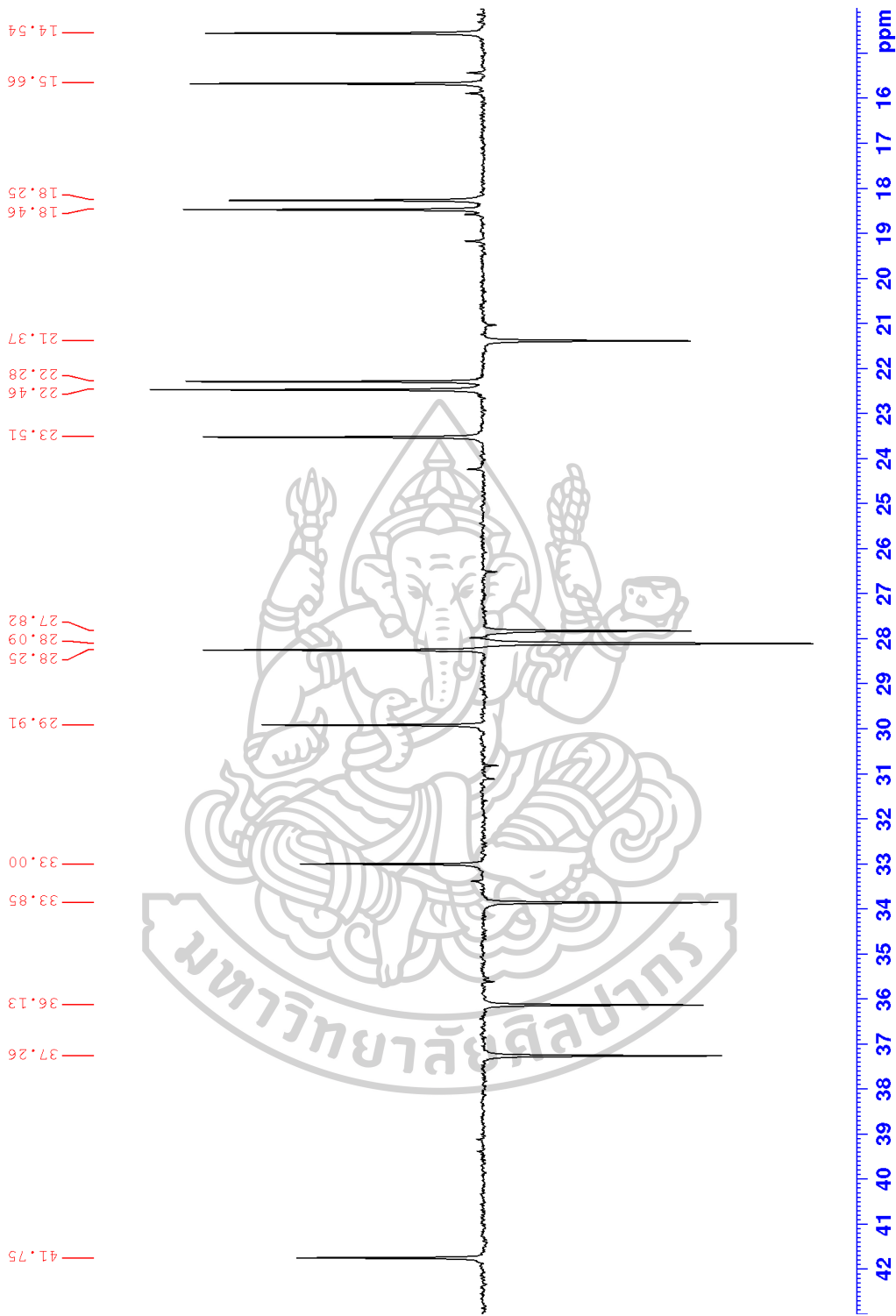


Figure S68 Zoom of the DEPT 135 spectrum of S68

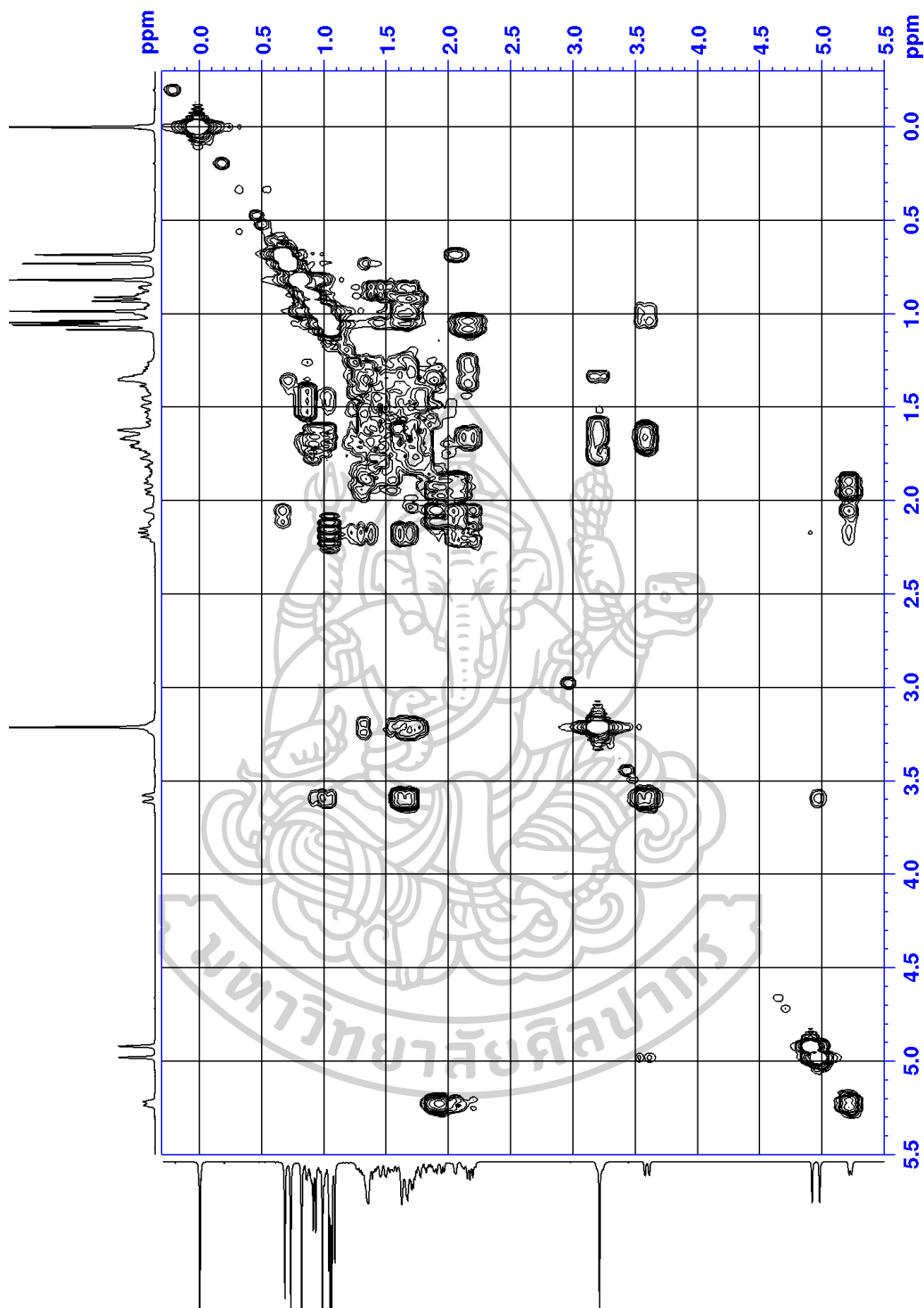


Figure S69 COSY spectrum of MS3 (300 MHz, CDCl₃)

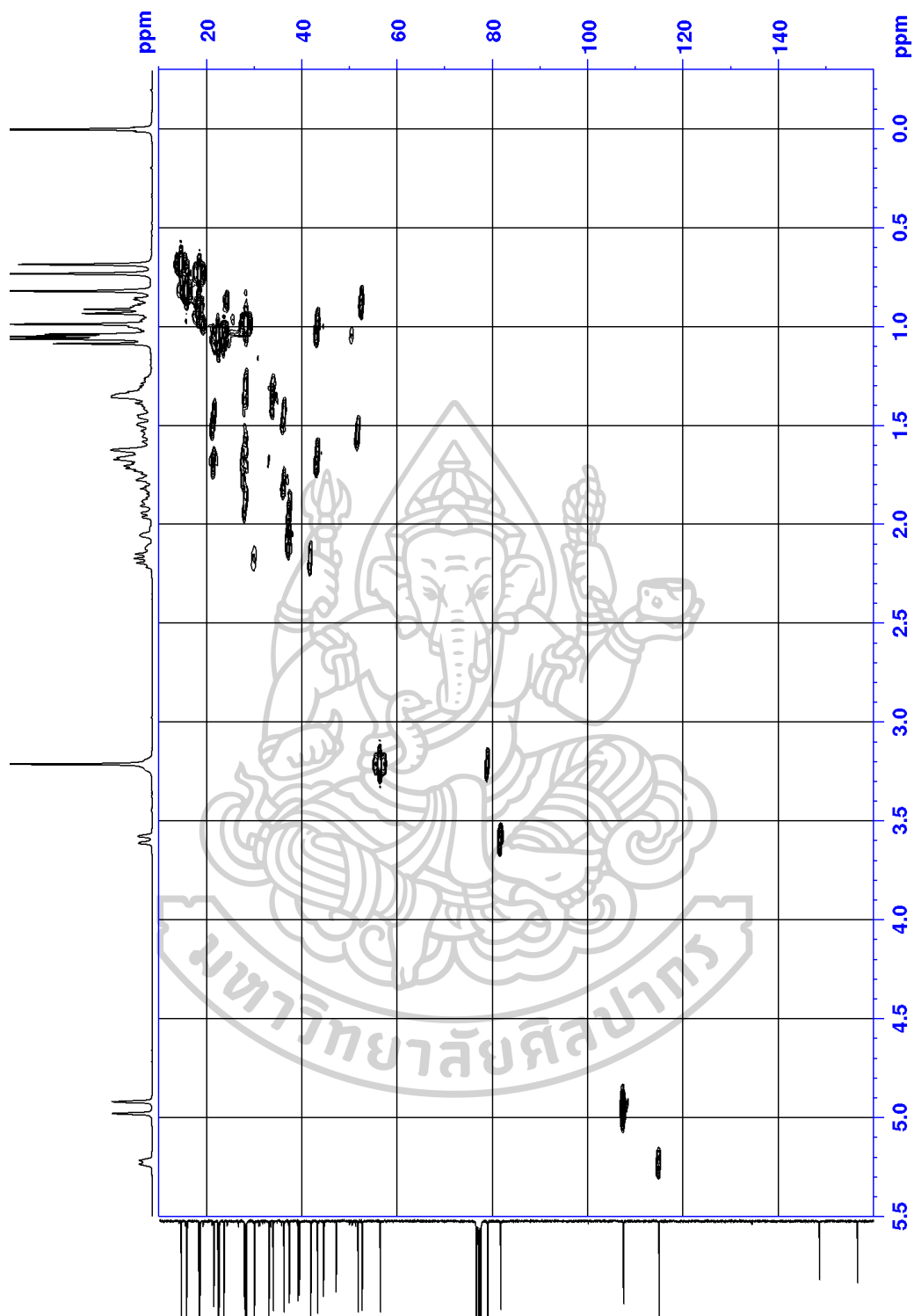


Figure S70 HMQC spectrum of MS3

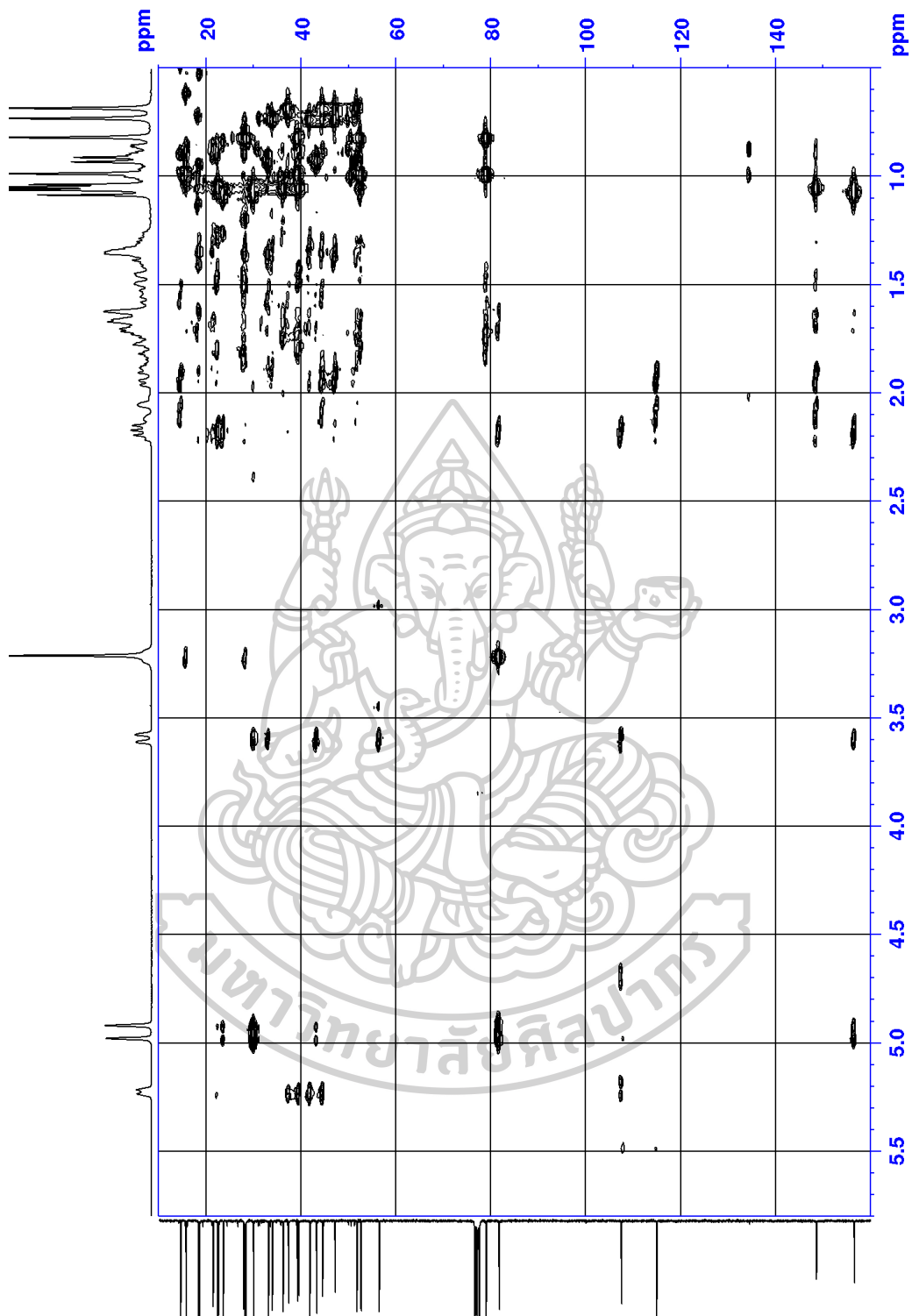
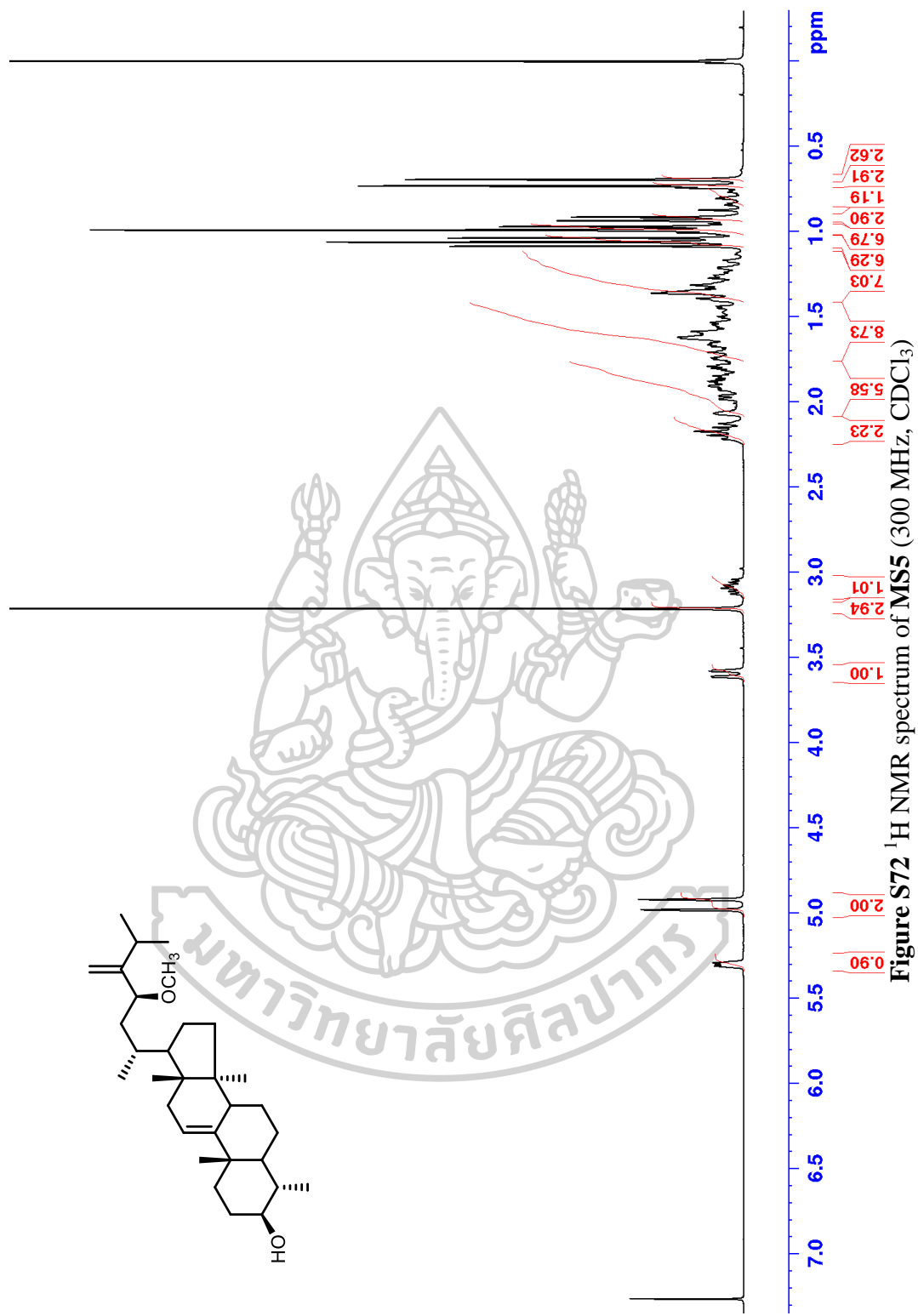


Figure S71 HMBC spectrum of MS3



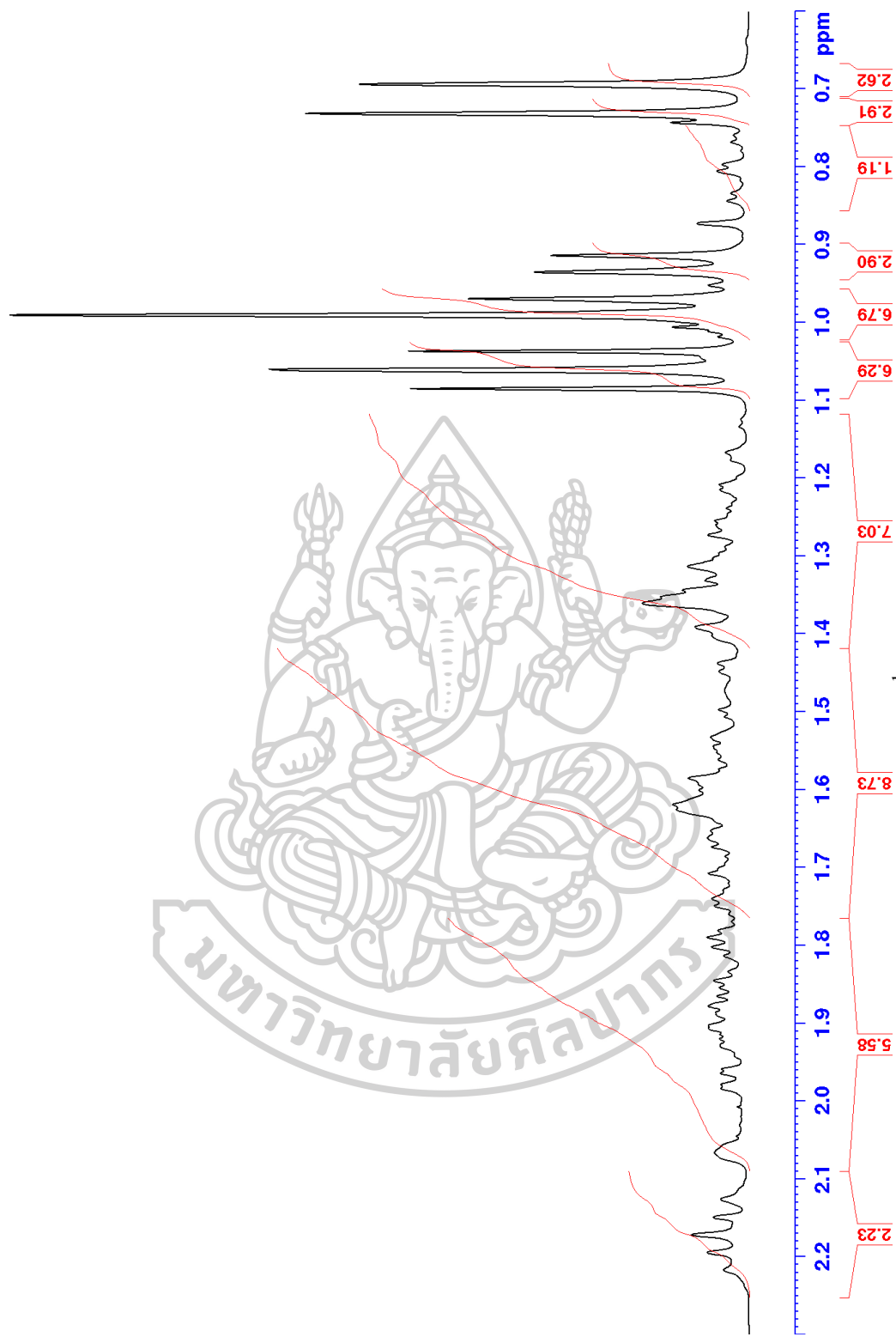


Figure S73 Zoom of the ^1H NMR spectrum of MS5

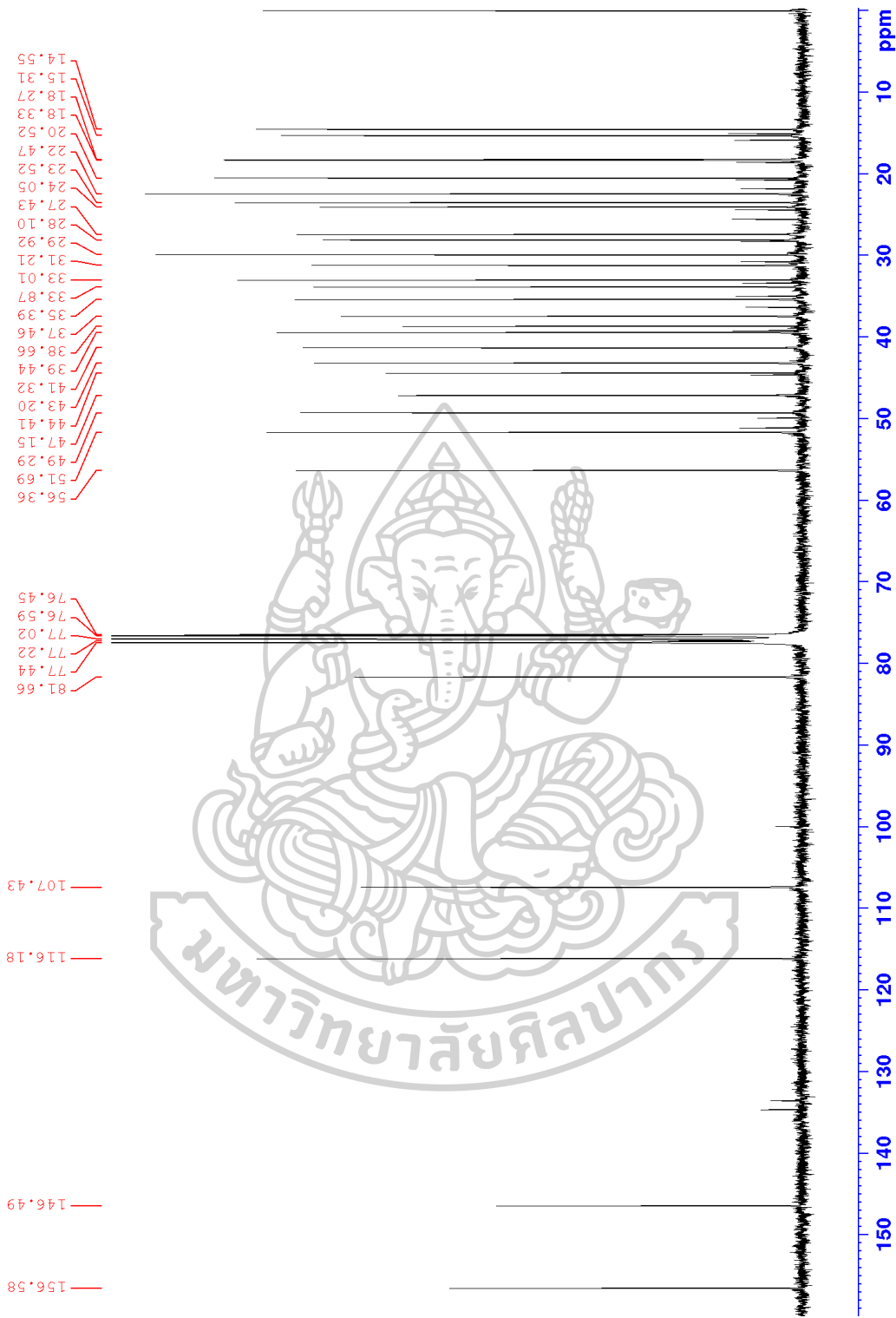


Figure S74 ¹³C NMR spectrum of MS5 (75 MHz, CDCl₃)

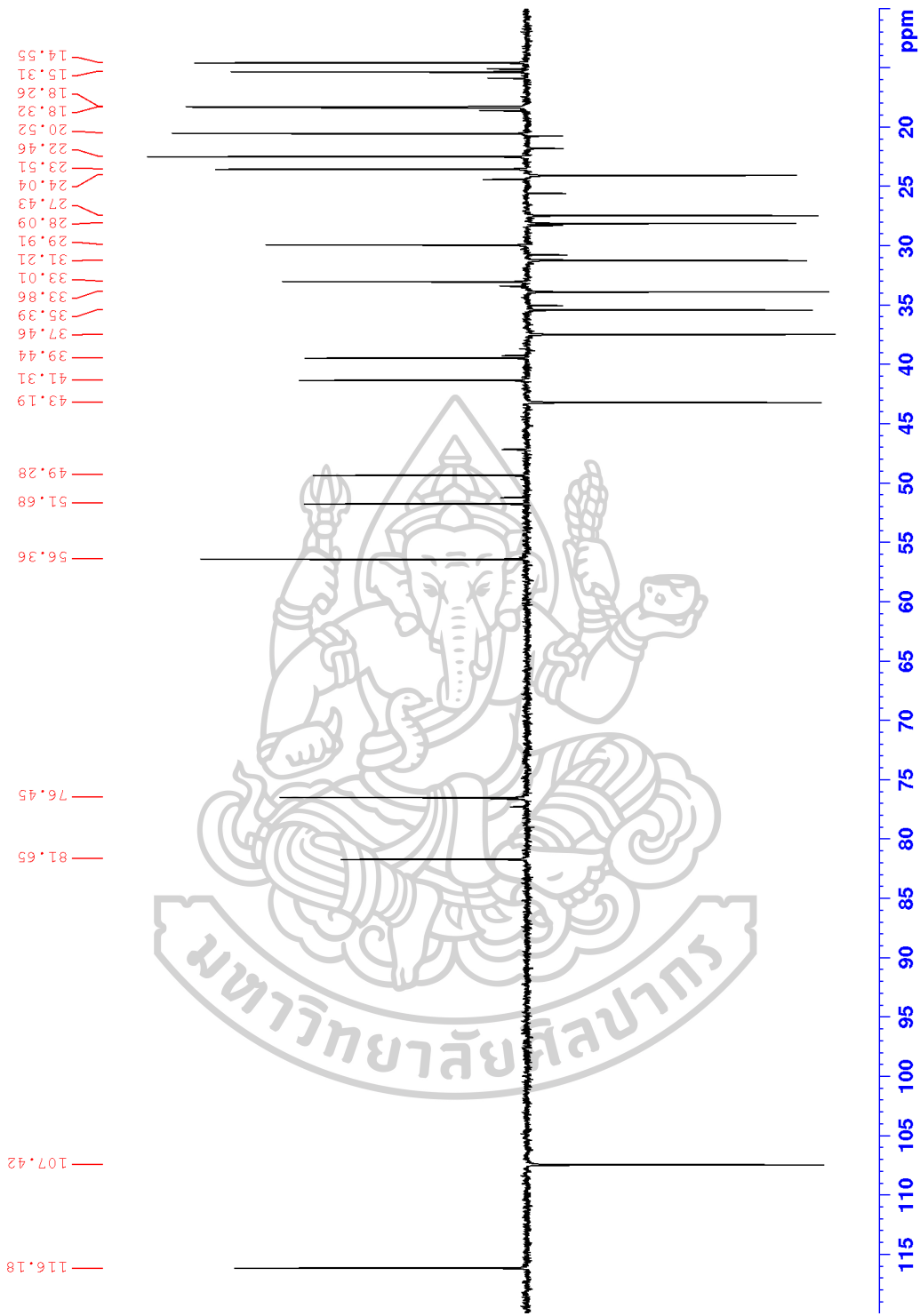


Figure S75 DEPT 135 spectrum of MS5 (75 MHz, CDCl₃)

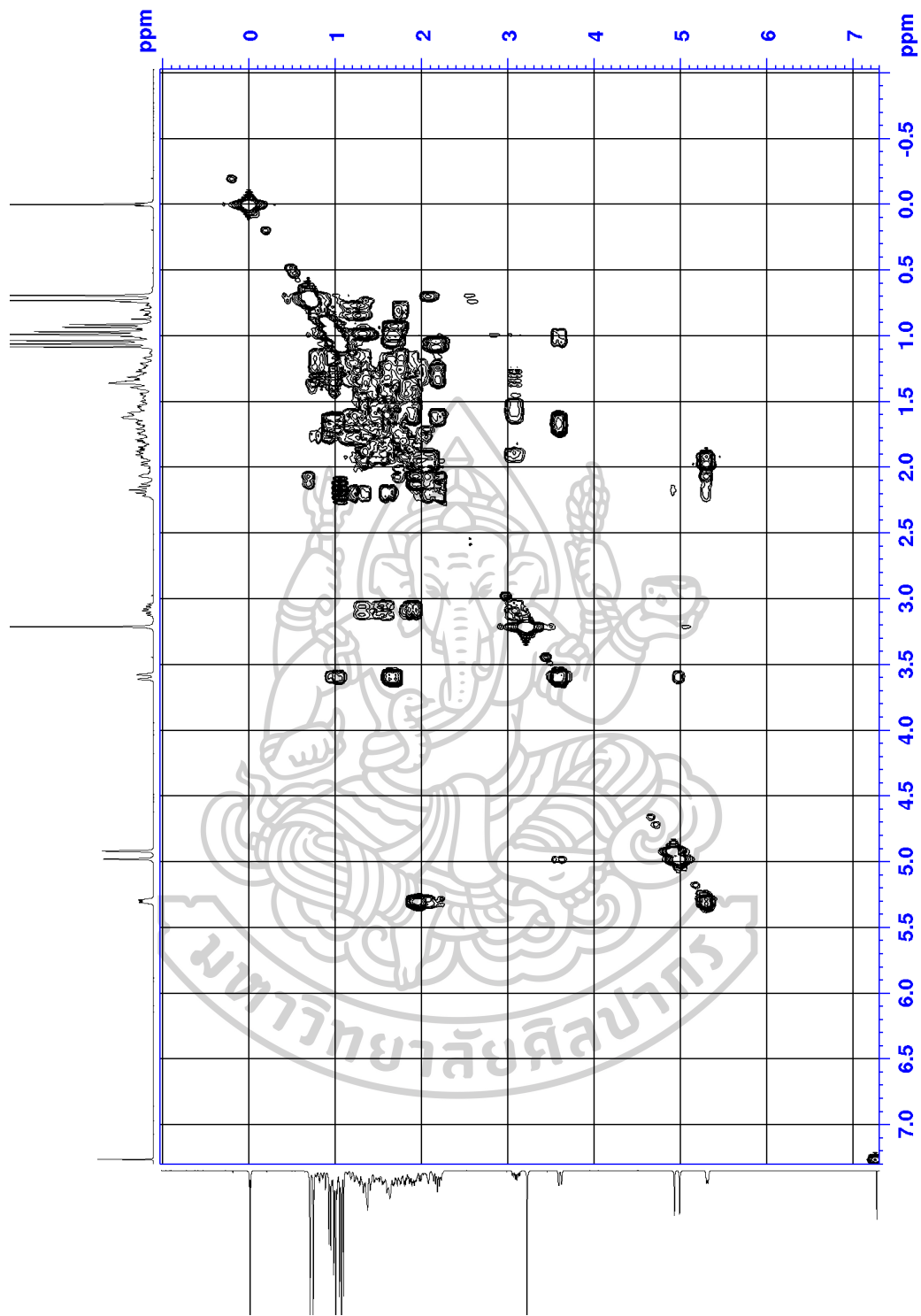


Figure S76 COSY spectrum of MS5 (300 MHz, CDCl₃)

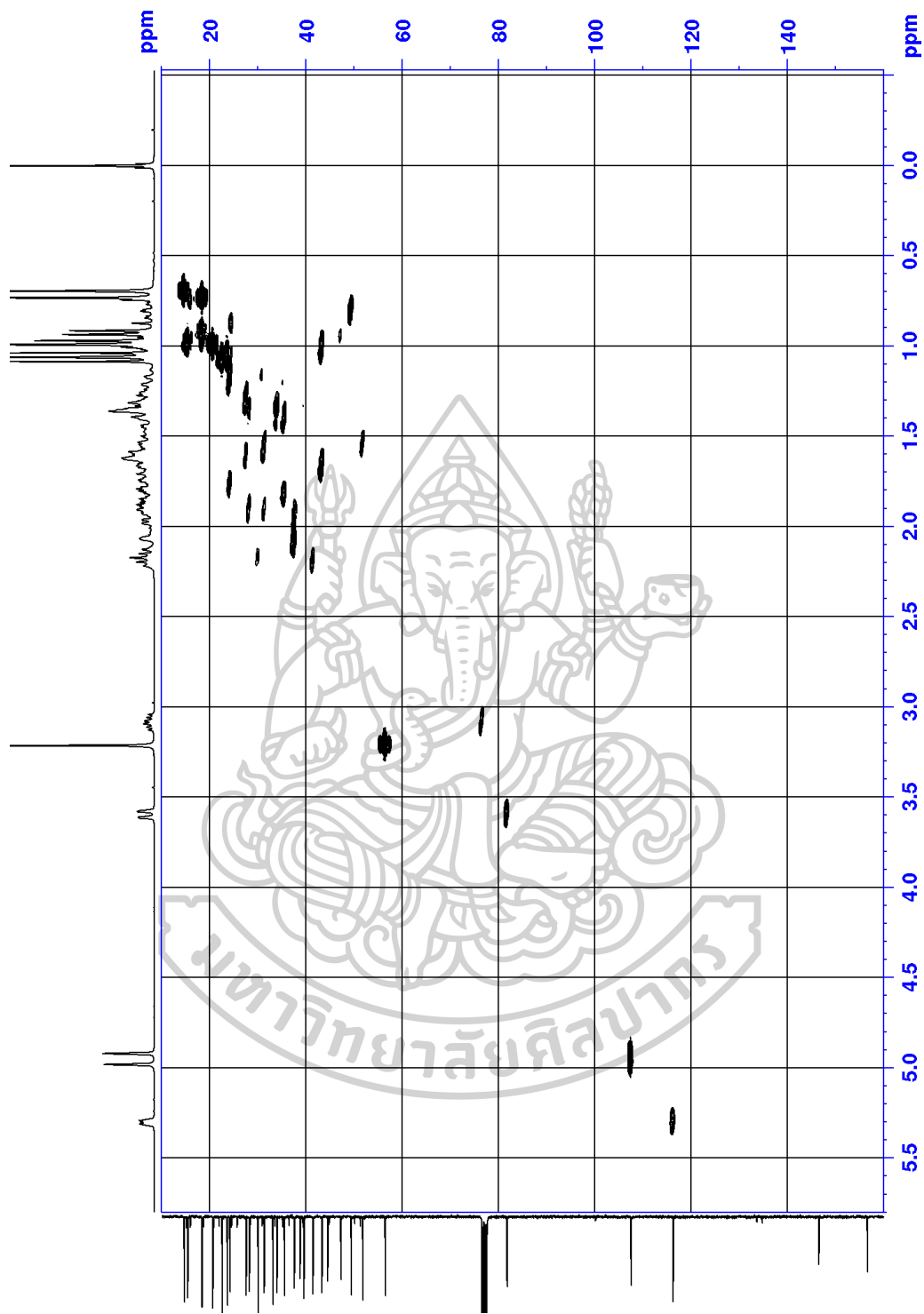


Figure S77 HMQC spectrum of MS5

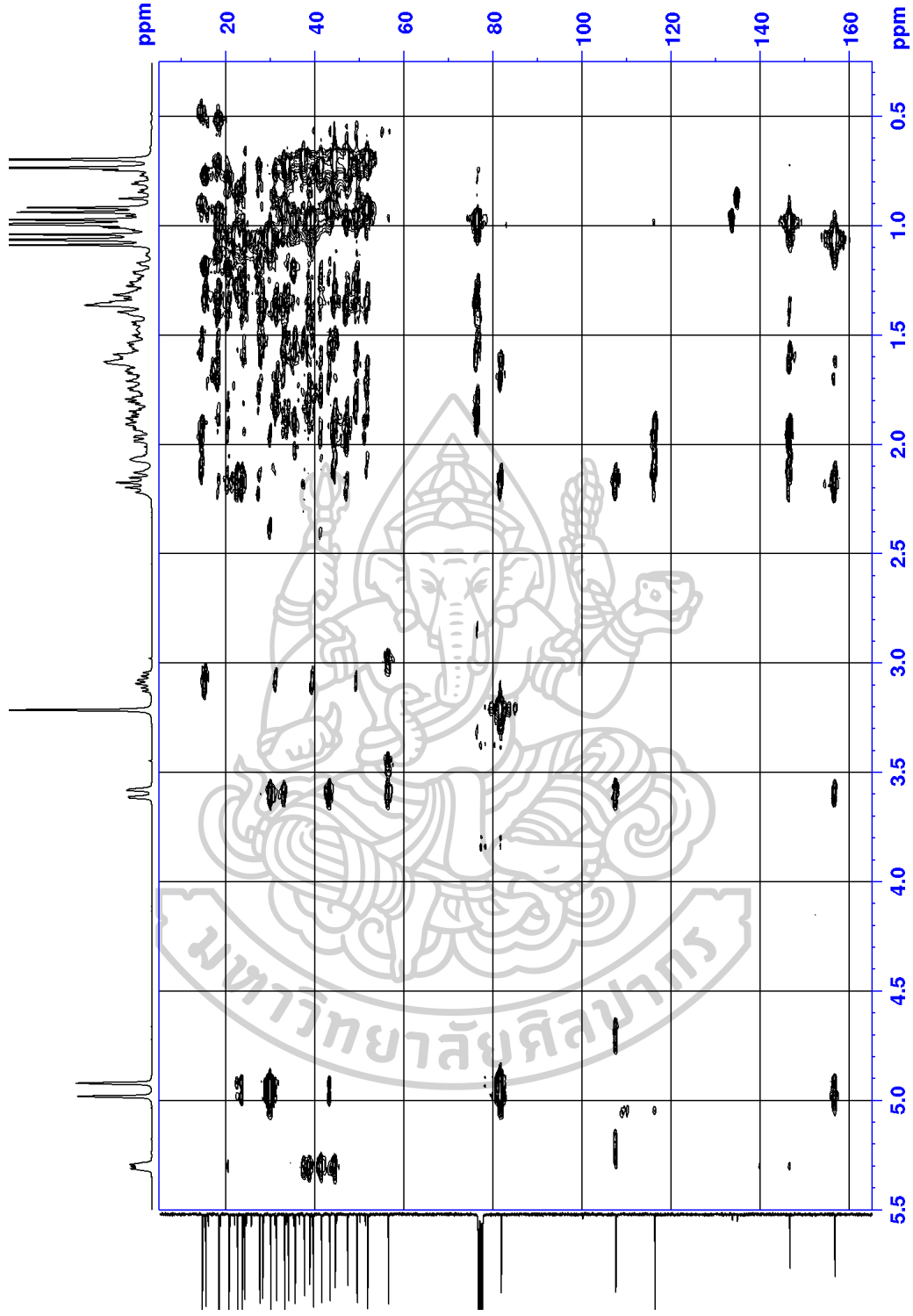
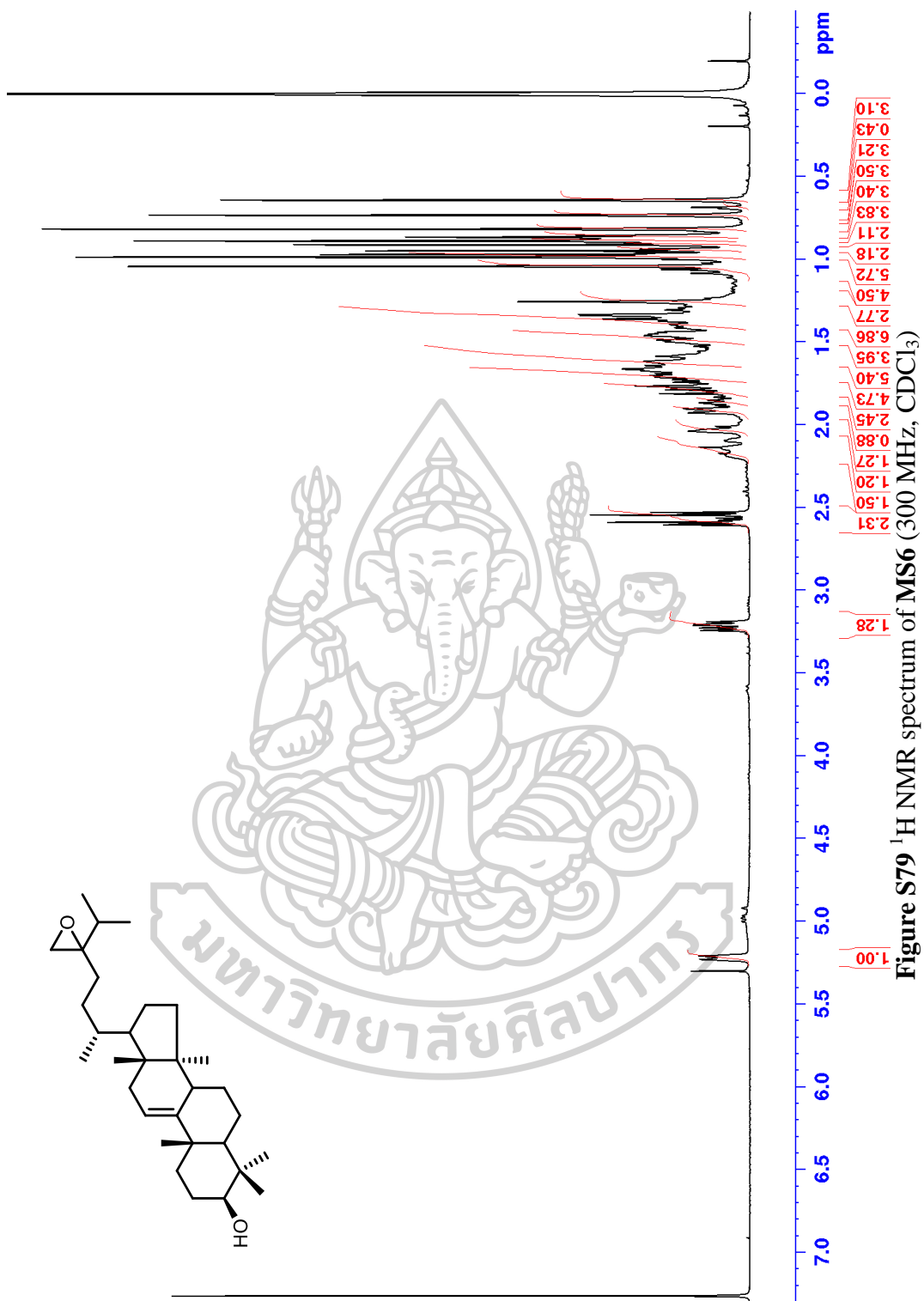


Figure S78 HMB spectrum of MS5



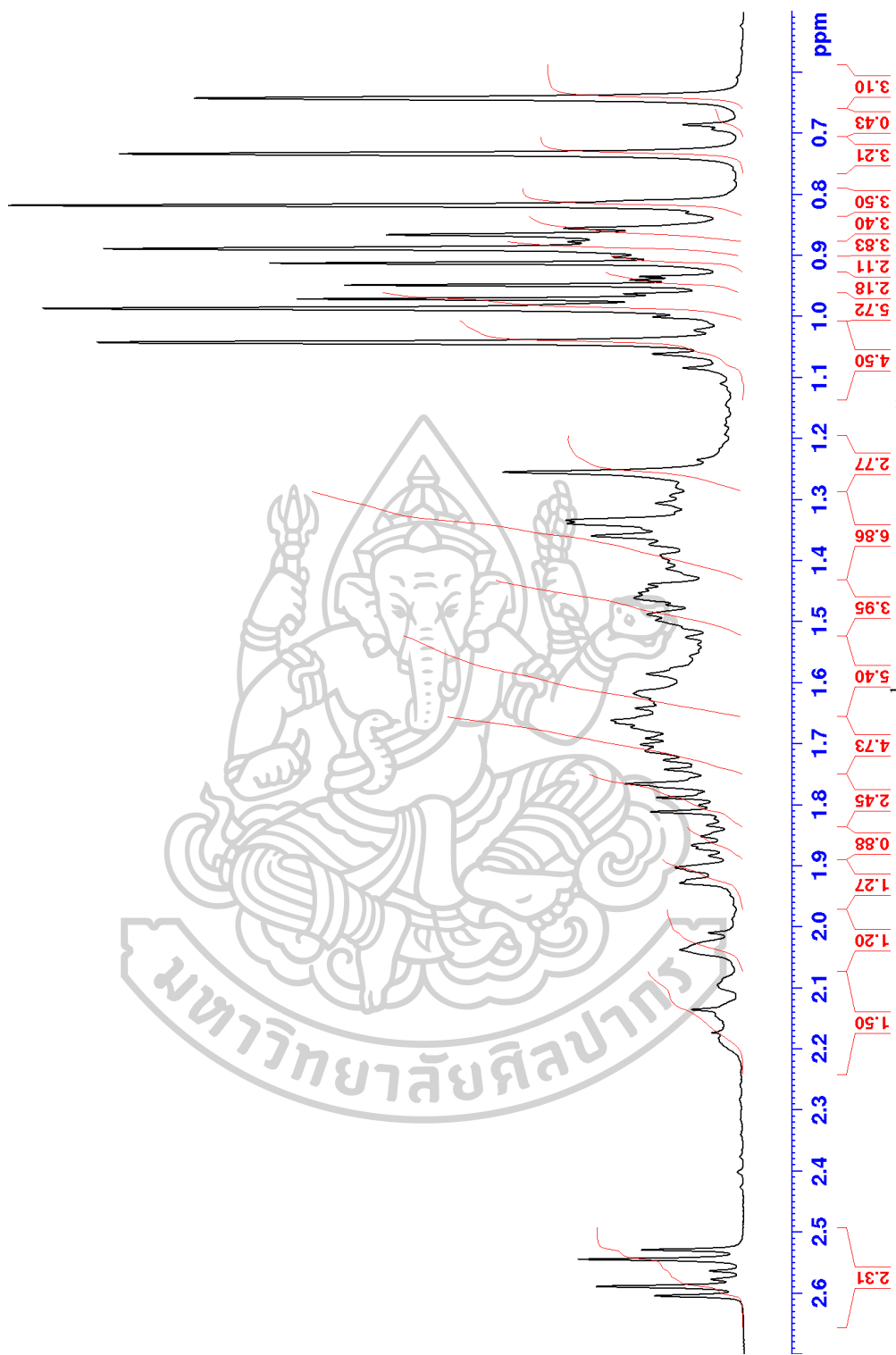


Figure S80 Zoom of the ¹H NMR spectrum of MS6

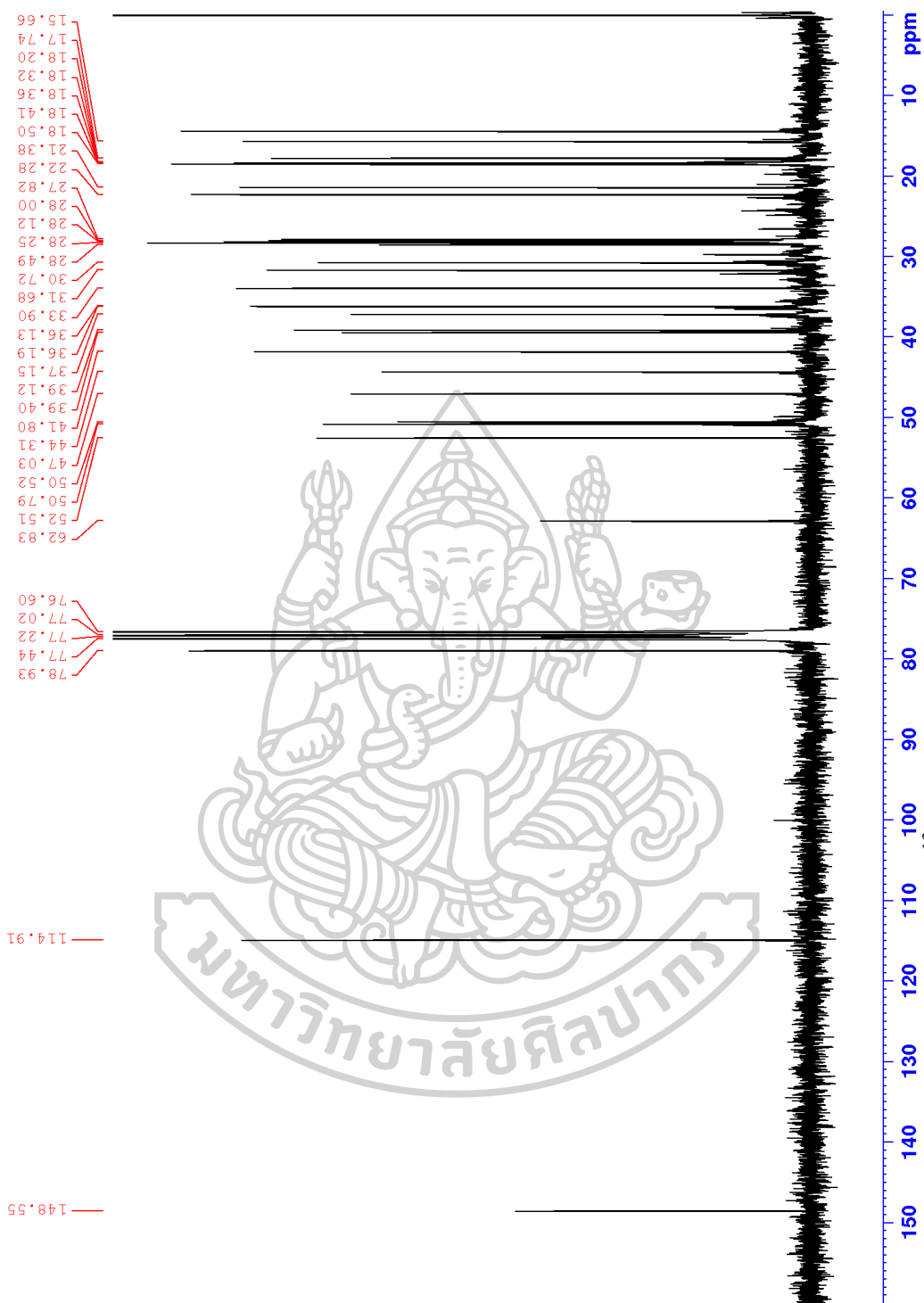
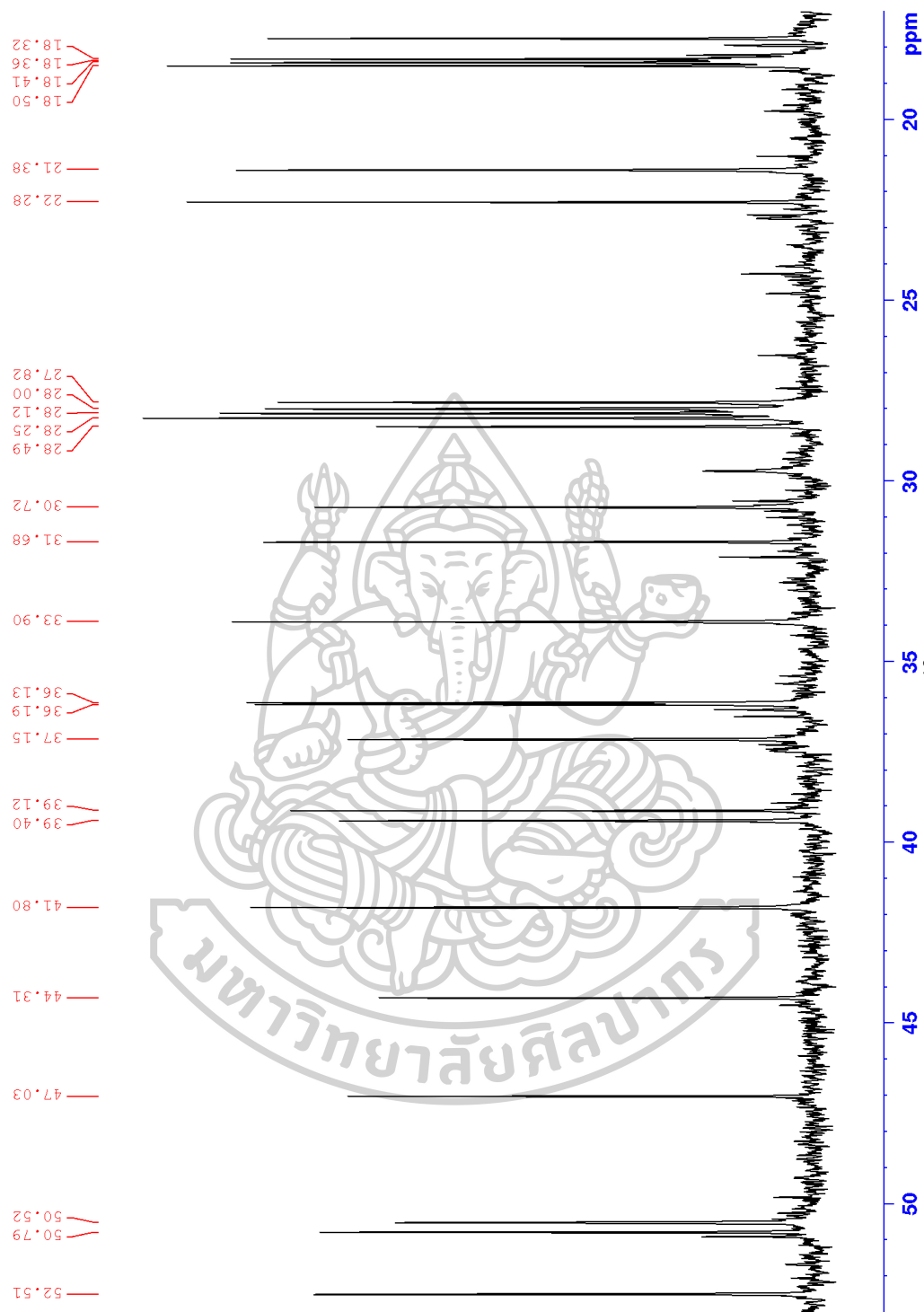


Figure S81 ^{13}C NMR spectrum of MS6 (75 MHz, CDCl_3)

Figure S82 Zoom of the ^{13}C NMR spectrum of MS6

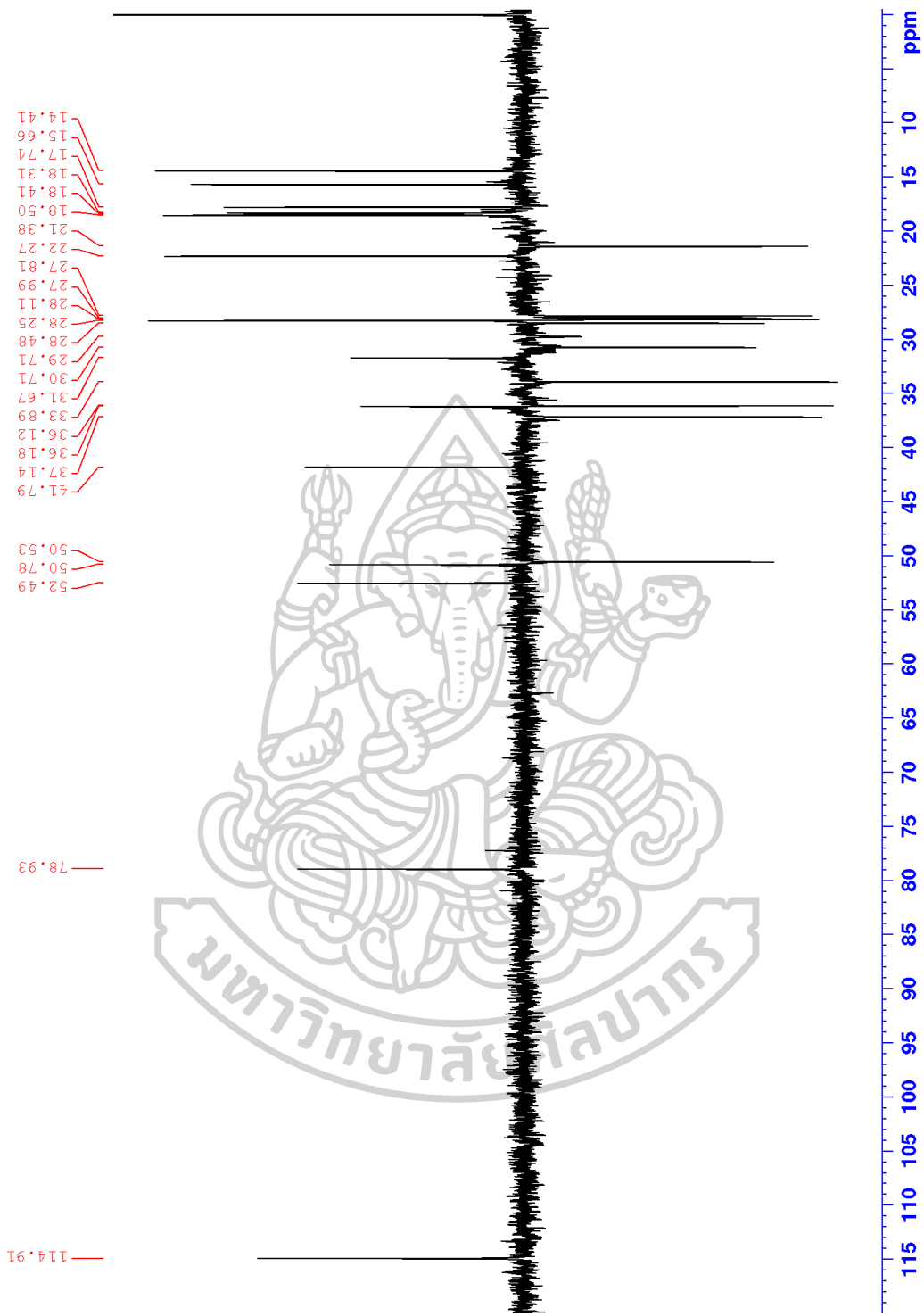


Figure S83 DEPT 135 spectrum of MS6 (75 MHz, CDCl₃)

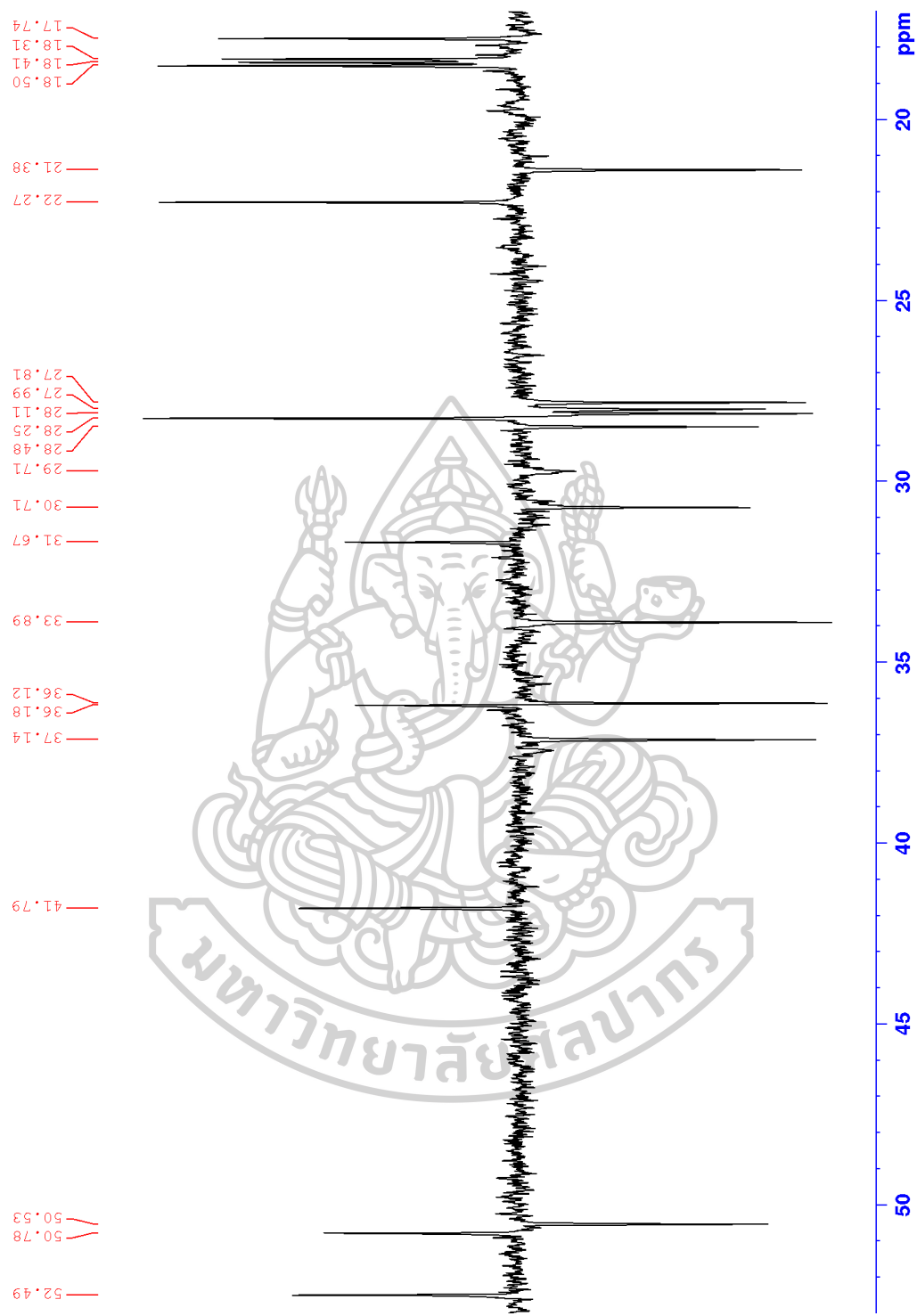


Figure S84 Zoom of the DEPT 135 spectrum of MS6

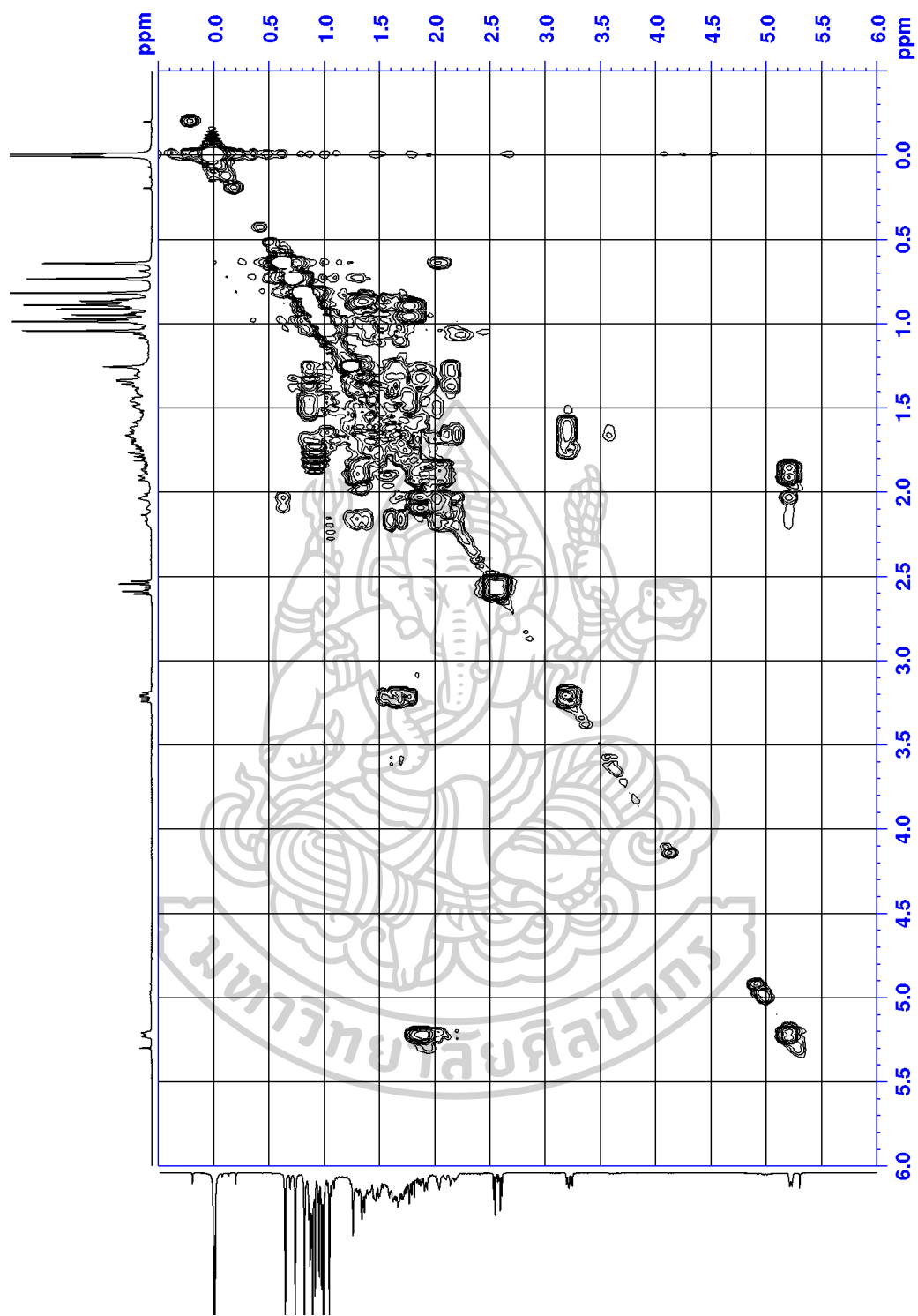


Figure S85 COSY spectrum of MS6 (300 MHz, CDCl₃)

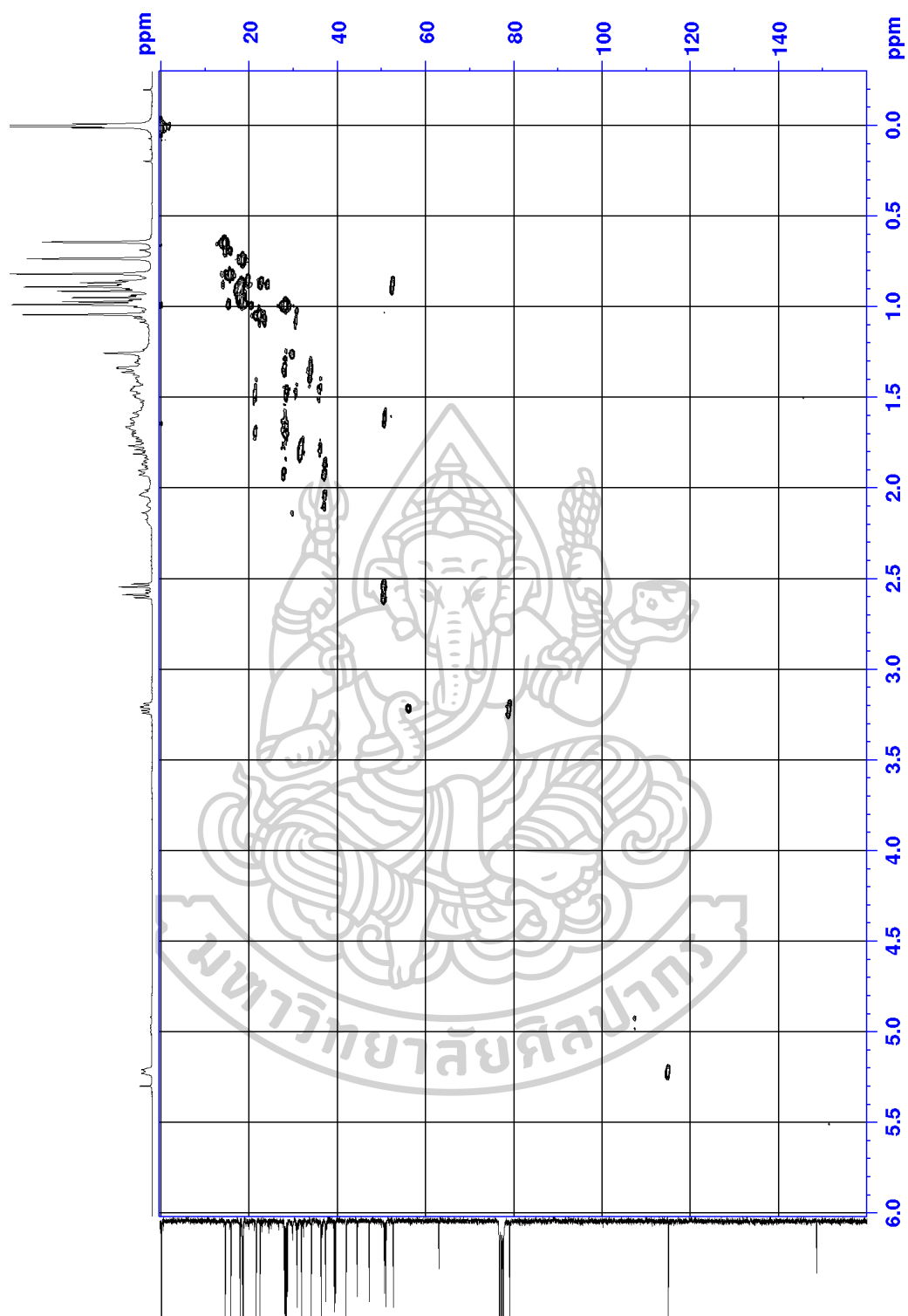


Figure S86 HMQC spectrum of MS6

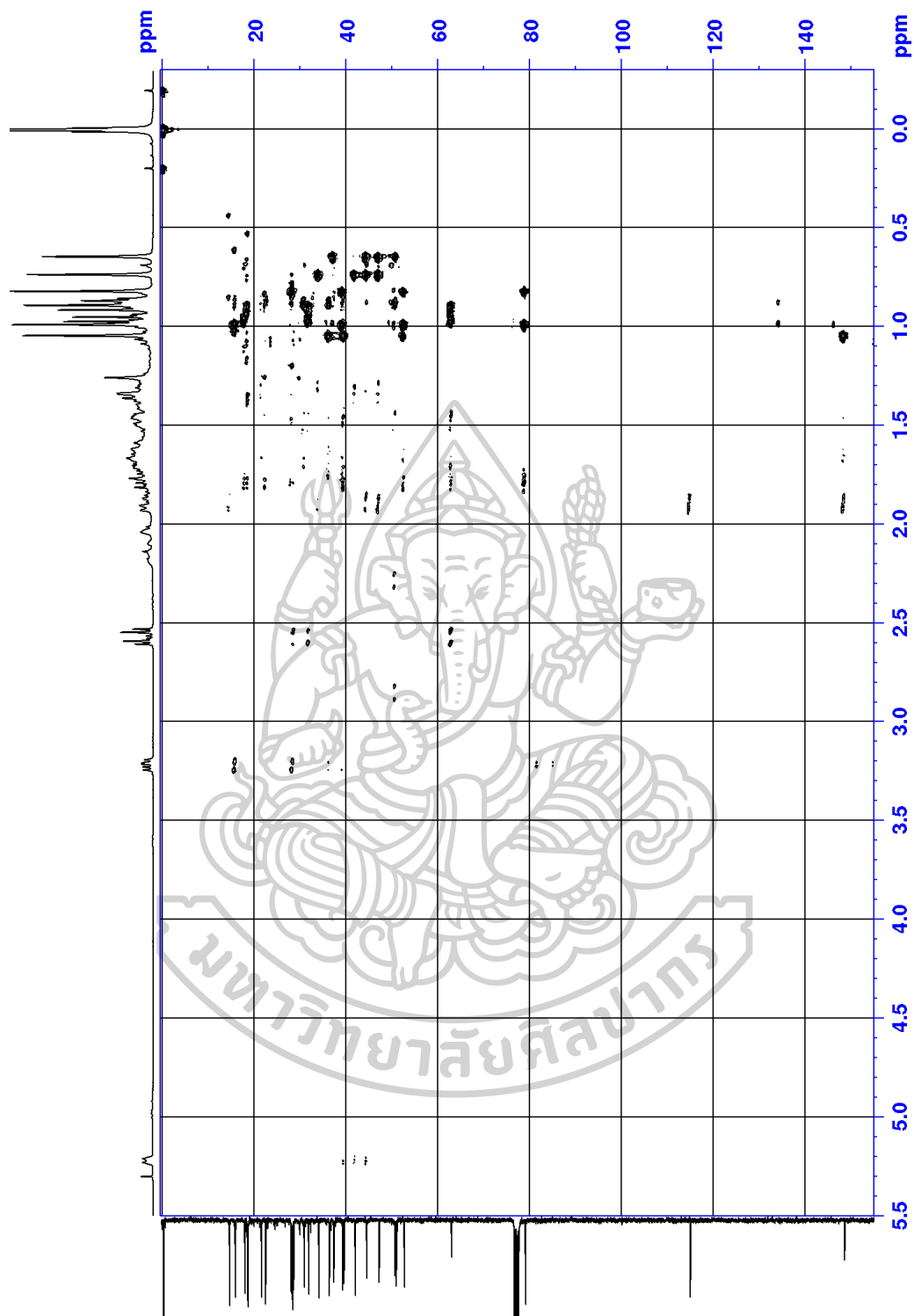


Figure S87 HMBC spectrum of MS6

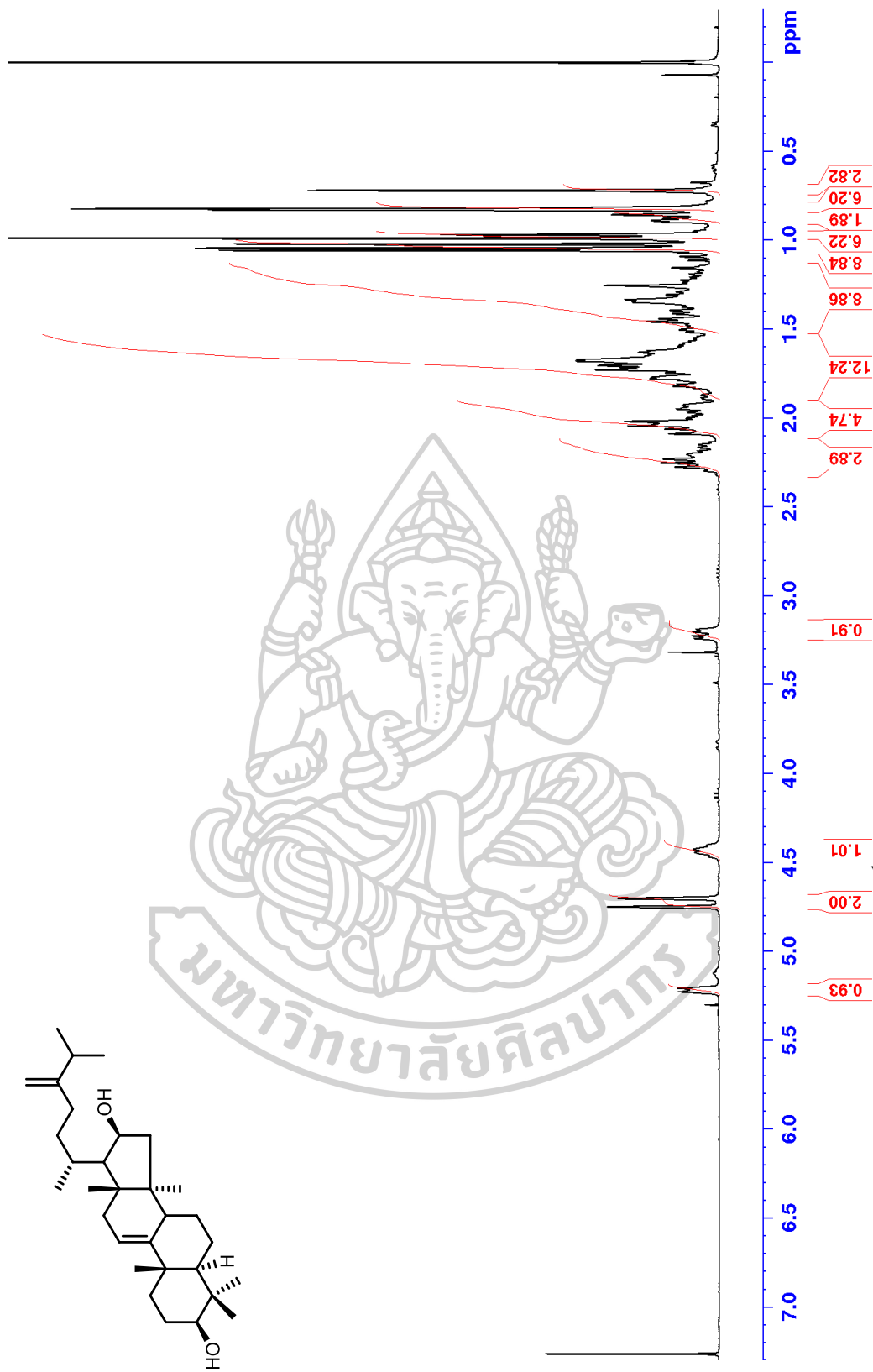


Figure S88 ^1H NMR spectrum of MS7 (300 MHz, CDCl_3)

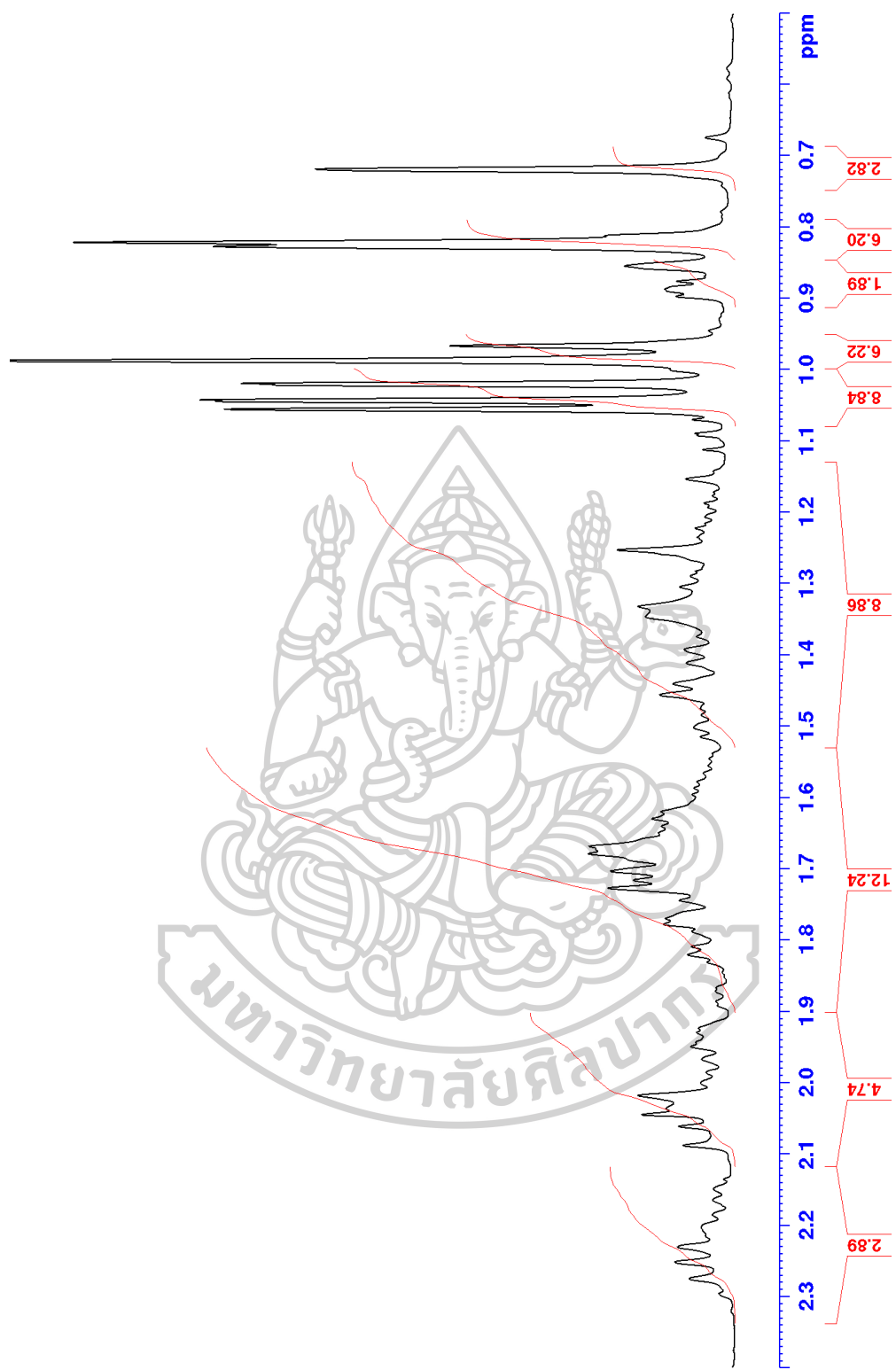


Figure S89 Zoom of the ^1H NMR spectrum of MS7

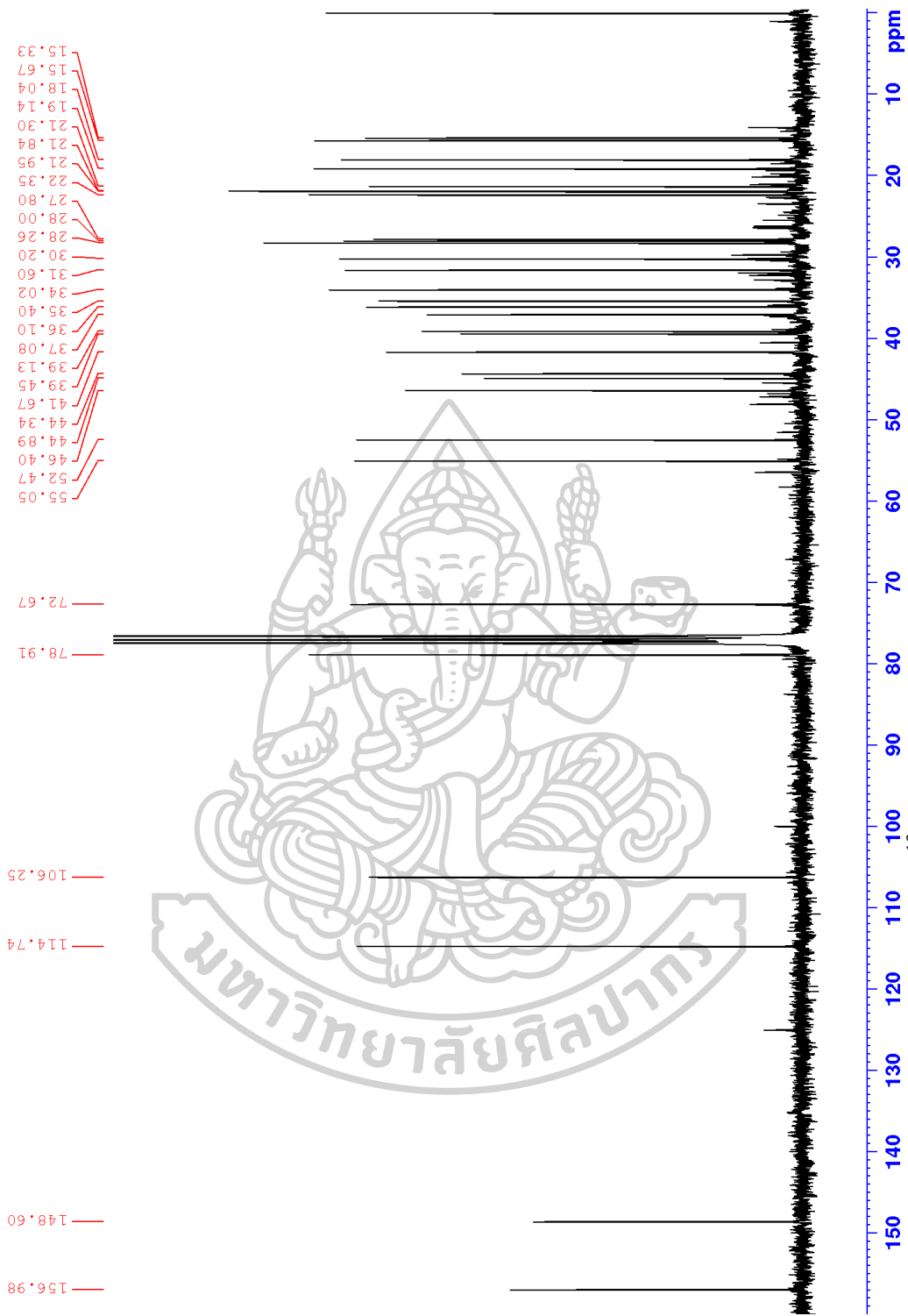


Figure S90 ^{13}C NMR spectrum of MS7 (75 MHz, CDCl_3)

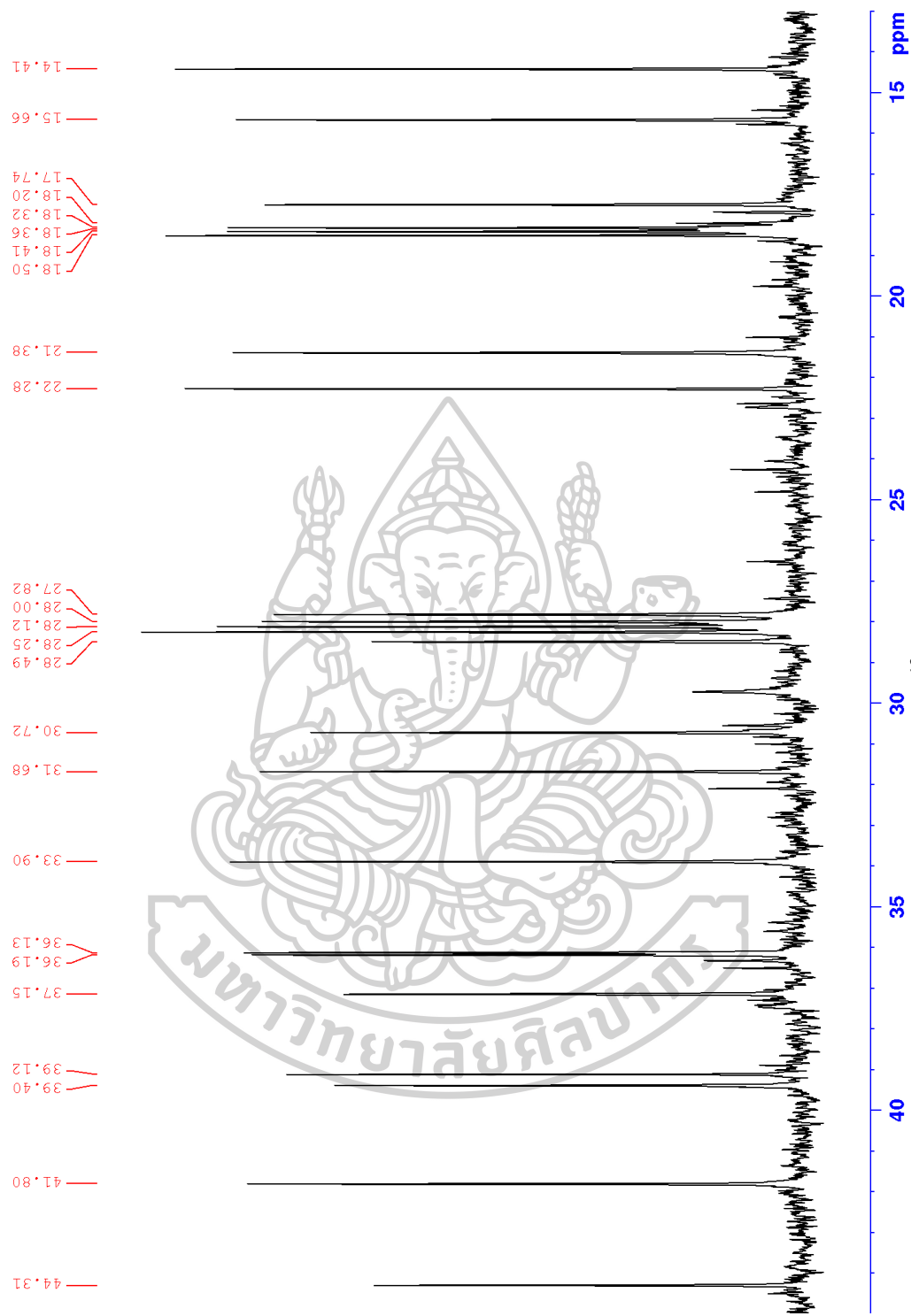


Figure S91 Zoom of the ^{13}C NMR spectrum of MS7

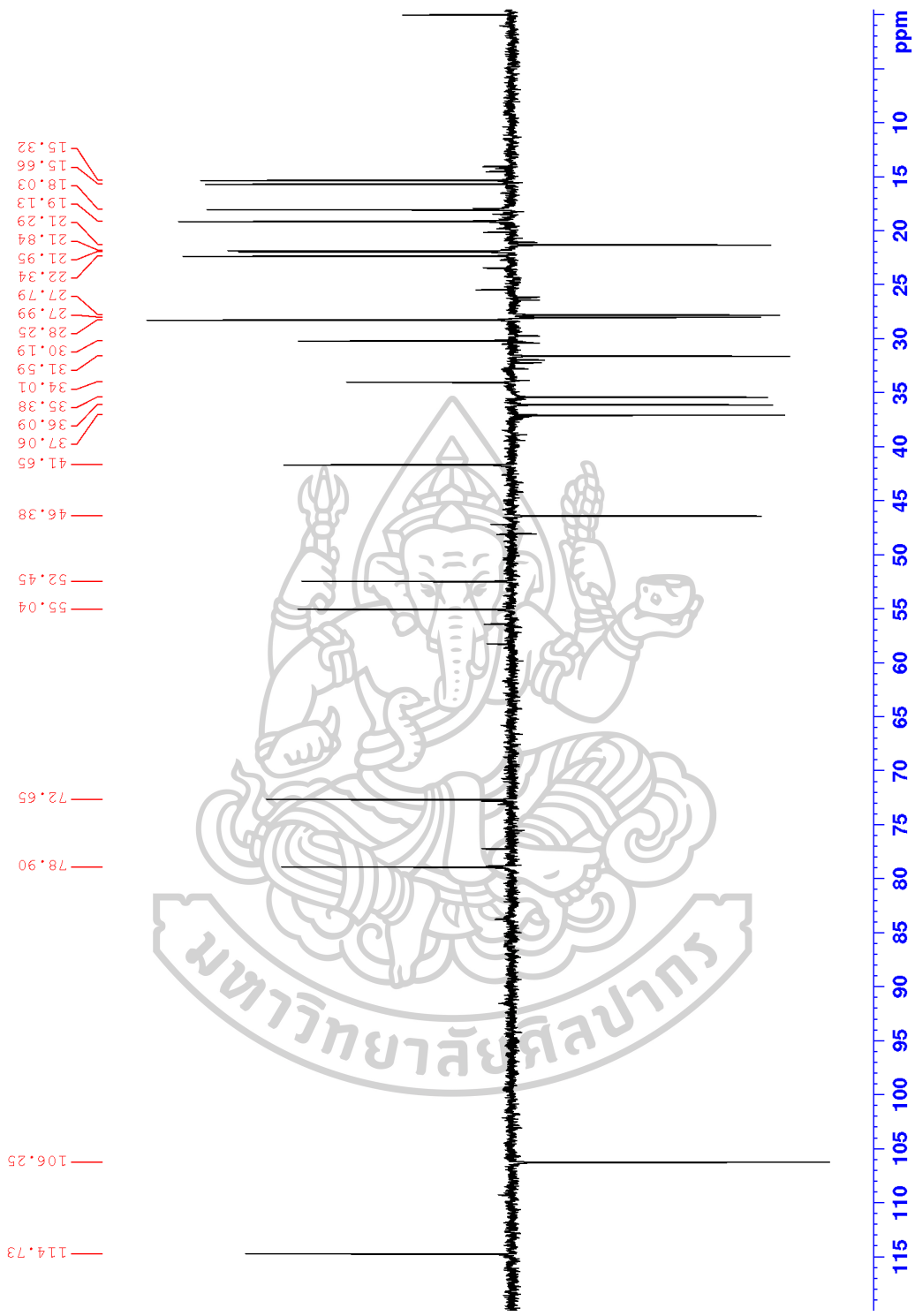


Figure S92 DEPT 135 spectrum of MS7 (75 MHz, CDCl₃)

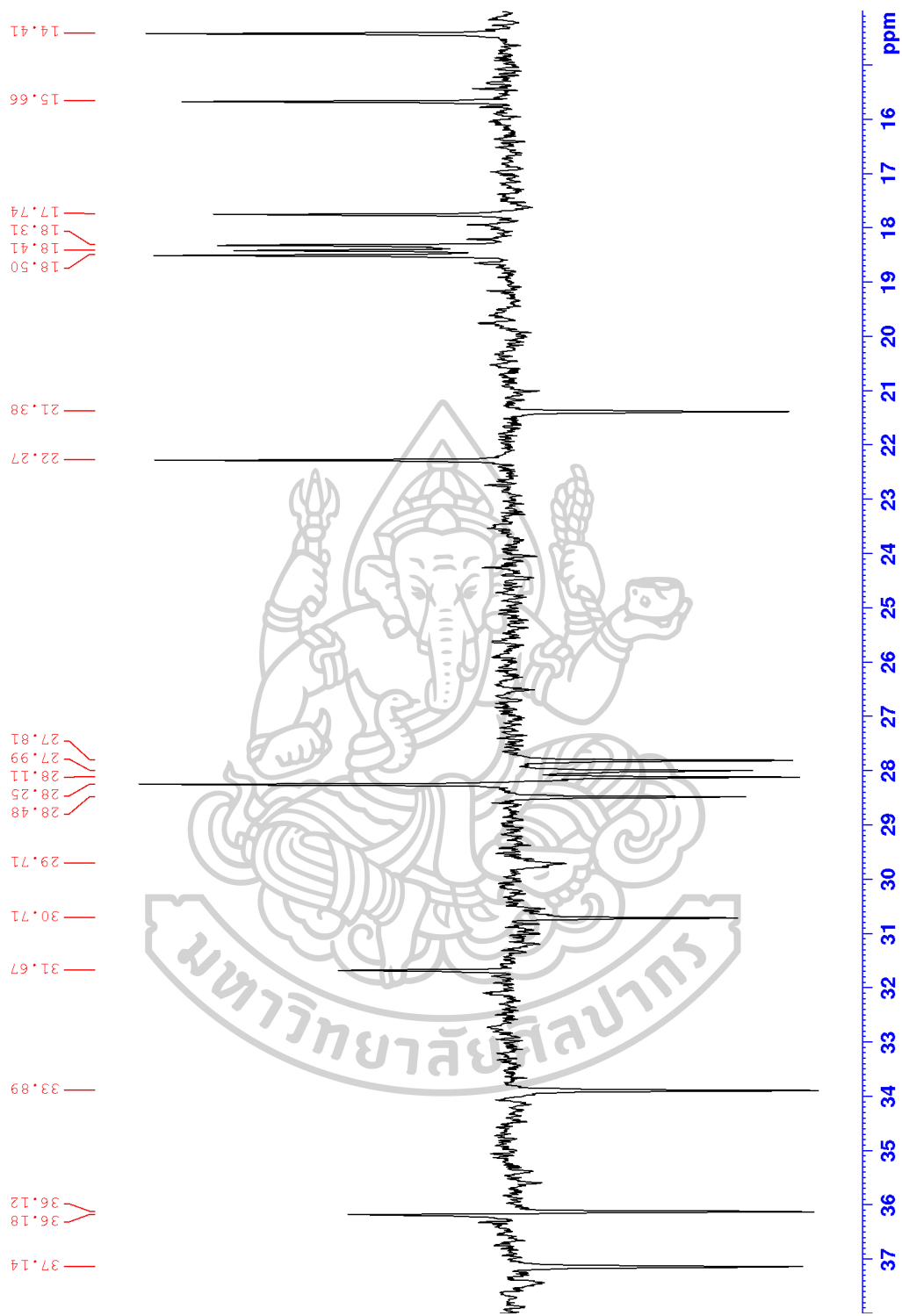


Figure S93 Zoom of the DEPT 135 spectrum of MS7

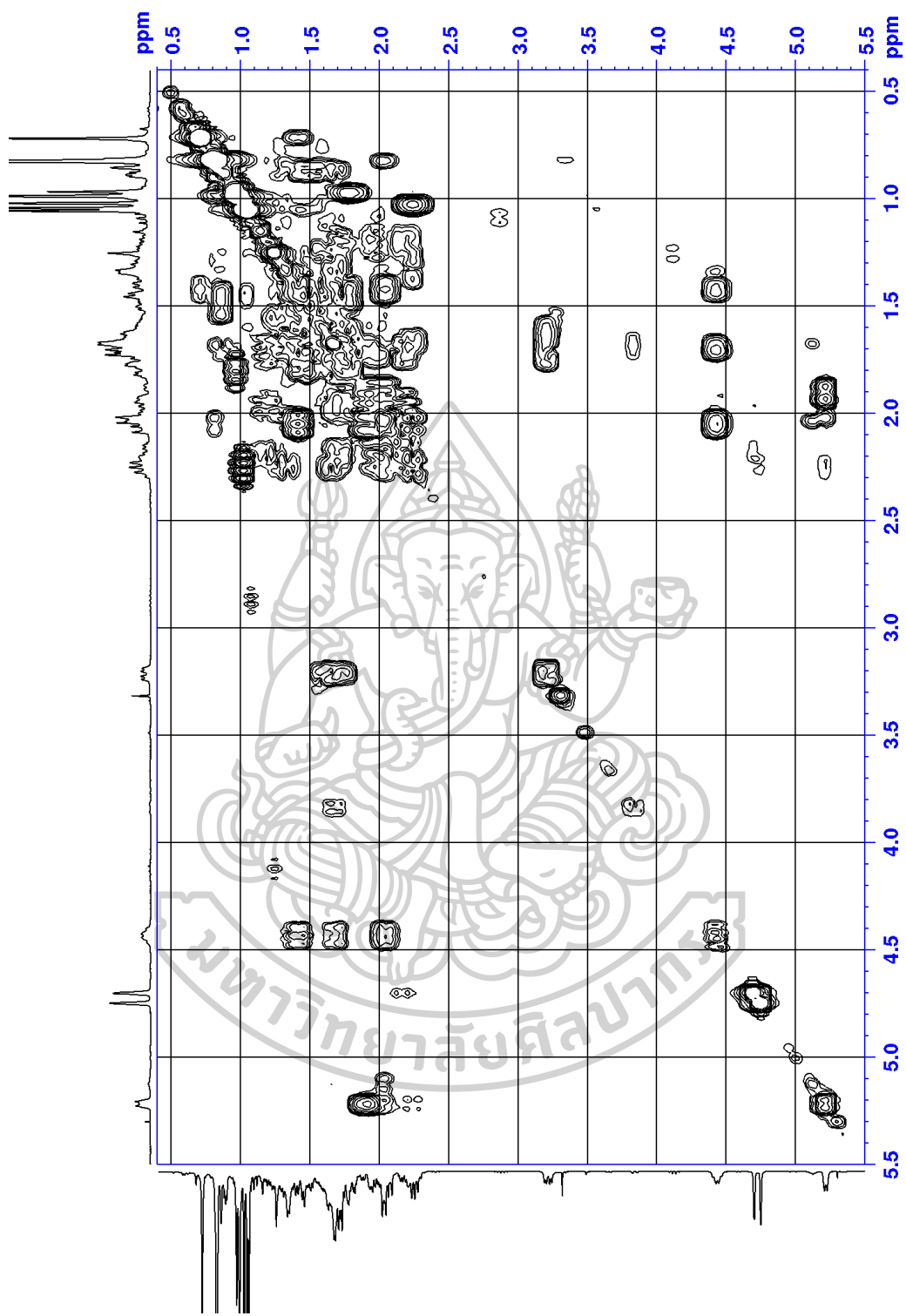


Figure S94 COSY spectrum of MS7 (300 MHz, CDCl₃)

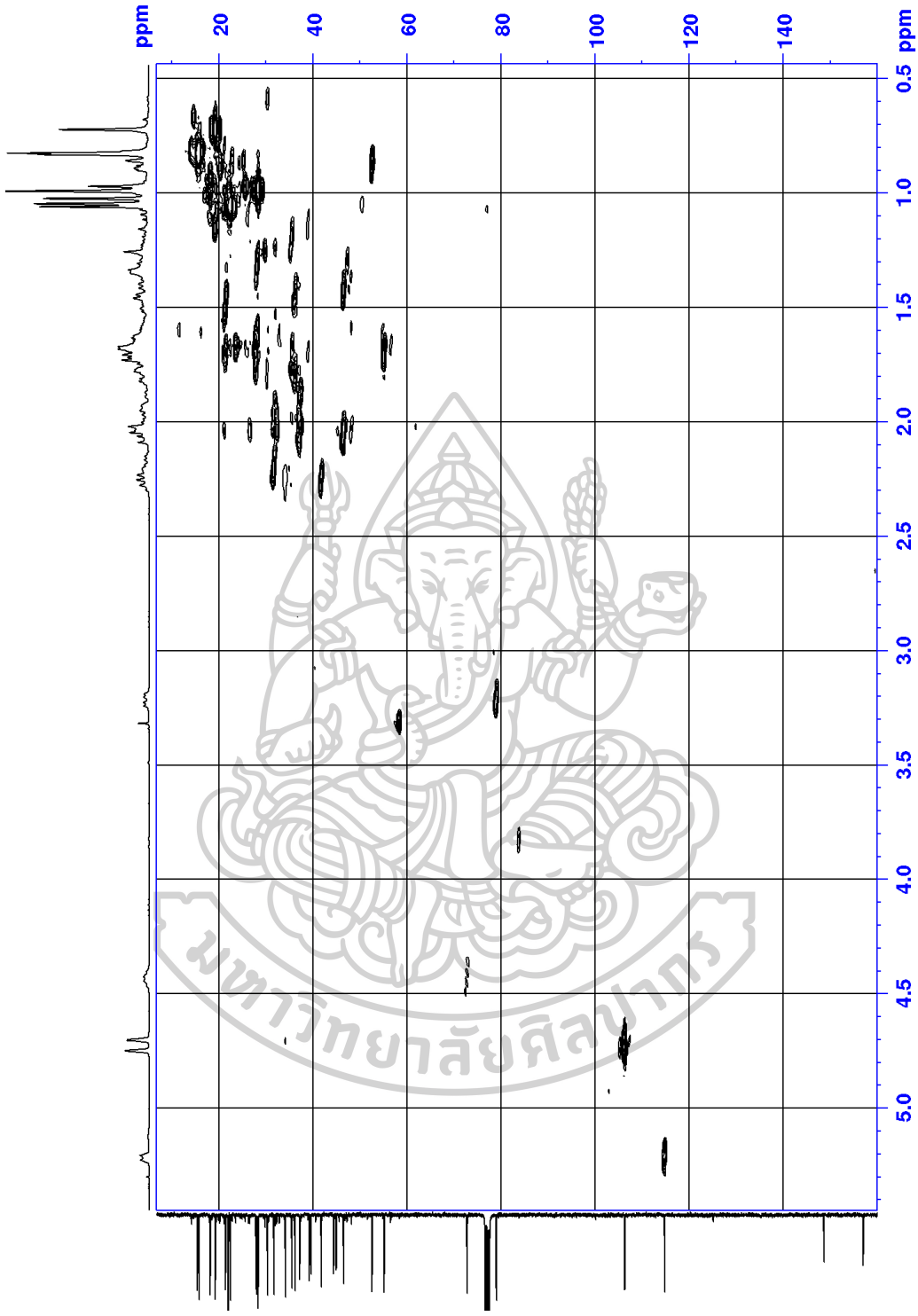


Figure S95 HMQC spectrum of MS7

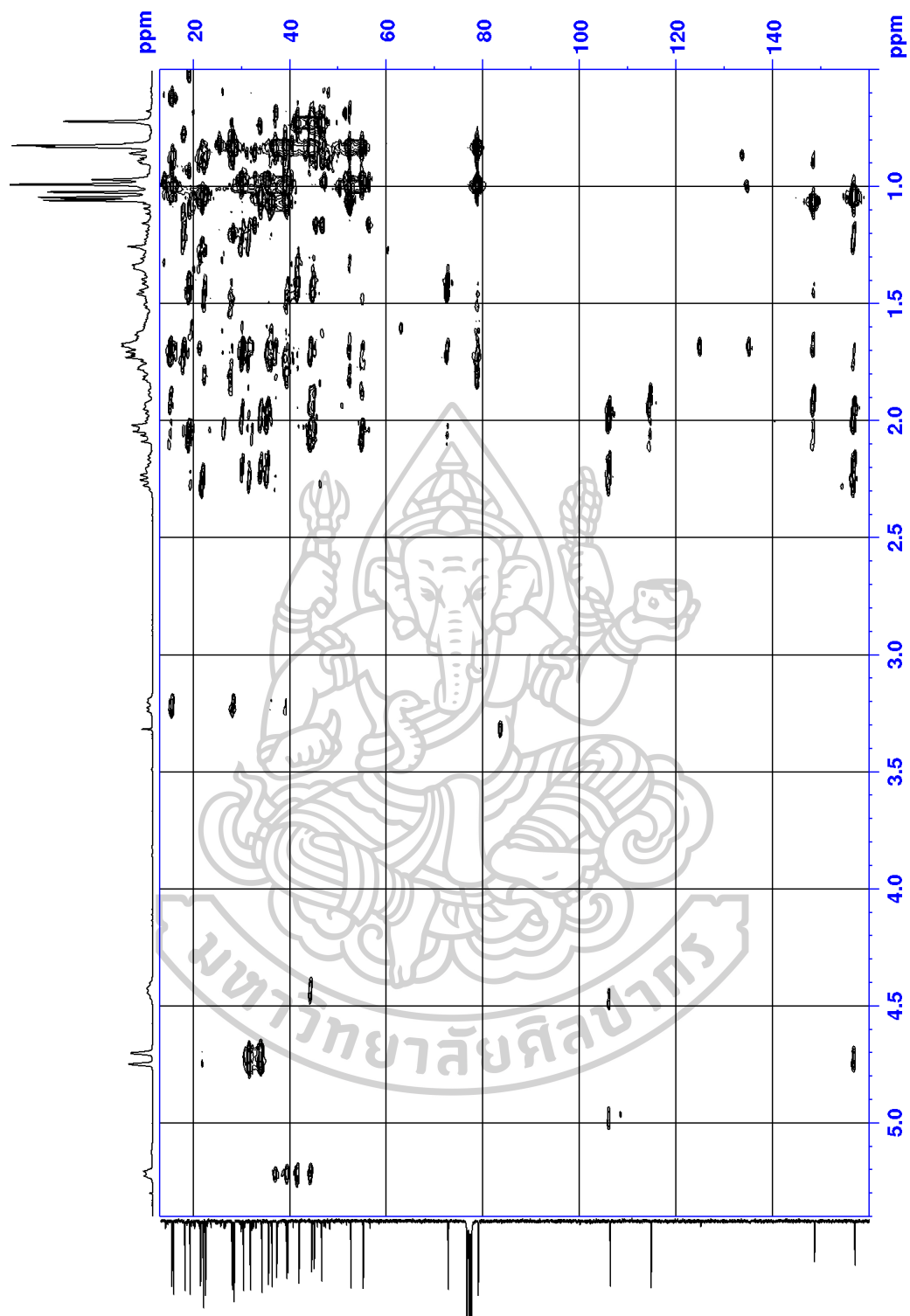


Figure S96 HMBC spectrum of MS7

APPENDIX C

LIST OF HRESIMS SPECTRUM OF ISOLATED COMPOUNDS

Figure	content	Page
Neolignans		
S97	HRESIMS spectrum of MS11	257
S98	HRESIMS spectrum of MS12	258
S99	HRESIMS spectrum of MS14	259
S100	HRESIMS spectrum of MS15	260
S101	HRESIMS spectrum of MS16	261
S102	HRESIMS spectrum of MS17	262
S103	HRESIMS spectrum of MS19	263
S104	HRESIMS spectrum of MS20	264
S105	HRESIMS spectrum of MS20a	265
Phenylpropanoid dimers		
S106	HRESIMS spectrum of MS18	266
Triterpenes		
S107	HRESIMS spectrum of MS3	267
S108	HRESIMS spectrum of MS5	268
S109	HRESIMS spectrum of MS6	269
S110	HRESIMS spectrum of MS7	270

Mass Spectrum List Report

Analysis Info

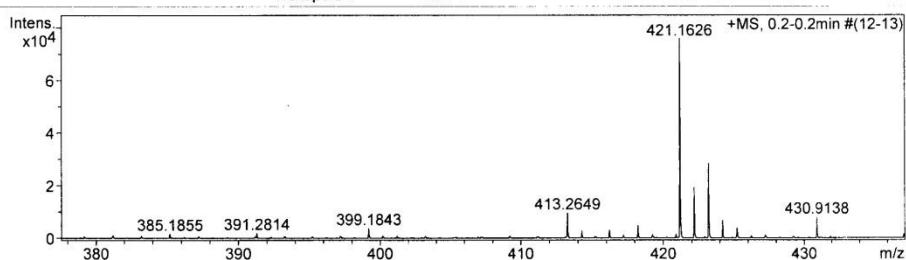
Analysis Name TOFSLP23404 Kanok-on YPMS-8 E+.d
 Method Nitirat_ESI pos 2017-2.m
 Sample Name ESIPos

Acquisition Date 12/1/2017 4:36:10 AM
 Operator Administrator
 Instrument micrOTOF 74

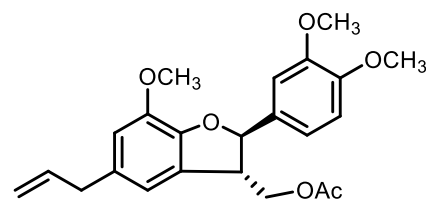
Acquisition Parameter

Source Type ESI
 Scan Range n/a
 Scan Begin 150 m/z
 Scan End 850 m/z
 Ion Polarity Positive
 Capillary Exit 90.0 V
 Hexapole RF 145.0 V
 Skimmer 1 30.0 V
 Hexapole 1 22.9 V

Set Corrector Fill 64 V
 Set Pulsar Pull 405 V
 Set Pulsar Push 405 V
 Set Reflector 1300 V
 Set Flight Tube 9000 V
 Set Detector TOF 1985 V



#	m/z	I	Res.
1	226.9515	18573	7247
2	271.1185	2756	7046
3	273.1674	2894	7346
4	294.9397	15410	8101
5	303.1784	2627	7870
6	329.1587	2580	7667
7	339.1592	9670	8367
8	362.9263	8604	8317
9	399.1843	3730	8193
10	413.2649	9516	8801
11	414.2689	2778	9396
12	416.2071	3055	8628
13	418.2211	4873	8877
14	421.1626	75849	8806
15	422.1652	19337	9155
16	423.1784	28440	8794
17	424.1809	6753	8793
18	425.2079	3937	7494
19	430.9138	7950	9300
20	489.1502	3435	9064
21	498.9012	5170	9664
22	566.8888	4017	9457
23	634.8737	3013	10102
24	702.8608	2603	10621
25	811.4386	2841	9864
26	819.3357	15971	10087
27	820.3383	7985	10177
28	821.3489	10389	9697
29	822.3527	4621	9762
30	823.3694	3615	9095



Chemical formula $C_{23}H_{26}O_6$

Exact mass 398.1729

HRMS m/z $[M+Na]^+$ 421.1626

calcd. for $C_{23}H_{26}O_6Na$ 421.1627

Figure S97 HRESIMS spectrum of MS11

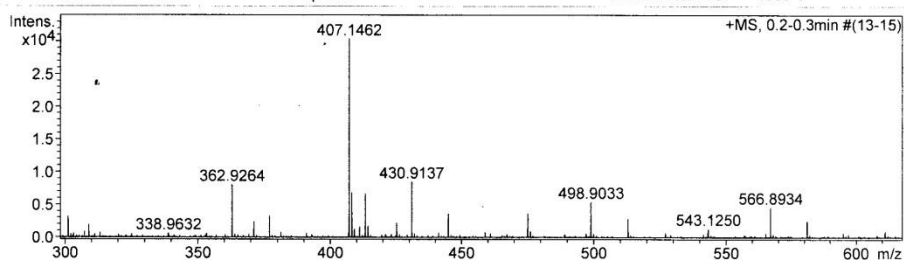
Mass Spectrum List Report

Analysis Info

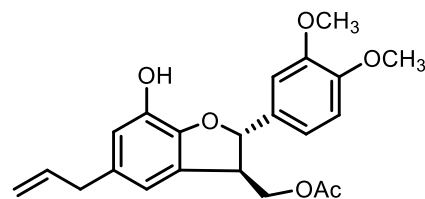
Analysis Name	TOFSLP23421 Kanok-on YPMS-7 E+.d	Acquisition Date	12/1/2017 4:31:55 AM
Method	Nitirat_ESI pos 2017-2.m	Operator	Administrator
Sample Name	ESIpos	Instrument	micrOTOF 74

Acquisition Parameter

Source Type	ESI	Ion Polarity	Positive	Set Corrector Fill	64 V
Scan Range	n/a	Capillary Exit	90.0 V	Set Pulsar Pull	405 V
Scan Begin	150 m/z	Hexapole RF	145.0 V	Set Pulsar Push	405 V
Scan End	850 m/z	Skimmer 1	30.0 V	Set Reflector	1300 V
		Hexapole 1	22.9 V	Set Flight Tube	9000 V
				Set Detector TCF	1985 V



#	m/z	I	Res.
1	197.0784	2694	6642
2	198.0631	2019	6467
3	226.9515	32159	7404
4	240.9670	8031	7589
5	270.9765	3676	7881
6	279.2280	2590	7873
7	294.9389	6273	7914
8	301.1410	3191	8216
9	308.9544	1959	8256
10	362.9264	8087	8803
11	371.0964	2387	8519
12	376.9423	3314	8811
13	407.1462	30412	8779
14	408.1502	6819	8445
15	411.1280	1597	8610
16	413.2655	6663	9179
17	414.2694	1715	9182
18	425.2153	2238	9145
19	430.9137	8518	9462
20	444.9301	3665	9368
21	475.1353	3646	9221
22	498.9033	5399	9286
23	512.9189	2860	9491
24	566.8934	4618	9878
25	580.9098	2512	9423
26	634.8822	3113	9348
27	648.8993	2226	10346
28	702.8758	2729	10084
29	716.8915	1920	10857
30	770.8680	1683	10129



Chemical formula $C_{22}H_{24}O_6$

Exact mass 384.1573

HRMS m/z $[M+Na]^+$ 407.1462

calcd. for $C_{22}H_{24}O_6Na$ 407.1471

Figure S98 HRESIMS spectrum of MS12

Mass Spectrum SmartFormula Report

Analysis Info

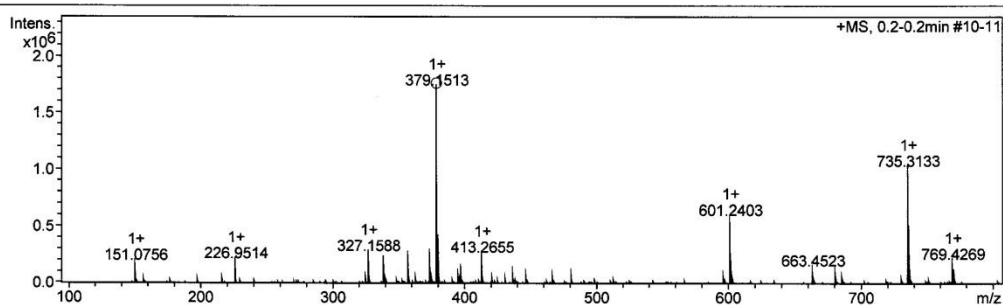
Analysis Name D:\Data\CRI\QSP02642 Kanok-on YPMS10 E+.d
 Method Nitirat esi pos low may2018-1.m
 Sample Name ESIpos
 Comment

Acquisition Date 4/10/2018 4:37:44 PM

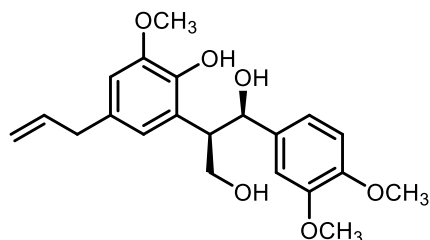
Operator BDAL@DE
 Instrument compact 8255754.20094

Acquisition Parameter

Source Type	ESI	Ion Polarity	Positive	Set Nebulizer	1.0 Bar
Focus	Not active	Set Capillary	4000 V	Set Dry Heater	135 °C
Scan Begin	100 m/z	Set End Plate Offset	-500 V	Set Dry Gas	6.5 l/min
Scan End	800 m/z	Set Charging Voltage	2000 V	Set Divert Valve	Source
		Set Corona	0 nA	Set APCI Heater	0 °C



Meas. m/z # Ion	Formula	m/z	err [ppm]	Mean err [ppm]	rdB	N-Rule	e ⁻	Conf	mSigma	Std I a	Std Mean m/z	Std VarNor m	Std I m	Std m/z	Std Diff	Std Comb Dev
379.151282 1	C ₂₁ H ₂₄ NaO ₅	379.151595	0.8	0.9	9.5	ok	even		1.9	3.0	n.a.	n.a.	n.a.	n.a.	n.a.	n.a.



Chemical formula C₂₁H₂₆O₆
 Exact mass 374.1729
 HRMS m/z [M+Na-H₂O]⁺ 379.1513
 calcd. for C₂₁H₂₄O₅Na 379.1522

Figure S99 HRESIMS spectrum of MS14

Mass Spectrum List Report

Analysis Info

Analysis Name TOFSLP24297 Kanokon YPMS-12 E+.d
 Method Nitirat ESI pos 2018-1.m
 Sample Name ESIpos

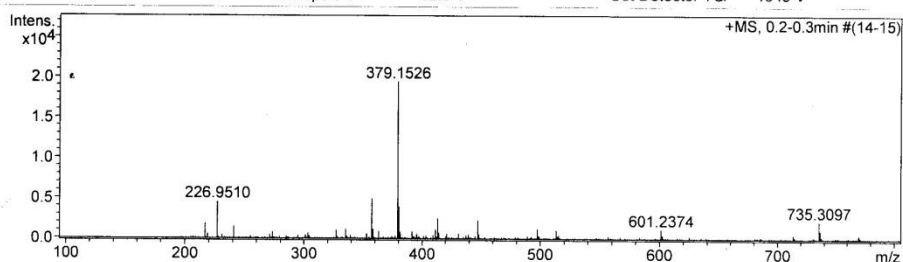
Acquisition Date 7/9/2018 3:11:22 AM
 Operator Administrator
 Instrument micrOTOF 74

Acquisition Parameter

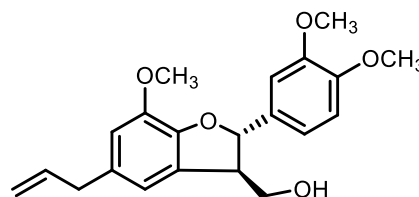
Source Type ESI
 Scan Range n/a
 Scan Begin 100 m/z
 Scan End 800 m/z

Ion Polarity Positive
 Capillary Exit 110.0 V
 Hexapole RF 150.0 V
 Skimmer 1 35.0 V
 Hexapole 1 22.9 V

Set Corrector Fill 64 V
 Set Pulsar Pull 405 V
 Set Pulsar Push 405 V
 Set Reflector 1300 V
 Set Flight Tube 9000 V
 Set Detector TOF 1945 V



#	m/z	I	Res.
1	216.9224	1906	8250
2	218.9193	585	8079
3	226.9510	4531	8384
4	240.9673	1462	8749
5	273.1673	793	8923
6	303.1792	717	8879
7	327.1612	1062	9509
8	335.1768	1160	9296
9	352.8972	626	10435
10	357.1670	4945	9097
11	358.1712	1180	8598
12	362.9288	925	10173
13	379.1526	19426	10147
14	380.1555	3956	9667
15	381.1667	852	6995
16	391.2837	928	10222
17	395.1370	601	7703
18	411.1655	1168	6398
19	413.2666	2555	9956
20	414.2709	786	10662
21	420.8848	607	10877
22	430.9153	658	10513
23	439.1710	573	9536
24	447.1386	2309	10825
25	497.2139	1221	10792
26	513.2435	1073	11326
27	601.2374	1189	10542
28	713.3127	557	10838
29	735.3097	2220	10793
30	736.3084	1015	11663



Chemical formula $C_{21}H_{24}O_5$
 Exact mass 356.1624
 HRMS m/z $[M+Na]^+$ 379.1526
 calcd. for $C_{21}H_{24}O_5Na$ 379.1522

Figure S100 HRESIMS spectrum of compound MS15

Mass Spectrum List Report

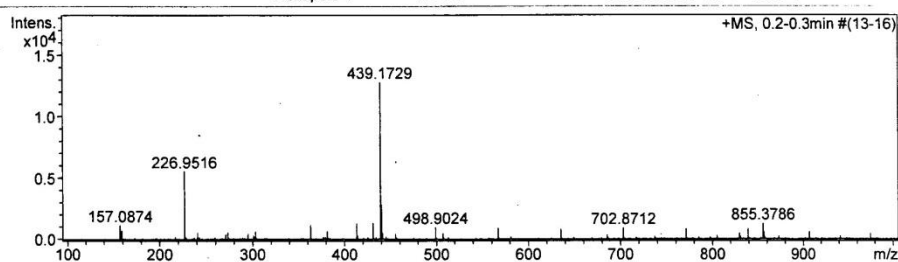
Analysis Info

Analysis Name TOFSP24209 Kanok-on YPMS-11 E+.d
 Method Nitirat ESI pos 2018-1.m
 Sample Name ESIpos

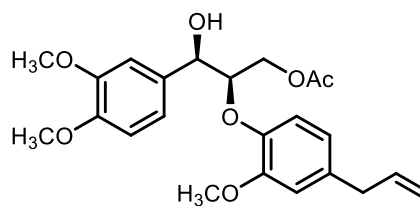
Acquisition Date 5/4/2018 2:55:54 AM
 Operator Administrator
 Instrument micrOTOF 74

Acquisition Parameter

Source Type	ESI	Ion Polarity	Positive	Set Corrector Fill	64 V
Scan Range	n/a	Capillary Exit	110.0 V	Set Pulsar Pull	405 V
Scan Begin	100 m/z	Hexapole RF	120.0 V	Set Pulsar Push	405 V
Scan End	1000 m/z	Skimmer 1	35.0 V	Set Reflector	1300 V
		Hexapole 1	22.9 V	Set Flight Tube	9000 V
				Set Detector TCF	1930 V



#	m/z	I	Res.
1	157.0874	1159	7774
2	158.9687	711	7424
3	226.9516	5545	8600
4	240.9674	520	9010
5	270.9767	354	10008
6	273.1673	551	8645
7	294.9387	446	9238
8	303.1776	613	9392
9	362.9267	1162	10305
10	381.1666	655	9970
11	413.2661	1286	11151
12	414.2673	319	10572
13	430.9136	1328	11128
14	439.1729	12791	11049
15	440.1769	2824	10684
16	441.1802	530	10804
17	455.1480	424	9992
18	498.9024	983	12088
19	507.1621	479	11138
20	566.8917	913	11201
21	634.8817	815	11180
22	685.4408	327	12072
23	702.8712	923	11420
24	770.8639	833	12195
25	829.4668	486	11449
26	838.8558	853	12420
27	855.3786	1288	11414
28	856.3788	628	11036
29	906.8493	607	12251
30	974.8453	469	12504



Chemical formula $C_{23}H_{28}O_7$
 Exact mass 416.1835
 HRMS m/z $[M+Na]^+$ 439.1729
 calcd. for $C_{23}H_{28}O_7Na$ 439.1733

Figure S101 HRESIMS spectrum of MS16

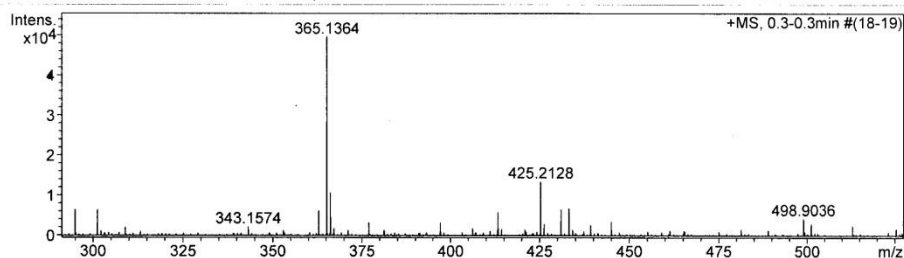
Mass Spectrum List Report

Analysis Info

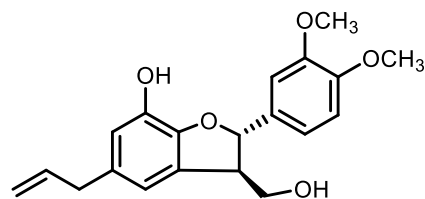
Analysis Name	TOFSLP23405 Kanok-on YPMS-9 E+.d	Acquisition Date	12/1/2017 4:37:15 AM
Method	Nitirat_ESI pos 2017-2.m	Operator	Administrator
Sample Name	ESIpos	Instrument	micrOTOF 74

Acquisition Parameter

Source Type	ESI	Ion Polarity	Positive	Set Corrector Fill	64 V
Scan Range	n/a	Capillary Exit	90.0 V	Set Pulsar Pull	405 V
Scan Begin	150 m/z	Hexapole RF	145.0 V	Set Pulsar Push	405 V
Scan End	850 m/z	Skimmer 1	30.0 V	Set Reflector	1300 V
		Hexapole 1	22.9 V	Set Flight Tube	9000 V
				Set Detector TCF	1985 V



#	m/z	I	Res.
1	199.0606	2160	6667
2	216.9229	2930	7374
3	219.0992	10263	6921
4	226.9515	31252	7283
5	240.9673	8144	7376
6	270.9780	3980	7849
7	271.0869	2387	4764
8	279.2282	2531	7585
9	294.9388	6505	8248
10	301.1419	6399	8317
11	308.9550	2061	8415
12	343.1574	2123	7798
13	362.9265	6207	8562
14	365.1364	49594	8614
15	366.1399	10631	8843
16	376.9431	3177	8781
17	397.1288	3205	8650
18	413.2655	5782	9021
19	425.2128	13425	8603
20	426.2162	2903	8998
21	430.9137	6490	9290
22	433.1232	6765	9263
23	439.1733	2604	8900
24	444.9303	3470	9680
25	498.9036	4183	9646
26	501.1109	2912	9847
27	512.9191	2433	9869
28	566.8908	3229	9994
29	634.8795	2006	9590
30	707.2863	2439	10123



Chemical formula $C_{20}H_{22}O_5$

Exact mass 342.1467

HRMS m/z $[M+Na]^+$ 365.1364

calcd. for $C_{20}H_{22}O_5Na$ 365.1365

Figure S102 HRESIMS spectrum of **MS17**

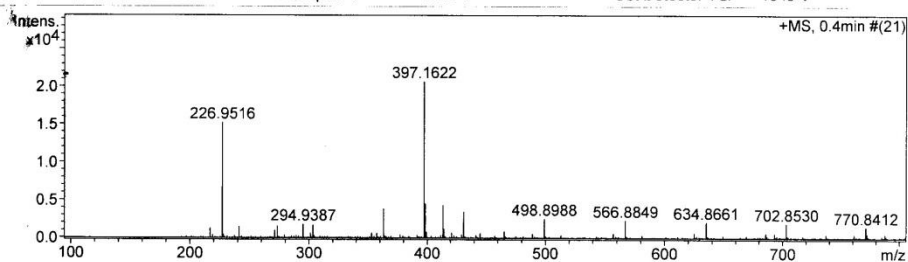
Mass Spectrum List Report

Analysis Info

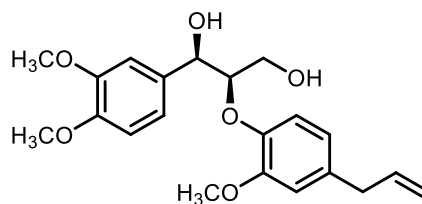
Analysis Name TOFSLP24298 Kanokon YPMS-13 E+.d	Acquisition Date 7/9/2018 3:12:32 AM
Method Nitirat ESI pos 2018-1.m	Operator Administrator
Sample Name ESIpos	Instrument micrOTOF 74

Acquisition Parameters

Source Type ESI	Ion Polarity Positive	Set Corrector Fill 64 V
Scan Range n/a	Capillary Exit 110.0 V	Set Pulsar Pull 405 V
Scan Begin 100 m/z	Hexapole RF 150.0 V	Set Pulsar Push 405 V
Scan End 800 m/z	Skimmer 1 35.0 V	Set Reflector 1300 V
	Hexapole 1 22.9 V	Set Flight Tube 9000 V
		Set Detector TCF 1945 V



#	m/z	I	Res.
1	216.9224	1298	8214
2	226.9516	15219	8172
3	240.9669	1439	8797
4	270.9784	1023	8903
5	273.1681	1546	8693
6	294.9387	1813	9365
7	301.1460	618	7439
8	303.1791	1704	9115
9	352.8984	673	10215
10	357.1669	618	8546
11	362.9266	3864	10058
12	397.1622	20691	9278
13	398.1652	4548	9941
14	399.1704	788	9375
15	413.2656	4323	10142
16	414.2693	1221	10520
17	420.8847	726	10508
18	430.9136	3459	10282
19	444.9307	619	10823
20	465.1496	869	10978
21	498.8988	2548	11263
22	556.8556	640	11607
23	566.8849	2332	11657
24	624.8404	651	12063
25	634.8661	2130	11826
26	685.4241	658	11695
27	702.8530	1931	11143
28	770.8412	1514	10991
29	771.3261	1497	11236
30	772.3310	593	10961



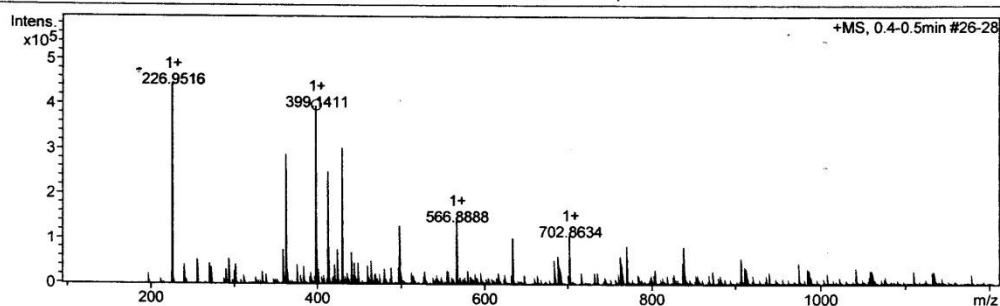
Chemical formula	C ₂₁ H ₂₆ O ₆
Exact mass	374.1729
HRMS m/z [M+Na] ⁺	397.1622
calcd. for C ₂₁ H ₂₆ O ₆ Na	397.1627

Figure S103 HRESIMS spectrum of MS19

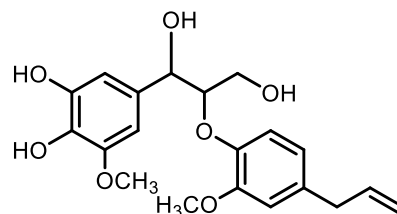
Mass Spectrum SmartFormula Report

Analysis Info		Acquisition Date	11/19/2018 1:21:59 PM
Analysis Name	D:\Data\CR\QSLP04307 Kanok-on YPMS15 E+.d	Operator	BDAL@DE
Method	Nitirat esi neg low may2018-2.m	Instrument	compact 8255754.20094
Sample Name	ESlpos		
Comment			

Acquisition Parameter					
Source Type	ESI	Ion Polarity	Positive	Set Nebulizer	1.0 Bar
Focus	Not active	Set Capillary	4000 V	Set Dry Heater	130 °C
Scan Begin	100 m/z	Set End Plate Offset	-500 V	Set Dry Gas	6.0 l/min
Scan End	1200 m/z	Set Charging Voltage	2000 V	Set Divert Valve	Source
		Set Corona	0 nA	Set APCI Heater	0 °C



Meas. m/z # Ion Formula	m/z	err [ppm]	Mean err [ppm]	rdB	N-Rule	e ⁻	Conf	mSigma	Std I a	Std Mean m/z	Std VarNor m	Std I m/z	Std Diff	Std Comb Dev
399.141122 1 C ₂₀ H ₂₄ NaO ₇	399.141424	0.8	0.6	8.5	ok	even		0.7	1.3	n.a.	n.a.	n.a.	n.a.	n.a.



Chemical formula	C ₂₀ H ₂₄ O ₇
Exact mass	376.1522
HRMS m/z [M+Na] ⁺	399.1411
calcd. for C ₂₀ H ₂₄ O ₇ Na	399.1420

Figure S104 HRESIMS spectrum of MS20

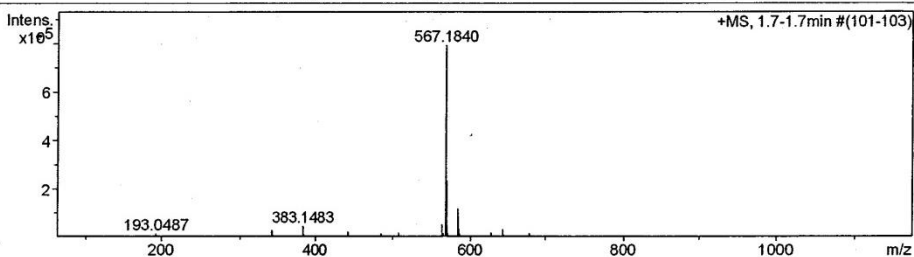
Mass Spectrum List Report

Analysis Info

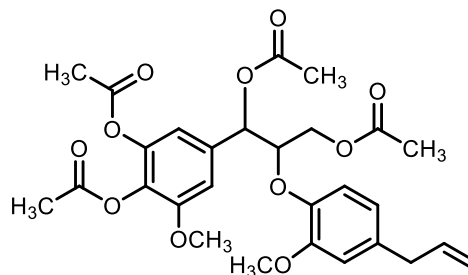
Analysis Name	OS17062019009.d	Acquisition Date	6/18/2019 8:57:22 AM
Method	Tune_low_1_POS_2019.m	Operator	Administrator
Sample Name	YPMS-15a	Instrument	micrOTOF 72
	YPMS-15a		

Acquisition Parameter

Source Type	ESI	Ion Polarity	Positive	Set Corrector Fill	50 V
Scan Range	n/a	Capillary Exit	110.0 V	Set Pulsar Pull	337 V
Scan Begin	50 m/z	Hexapole RF	150.0 V	Set Pulsar Push	337 V
Scan End	3000 m/z	Skimmer 1	45.0 V	Set Reflector	1300 V
		Hexapole 1	24.3 V	Set Flight Tube	9000 V
				Set Detector TOF	2295 V



#	m/z	I	I %	S/N	Res.
1	177.0542	5665	0.7	26.2	4223
2	193.0487	13646	1.7	64.0	4120
3	212.1167	6572	0.8	31.0	4467
4	341.1371	30219	3.8	154.8	4371
5	342.1379	7153	0.9	36.2	4478
6	383.1483	44961	5.7	227.1	4461
7	384.1511	11067	1.4	55.4	4635
8	425.1586	7376	0.9	36.0	4740
9	443.1683	22805	2.9	112.3	4396
10	444.1711	6455	0.8	31.1	4968
11	485.1767	15448	1.9	74.6	4646
12	507.1601	19191	2.4	92.1	4689
13	562.2273	54439	6.9	265.8	4615
14	563.2303	17974	2.3	87.1	4701
15	564.1871	16284	2.1	78.8	3600
16	564.6761	8971	1.1	42.9	3999
17	567.1840	793692	100.0	3907.4	4488
18	568.1869	235454	29.7	1159.3	4625
19	569.1886	48373	6.1	237.4	4504
20	570.1889	8517	1.1	40.9	4355
21	583.1584	116778	14.7	581.6	4617
22	584.1613	35275	4.4	175.0	4585
23	585.1587	16132	2.0	79.5	4749
24	627.1921	17782	2.2	91.0	4589
25	628.1967	8012	1.0	40.4	4540
26	629.1900	5483	0.7	27.3	4568
27	643.1688	34167	4.3	178.5	4771
28	644.1719	11733	1.5	60.6	4706
29	679.2362	16798	2.1	90.2	4589
30	680.2395	6078	0.8	32.0	4351



Chemical formula C₂₈H₃₂O₁₁

Exact mass 544.1945

HRMS m/z [M+Na]⁺ 567.1840

calcd. for C₂₈H₃₂O₁₁Na 567.1763

Figure S105 HRESIMS spectrum of MS20a

Mass Spectrum SmartFormula Report

Analysis Info

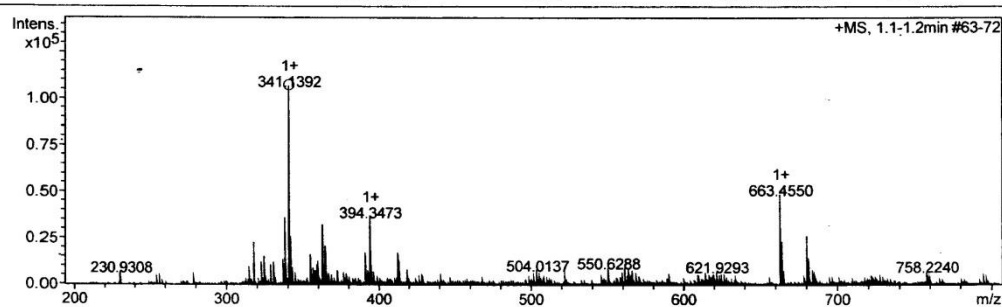
Analysis Name D:\Data\CRI\QSLP04324 Kanok-on YPMS-14 E+.d
 Method Nitrat esi neg low may2018-2.m
 Sample Name ESipos
 Comment

Acquisition Date 11/20/2018 12:58:24 PM

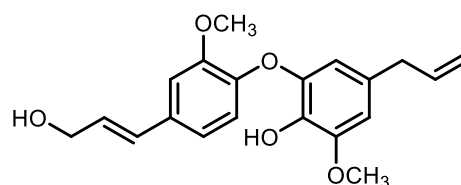
Operator BDAL@DE
 Instrument compact 8255754.20094

Acquisition Parameter

Source Type	ESI	Ion Polarity	Positive	Set Nebulizer	1.0 Bar
Focus	Not active	Set Capillary	4000 V	Set Dry Heater	150 °C
Scan Begin	200 m/z	Set End Plate Offset	-500 V	Set Dry Gas	6.0 l/min
Scan End	800 m/z	Set Charging Voltage	2000 V	Set Divert Valve	Source
		Set Corona	0 nA	Set APCI Heater	0 °C



Meas. m/z # Ion Formula	m/z	err [ppm]	Mean err [ppm]	rdB	N-Rule	e ⁻	Conf	mSigma	Std I	Std Mean m/z	Std Var	Std I Nor m	Std m/z Diff	Std Comb Dev
341.139212 1 C ₂₀ H ₂₁ O ₅	341.138350	-2.5	-5.0	10.5	ok	even		22.9	40.0	n.a.	n.a.	n.a.	n.a.	n.a.



Chemical formula C₂₀H₂₂O₅

Exact mass 342.1467

HRMS m/z [M-H]⁺ 341.1392

calcd. for C₂₁H₂₁O₅ 341.1389

QSLP04324 Kanok-on YPMS-14 E+.d

Bruker Compass DataAnalysis 4.3

printed: 11/20/2018 1:05:56 PM

by: BDAL@DE

Page 1 of 1

Figure S106 HRESIMS spectrum of MS18

Mass Spectrum SmartFormula Report

Analysis Info

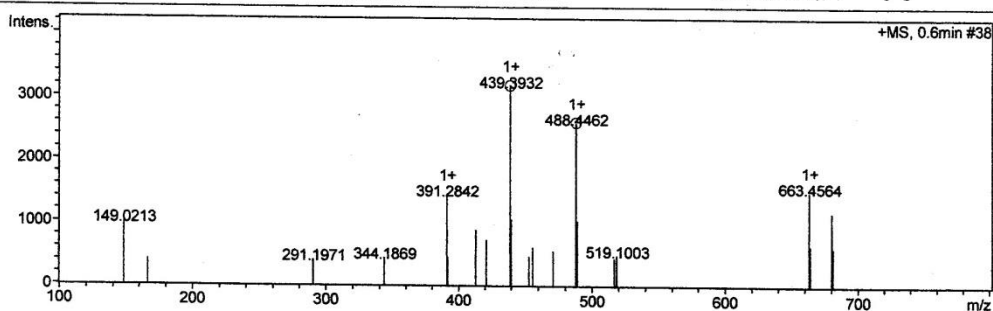
Analysis Name D:\Data\CRI\QSLP1795 Kanokon YPMS4 E+.d
 Method Nitirat esi pos low may2017-2.m
 Sample Name ESIpos
 Comment

Acquisition Date 7/21/2017 4:06:09 PM

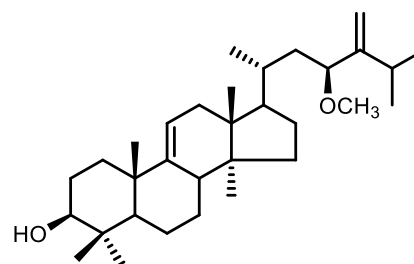
Operator BDAL@DE
 Instrument compact 8255754.20094

Acquisition Parameter

Source Type	ESI	Ion Polarity	Positive	Set Nebulizer	0.8 Bar
Focus	Not active	Set Capillary	3500 V	Set Dry Heater	110 °C
Scan Begin	100 m/z	Set End Plate Offset	-500 V	Set Dry Gas	7.0 l/min
Scan End	800 m/z	Set Charging Voltage	2000 V	Set Divert Valve	Source
		Set Corona	0 nA	Set APCI Heater	0 °C



Meas. m/z	#	Ion Formula	Score	m/z	err [mDa]	err [ppm]	mSigma	rdb	e ⁻ Conf	N-Rule	Adduct
439.393223	1	C31H51O	100.00	439.393443	0.2	0.5	36.1	6.5	even	ok	M+H
488.446241	1	C32H58NO2	100.00	488.446207	-0.0	-0.1	35.5	4.5	even	ok	M+H



Chemical formula $C_{32}H_{54}O_2$
 Exact mass 470.4124
 HRMS m/z $[M+NH_4]^+$ 488.4462
 calcd. for $C_{21}H_{21}O_5$ 488.4467

Figure S107 HRESIMS spectrum of MS3

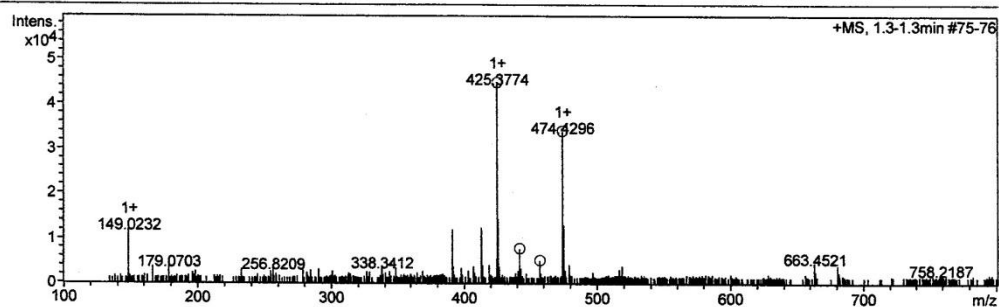
Mass Spectrum SmartFormula Report

Analysis Info
 Analysis Name: D:\Data\CRI\QSLP1796 Kanokon YPMS5 E+.d
 Method: Nitirat esi pos low may2017-2.m
 Sample Name: ESipos
 Comment:

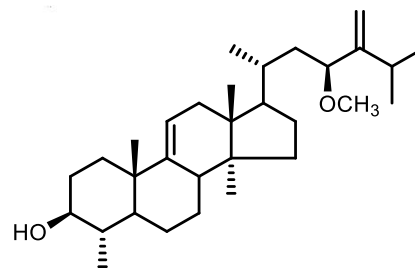
Acquisition Date: 7/21/2017 4:13:37 PM
 Operator: BDAL@DE
 Instrument: compact 8255754.20094

Acquisition Parameter

Source Type	ESI	Ion Polarity	Positive	Set Nebulizer	0.8 Bar
Focus	Not active	Set Capillary	3500 V	Set Dry Heater	130 °C
Scan Begin	100 m/z	Set End Plate Offset	-500 V	Set Dry Gas	7.5 l/min
Scan End	800 m/z	Set Charging Voltage	2000 V	Set Divert Valve	Source
		Set Corona	0 nA	Set APCI Heater	0 °C



Meas. m/z	#	Ion Formula	Score	m/z	err [mDa]	err [ppm]	mSigma	rdb	e ⁻ Conf	N-Rule	Adduct
425.377414	1	C30H49O	100.00	425.377793	0.4	0.9	14.4	6.5	even	ok	M+H
442.403825	1	C30H52NO	100.00	442.404342	0.5	1.2	30.5	5.5	even	ok	M+H
457.402771	1	C31H53O2	100.00	457.404007	1.2	2.7	47.8	5.5	even	ok	M+H
474.429635	1	C31H56NO2	100.00	474.430556	0.9	1.9	11.5	4.5	even	ok	M+H



Chemical formula C₃₁H₅₂O₂

Exact mass 456.3967

HRMS m/z [M+NH₄]⁺ 474.4296

QSLP1796 Kanokon YPMS5 E+.d
 Bruker Compass DataAnalysis 4.3

calcd. for C₂₁H₂₁O₅

474.4310

printed: 7/24/2017 11:43:50 AM

by: BDAL@DE

Page 1 of 1

Figure S108 HRESIMS spectrum of MS5

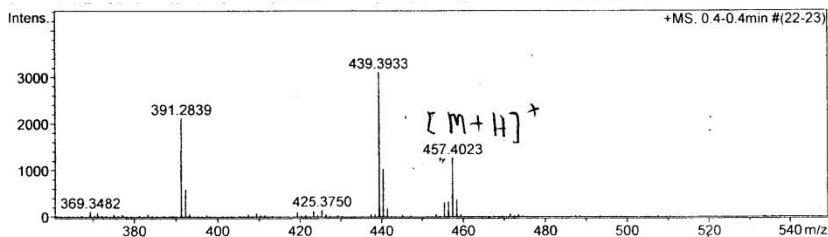
Mass Spectrum List Report

MSLH-1-51-1

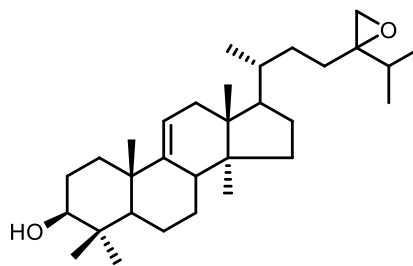
Analysis Info			
Analysis Name	TOFSLP24961 Kanok-on YPMS-16 A+.d	Acquisition Date	11/21/2018 4:06:22 AM
Method	Nitrat APCI pos 2018-1.m	Operator	Administrator
Sample Name	APCIpos	Instrument	micrOTOF 74

Acquisition Parameter

Source Type	APCI	Ion Polarity	Positive	Set Corrector Fill	64 V
Scan Range	n/a	Capillary Exit	115.0 V	Set Pulsar Pull	405 V
Scan Begin	100 m/z	Hexapole RF	120.0 V	Set Pulsar Push	405 V
Scan End	700 m/z	Skimmer 1	35.0 V	Set Reflector	1300 V
		Hexapole 1	22.9 V	Set Flight Tube	9000 V
				Set Detector TOF	1980 V



#	m/z	I	Res.
1	149.0240	450	6529
2	153.1214	304	6575
3	163.0788	256	6684
4	169.0876	345	6577
5	179.0862	267	3085
6	183.0880	254	4327
7	201.1741	306	5345
8	203.1741	477	7708
9	205.1908	1373	7899
10	206.1934	249	7417
11	219.1711	541	7830
12	221.1525	261	3469
13	229.2119	537	7531
14	253.1204	979	8043
15	257.2444	557	8316
16	271.2593	506	8173
17	279.1579	316	7552
18	281.0958	279	8281
19	294.1031	261	9329
20	295.1093	729	8777
21	297.2760	513	8140
22	308.9760	308	9114
23	391.2839	2126	10305
24	392.2860	592	9695
25	439.3933	3113	10528
26	440.3960	1034	10575
27	455.3844	312	11343
28	456.3954	337	10382
29	457.4023	1273	10427
30	458.4061	382	9496



Chemical formula	C ₃₁ H ₅₂ O ₂
Exact mass	456.3967
HRMS m/z [M+H] ⁺	457.4023
calcd. for C ₃₁ H ₅₃ O ₂ ,	457.4045)

Figure S109 HRESIMS spectrum of MS6

Mass Spectrum SmartFormula Report

Analysis Info

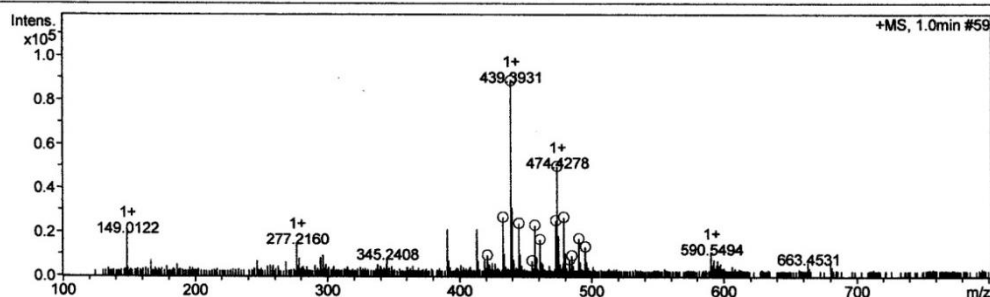
Analysis Name D:\Data\CR\QSLP1797 Kanokon YPMS6 E+.d
 Method Nitirat esi pos low may2017-2.m
 Sample Name ESipos
 Comment

Acquisition Date 7/21/2017 4:18:38 PM

Operator BDAL@DE
 Instrument compact 8255754.20094

Acquisition Parameter

Source Type	ESI	Ion Polarity	Positive	Set Nebulizer	0.8 Bar
Focus	Not active	Set Capillary	3500 V	Set Dry Heater	130 °C
Scan Begin	100 m/z	Set End Plate Offset	-500 V	Set Dry Gas	7.5 l/min
Scan End	800 m/z	Set Charging Voltage	2000 V	Set Divert Valve	Source
		Set Corona	0 nA	Set APCI Heater	0 °C



Meas. m/z	#	Ion Formula	Score	m/z	err [mDa]	err [ppm]	mSigma	rdb	e ⁻ Conf	N-Rule	Adduct
421.382144	1	C31H49	100.00	421.382878	0.7	1.7	69.5	7.5	even	ok	M+H
	2	C29H50Na	38.96	421.380472	-1.7	-4.0	79.2	4.5	even	ok	M+H
433.367816	1	C28H49O3	100.00	433.367622	-0.2	-0.4	28.6	4.5	even	ok	M+H
439.393143	1	C31H51O	100.00	439.393443	0.3	0.7	3.6	6.5	even	ok	M+H
445.367217	1	C29H49O3	100.00	445.367622	0.4	0.9	45.7	5.5	even	ok	M+H
455.389497	1	C31H51O2	100.00	455.388357	-1.1	-2.5	637.7	6.5	even	ok	M+H
457.403178	1	C31H53O2	100.00	457.404007	0.8	1.8	21.3	5.5	even	ok	M+H
461.361589	1	C29H49O4	100.00	461.362536	0.9	2.1	108.0	5.5	even	ok	M+H
473.392103	1	C33H49N2	100.00	473.389026	-3.1	-6.5	n.a.	10.5	even	ok	M+H
474.427803	1	C31H56NO2	100.00	474.430556	2.8	5.8	6.6	4.5	even	ok	M+H
479.384956	1	C31H52NaO2	92.37	479.385952	1.0	2.1	7.0	5.5	even	ok	M+H
	2	C33H51O2	11.87	479.388357	3.4	7.1	13.1	8.5	even	ok	M+H
	3	C28H51N2O4	100.00	479.384335	-0.6	-1.3	13.5	4.5	even	ok	M+H
483.343477	1	C29H48NaO4	94.40	483.344481	1.0	2.1	32.7	5.5	even	ok	M+H
	2	C31H47O4	13.41	483.346886	3.4	7.1	33.0	8.5	even	ok	M+H
	3	C26H47N2O6	100.00	483.342864	-0.6	-1.3	38.5	4.5	even	ok	M+H
485.361067	1	C31H49O4	94.79	485.362536	1.5	3.0	32.3	7.5	even	ok	M+H
	2	C29H50NaO4	100.00	485.360131	-0.9	-1.9	42.5	4.5	even	ok	M+H
	3	C26H49N2O6	22.75	485.358514	-2.6	-5.3	53.4	3.5	even	ok	M+H
490.425213	1	C31H56NO3	100.00	490.425471	0.3	0.5	24.5	4.5	even	ok	M+H
495.379981	1	C33H51O3	20.72	495.383272	3.3	6.6	65.2	8.5	even	ok	M+H
	2	C31H52NaO3	100.00	495.380866	0.9	1.8	73.7	5.5	even	ok	M+H
	3	C28H51N2O5	77.35	495.379249	-0.7	-1.5	82.2	4.5	even	ok	M+H

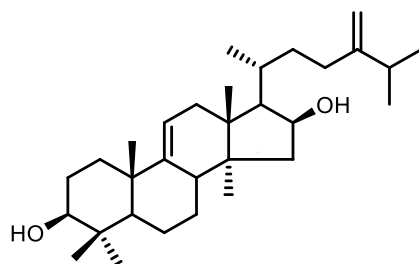
QSLP1797 Kanokon YPMS6 E+.d

Bruker Compass DataAnalysis 4.3

printed: 7/24/2017 11:46:11 AM

by: BDAL@DE

Page 1 of 1



Chemical formula	C ₃₁ H ₅₂ O ₂
Exact mass	456.3967
HRMS m/z [M+NH ₄] ⁺	474.4278
calcd. for C ₂₁ H ₂₁ O ₅	474.4310

Figure S94 HRESIMS spectrum of MS7

VITA

NAME Yupa Pootaeng-on

DATE OF BIRTH 12 Dec 1977

PLACE OF BIRTH Nakhon Pathom

INSTITUTIONS ATTENDED Department of Chemistry, Faculty of Science, Silpakorn University

HOME ADDRESS 9/6 Village No. 6, Tupluang Sub-district, Mueang Nakhon Pathom District, Nakhon Pathom Province

PUBLICATION Pootaeng-on, Y., Charoensuksai, P., Wongprayoon, P., Jiajaroen, S., Chainok, K., Rayanil, K. 2020. Miliusins; cytotoxic neolignans from the leaves of *Miliusa sessilis*. *Phytochemistry*, 176: 112417.

